

Technical Report

Hybrid growth models for *Eucalyptus globoidea* and *E. bosistoana*: Explaining within and between site variability

Author/s: Serajis Salekin

Date: 15th February 2019

Report: SWP-T070

TABLE OF CONTENTS

EXECUTIVE SUMMARY	1
Thesis – embedded here	2

Disclaimer

This report has been prepared by University of Canterbury for Forest Growers Research Ltd (FGR) subject to the terms and conditions of a research services agreement dated 1 July 2015.

The opinions and information provided in this report have been provided in good faith and on the basis that every endeavour has been made to be accurate and not misleading and to exercise reasonable care, skill and judgement in providing such opinions and information.

Under the terms of the Services Agreement, University of Canterbury's liability to FGR in relation to the services provided to produce this report is limited to the value of those services. Neither University of Canterbury nor any of its employees, contractors, agents or other persons acting on its behalf or under its control accept any responsibility to any person or organisation in respect of any information or opinion provided in this report in excess of that amount.

EXECUTIVE SUMMARY

Plantation forests play a major role in satisfying many forestry needs such as demand for wood and different ecosystem services, which are projected to increase in the future. In New Zealand, the plantation forestry industry is dominated by *Pinus radiata*, which comprise approximately 90% of the net stocked area. Diversification of the New Zealand plantation forest estate by introducing new species is prudent, especially in arid parts of the country where *Pinus radiata* growth cannot achieve its full potential. Several *Eucalyptus* species are potential alternatives to *Pinus radiata*. However, there is currently very little information on their growth dynamics.

Forest growth and yield models are used to understand the growth dynamics of forest trees and are generally mensurational models for mature stands created from inventory data that span several years. Growth models of plantation trees at juvenile ages can generate information useful for plantation establishment, but such models are rarely created. Although mensurational growth and yield models project and create useful information to help management decisions, they provide little understanding of ecophysiological tree growth process. However, ecophysiological process information is important, especially in young plantations. This information can be created through process-based models, but these models are data intensive. Therefore, combining the two modelling approaches through hybridisation can give access to both mensurational and processbased modelling information, without violating basic growth and yield modelling assumptions.

Most existing growth and yield models are developed at stand level or individual tree-level, and productivity of the site is assumed to be homogenous due to silvicultural management and site preparation practices. However, in most sites growth is not homogenous throughout, especially juvenile plantation growth. Therefore, it is important to explore the factors affecting plantation growth within stands. This doctoral thesis investigates and develops models that include within and between stand factors for juvenile *Eucalyptus bosistoana* and *Eucalyptus globoides* by using a hybrid ecophysiological modelling approach. The study further tests and compares different hybridisation approaches. It concludes with a preliminary mature-stand mensurational growth and yield model for *E. globoides*, developed from sparse available data by use of algebraic difference approach (ADA) equations.

The availability of high-resolution digital elevation models (DEMs) is inadequate for rural New Zealand, including the unproductive ex-pastoral lands where this study is sited. However, it is important to have high-resolution DEMs for hybrid ecophysiological study of growth and yield. Field surveys conducted with global positioning system (GPS) receivers, can be an efficient, useful and simple method for creating high-resolution DEMs. This study reports on an optimisation procedure for producing DEMs by comparing three non-geostatistical interpolation procedures carried out with field collected GNSS data. Results show that the ANUDEM interpolation algorithm produced DEMs with the highest accuracy. The study also reports that data density influences final DEM resolution.

Within-stand height growth and survival proportion models indicate that topographic, wind exposure, morphometric protection, position index, and distance from ridge top significantly influenced juvenile height growth and survival proportion. These topographic indices were also found to be significant for between-site juvenile height growth and survival proportion, along with temperature. Overall, each of the final models had high precision and minimal bias, therefore they can predict juvenile tree height yield and survival proportion well.

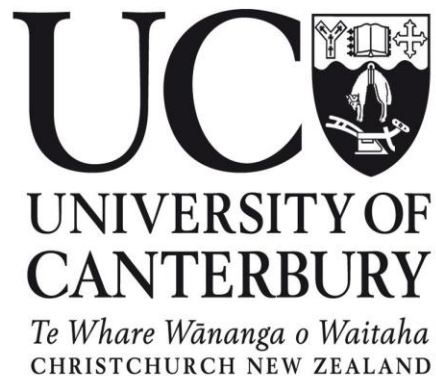
Potentially useable light sum equations (PULSE) with augmented topographic indices were better than PULSE alone, or traditional hybridisation approaches, for explaining between-site growth. In addition to height growth and survival predictions, these hybrid models offer many other uses, including generating useful ecophysiological information, and they offer an improved understanding of tree growth processes.

Finally, the preliminary mensurational growth and yield models for *E. globoidea* were developed to project growth over time with high precision and minimal error. These models create useful growth dynamics information for forest managers, as well as suggesting future research avenues for growing *Eucalyptus* in New Zealand.

THESIS – NEXT PAGE

Hybrid growth models for *Eucalyptus globoidea* and *E. bosistoana*:

Explaining within and between site variability



School of Forestry
University of Canterbury
2019

Hybrid growth models for *Eucalyptus globoidea* and *E. bosistoana*: Explaining
within and between site variability

by
Serajis Salekin

A THESIS
submitted to
University of Canterbury

in partial fulfilment of
the requirements for the
degree of
Doctor of Philosophy

2019

To all the mothers, who bring us the first light.

Acknowledgements

Thinking of these last four years, dedicated to works that are part of this thesis, all the people who have been part of this and without whom it would not have been possible, come to mind.

First and foremost, I would like to thank my doctoral supervisory team, composed of Professor Euan Mason (Principal supervisor), Dr Justin Morgenroth (Co-supervisor), Dr Mark Bloomberg (Associate supervisor), and Dr Dean Meason (Associate supervisor) for giving me the opportunity to work on this project and believe in me. Also, I appreciate their timely and constructive feedback, which helped greatly to improve this work. I am especially grateful to Professor Euan Mason for his great enthusiasm, advice on the topic, lessons on modelling, and inestimable assistance with R environment and programming. I am also greatly indebted, to Dr Justin Morgenroth for his enormous support with GIS and time management. Their encouragement and appreciation helped me pass through the most difficult stages.

Many thanks to all the postgraduate fellows and friends for creating a comfortable environment within the school with their humour and words beyond forestry. Special thanks to the people who helped me in the field and laboratory work. In particular Jack Henry Burgess, Satoru Kuwabara, Dr Huimin Lin, Fei Guo, Xuan Nguyen, Ash Millen, Neil Smith and Md. Azharul Alam. Special thanks to Paul Millen, NZDFI team, SCION and all the landowners who kindly gave access to data for this project. I would like to express my sincere gratitude to Dr Horacio Bown for his constructive feedback on modelling chapters, and Yannina Whiteley, Walter Raymond, Darius Phiri and Cristian Higuera for helping me to greatly improve the readability of this document. I am grateful to the School of Forestry for hosting me and providing all the necessary logistics, especially to Jeanette Allen and Vicki Wilton.

I would like to acknowledge the generous financial support I have received from the Agricultural and Marketing Research and Development Trust (2015-20117), Speciality Wood Product programme (2017-2018), T W Adams postgraduate scholarship (2018), the McKelvey Prize (2017).

Finally, thanks to my family, friends, and Niger for helping me to see this endeavour through with their love and support.

Abstract

Plantation forests play a major role in satisfying many forestry needs such as demand for wood and different ecosystem services, which are projected to increase in the future. In New Zealand, the plantation forestry industry is dominated by *Pinus radiata*, which comprise approximately 90% of the net stocked area. Diversification of the New Zealand plantation forest estate by introducing new species is prudent, especially in arid parts of the country where *Pinus radiata* growth cannot achieve its full potential. Several *Eucalyptus* species are potential alternatives to *Pinus radiata*. However, there is currently very little information on their growth dynamics.

Forest growth and yield models are used to understand the growth dynamics of forest trees and are generally mensurational models for mature stands created from inventory data that span several years. Growth models of plantation trees at juvenile ages can generate information useful for plantation establishment, but such models are rarely created. Although mensurational growth and yield models project and create useful information to help management decisions, they provide little understanding of ecophysiological tree growth process. However, ecophysiological process information is important, especially in young plantations. This information can be created through process-based models, but these models are data intensive. Therefore, combining the two modelling approaches through hybridisation can give access to both mensurational and process-based modelling information, without violating basic growth and yield modelling assumptions.

Most existing growth and yield models are developed at stand level or individual tree-level, and productivity of the site is assumed to be homogenous due to silvicultural management and site preparation practices. However, in most sites growth is not homogenous throughout, especially juvenile plantation growth. Therefore, it is important to explore the factors affecting plantation growth within stands.

This doctoral thesis investigates and develops models that include within and between stand factors for juvenile *Eucalyptus bosistoana* and *Eucalyptus globoidea* by using a hybrid ecophysiological modelling approach. The study further tests and compares different hybridisation approaches. It concludes with a preliminary mature-stand mensurational growth and yield model for *E. globoidea*, developed from sparse available data by use of algebraic difference approach (ADA) equations.

The availability of high-resolution digital elevation models (DEMs) is inadequate for rural New Zealand, including the unproductive ex-pastoral lands where this study is sited. However, it is important to have high-resolution DEMs for hybrid ecophysiological study of growth and yield. Filed surveys conducted with global positioning system (GPS) receivers, can be an efficient, useful and simple method for creating high-resolution DEMs. This study reports on an optimisation procedure for producing DEMs by comparing three non-geostatistical interpolation procedures carried out with field collected GNSS data. Results show that the ANUDEM interpolation algorithm produced DEMs with the highest accuracy. The study also reports that data density influences final DEM resolution.

Within-stand height growth and survival proportion models indicate that topographic, wind exposure, morphometric protection, position index, and distance from ridge top significantly influenced juvenile height growth and survival proportion. These topographic indices were also found to be significant for between-site juvenile height growth and survival proportion, along with temperature. Overall, each of the final models had high precision and minimal bias, therefore they can predict juvenile tree height yield and survival proportion well.

Potentially useable light sum equations (PULSE) with augmented topographic indices were better than PULSE alone, or traditional hybridisation approaches, for explaining between-site

growth. In addition to height growth and survival predictions, these hybrid models offer many other uses, including generating useful ecophysiological information, and they offer an improved understanding of tree growth processes.

Finally, the preliminary mensurational growth and yield models for *E. globoidea* were developed to project growth over time with high precision and minimal error. These models create useful growth dynamics information for forest managers, as well as suggesting future research avenues for growing *Eucalyptus* in New Zealand.

Table of contents

ACKNOWLEDGEMENTS	V
ABSTRACT	VII
LIST OF FIGURES	XVII
LIST OF TABLES	XXIII
LIST OF ABBREVIATIONS	XXV
1. INTRODUCTION	28
1.1 PLANTATION FOREST	28
1.2 FOREST PLANTATION ESTABLISHMENT	29
1.3 FOREST PLANTATION SITE	31
1.3.1 Site productivity	32
1.3.2 Micro-site variation in plantation forestry	33
1.3.3 Documented factors of micro-site variation and their role	35
1.3.5 Importance of being subtle	39
1.4 FOREST GROWTH AND YIELD MODELLING	40
1.4.1 Classification of growth and yield models	42
1.4.1.1 Forest models based on the level of focus	42
1.4.1.2 Forest models based on the approach of development	44
1.4.2 Hybrid models: a way to deal with complexity	46
1.4.3 Hybridisation strategies	48
1.4.3.1 Augmented hybridisation approach	48
1.4.3.2 Potentially useable radiation sums approach	49
1.4.4 Modelling juvenile growth and yield	50

1.5 NEW ZEALAND DRY LAND FOREST INITIATIVE (NZDFI) AND TWO SPECIES OF INTEREST	51
1.6 OBJECTIVES AND THESIS STRUCTURE	55
1.7 REFERENCES	58
2. A COMPARATIVE STUDY OF THREE NON-GEOSTATISTICAL METHODS TO OPTIMISE DIGITAL ELEVATION MODEL INTERPOLATION.	75
2.1 INTRODUCTION	75
2.2 MATERIALS AND METHODS	78
2.2.1 Study sites	78
2.2.3 Interpolation methods and parameters	81
2.2.3.1 Inverse Distance Weighted (IDW)	82
2.2.3.2 Topo to Raster (ANUDEM)	83
2.2.3.3 Natural Neighbours (NaN)	84
2.2.4 Analysis	84
2.3 RESULTS	86
2.3.1 DEM resolution analysis	86
2.3.2 Interpolation methods and data density	88
2.4 DISCUSSION	94
2.4.1 An alternate data source	94
2.4.2 Optimal resolution	94
2.4.3 Influencers of DEM quality	95
2.4.4 Deterministic interpolation method	96
2.5 SUMMARY AND CONCLUSIONS	96

2.6 REFERENCES	98
3. MODELLING THE EFFECT OF ENVIRONMENTAL MICRO-SITE INFLUENCES ON THE GROWTH OF JUVENILE <i>EUCALYPTUS GLOBOIDEA</i> AND <i>EUCALYPTUS BOSISTOANA</i> IN NEW ZEALAND.	106
3.1 INTRODUCTION	106
3.2 MATERIALS AND METHODS	109
3.2.1 Experimental sites	109
3.2.2 Data collection and preparation	110
3.2.2.1 Tree data	110
3.2.2.2 Topographic data	113
3.2.2.3 Soil data	116
3.2.2.4 Climatic data	117
3.2.3 Modelling approach	119
3.2.3.1 Soil rooting depth model	119
3.2.3.2 Temperature model	119
3.2.3.3 Juvenile height model	120
3.2.3.4 Survival model	121
3.2.4 Model testing and validation	122
3.2.5 Statistical analysis	123
3.3 RESULTS	124
3.3.1 Soil rooting depth	124
3.3.2 Temperature variation at Avery and Lawson sites	125
3.3.3 Juvenile height model	126
3.3.4 Key variables for micro-site height growth	129
3.3.5 Juvenile survival model	135
3.3.6 Key factors to juvenile micro-site survival	137

3.4 DISCUSSION	140
3.4.1 Juvenile micro-site models	140
3.4.2 Micro-site variables affect juvenile tree height growth	140
3.4.3 Micro-site variability on juvenile tree survival	141
3.4.4 Data constraints	142
3.5 CONCLUSION	142
3.6 REFERENCES	144
4. MODELLING THE GROWTH AND SURVIVAL OF JUVENILE <i>EUCALYPTUS GLOBOIDEA</i> AND <i>EUCALYPTUS BOSISTOANA</i> IN NEW ZEALAND.	153
4.1 INTRODUCTION	153
4.2 MATERIALS AND METHODS	155
4.2.1 Experimental sites	155
4.2.2 Data collection and preparation	156
4.2.2.1 Tree data	157
4.2.2.2 Topographic data	159
4.2.2.3 Soil data	160
4.2.2.4 Climatic data	162
4.2.3 Modelling approach	164
4.2.4 Model testing and validation	164
4.2.5 Statistical analysis	165
4.3 RESULTS	166
4.3.1 Site-specific juvenile height yield models	166
4.3.2 Key juvenile height growth factors	170
4.3.3 Site-specific survival model	171

4.3.4 Key site-specific factors for juvenile survival	175
4.4. DISCUSSION	176
4.4.1. Site-specific growth and survival models	177
4.4.2. Juvenile height growth factors	178
4.4.3. Factors affecting juvenile survival	180
4.5 CONCLUSION	181
4.6 REFERENCES	183
5. MODELLING JUVENILE GROWTH AND SURVIVAL USING A HYBRID ECOPHYSIOLOGICAL APPROACH.	190
5.1. INTRODUCTION	190
5.2. METHODS	193
5.2.1 Data description	193
5.2.2 Calculation of modifiers	194
5.2.3 Model building and evaluation	200
5.3. RESULTS	201
5.3.1. Site-specific height yield PULSE models	201
5.3.2 Augmented PULSE model for juvenile height yield	208
5.3.3 Site-specific survival PULSE model	214
5.3.4 Augmented PULSE model for juvenile survival proportion	220
5.4 DISCUSSION	226
5.4.1 Juvenile PULSE models	226
5.4.2 Topographic variables	227

5.5 CONCLUSION	228
5.6 REFERENCES	230
6. COMPARISON OF HYBRID ECOPHYSIOLOGICAL MODELLING APPROACHES BETWEEN SITES.	235
6.1 INTRODUCTION	235
6.2 METHODOLOGY	236
6.3. RESULTS AND DISCUSSION	237
6.3.1. Time versus radiation	237
6.3.2 Information used	239
6.3.3 Precision and bias	241
6.3.4 System integration	243
6.4 CONCLUSION	244
6.5 REFERENCES	245
7. A PRELIMINARY GROWTH AND YIELD MODEL FOR MATURE <i>EUCALYPTUS GLOBOIDEA</i> PLANTATIONS IN NEW ZEALAND	248
7.1 INTRODUCTION	248
7.2 MATERIALS AND METHODS	249
7.2.1 Data preparation and description	249
7.2.2 Modelling and evaluation	252
7.3 RESULTS	254
7.3.1 Mean top height (MTH) model	254
7.3.2 Basal area (G) model	255

7.3.3 Maximum diameter (D_{\max}) model	257
7.3.4 Standard deviation of diameter (SD_D) model	258
7.3.5 Stand volume (V) model	260
7.3.6 Height diameter (H-D) model	262
7.3.7 Self-thinning model	263
7.4 DISCUSSION	264
7.5 CONCLUSION	266
7.6 REFERENCES	267
8. A GENERAL DISCUSSION	272
8.1 WITHIN-SITE AND BETWEEN-SITES GROWTH AND SURVIVAL FACTORS	272
8.3 PRELIMINARY GROWTH AND YIELD MODEL FOR <i>E. GLOBOIDEA</i>	273
8.4 MANAGEMENT IMPLICATIONS	274
8.5 RESEARCH NEEDS AND RESEARCH QUESTIONS	274
8.6 CONCLUSION	275
8.7 REFERENCES	276
APPENDICES	277
Appendix I	277
Appendix II	280
Appendix III	282
Appendix IV	285

List of figures

Figure 1.1 Adapted conceptual model of plantation establishment (Mason, 1992).	30
Figure 1.2 General organisation of the research chapters in the thesis based on the data, stand status and different modelling strategies.	56
Figure 2.1 Location of the experimental site. Aerial imagery overlaid on a hillshade model.	79
Figure 2.2 Layout of the collected data points.	80
Figure 2.3 Training points were thinned by A) 0%, B) 25%, C) 50%, and D) 75%.	81
Figure 2.4 Effect of resolution at each observation point by A) RMSE (root mean square error) and B) MAE (mean absolute error).	88
Figure 2.5 Residuals plotted against predicted elevation (m) for different models and levels of data thinning. Red line shows the model prediction trend.	90
Figure 2.6 Comparison of three interpolation method in regards to different data density A) Root mean square error (RMSE) and B) Mean absolute error (MAE).	91
Figure 2.7 Hillshade surfaces produced from DEMs interpolated by: A) Nearest neighbour, B) ANUDEM and C) IDW. Numbers 0 to 3 represent 0%, 25%, 50%, and 75% elevation data thinning prior to DEM interpolation.	93
Figure 3.1 Study site locations.	110
Figure 3.2 Daily maximum temperature by month at A) A, and B) B sites (red line showed the general monthly temperature trend); C) and D) represents the temperature difference at A and B sites from the independent weather station temperature (blue line showed the general trend).	118
Figure 3.3 <i>E. globoidea</i> juvenile height model residual plots: A) final model residuals and B) validation residuals with the loess line (blue); C) and D) respectively final model and validation residuals distribution.	127

- Figure 3.4 *E. bosistoana* juvenile height models residuals (m) plot for site B; A) Final model residuals and B) validation residuals representation with the loess line (blue); C) and D) represents the residuals distribution of model fit and validation dataset. 128
- Figure 3.5 *E. bosistoana* juvenile height models residuals (m) plot for site C; A) Final model residuals and B) validation residuals representation with loess line (blue); C) and D) represents the residuals distribution of model fit and validation dataset. 129
- Figure 3.6 Micro-topographic effect of *E. globoidea* height growth: (A) Wind exposure effect, (B) Morphometric protection effect, and (C) Distance from the top ridge effect. 131
- Figure 3.7 Micro-topographic effects on *E. bosistoana* height growth at site B; (A) Plan curvature, (B) Morphometric protection effect, (C) Distance from the top ridge effect, (D) Topographic position effect, (E) Wind exposure effect and (F) WEI and DIST interaction effect. 133
- Figure 3.8 Micro-topographic effect of *E. bosistoana* height growth at site C: (A) Wind exposure, (B) Wetness effect, (C) Distance from the top ridge effect, (D) Topographic position effect, and (E) Morphometric protection effect. 134
- Figure 3.9 *E. globoidea* juvenile survival models residuals (m) plot for site A; A) Final model residuals and B) validation residuals representation with the loess line (blue); C) and D) represents the residuals distribution of model fit and validation dataset. 136
- Figure 3.10 *E. bosistoana* juvenile survival models residuals (m) plot for site C; A) Final model residuals and B) validation residuals representation with loess line (blue); C) and D) represents the residuals distribution of model fit and validation dataset. 137
- Figure 3.11 Micro-topographic effect of *E. globoidea* survival at Site A: (A) Plan curvature, (B) Profile curvature effect, (C) Wind exposure effect, and (D) Distance from the ridge top effect; E) *E. bosistoana* survival with profile curvature effect at the site C. 139
- Figure 4.1 Locations of permanent sample plots (PSPs) and virtual climatic stations (VCSN). 156
- Figure 4.2 Height yield model prediction and residual plot: A1) predicted height yield against model residuals (blue points-model fitting, grey points-model validation residuals and blue line-loess line); B1) model fitting residuals distribution for *E. bosistoana*; A2) predicted height yield against models residuals (red points-model fitting, grey points-model validation residuals and red line shows the loess fit); and B2) model fitting residuals distribution for *E. globoidea*. 168

- Figure 4.3 Decision trees from the recursive partitioning of independent variables against height yield at a single age. Each factor presents with a threshold value, and each node represents with its splitting values and a number of observations of predicted class. A) represents *E. globoidea*, and B) *E. bosistoana*. 170
- Figure 4.4 Effect of A1) topographic wetness index (TWI), B1) wind exposure index (WEI) on *E. bosistoana*; A2) maximum temperature, and B2) radiation on *E. globoidea* height growth. 171
- Figure 4.5 Survival models predicted, and residuals plots: A1) predicted survival against model residuals (red points-model fitting, grey points-model validation residuals and blue line-loess line); B1) model fitting residuals distribution for *E. bosistoana* (red dashed line shows the mean); A2) predicted survival proportion against model residuals; and B2) model fitting residuals distribution for *E. globoidea* (the red dashed line shows the mean). 173
- Figure 4.6 Decision trees from the recursive partitioning of independent variables against survival proportion at a single age. Each factor presents a threshold value, and each node represents its splitting values and a number of observations of the predicted class: A) *E. globoidea* and B) *E. bosistoana*. 175
- Figure 4.7 Effect of A1) topographic wetness index (TPI), B1) minimum temperature (Tmin) on *E. bosistoana*, A2) minimum temperature (Tmin), and B2) radiation on *E. globoidea* survival. 176
- Figure 5.1 Generic leaf area index (LAI) estimation models. 197
- Figure 5.2 Residuals against predicted of *E. bosistoana* PULSE height yield models (blue line indicating the loess fit), with A) All modifiers (R_M); B) temperature (R_T); C) temperature and vapour pressure deficit (R_{TVPD}); D) available soil water ($R_{T\theta}$) modified radiation sum. 203
- Figure 5.3 Residuals against predicted of *E. globoidea* PULSE height yield models (blue line indicating the loess fit), with A) All modifiers (R_M); B) temperature (R_T); C) temperature and vapour pressure deficit (R_{TVPD}); D) available soil water ($R_{T\theta}$) modified radiation sum. 204
- Figure 5.4 Residuals distribution of *E. bosistoana* PULSE height yield models (red dashed line shows the mean), A) All modifiers (R_M); B) temperature (R_T); C) temperature and vapour pressure deficit (R_{TVPD}); D) available soil water ($R_{T\theta}$) modified radiation sum. 206
- Figure 5.5 Residuals distribution of *E. globoidea* PULSE height yield models (red dashed line showed the mean), A) All modifiers (R_M); B) temperature (R_T); C) temperature and vapour pressure deficit (R_{TVPD}); D) available soil water ($R_{T\theta}$) modified radiation sum. 207

- Figure 5.6 Residuals distribution from the model validation, A) predicted against residuals distribution with the loess fit line in blue and B) frequency distribution (red dashed line showing the mean). A1 and B1 for *E. bosistoana*; A2 and B2 for *E. globoidea*. 208
- Figure 5.7 Augmented PULSE height model for *E. bosistoana* residuals: A) residuals against predicted plot, the blue line indicates the loess fit; B) residuals distribution; C) morphometric protection index (MPI) effect; and D) wind exposure index (WEI) effect. 210
- Figure 5.8 Augmented PULSE height model for *E. globoidea* residuals: A) residuals against predicted plot, the blue line indicating the loess fit; B) residuals distribution; C) Morphometric protection index (MPI) effect. 211
- Figure 5.9 Residuals distribution from augmented models validation: A) predicted against residuals distribution with the loess fit line in blue and B) frequency distribution (red dashed showing the mean line). A1 and B1 for *E. bosistoana*; A2 and B2 for *E. globoidea*. 212
- Figure 5.10 Residuals against predicted survival proportion of *E. bosistoana* PULSE survival proportion models (blue line indicating the loess fit): with A) all modifiers (R_M); and PULS modified by B) temperature (R_T); C) temperature and vapour pressure deficit (R_{TVPD}); and D) available soil water ($R_{T\theta}$). 215
- Figure 5.11 Residuals against predicted survival proportion of *E. globoidea* PULSE survival proportion models (blue line indicating the loess fit) and PULS modified by A) all modifiers (R_M); B) temperature (R_T); C) temperature and vapour pressure deficit (R_{TVPD}); D) available soil water ($R_{T\theta}$). 216
- Figure 5.12 Residual distributions of *E. bosistoana* PULSE survival proportion models (red dashed line showing the mean), and PULS modified by A) all modifiers (R_M); B) temperature (R_T); C) temperature and vapour pressure deficit (R_{TVPD}); D) available soil water ($R_{T\theta}$) modified radiation sum. 217
- Figure 5.13 Residuals distribution of *E. globoidea* PULSE survival proportion models (red dashed line showing the mean), and PULS modified by A) all modifiers (R_M); B) temperature (R_T); C) temperature and vapour pressure deficit (R_{TVPD}); D) available soil water ($R_{T\theta}$) modified radiation sum. 218
- Figure 5.14 Residuals distribution for validation of survival proportion models: A) predicted against residuals distribution with the loess fit line in blue, and B) frequency distribution (red dashed line showing the mean). A1 and B1 for *E. bosistoana*; A2 and B2 for *E. globoidea*. 220

- Figure 5.15 Augmented PULSE survival proportion model for *E. bosistoana*: A) residuals against predicted plot, the blue line indicating the loess fit; B) residuals distribution (red dashed line indicating the mean); C) topographic wetness index (TWI) effect. 222
- Figure 5.16 Augmented PULSE survival proportion model for *E. globoidea*: A) residuals against predicted plot, blue line indicating the loess fit; B) residuals distribution (red dashed line indicating the mean); C) wind exposure index (WEI) effect. 223
- Figure 5.17 Residuals distribution from augmented survival proportion model validation: A) predicted against residuals distribution with the loess fit line (blue line) and B) frequency distribution (red dashed line shows the mean). A1 and B1 for *E. bosistoana*; A2 and B2 for *E. globoidea*. 224
- Figure 6.1 Relationship between height (m) with modified PULS and time (age) with correlation coefficients: A) all modifiers; B) temperature modifier; C) temperature and VPD modifiers; D) temperature and ASW modifiers; and E) age in years. 238
- Figure 6.2 Relationship between survival proportion with modified PULS and time (age) with correlation coefficients: A) all modifiers; B) temperature modifier; C) temperature and VPD modifiers; D) temperature and ASW modifiers; and E) age in years. 239
- Figure 6.3 Comparison of three different height model approaches based on residual against predicted values: A) augmented time-based model; B) simple PULSE; and C) augmented PULSE. 1) *E. bosistoana*, and 2) *E. globoidea*. 242
- Figure 6.4 Comparison of three different survival proportion model approaches based on residual against predicted values: A) augmented time-based model; B) simple PULSE; and C) augmented PULSE. 1) *E. bosistoana*, and 2) *E. globoidea*. 243
- Figure 7.1 Permanent sample plot (PSP) locations and topography. 250
- Figure 7.2 Mean top height (MTH) model results: A) Residuals against prediction plot of first Von Bertalanffy-Richards polymorphic equation, light blue points represent model fitting, red points indicate validation residuals, and model fit is shown by the black line; B) Residuals frequency distribution, red dashed line shows the mean; and C) Model fit (blue lines) over measured MTH (thin black lines). 255
- Figure 7.3 Basal area (G) model results: A) Residuals against prediction plot of first Schumacher anamorphic equation, light blue points represent model fitting, the red points indicate

validation residuals, and model fit is shown by the black line; B) Residuals frequency distribution, red dashed line shows the mean; and C) Model fit (blue lines) over measured G (thin black lines). 256

Figure 7.4 Maximum diameter (D_{max}) model results: A) Residuals against prediction plot of Hossfeld polymorphic equation, light blue points represent model fitting, the red points indicate validation residuals, and the model fit is shown by the black line; B) Residuals frequency distribution, red dashed line shows the mean; and C) Model fit (blue lines) over measured D_{max} (thin black lines). 258

Figure 7.5 Maximum diameter (D_{max}) model results: A) Residuals against prediction plot of Hossfeld polymorphic equation, light blue points represent model fitting, the red points indicate validation residuals, and the model fit is shown by the black line; B) Residuals frequency distribution, red dashed line shows the mean; and C) Model fit (blue lines) over measured SD_D (thin black lines). 260

Figure 7.6 Stand volume (V) model results: A) Estimated stand volume from measured data; B) Residuals against prediction plot, light blue points represent model fitting, red points indicate validation residuals, and model fit is shown by the black line; and C) Residuals frequency distribution, red dashed line is shown the mean. 261

Figure 7.7 A) Measured height-diameter ($H-D$), blue line shows the linear trend; B) Residuals against prediction plot, light blue points represent model fitting, red points indicate validation residuals, model fit is shown by the blue line; and C) Residuals frequency distribution, red dashed line is shown the mean. 263

Figure 7.8 A) Reineke's SDI curve represented with self-thinning lines and A) SDI distribution plot. 264

List of tables

Table 1.1 Summary of documented cases of micro-site variation with different measurement indicators and ecosystems.	37
Table 1.2 Summary of characteristics of two growth and yield models depend on the level of focus.	43
Table 1.3 Comparison of major features of growth and yield models (mensurational versus ecophysiological) (Peng, 2000).	46
Table 2.1 Summary of elevations resulting from different training data thinning intensities.	81
Table 2.2 Statistical metrics to assess interpolation quality.	85
Table 2.3 Results of statistical analysis for different DEM resolutions.	87
Table 2.4 Comparison of the three methods at 0.5m resolution with different data density.	89
Table 3.1 Summary of the plantation inventory data.	112
Table 3.2 Description of the topographic attributes.	114
Table 3.3 Summary of the topographic attributes for study sites.	116
Table 3.4 Summary statistics of soil pits with rooting depth.	117
Table 3.5 Soil description of three sites according to Hewitt (2010).	117
Table 3.6 Summary of the average daily maximum monthly temperature.	118
Table 3.7 Results of rooting depth analysis.	125
Table 3.8 Coefficients for final full linear mixed models for air temperature difference within site.	126
Table 3.9 Fitting and validation statistics of the final height growth equations.	128
Table 3.10 Tested variables and their significance on juvenile height growth.	130
Table 3.11 Juvenile survival proportion model fitting statistics.	135
Table 3.12 Tested variables and their significance on juvenile <i>Eucalyptus</i> survival proportion.	138
Table 4.1 Summary of plantation inventory data.	158
Table 4.2 Summary of estimated topographic attributes.	159
Table 4.3 Summary statistics of soil data.	161
Table 4.4 Summary of climatic data from VCSN points.	163
Table 4.5 Height growth model fitting and validation statistics.	169
Table 4.6 Survival model fitting and validation statistics.	174
Table 5.1 List of parameters used in PULSE.	199
Table 5.2 Fitting statistics for PULSE height yield models.	205

Table 5.3 Validation statistics for the best PULSE height yield models.	205
Table 5.4 Augmented variables and their significant status.	209
Table 5.5 Fitting and validation statistics for augmented PULSE height yield models.	213
Table 5.6 Fitting statistics for the PULSE survival proportion models.	219
Table 5.7 Validation statistics for the best PULSE survival proportion models.	219
Table 5.8 Augmented variables and their significance status.	221
Table 5.9 Fitting and validation statistics for augmented survival proportion PULSE models.	225
Table 6.1 Data used in different modelling approaches.	240
Table 6.2 Comparison of precision, bias and performance of the different approaches. Bold faces show the best values in the group.	241
Table 7.1 Summary of the variables used for modelling.	251
Table 7.2 Different forms of difference equations.	252
Table 7.3 Volume equations.	253
Table 7.4 Mean top height (MTH) model fitting and validation statistics.	254
Table 7.5 Basal area (G) model fit and validation statistics.	256
Table 7.6 Maximum diameter (D _{max}) model fitting and validation statistics.	257
Table 7.7 Standard deviation of DBH (SD _D) model fitting and validation statistics.	259
Table 7.8 Stand volume(V) model fitting and validation statistics.	261
Table 7.9 Height-diameter relationship (H-D) model fitting and validation statistics.	262

List of abbreviations

<i>DEM</i>	Digital elevation model
<i>ANUDEM</i>	Topo to raster algorithm in ArcGIS
<i>IDW</i>	Inverse distance weighted regression
<i>NaN</i>	Natural neighbours
<i>RUE</i>	Radiation use efficiency
<i>LUE</i>	Light use efficiency
<i>LAI</i>	Leaf area index
<i>SLA</i>	Specific leaf area
<i>RMSE</i>	Root mean square error
<i>MAE</i>	Mean absolute error
<i>SE</i>	Standard error
<i>AICc</i>	Corrected Akaike information criterion
<i>R² adj.</i>	Adjusted regression coefficient
<i>r</i>	Correlation coefficient
<i>SD</i>	Standard deviation
<i>VPD</i>	Vapour pressure deficit
<i>PULSE</i>	Potentially useable light sum equations
<i>PULS</i>	Potentially usable light sum
<i>TWI</i>	Topographic wetness index
<i>WEI</i>	Wind exposure index

<i>DIST</i>	Distance from the top ridge
<i>TPI</i>	Topographic position index
<i>MPI</i>	Morphometric position index
<i>MPRESS</i>	Mean predicted residual error sum of squares
<i>MAPRESS</i>	Mean absolute predicted residual error sum of squares
<i>DBH</i>	Diameter at breast height (1.4m)
<i>MTH</i>	Mean top height
<i>G</i>	Basal area
<i>V</i>	Volume over bark
<i>SDI</i>	Stand density index
<i>SD_D</i>	Standard deviation of DBH
<i>D_{max}</i>	Maximum diameter
<i>Stocking</i>	Number of stems per hectore

1

Introduction

1. Introduction

1.1 Plantation forest

In the modern era, the pressure on the world's forests to deliver and satisfy multiple demands is increasing (Angelsen & Wunder, 2003, p. 3; Gustafsson et al., 2012) and approximately 30% of the world's land surface is considered to be forested (FAO, 2010). Moreover, nowadays, forest products are promoted as environmentally friendly materials (FAO, 2014). In spite of that, native, "natural", forests will continue to be preserved for their intrinsic values, as refugia for numerous associated organisms, and as learning hubs for research (Boyle, 1999). Different and contradictory expectations from society have led to conflict over forest use (Freer-Smith & Carnus, 2008). Forest plantations are promoted as a solution, though debates continue. For example, Stephens and Wagner (2007, p. 312) called plantations "biological deserts" and Carrere and Fonseca (2004, p. 3) even argued that "plantations are not forests". However, tree plantations are conceptually and practically established to fulfil the diverse global demands for goods and services from forests (Paquette & Messier, 2009).

It can be hard to define a plantation forest (Evans, 1992), as it is often confused with afforestation (Kanowski, 1997). The FAO (2010, p. 212) defines "a planted forest as those forests composed of trees established through planting and deliberate seeding of native or introduced species". Moreover, Owens and Lund (2009, p. 200) elaborate the idea of plantation forest as "forest by origin which still possesses features of uniformity, shape, and often the intensity of management, which readily distinguish them as artificial. Often although not always, they will have been established on land devoid of tree cover, at least in the previous 50 years". Besides this, plantation forests can exhibit natural ecological processes at different scales, depending on the species and degree of naturalness (INDUFOR, 2012).

The planted forest has long been mentioned in history. With some early references from the sixteenth century in Britain, it originally started in its modern, organised form in Germany during the eighteenth century. In the twentieth century, major plantation establishment happened in the temperate and Mediterranean climatic regions. Moreover, introduction of exotic trees accelerated the development of plantations, and experience of these species was gained this way (Evans, 1999). Now in the twenty-first century, the total global plantation forest area has been estimated to be 264 million hectares, which corresponds to an increase in area of just over 8% between 2005 and 2010 (FAO, 2010). In addition, it is projected to increase at a rate of 1.8% annually (INDUFOR, 2012). So, it is evident that plantation forests will significantly expand to satisfy global needs, including a wide range of services related to forests and their associated societies, for example, forest protection and restoration, and ecological services such as climate regulation and protection of soil and water resources. These services have been explored in the last few decades (see, Barua et al., 2014; Charnley, 2006; Onyekwelu et al., 2011; Sedjo & Botkin, 1997) and plantation forests are classified to serve specific purposes (Evans, 1999). However, production of industrial wood, which was the initial purpose of plantation forests, has increased and Sedjo (1999) predicted that it would grow even more rapidly in the future.

1.2 Forest plantation establishment

The establishment phase of a plantation is critical (Margolis & Brand, 1990): poor establishment may incur some extra cost. Mason (1992) suggested a conceptual model for plantation establishment, where the state of a stand is a function of the condition of the seedlings immediately after planting and their associated micro-environment, where both seedling state and micro-environment can be altered through management practices. Moreover, the costs incurred for overall management practices and site characteristics need to be considered (Figure 1.1). Further,

Schönau and Herbert (1989) reported species-specific silvicultural treatment and site preparation by means of fertilisation is required for proper establishment, which is also in line with the model.

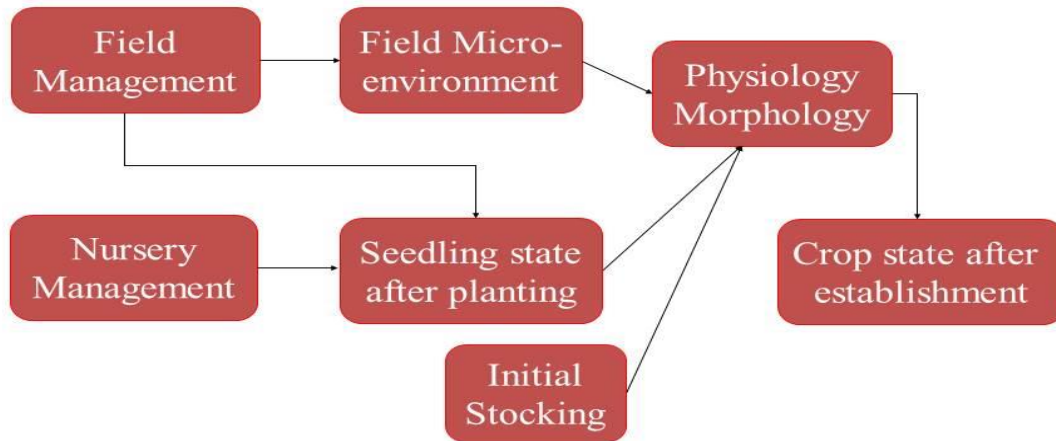


Figure 1.1 Adapted conceptual model of plantation establishment (Mason, 1992).

Traditionally, the most emphasised measures of juvenile crop performance are survival and initial height growth (Chavasse, 1977). In plantation forests, these depend on crop characteristics and other factors (Mason, 1992; Millner, 2006). For example, crop uniformity (West, 1984), stocking (Maclaren et al., 1995), and juvenile tree stability (Mason, 1985) are considered important characteristics. Moreover, the success of the plantation by way of survival is an indicator, which is measured by the number of quality stems prior to the first thinning (Mason, 1992). The desired numbers of stems/ha in the final crop will determine the numbers required after establishment through a “selection ratio” that varies with the purposes and conditions of the plantations.

During establishment, for measuring the growth of the stand at the beginning, the ground-line diameter (GLD) and height of the stems are readily available after planting. However, diameter

at breast height over bark (dbhob) is preferable for managers as it can be a state variable when expressed as basal area in a growth and yield model (Garcia, 1988).

1.3 Forest plantation site

In the case of forest land, “site” is a well-established term often used as a primary ecological unit. It refers to a geographic location which is relatively homogenous in terms of its physical and biological environment (Bailey et al., 1978; Grey, 1980). The forest plantation site refers to the composition of a site’s edaphic and climatic characteristics as a whole and its potential to sustain plant growth with a focus on site-specific silviculture (Skovsgaard & Vanclay, 2008). Louw (1995, p. 165) defined forest site as “an area that requires homogenous silvicultural practice, regarding species choice, management and amelioration techniques, and expected yields. In addition, it will have relatively similar soils, climate, parent material and topography.”

The forest site plays an important role as one of the principal modulators of survival and growth at different scales (Radford et al., 2002). One of the main components of a site is soil. The soil (Burdett et al., 1983; Koch et al., 2004) and its microorganisms flourish in the environment by developing plant-soil interactions and regulating nutrient cycling, gas exchange and transformation of aqueous solutes (Bohlen et al., 2001; Mooney et al., 1987).

Site preparation can help to correct site problems. For example, Mason (2004) reported that plant height growth was directly related to soil cultivation and fertilisation. Moreover, forest floor heterogeneity regulates plantation establishment and growth and can be a consideration during forest management decision making (Bartels & Chen, 2009; Nambiar, 1996).

Another component that directly regulates site condition, and also influences the soil, is climate. Parton et al. (1987) reported climatic effects on soil properties. Soil gas exchange and water potential are influenced by climate, particularly associated air temperature, wind, and

precipitation (Mooney et al., 1987). Ralston (1964) considered these as meteorological variables. The effects produced by meteorological variables can vary on a small scale in ways that directly affect forest productivity.

1.3.1 Site productivity

Variation in site capability to produce high yields has been a subject of continuous interest. Some sites support luxuriant forest, while others are capable of supporting only poor forest, and this is related to the site productivity (Czerepko, 2008). Forests proceed through a faster development sequence on highly productive sites (Franklin et al., 2002) and toward a more complex structure (Larson et al., 2008). The terms “site quality” and “site productivity” are often interchangeable, though they are not synonymous. Site quality is a descriptive measure of site determined by subjective methods, often by visual assessment into a relative classification, whereas site productivity is a general term for the potential of certain species on the site to produce over time (Ford Robertson, 1971; Vanclay, 1992). To be specific, site quality is a qualitative measure, whereas site productivity is a quantitative estimate. Moreover, site productivity is more the potential of a particular forest stand or site to produce aboveground wood volume (Skovsgaard & Vanclay, 2008).

Generally, above-ground volume production is calculated as stem wood volume for conifers, and sometimes it includes branch volume for broadleaved tree species (Vanclay, 1994). In this context site productivity is often quantified as an index, typically site class or site index. Such indices are defined in different ways (Bravo & Montero, 2001). Most universally used site indices are based on the stand height of the dominant trees at a given age (Kimberley et al., 2005; Louw & Scholes, 2002; Skovsgaard & Vanclay, 2013; Tesch, 1980) Indices also reflect site quality as the site potential to volume growth is related to site productivity. Moreover, productivity

depends on both natural factors inherent to the site and on management regimes. However, in a managed site, it is influenced greatly by the climatic and edaphic factors, as well as forest management (Skovsgaard & Vanclay, 2008; Skovsgaard & Vanclay, 2013).

In a broader context, the use of stand height as an indicator of site productivity is based on the general belief that, in an even-aged stand, the height growth of the largest trees is roughly independent of stocking (Perry, 1985; Voelker et al., 2008). Moreover, all the biological and environmental variables that have influenced growth are considered as integrated into the indices, rather than examined for their explicit effects (Assmann, 1970; Ralston, 1964). This is because height, as a variable that can be obtained easily and correlates with a number of productivity measures (Skovsgaard & Vanclay, 2013). In addition, it is easy and inexpensive to measure and is less affected by management practices than stem diameter. However, this could only happen with sites where there are good management records. This implies that site productivity can be classified based on height growth, but there is a lot of remaining complexity especially in a site with different and heterogeneous information (Vanclay, 1992; Vanclay & Henry, 1988). Thus, the evaluation of forest site productivity involves problems of isolating biological and environmental variables and their quantitative effects on growth. However, researchers have incorporated additional inputs to make a more precise classification of site productivity (e.g., Site index, 300 index), which could evaluate site productivity on a more specific scale (e.g., Battaglia & Sands, 1997; Kimberley et al., 2005; Louw & Scholes, 2002; Woollons et al., 1997).

1.3.2 Micro-site variation in plantation forestry

Forests, as long term and dynamic natural resources, can be organised on different scales (Wiens, 1989). In most cases, forest models are simplified. The general assumption about the natural site conditions and site productivity that they change gradually and predictably. For this

reason, uni-dimensional productivity indicators such as the commonly used site index are employed (Vanclay, 1992). Besides this, traditionally, forest scientists and ecologists are more focused on large-scale variation. This is because the costs involved in quantifying variation at micro-scales are large, and so researchers have avoided it by sampling to capture the “mean” value for a site or plot. Recently, small scale variation that occurred at the level of single trees or small patches has been discovered (Coates, 2002; Kuuluvainen, 2002). In addition, small scale variation has particular roles in forest productivity (Kuuluvainen & Juntunen, 1998). However, in natural forest, various disturbances and practises within sites create diversity, which is much more complex and dynamic and has been explored in a rigorous way (Martín-Alcón et al., 2015; Peterson & Pickett, 1990; Runkle, 1981; Runkle & Yetter, 1987). For example, gap phase dynamics (Narukawa & Yamamoto, 2001; Yamamoto, 2000) and gap models (Bugmann, 2001) are used to study those complex micro-site characteristics for old growth forest. Lilja-Rothsten et al. (2008) defined micro-site as local features of the forest floor that characterise a seedling’s growing environment, such as substrate type, e.g. dead wood at various stages of decay or exposed mineral soil, or locations with a microclimate that differs from that of the surroundings, e.g. under a fallen tree.

Compared to natural forest stands, micro-site variation often decreases in managed forest stands (Kuuluvainen & Laiho, 2004). The decreased variation is not only due to different types of silvicultural treatments but also to site preparation which makes the site homogenously productive (Mason, 2004). However, in the case of individual tree growth in monocultures, micro-site variation is a comparatively new and emerging discipline, especially with the introduction of the new geographic information system and remote sensing technology. Most often juvenile plantations are studied to quantify the role of the micro-sites (Kohama et al., 2006) as mature

plantations can modify their site with time (Maclaren, 1996). Therefore, micro-sites influence juvenile and mature plantations in different ways.

1.3.3 Documented factors of micro-site variation and their role

The study of microsite in plantation forestry has only recently advanced, and there are several reports from those who have tried to understand sources of variation on different scales. Much of the research undertaken in recent experimental trials established in different ecosystems were focused on within stand or micro-site variation sources (Table 1.1). Specific studies have shown significant effects of micro-site variation. First of all, variation is divided into two broad classes: spatial and temporal. Here spatial variations mainly cover the topographic and associated edaphic factors, whereas temporal variation mainly represents seasonal and related climatic variables that can also vary from year to year.

Interestingly, to identify sources of variation, different indicators are used. Specific leaf area (SLA) and leaf area index (LAI) are important ecophysiological indicators used as a representative to quantify the sources (Nippert & Marshall, 2003; Nouvellon et al., 2010; Weiskittel et al., 2008). Besides this, canopy structure (Kohama et al., 2006), net primary productivity (NPP) (Fontes et al., 2006), mean annual increment (MAI) (Battaglia & Sands, 1997), and needle length for conifers (Morgan et al., 1983) are also used to measure the effects of spatial and temporal micro-site variation.

From the above indicators, it is established by Monteith and Moss (1977) that light levels have a profound influence over plant growth. As a whole, light is found to be the most vital factor for both the spatial and temporal classes mentioned above. It is also true that all the other factors usually considered in studies of forest productivity somehow contribute to light /radiation use by trees.

The proportion of incoming light that is actively used is called radiation use efficiency (RUE) (Sinclair & Muchow, 1999). Nagel and O'Hara (2001) found a strong relationship between stand basal area and light interception. Moreover, it is reported that productivity is often correlated with precipitation along with temperature and day length (Binkley et al., 2013) or mode of light interception (António et al., 2007; Millner & Kemp, 2012). However, light use efficiency or radiation use efficiency (LUE/RUE) is also dependent on plant functional traits, such as leaf trait and age (Bond et al., 1999; Nippert & Marshall, 2003). Furthermore, light availability is highly varied by spatial heterogeneity (Nicotra et al., 1999). For example land sloped to face different aspects intercept different amounts of light.

Soil properties can also vary greatly within a plant community and result in spatial heterogeneity (Robertson et al., 1988). It is well known that soil properties vary widely with topographic gradients (Bathgate et al., 1993; Brubaker et al., 1994; Garten et al., 1994) and meteorological variables. Besides the effects induced by direct topographic and soil properties, soil chemical properties have significant effects on RUE (Bellingham & Tanner, 2000; Heaphy et al., 2014). Again, there are effects of light on stand development and growth beyond those limitations (Montgomery & Chazdon, 2002).

On the other hand, temporal variation represents seasonal variation, specifically differences in a variety of climatic factors, such as precipitation, temperature and solar radiation. Those factors are found to be most important, not only for the individual trees but also for the site as a vital modulator (Ralston, 1964).

Table 1.1 Summary of documented cases of micro-site variation with different measurement indicators and ecosystems.

Species	Environmental constraints	Scale	Zone	Indicator	References
<i>Pseudotsuga menziesii</i>	Aspect, Soil water limitation	Within Site	Distinct dry summer and cool, wet winter.	Specific leaf area (SLA)	Weiskittel et al. (2008)
Hybrid spruce	Aspect, Soil water limitation	Within Site	Moist-cold subzone of the interior Cedar hemlock biogeoclimatic zone	Specific leaf area (SLA)	Weiskittel et al. (2008)
<i>Pinus ponderosa</i>	Aspect, Soil water limitation	Within Site	Continental climate with long, cold winters and warm, dry summers.	Specific leaf area (SLA)	Weiskittel et al. (2008)
Clonal <i>Eucalyptus spp.</i>	Seasonal variation, Soil water limitation	Within Site	African savannah	Specific leaf area (SLA)	Nouvellon et al. (2010)
<i>Eucalyptus globulus</i>	Stocking density, Soil physical properties	Within & Between Site	Maritime Mediterranean climatic zone	Net primary productivity (NPP)	Fontes et al. (2006)
<i>Eucalyptus globulus</i>	Temperature, Soil water availability, Solar radiation	Within & Between site	Tasmanian and Western Australian climatic zone	Mean annual increment (MAI)	Battaglia and Sands (1997)
<i>Abies balsamea</i>	Spacing	Within site	-	Needle length	Morgan et al. (1983)

<i>Pseudotsuga menziesii</i> & <i>Abies grandis</i>	Seasonal variation	Within site	Interior North-west USA	Specific leaf area (SLA)	Nippert and Marshall (2003)
<i>Pinus halepensis</i>	Seasonal variation, Topographic variables (Slope inclination, Aspect, Compound topographic index, Flow accumulation) & Stock quality	Within & Between site	Maritime to Continental Mediterranean	Survival and Growth (DBH & Height)	Navarro-Cerrillo et al. (2014)
<i>Cryptomeria japonica</i>	Light, Site slope	Within site	Japanese mountainous region	Tree size and growth (DBH & Height)	Kohama et al. (2006)
<i>Pinus thunbergii</i>	Soil properties (Thickness and texture) and topography of the site (Slope and undulation)	Within site	Shiga Prefecture, Japan	Tree growth (DBH, Height and volume)	Enoki et al. (1996)

However, plant survival and growth are complex processes, and are highly context-dependent and species-specific (Holzwarth et al., 2013). An important role is played by the stock quality and spacing as there is ultimately competition for seedling survival and growth once trees are large enough to influence one another. The trees in any young plantation are involved in both interspecific and intraspecific competition (Brand, 1986; Fontes et al., 2006) and the former is reported to happen most likely at the juvenile stage of the plant (Liu & Burkhardt, 1994).

1.3.5 Importance of being subtle

Site productivity, which is important for sustainable forest management, is established on a stand height centred hypothesis (Skovsgaard & Vanclay, 2013). In the case of forest growth modelling, in particular, it is considered to be one of the basic variables. However, in the modern era with many latest experiments and instruments (i.e., GIS & remote sensing facilities) in forest science, the idea needs to be revisited. It is already noted that for several species and site types, site index and volume growth are poorly correlated (Grey, 1983; McMurtrie et al., 1990; Watt et al., 2010). In addition, site productivity depends rather on natural factors inherent to the site and on management related factors.

The studies mentioned above provide clear evidence of the utility of incorporating micro-site variables into forest growth and yield modelling that includes objectives beyond maximum sustained yield. However, it becomes increasingly apparent that tree and stand level responses can vary considerably within and between sites at different intensities. Therefore, interpretations concerning short and long term effects must be made cautiously and by avoiding generalisations.

Another important issue is the introduction of managed relocation under a global change umbrella (see, Sax et al., 2009; Vitt et al., 2010). Minter and Collins (2010) defined managed relocation as a “conservation strategy involving the translocation of species to novel ecosystems

in anticipation of range shifts forced by climate change”. However, until now it is a debatable issue among scientists and conservationists and needs to be more precise in order to make decisions. Moreover, forestry is moving towards a system called “precision science” (Dyck, 2003), where the elements can be optimised in a more nuanced sense. So, a major challenge for forest managers and scientists is to understand stand structure and behaviour and to develop a more efficient system or tool to manage it. To cover all these aspects, it is important to be imaginative as well as to look through a more complex, subtle lens.

1.4 Forest growth and yield modelling

According to Vanclay (1994, p. 4), “a model is an abstraction or a simplified representation of some aspect of reality”. It can be both quantitative and conceptual, but all models are integrators of multiple fields of knowledge. Consequently, models generally have several important and varied uses (Vanclay, 2006; Weiskittel et al., 2011). Interestingly, from the beginning of mankind we have frequently used models unconsciously: we try to predict the future, and this also happens in the case of forest growth and yield. As forests are long-lived dynamic biological systems that are continuously changing (Peng, 2000), we always try to predict and assume their future growth in terms of a given specific unit. Growth is the dimensional change over time of one or more individuals in a stand (Vanclay, 1994). In that sense, forest growth and yield models are abstractions of the natural dynamics of trees, stands and whole forests, and may encompass growth, mortality and any other changes that happen in stand structure and composition (Burkhardt & Brooks, 1990; Vanclay, 1994; Weizhong Zhao, 1999). Again, an ideal model would be one with which, given any stand, forecasts of some trait may be made with a high degree of precision for a given time horizon Curtis (1972).

Growth and yield modelling in forestry is a long-established approach to predict the future to make decisions (Weiskittel et al., 2011). It started with experience-based methods in the 1700s (Kimmins et al., 2008), followed by graphical methods in the 1850s in Central Europe (Assmann, 1970). Such experience-based tools are excellent for single values (e.g., timber) but they assume highly generalized future circumstances (e.g., climate, soil characteristics, operation etc.) by keeping them unchanged. They are unable to predict multiple values and are unreliable in cases of significant change in circumstances. Yield tables are based on complete observations of yield throughout entire rotations and were constructed for important tree species (Vuokila, 1965). In contrast, American yield tables were based on guide curve assumptions (Monserud, 1984; Spurr, 1951). Despite this early demonstration, the breadth and complexity of modelling efforts increased with advances in information technology. During recent decades, along with advances in mathematical statistics and rapidly developed computer technology, growth and yield modelling technology, and methodology moved forward significantly (Garcia, 1988; Johnsen et al., 2001; Kimmins et al., 2008; Peng, 2000). Functions used to describe growth and yield are compatible in that growth is a derivative of yield. Clutter (1963) was among the first to describe growth and yield systems in terms of difference equations, where future yield is expressed as a function of existing yield and the interval in time between the two observations. Moreover, growth and yield modelling started to proceed in a multi-dimensional way by focusing on several other basic ecological perspectives such as gap dynamics model to forecast the future of the uneven-aged forest (Bugmann, 2001). The dependent variables were changed on different scales from whole stands to individual trees, and the objectives extended from stand yield prediction to ecological process description.

1.4.1 Classification of growth and yield models

Development of forest growth and yield models involves a cyclic procedure of data preparation, model construction, model validation, model implementation, and model recalibration with a refreshed database (Vanclay & Skovsgaard, 1997). In addition, model uses vary among users. Forest managers use models for management planning and decision making, whereas forest scientists use them for understanding underlying biological processes (e.g., carbon sequestration, photosynthesis mechanism). So, models can be classified in many ways by focusing on end use. Traditionally, they can be classified in two ways: 1) scale of focus, which means areal unit at which the model functions (e.g., individual or stand-level); and 2) approach of development, or the underlying mechanism of development (e.g., mensurational or ecophysiological) (Munro, 1974).

1.4.1.1 Forest models based on the level of focus

Munro (1974), and then Burkhart and Brooks (1990), classified whole stand models into two major groups, depending on their level of focus. They are as follows: 1) stand-level models and 2) individual tree models.

Stand-level models use stand variables such as basal area, volume, stocking, and variables characterising the underlying diameter distribution to simulate stand growth and yield. They can be further classified into growth and yield equations and size-class (diameter) distribution categories (Avery & Burkhart, 2015; Vanclay, 1994). Most stand-level models are usually simple and robust and require relatively little data to simulate stand growth and development. However, they provide little or no information on individual trees within stands. They can be useful for modelling plantations, but not for more complex features or variables (Fox et al., 2001; Vanclay,

1994). Size-class models provide some information relating to stand structure and are widely used in uneven-aged stands to project stand tables (Ek, 1974).

On the other hand, individual tree models use individual trees as the basic units to model growth of tree diameters (or basal area), heights, mortality, and possibly crown characteristics (Weizhong Zhao, 1999). They require detailed inputs and provide detailed outputs. They also, provide a useful alternative to whole stand models for irregular size-class distributions. Most individual tree models describe the increment of diameter or basal area and a few models predict diameter and height, based on differential equations (Monserud & Sterba, 1996). Individual tree models can be further subdivided into distance dependent and independent, based on spatial location of the trees. A distance-dependent individual-tree model requires measurements not only of tree size but also of tree location (Daniels & Burkhart, 1988; Tennent, 1982). Distance-independent individual tree models require no spatial data about neighbours (Clutter & Allison, 1974; Clutter & Jones Jr, 1980). Table 1.2 shows a simple comparison of these model types.

Table 1.2 Summary of characteristics of two growth and yield models depend on the level of focus.

Indicators	Whole stand model	Individual tree model
<i>Dependency</i>	Stand parameters	Both stand and tree parameters
<i>Complexity</i>	Relatively simple, low dimensionality	Relatively simple, low dimensionality
<i>Drivers</i>	Generally driven by stand density, age and site productivity	Tree component based on tree dimension and stand parameters
<i>Resolution</i>	Stand-level	Tree-level
<i>Level</i>	Holistic	Reductionist

1.4.1.2 Forest models based on the approach of development

A forest is a complex system and is hard to sketch through a single approach. So, the right approach depends on the objectives of end users, that identify the purpose at the practical level (Fontes et al., 2010). There are mostly two types of models, each based on their approach to modelling: mensurational and ecophysiological (Kimmins, 1990; Mohren & Burkhardt, 1994; Vanclay, 1994). Most forest models have been developed using elements of both approaches. From this point of view, models vary across a wide-ranging and complex spectrum. Therefore, forest models can be categorised principally by the degree to which each approach has been emphasised in their development (Korzukhin et al., 1996).

Mensurational models are derived from large amounts of field data, and describe growth rate as a regression function of variables such as site index, age, tree density and basal area (Clutter, 1963). Mensurational models have often been criticised as being too simplistic and unrealistic, but the major strength of the mensurational approach is in describing the best relationship between the measured data and the growth determining variables using specified mathematical function or curves (Fox et al., 2001). In implementation, mensurational models require only simple inputs and are easily constructed. They are also easily integrated into diversified management analyses and silvicultural treatments and can achieve greater efficiency and accuracy in providing quantitative information for forest management (Burkhardt & Tomé, 2012). They may be a suitable method for predicting short-term yield for time scales but cannot be used to analyse the consequences of climatic changes or environmental stress (Kimmins, 1990; Seynave et al., 2008; Shugart et al., 1992).

Unlike mensurational models, ecophysiological models are developed using knowledge gained empirically to describe underlying processes associated with growth, for example,

photosynthesis, respiration, carbon allocation and nutrient cycling. Ecophysiological modelling is defined as a procedure by which the system is analysed with a set of functional components and their interactions with each other and their system environment, through mechanistic processes occurring over time (Bossel, 2013; Mäkelä, 2003; Monserud, 2003). Actually, such a model is a framework for testing and generating alternative hypotheses and has potential to help accurately evaluate processes in the system (Blake et al., 1990). The application of ecophysiological modelling is reviewed in detail by Battaglia and Sands (1998). The questions being asked in forest management have changed, and the potential applications of the process have increased. Despite their benefits and applications, ecophysiological models need to be at least as precise and unbiased as mensurational models in order to be considered in the field of forestry (Peng, 2000).

In essence, the weaknesses and strengths are reciprocal in mensurational versus ecophysiological models. It is almost always possible to find a mensurational model that provides a better fit for a given set of data, chiefly due to the constraints imposed by the assumptions of ecophysiological models (Battaglia & Sands, 1998; Mäkelä et al., 2000; Peng, 2000; Peng et al., 2002a). The greater model complexity of ecophysiological models arising from the use of many submodels and prediction of growth over short time increments can cause recursion and compounding of errors (Pinjuv, 2006). However, mensurational growth and yield models tend to be too site-specific and lack the ability to make predictions under changing future environmental conditions (Woollons et al., 1997). Table 1.3 briefly presents the characteristic comparison of the mensurational and ecophysiological models.

Table 1.3 Comparison of major features of growth and yield models (mensurational versus ecophysiological) (Peng, 2000).

Indicators	Mensurational models	Ecophysiological models
<i>End users</i>	Foresters and forest managers	Researchers
<i>Research</i>	Intermediate	High
<i>Complexity</i>	Low to high	High
<i>Flexibility</i>	Intermediate	Low
<i>Model parameters</i>	Few to many	Many
<i>Environmental measured factors (general)</i>	Site index, site characteristics	Climatic, edaphic and disturbance

1.4.2 Hybrid models: a way to deal with complexity

Ecophysiological models could be important tools to support decisions in forest management, although detailed ecophysiological models are often data-intensive and difficult to apply for management related applications (Blanco et al., 2005; Grant et al., 2005). The inflexibility of experience-based predictive models can be addressed by combining both causal and mensurational elements of the same model in a hierarchical procedure: more specifically, incorporating the key elements of both mensurational and ecophysiological approaches into a model that could give insight into the underlying mechanism as well as give predictions for both short and long term (Peng et al., 2002a). More precisely, hybrid models are a mix of ecophysiological and mensurational principles in models which can avoid the shortcomings of both approaches (Kimmins, 1990; Mäkelä et al., 2000; Peng, 2000; Weiskittel et al., 2011).

Hybrid models have been further broken down into two basic types: simplified mechanistic models, and classical growth and yield models with mechanistic terms. The first type can make projections at a stand level and may use empirical methods as sub-models, but the main model

format is mechanistic in nature. The second type of hybrid model uses classical growth and yield methods with the addition of mechanistic predictor variables (Pinjuv, 2006). The basic idea behind all of these methods is that some of the parameters can be determined exactly on the basis of a priori information; others can be given intervals of likely variation, and some cannot be determined at all on the basis of current knowledge (Mäkelä et al., 2000). In other words, they combine one's understanding of the ecophysiology of growth and allocation with the output of a mensurational model and certain other data that are generally available. This approach greatly reduces the calibration requirement for the different ecosystems (Kimmins et al., 1996; Mäkelä et al., 2000).

The quality of predictions of these models would also be statistically testable via residual analysis to ascertain the quality of their predictions. Woollons et al. (1997) have included driving variables of mechanistic models such as mean temperature, solar radiation, rainfall, and soil type into a classical growth and yield modelling system, and have shown an improvement in predictions of basal area/ha over strict growth and yield curves. Snowdon et al. (1999) incorporated indices of annual climatic variation and photosynthesis into a growth model for *Pinus radiata*, and they found a significant improvement in short term predictions. They used predicted photosynthesis rates from a ecophysiological model at a single site in the forest estate as an index for growth that was added to a Schumacher growth curve, while Mason et al. (2011) replaced the time in traditional differential equations with potentially useable light sums (PULS) and found an improved fit to independent permanent plot data for basal area per ha. Moreover, Mason (2013) showed that hybrid modelling can provide useful rotation length estimates of gain from short-term site preparation treatments. The hybrid modelling approach essentially prevents the past patterns and frequencies from re-occurring in the future during stand development if the key elements and their interactions are changed. However, in agreement with "Occam's razor" (Blumer et al., 1987), it is

decided that those elements which are logically expected to change should be included in a hybrid model (Kimmins et al., 2008). It also brings on board the different processes that should be included, or, the level of complexity with which a model needs to deal.

1.4.3 Hybridisation strategies

Hybrid models are formulations that mix different approaches for achieving specific prediction and analysis goals. Hybridisation between mensurational and ecophysiological models is similarly varied as a methodology for estimating forest growth.

The investigation of hybridisation strategies to use the best features of each approach and satisfy modelling objectives has led to a large number of models. In general, a hybrid ecophysiological, mensurational model can represent one or a mix of the following categories:

- i. A structural hybrid approach, representing a mix of both approaches from the conception of the internal structure. In an increasing grade of resolution, there can be either improved mensurational equations or simplified physiological relationships.
- ii. An aggregative approach, where the output of one kind of model is the input for the other, either by using modules or entire models to form one complex structure.

1.4.3.1 Augmented hybridisation approach

The augmented modelling approach was the first step towards hybridisation. Thus, much work has been done to improve mensurational equations by adding environmental factors, and hence a range of strategies has been explored. In this approach, normally physiological indices are integrated with the appropriate mensurational equation to test the gain.

Woollons et al. (1997) tested the augmented effect of climatic and soil variables on quality of predictions of mean top height and basal area of *Pinus radiata*, and they found that they partially improved the predictions. Snowdon et al. (1999) studied the inclusion of several climatic indices

from two physiological models into various forms of Schumacher's equation among which annual growth index was the most effective one. There are several examples of this approach (e.g. Henning & Burk, 2004; Mason, 2001; Pinjuv et al., 2006; Snowdon, 2002).

1.4.3.2 Potentially useable radiation sums approach

Radiant energy is the key driver of photosynthesis and hence the main responsible growth factor. But only specific bands of radiation (~ 400-700nm) are actively involved in photosynthesis, named "photosynthetically active radiation (PAR)", and only the fraction that falls directly on leaf surfaces is potentially available for photosynthesis (absorbed photosynthetically active radiation or APAR). Nonetheless, the use of the radiant resource depends on the availability of other necessary resources. Following this concept, net primary production (NPP) is defined by Landsberg and Waring (1997) (Equation 1),

$$NPP = \varepsilon \sum APAR t_{min}\{f_{\theta}f_d f_k\}f_r f_{Fr} f_s \quad (1)$$

where NPP = net primary productivity; ε = maximum quantum efficiency; APAR = absorbed photosynthetically active radiation; f_{θ} = soil water modifier; f_d = vapour pressure deficit modifier; t_{min} = minimum average monthly temperature; f_k = temperature modifier; f_F = fertility modifier; f_s = senescence modifier; and f_{Fr} = frost modifier.

Mason et al. (2007) substituted radiation sum since the time of planting for time in a non-linear equation, but with radiation modified by adaptations of the physiological modifiers developed for the 3-PG model (Landsberg et al., 2001). This way, the errors related to the estimation and also accumulated errors from recursion were avoided (Mason et al., 2011). The potentially useable light term to be substituted for time is as follows (Equation 2):

$$RT = \sum R t_{min}\{f_{\theta}f_d\}f_k f_{Cl} \quad (2)$$

where RT = potentially useable light sum; R_t = radiation in month; t_{min} =minimum average monthly temperature; f_{θ} = soil water modifier; f_d = vapour pressure deficit modifier; f_k = temperature modifier; and f_{Cl} = light competition modifier and summation in months.

This approach was first tested by Mason et al. (2007) for *Pseudotsuga menziesii* and later for *Pinus radiata* (Mason et al., 2011). Results obtained showed consistent improvements in precision and flexibility comparing modified equations with traditional time-based equations for basal area (G), but not for mean top height (MTH).

1.4.4 Modelling juvenile growth and yield

Most models are designed for established trees from slightly before the beginning of the stem exclusion phase (Spiecker et al., 1996) when different tending operations are made, and harvest age is decided. However, some decisions need to be made earlier in the life of the stand.

Growth at the juvenile stage of a plantation is important as well as sensitive to the environment and establishment procedure (Rauscher et al., 1990). The main aim of plantation establishment is to maximise growth response, and for that, it needs to identify the main factors and predict responses of trees to different sites (Mátyás et al., 2009; Weizhong Zhao, 1999). In this context, modelling juvenile growth is important for better understanding the whole process of stand development and for helping to improve a young stand. Though in terms of modelling, juvenile growth is less highlighted over time (Zhang et al., 1996). Moreover, juvenile growth is often more complex than the growth of mature stands as both inter and intra-specific competition occurs among the trees. Individual-tree models often focus on increment of height and diameter or increment of basal area (Nyström & Kexi, 1997; Zhang et al., 1996). Modelling for juvenile growth demands a choice between diameter or sectional area at ground level, and diameter at breast height (DBH) or basal area, or both. To provide compatibility with older growth models, DBH or basal

area is needed. Usually, no suitable individual tree volume equation is available for such young trees. Tree form has rarely been modelled due to the lack of availability of necessary measurements. Yield-age equations have been employed by most modellers (Belli & Ek, 1988; Mason, 1992; Mason et al., 1996) to reflect the growth response fully for different operations and site conditions from time of planting.

Juvenile growth and yield can be explained as a function of site and climatic variables. Zhao (1999) reported juvenile yield as a function of conditions of sites, status of seedlings, treatments and competition forces from various weeds, and trees themselves due to the crown being closer. Seedling quality can be described physically and morphologically, while it can be altered by several factors (e.g., genetics, nursery techniques) (Mason, 2001). Hunter and Gibson (1984) reported that climatic and edaphic factors modified site quality. In addition, the microenvironmental effect needs to be taken into account as it is changed in plantations by site preparation (Amateis et al., 1997; Mason, 2004) and further changes with time after planting (Maclaren, 1996). This is expected to play an essential role for further understanding the decision-making process.

Some equation forms for early growth and yield of tree height, diameter, and survival have been proposed and used (e.g. Bullock & Burkhart, 2005; Mason & Whyte, 1997; Mason et al., 1997; Richardson et al., 2006). The relationship issue between juvenile and older growth models has arisen since juvenile growth models have been formulated. But juvenile growth in relation to micro-site variables is yet to be modelled as previous studies concentrated on yield at a stand level.

1.5 New Zealand dry land forest initiative (NZDFI) and two species of interest

In New Zealand, forest industries are mostly based on plantation forestry, and interestingly they utilise exotic species to produce major forest products (Maclaren, 2005; Millner, 2006). This

sector is heavily dependent on *Pinus radiata* with a minor proportion of *Pseudotsuga menziesii* (Maclaren, 1993). These species display several notable features, but they are not suited to some severe conditions, for example, increasingly dry conditions, and their end uses are limited by their wood properties (Apiolaza et al., 2011). Therefore, it is important to move to a more diverse practice by introducing new species for tackling future challenges.

New Zealand plantation forests are established and extended on land less valued for pastoral agriculture (Millner, 2006), most of which are situated on the hilly parts of the country. The characteristic features of hill country are heterogeneity and a mosaic of microsites resulting from several climatic and edaphic factors, such as aspect, slope gradient, and soil variation (see, Gillingham & During, 1973; Lambert & Roberts, 1976, 1978; Radcliffe & Lefever, 1981). Moreover, the dry parts of these areas are very heterogeneous. Apiolaza et al. (2011) characterised the dryland areas of New Zealand as areas receiving rainfall of 500-1000 mm/year, which covers a large part of the country. Dryland covers a significant portion of the earth's ecosystems (Schimel, 2010), yet global literature has ignored this by focusing on more productive ecosystems. Generally, this area is used for farming, but alternatives are needed.

The trends of managing plantation forest in New Zealand are similar to other countries, which produce both long and short term forest products. However, good forest management requires accurate information on the current growing stock and future growth potential (Peng, 2000). This is normally obtained through several stands alone or mixed approaches, including forest inventories and projections through growth and yield modelling. Early growth models or juvenile growth models make available the opportunity for the forest managers to access the right information and understand the impacts of site variables (Pretzsch, 2009). Thus, they can adapt the right approaches beforehand efficiently and effectively. So, managers should have the best set

of information before deciding on crop establishment so that all potential benefits can accrue (Mason, 1992).

Eucalyptus species play only a minor role in New Zealand forestry, as they have failed to achieve the critical mass to be economically viable (Apiolaza et al., 2011). Normally, they are intolerant to environmental conditions to which they are not adapted (Barr, 1996; Johnson & Wilcox, 1989), but Barr (1996) reported that several species of this genus have the potential to be introduced in unusual conditions in New Zealand. Some of the species of *Eucalyptus* produce wood of hard, strong and naturally durable quality, while the others produce decorative wood (Menzies, 1995).

The New Zealand Dryland Forest Initiative (NZDFI) begun in 2008 aiming to provide and advocate sustainable and commercially oriented alternative species to New Zealand forest industries. The main aims of this project are to breed and improve drought tolerant and ground durable *Eucalyptus* species which do not require chemical treatment (Van Ballekom & Millen, 2017). Since the beginning of the NZDFI, the coast grey box (*Eucalyptus bosistoana*) and white stringybark (*Eucalyptus globoidea*) were considered two promising species among several that have been tested (Millen, 2006).

Eucalyptus bosistoana is commonly known as coast grey box (or Gippsland grey box) and is the largest of the box group of *Eucalyptus*. It is commonly 30-40m in height and up to one meter in diameter at breast height (DBH), while some trees attain 60m in height (Williams & Woinarski, 1997). The tree occurs naturally within the latitudinal range of 33-37.5°S at elevations between sea level and 500 m. The distribution of *E. bosistoana* is confined to mixed coastal forests along the South East coast of Australia (Boland et al., 2006). The preferable climatic condition is warm humid to sub-humid, with the mean maximum temperature of the hottest month range 24-29°C

and the mean minimum of the coldest month around 1-6°C. It can grow in deep soil, with moderate salinity. Moreover, it can resist a few frosty occurrences as well as waterlogged and somewhat dry conditions. In addition, it shows a marked preference for good soil quality (FAO, 2015). The wood of *E. bosistoana* is used for heavy engineering construction, poles, cross-arms, railway sleepers and fences (Bootle, 1983). It is very tough and durable, and because individual trees can grow tall and straight, this species has been sought after for milling into poles and for uses such as heavy construction (Boland et al., 2006). Its green wood has 103 MPa modulus of rupture, 17GPa modulus of elasticity, hardness of 1180kN and basic density of 880kg/m³. Overall the wood is considered a highly durable timber (class 1 and 2 Australian standards, AS5606-2005) (Nicholas & Millen, 2012a).

Eucalyptus globoidea, commonly known as white stringybark, attains 25-30m in height and 1 m DBH, with straight trunks which may be up to two-thirds of the tree height. The crowns are usually compact and moderately dense (Boland et al., 2006). It is a common tree in central and southern coastal New South Wales, on the edges of the tablelands adjacent to the coastal areas in central and lower northern parts of the state, and also in eastern Victoria. The species is distributed from latitude 30-38°S and from near sea level to about 1100m in altitude. The suitable climatic range is warm sub-humid to humid with the mean maximum temperature of the hottest month in the range of 22-31°C, and the mean annual rainfall of about 650-1400mm with relatively even distribution (Boland et al., 2006). This species can grow on various topographical sites from gently undulating country and hills near the coast to mountain slopes at the junction of the tablelands and the coastal areas. Soils are commonly sandy, but the species also occurs on gravelly loams and clays and on skeletal soils. It can grow in less productive sites (Bullock, 1991), but not on sites with poor drainage capacity (Barr, 1980). The timber of *E. globoidea* is used for building

framework (Bootle, 1983). The sapwood is resistant to *Lyctus* borers; the heartwood is light brown, occasionally light pink, moderately fine textured, and generally straight-grained; density is about 900 kg/m³. In Australian standards (AS5606-2005) it is considered as a highly durable timber class 1 or 2 (Nicholas & Millen, 2012b).

1.6 Objectives and thesis structure

The main objectives of this study are (i) to explore the edaphic, topographic and climatic factors that influence the growth dynamics of juvenile *Eucalyptus* plantations by considering within and between site variability, and (ii) to develop a preliminary field applicable mensuration growth and yield model for *E. globoidea* from the available data. Furthermore, this study aims to explore different modelling strategies to enhance the understanding of the overall processes. The assessment of these objectives has required different approaches and tools, from field inventory, geographic information system (GIS) based topographic characterisation.

The thesis has been structured in chapters, written in the format of scientific articles. It consists of an overall introduction, six research chapters, and a general discussion and conclusion. Different ideas and topics touched by this thesis were briefly discussed under introduction, associated literature and justification of the study were presented with each research chapter. An overall organisation of the research chapters is presented by Figure 1.2. In the first research chapter (Chapter 2) three different non-geostatistical interpolation methods are tested to optimise the digital elevation model (DEM) from GNSS (RTK-GPS) acquired data. The DEM is used in subsequent modelling chapters.

The next chapter (Chapter 3) focuses on the within-site variables in relation to juvenile tree height and survival. The main aims of this chapter are to find out the most important variables that influence juvenile tree height and survival and model them by applying an augmented time-based

approach. Within-site topographical attributes, temperature and soil rooting depth are tested from three different sites for *E. globoidea* and *E. bosistoana*.

In Chapter 4, between sites variables (soil, climatic and topographic variables) are identified and modelled for height growth and survival by applying the same procedure described in Chapter 3. Chapter 5 explores and develops the modelling by applying a Potentially Useable Light Sum Equations (PULSE) approach and augmented PULSE approach. For these studies, a set of 84 permanent sample plots (PSPs) are used from the NZDFI PSP network, which were located in 25 different sites in New Zealand. Chapter 6 presents a comparative study on different approaches of juvenile tree height growth and survival model based on the results presented in Chapter 4 and 5.

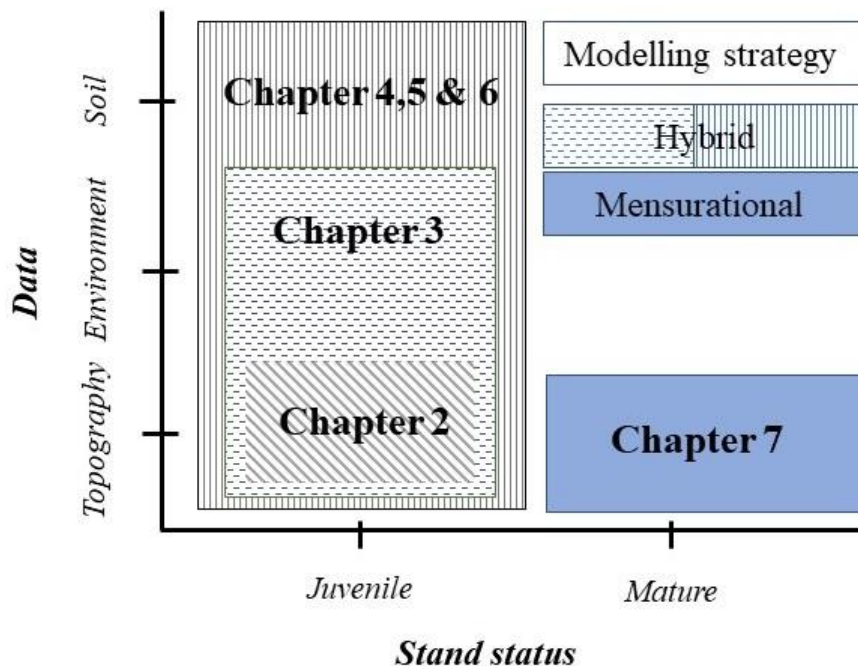


Figure 1.2 General organisation of the research chapters in the thesis based on the data, stand status and different modelling strategies.

The juvenile height growth and survival models are useful for plantation establishment, whereas the mature stand models are useful for the later stage of the plantation. The mature stand models can help to project future growth and plan the silvicultural regime. Chapter 7 presents a set of mature stand preliminary growth and yield models for *E. globoidea* in New Zealand. The main aim of this chapter is to build a field compatible mature stand growth and yield model from the available data.

Finally, Chapter 8 presents a general discussion of the key findings of the thesis and an overall conclusion.

1.7 References

- Amateis, R. L., Burkhart, H. E., & Liu, J. (1997). Modelling survival in juvenile and mature loblolly pine plantations. *Forest Ecology and Management*, 90(1), 51-58. doi:http://dx.doi.org/10.1016/S0378-1127(96)03833-9
- Angelsen, A., & Wunder, S. (2003). *Exploring the forest-poverty link: key concepts, issues and research implications*. Retrieved from
- António, N., Tomé, M., Tomé, J., Soares, P., & Fontes, L. (2007). Effect of tree, stand, and site variables on the allometry of *Eucalyptus globulus* tree biomass. *Canadian Journal of Forest Research*, 37(5), 895-906. doi:10.1139/X06-276
- Apiolaza, L., Mcconnochie, R., & Millen, P. (2011). *Introducing Durable Species to New Zealand Drylands: Genetics of Early Adaptation of Eucalyptus bosistoana*. Paper presented at the Developing A Eucalypt Resource: Learning from Australia and Elsewhere, Wood Technology Research Centre.
- Assmann, E. (1970). *The principles of forest yield study: studies in the organic production, structure, increment, and yield of forest stands*: Pergamon Press.
- Avery, T. E., & Burkhart, H. E. (2015). *Forest measurements*: Waveland Press.
- Bailey, R. G., Pfister, R. D., & Henderson, J. A. (1978). Nature of land and resource classification - a review. *Journal of Forestry*, 76(10), 650-655.
- Barr, N. (1980). Eucalypts for Hawkes bay and other East coast districts. *New Zealand Tree Grower*, 1(3), 12-14.
- Barr, N. (1996). *Growing eucalypt trees for milling on New Zealand farms*: New Zealand Farm Forestry Association.
- Bartels, S. F., & Chen, H. Y. H. (2009). Is understory plant species diversity driven by resource quantity or resource heterogeneity? *Ecology*, 91(7), 1931-1938. doi:10.1890/09-1376.1
- Barua, S. K., Lehtonen, P., & Pahkasalo, T. (2014). Plantation vision: potentials, challenges and policy options for global industrial forest plantation development. *International Forestry Review*, 16(2), 117-127. doi:10.1505/146554814811724801
- Bathgate, J. L., Guo, L. B., Allbrook, R. F., & Payn, T. W. (1993). Microsite effect on *Eucalyptus regnans* growth. *New Zealand Journal of Forestry Science*, 23, 154-162.

- Battaglia, M., & Sands, P. (1997). Modelling site productivity of *Eucalyptus globulus* in response to climatic and site factors. *Functional Plant Biology*, 24(6), 831-850. doi:http://dx.doi.org/10.1071/PP97065
- Battaglia, M., & Sands, P. J. (1998). Process-based forest productivity models and their application in forest management. *Forest Ecology and Management*, 102(1), 13-32. doi:http://dx.doi.org/10.1016/S0378-1127(97)00112-6
- Belli, K. L., & Ek, A. R. (1988). Growth and survival modeling for planted conifers in the Great Lakes region. *Forest Science*, 34(2), 458-473.
- Bellingham, P., & Tanner, E. (2000). The influence of topography on tree growth, mortality, and recruitment in a tropical montane forest. *Biotropica*, 32(3), 378-384.
- Binkley, D., Campoe, O. C., Gspaltl, M., & Forrester, D. I. (2013). Light absorption and use efficiency in forests: Why patterns differ for trees and stands. *Forest Ecology and Management*, 288, 5-13.
- Blake, J., Somers, G., & Ruark, G. (1990). Perspectives on process modeling of forest growth responses to environmental stress. In R. Dixon, R. Meldahl, G. Ruark, & W. Warren (Eds.), *Process modeling of forest growth responses to environmental stress*. (pp. 9-17). Timber Press, Portland, Oregon.
- Blanco, J. A., Zavala, M. A., Imbert, J. B., & Castillo, F. J. (2005). Sustainability of forest management practices: Evaluation through a simulation model of nutrient cycling. *Forest Ecology and Management*, 213(1), 209-228.
- Blumer, A., Ehrenfeucht, A., Haussler, D., & Warmuth, M. K. (1987). Occam's razor. *Information Processing Letters*, 24(6), 377-380.
- Bohlen, P. J., Groffman, P. M., Driscoll, C. T., Fahey, T. J., & Siccama, T. G. (2001). Plant-soil-microbial interactions in a northern hardwood forest. *Ecology*, 82(4), 965-978.
- Boland, D. J., Brooker, M. I. H., Chippendale, G., Hall, N., Hyland, B., Johnston, R. D., . . . Turner, J. (2006). *Forest trees of Australia*: CSIRO Publishing.
- Bond, B. J., Farnsworth, B. T., Coulombe, R. A., & Winner, W. E. (1999). Foliage physiology and biochemistry in response to light gradients in conifers with varying shade tolerance. *Oecologia*, 120(2), 183-192. doi:10.1007/s004420050847
- Bootle, K. R. (1983). *Wood in Australia. Types, properties and uses*: McGraw-Hill Book Company.

- Bossel, H. (2013). *Modeling and simulation*: Springer-Verlag.
- Boyle, J. (1999). Planted forests: views and viewpoints. In J. Boyle, J. Winjum, K. Kavanagh, & E. Jensen (Eds.), *Planted forests: contributions to the quest for sustainable societies* (Vol. 56, pp. 5-9): Springer Netherlands.
- Brand, D. G. (1986). A competition index for predicting the vigour of planted Douglas-fir in southwestern British Columbia. *Canadian Journal of Forest Research*, 16(1), 23-29. doi:10.1139/x86-005
- Bravo, F., & Montero, G. (2001). Site index estimation in Scots pine (*Pinus sylvestris* L.) stands in the high Ebro Basin (northern Spain) using soil attributes. *Forestry*, 74(4), 395-406. doi:10.1093/forestry/74.4.395
- Brubaker, S., Jones, A., Frank, K., & Lewis, D. (1994). Regression models for estimating soil properties by landscape position. *Soil Science Society of America Journal*, 58(6), 1763-1767.
- Bugmann, H. (2001). A review of forest gap models. *Climatic Change*, 51(3-4), 259-305.
- Bulloch, B. T. (1991). Eucalypts species selection for soil conservation in seasonally dry hill country - twelfth year assessment. *New Zealand Journal of Forestry Science*, 21(1), 10-31.
- Bullock, B. P., & Burkhart, H. E. (2005). An evaluation of spatial dependency in juvenile loblolly pine stands using stem diameter. *Forest Science*, 51(2), 102-108.
- Burdett, A. N., Simpson, D. G., & Thompson, C. F. (1983). Root development and plantation establishment success. *Plant and Soil*, 71(1-3), 103-110. doi:10.1007/BF02182645
- Burkhart, H., & Brooks, T. (1990). Status and future of growth and yield models. *USDA Forest Service general technical report PNW-GTR-Pacific Northwest Research Station (USA)*.
- Burkhart, H. E., & Tomé, M. (2012). *Modeling Forest Trees and Stands*: Springer.
- Carrere, R., & Fonseca, H. (2004). Plantations are not forests. *Watershed*, 9(3), 2-3.
- Charnley, S. (2006). Industrial plantation forestry: Do local communities benefit? *Journal of Sustainable Forestry*, 21(4), 35-57.
- Chavasse, C. G. R. (1977). The Significance of planting height as an indicator of subsequent seedling growth. *New Zealand Journal of Forestry*, 22(2), 283-295.
- Clutter, J., & Allison, B. (1974). A growth and yield model for *Pinus radiata* in New Zealand. *Growth Models for Tree and Stand Simulation. Proc. IUFRO Working Party S, 4*, 01-04.

- Clutter, J. L. (1963). Compatible growth and yield models for Loblolly Pine. *Forest Science*, 9(3), 354-371.
- Clutter, J. L., & Jones Jr, E. P. (1980). Prediction of growth after thinning in old-field slash pine plantations [Pinus elliottii, yield, mensuration]. *USDA Forest Service Research Paper SE (USA)*.
- Coates, K. D. (2002). Tree recruitment in gaps of various size, clearcuts and undisturbed mixed forest of interior British Columbia, Canada. *Forest Ecology and Management*, 155(1), 387-398.
- Curtis, R. O. (1972). Yield Tables Past and Present. *Journal of Forestry*, 70(1), 28-32.
- Czerepko, J. (2008). A long-term study of successional dynamics in the forest wetlands. *Forest Ecology and Management*, 255(3-4), 630-642. doi:<http://dx.doi.org/10.1016/j.foreco.2007.09.039>
- Daniels, R. F., & Burkhardt, H. E. (1988). An integrated system of forest stand models. *Forest Ecology and Management*, 23(2), 159-177.
- Dyck, B. (2003). *Precision forestry—The path to increased profitability*. Paper presented at the Proceedings, The 2nd International Precision Forestry Symposium.
- Ek, A. R. (1974). Nonlinear models for stand table projection in northern hardwood stands. *Canadian Journal of Forest Research*, 4(1), 23-27.
- Enoki, T., Kawaguchi, H., & Iwatsubo, G. (1996). Topographic variations of soil properties and stand structure in a Pinus thunbergii plantation. *Ecological Research*, 11(3), 299-309. doi:10.1007/BF02347787
- Evans, J. (1992). *Plantation forestry in the tropics: tree planting for industrial, social, environmental, and agroforestry purposes*: Oxford University Press.
- Evans, J. (1999). Planted forests of the wet and dry tropics: their variety, nature, and significance. *New Forests*, 17(1-3), 25-36. doi:10.1023/A:1006572826263
- FAO. (2010). *Global forest resources assessment: Main report* (Food and Agriculture Organization of the United Nations, Italy Ed.). Rome, Italy.
- FAO. (2014). *State of the World's Forest: Enhancing the Socioeconomic Benefit from the Forest* (Food and Agriculture Organisation of the United Nations Ed.). Rome, Italy.

- Fontes, L., Bontemps, J. D., Bugmann, H., Van Oijen, M., Gracia, C., Kramer, K., . . . Skovsgaard, J. P. (2010). Models for supporting forest management in a changing environment. *Forest Systems*, 19, 22. doi:10.5424/fs/201019S-9315
- Fontes, L., Landsberg, J., Tomé, J., Tomé, M., Pacheco, C. A., Soares, P., & Araujo, C. (2006). Calibration and testing of a generalized process-based model for use in Portuguese eucalyptus plantations. *Canadian Journal of Forest Research*, 36(12), 3209-3221. doi:10.1139/x06-186
- Ford Robertson, F. C. (1971). *Terminology of forest science, technology, practice and products*. : Society of American Foresters, Washington Dc.
- Fox, J. C., Ades, P. K., & Bi, H. (2001). Stochastic structure and individual-tree growth models. *Forest Ecology and Management*, 154(1), 261-276.
- Franklin, J. F., Spies, T. A., Van Pelt, R., Carey, A. B., Thornburgh, D. A., Berg, D. R., . . . Shaw, D. C. (2002). Disturbances and structural development of natural forest ecosystems with silvicultural implications, using Douglas-fir forests as an example. *Forest Ecology and Management*, 155(1), 399-423.
- Freer-Smith, P., & Carnus, J.-M. (2008). The sustainable management and protection of forests: analysis of the current position globally. *AMBIO: A Journal of the Human Environment*, 37(4), 254-262. doi:10.1579/0044-7447(2008)37[254:TSMAP0]2.0.CO;2
- Garcia, O. (1988). Growth modelling — A review. *New Zealand Forestry*, 33(3), 14-17.
- Garten, C. T., Huston, M. A., & Thoms, C. A. (1994). Topographic variation of soil nitrogen dynamics at Walker Branch Watershed, Tennessee. *Forest Science*, 40(3), 497-512.
- Gillingham, A., & During, C. (1973). Pasture production and transfer of fertility within a long-established hill pasture. *New Zealand journal of experimental agriculture*, 1(3), 227-232.
- Grant, R., Arain, A., Arora, V., Barr, A., Black, T., Chen, J., . . . Zhang, Y. (2005). Intercomparison of techniques to model high temperature effects on CO₂ and energy exchange in temperate and boreal coniferous forests. *Ecological Modelling*, 188(2), 217-252.
- Grey, D. (1980). On the concept of site in forestry. *South African Forestry Journal*, 113(1), 81-83.
- Grey, D. C. (1983). The Evaluation of Site Factor Studies. *South African Forestry Journal*, 127(1), 19-22. doi:10.1080/00382167.1983.9628908

- Gustafsson, L., Baker, S. C., Bauhus, J., Beese, W. J., Brodie, A., Kouki, J., . . . Franklin, J. F. (2012). Retention forestry to maintain multifunctional forests: a world perspective. *BioScience*, *62*(7), 633-645. doi:10.1525/bio.2012.62.7.6
- Heaphy, M., Lowe, D., Palmer, D., Jones, H., Gielen, G., Oliver, G., & Pearce, S. (2014). Assessing drivers of plantation forest productivity on eroded and non-eroded soils in hilly land, eastern North Island, New Zealand. *New Zealand Journal of Forestry Science*, *44*(1), 24.
- Henning, J. G., & Burk, T. E. (2004). Improving growth and yield estimates with a process model derived growth index. *Canadian Journal of Forest Research*, *34*(6), 1274-1282.
- Holzwarth, F., Kahl, A., Bauhus, J., & Wirth, C. (2013). Many ways to die – partitioning tree mortality dynamics in a near-natural mixed deciduous forest. *Journal of Ecology*, *101*(1), 220-230. doi:10.1111/1365-2745.12015
- Hunter, I. R., & Gibson, A. R. (1984). Predicting *Pinus radiata* site index from environmental variables. *New Zealand Journal of Forestry Science*, *14*(1), 53-64.
- Ian Nicholas, & Paul Millen. (2012). Durable Eucalypt leaflet Series: *Eucalyptus bosistoana*. In New Zealand Dryland Forest Initiative (Ed.).
- INDUFOR. (2012). *Strategic Review on the Future of Forest Plantations in the World*. Retrieved from Helsinki, Finland:
- Jerome. L. Clutter. (1963). Compatible growth and yield models for loblolly pine. *Forest Science*, *9*(3), 354-371.
- Johnsen, K., Samuelson, L., Teskey, R., McNulty, S., & Fox, T. (2001). Process models as tools in forestry research and management. *Forest Science*, *47*(1), 2-8.
- Johnson, G., & Wilcox, M. (1989). *Eucalyptus* species trials on pumiceland. *New Zealand Forestry*, *34*(1), 24-27.
- Kanowski, P. J. (1997). *Afforestation and Plantation Forestry*. Paper presented at the XI World Forestry Congress, Turkey.
- Kimberley, M., West, G., Dean, M., & Knowles, L. (2005). The 300 Index - a volume productivity index for radiata pine. *New Zealand Journal of Forestry*, *50*(2), 13-18.
- Kimmins, J. (1990). Modelling the sustainability of forest production and yield for a changing and uncertain future. *The Forestry Chronicle*, *66*(3), 271-280.

- Kimmins, J., Brunner, A., & Maily, D. (1996). *Modeling the sustainability of managed forests: hybrid ecosystem simulation modeling from individual tree to landscape*. Paper presented at the proceedings of the Society of American Foresters National Convention.
- Kimmins, J. P. H., Blanco, J. A., Seely, B., Welham, C., & Scoullar, K. (2008). Complexity in modelling forest ecosystems: how much is enough? *Forest Ecology and Management*, 256(10), 1646-1658.
- Koch, G. W., Sillett, S. C., Jennings, G. M., & Davis, S. D. (2004). The limits to tree height. *Nature*, 428(6985), 851-854.
- Kohama, T., Mizoue, N., Ito, S., Inoue, A., Sakuta, K., & Okada, H. (2006). Effects of light and microsite conditions on tree size of 6-year-old *Cryptomeria japonica* planted in a group selection opening. *Journal of Forest Research*, 11(4), 235-242. doi:10.1007/s10310-005-0202-7
- Korzukhin, M. D., Ter-Mikaelian, M. T., & Wagner, R. G. (1996). Process versus empirical models: which approach for forest ecosystem management? *Canadian Journal of Forest Research*, 26(5), 879-887. doi:10.1139/x26-096
- Kuuluvainen, T. (2002). Natural variability of forests as a reference for restoring and managing biological diversity in boreal Fennoscandia. *Silva Fennica*, 36(1), 97-125.
- Kuuluvainen, T., & Juntunen, P. (1998). Seedling establishment in relation to microhabitat variation in a windthrow gap in a boreal *Pinus sylvestris* forest. *Journal of Vegetation Science*, 9(4), 551-562. doi:10.2307/3237271
- Kuuluvainen, T., & Laiho, R. (2004). Long-term forest utilization can decrease forest floor microhabitat diversity: evidence from boreal Fennoscandia. *Canadian Journal of Forest Research*, 34(2), 303-309. doi:10.1139/x03-159
- Lambert, M., & Roberts, E. (1976). Aspect differences in an unimproved hill country pasture: I. climatic differences. *New Zealand Journal of Agricultural Research*, 19(4), 459-467.
- Lambert, M., & Roberts, E. (1978). Aspect differences in an unimproved hill country pasture: II. edaphic and biotic differences. *New Zealand Journal of Agricultural Research*, 21(2), 255-260.
- Landsberg, J., & Waring, R. (1997). A generalised model of forest productivity using simplified concepts of radiation-use efficiency, carbon balance and partitioning. *Forest Ecology and Management*, 95(3), 209-228.

- Landsberg, J. J., Johnsen, K. H., Albaugh, T. J., Allen, H. L., & McKeand, S. E. (2001). Applying 3-PG, a simple process-based model designed to produce practical results, to data from Loblolly Pine experiments. *Forest Science*, 47(1), 43-51.
- Larson, A. J., Lutz, J. A., Gersonde, R. F., Franklin, J. F., & Hietpas, F. F. (2008). Potential site productivity influences the rate of forest structural development. *Ecological Applications*, 18(4), 899-910. doi:10.2307/40062198
- Lilja-Rothsten, S., Chantal, M. d., Peterson, C., Kuuluvainen, T., Vanha-Majamaa, I., & Puttonen, P. (2008). Microsites before and after restoration in managed *Picea abies* stands in southern Finland: effects of fire and partial cutting with dead wood creation. *Silva Fennica*, 42(2), 165-176.
- Liu, J., & Burkhart, H. E. (1994). Spatial characteristics of diameter and total height in juvenile Loblolly Pine (*Pinus taeda* L.) plantations. *Forest Science*, 40(4), 774-786.
- Louw, J. H. (1995). *Site classification and evaluation for commercial forestry in the Crocodile River catchment, Eastern Transvaal*. (M.Sc.), Faculty of Forestry, University of Stellenbosch.
- Louw, J. H., & Scholes, M. (2002). Forest site classification and evaluation: a South African perspective. *Forest Ecology and Management*, 171(1-2), 153-168. doi:http://dx.doi.org/10.1016/S0378-1127(02)00469-3
- Maclaren, J. P. (1993). *Radiata Pine Growers' Manual*: New Zealand Forest Research Institute.
- Maclaren, J. P. (1996). Environmental effects of planted forests in New Zealand: the implications of continued afforestation of pasture. *FRI bulletin*(198).
- Maclaren, J. P., Grace, J. C., Kimberley, M. O., Knowless, R. L., & West, G. G. (1995). Height growth of *Pinus Radiata* as affected by stocking. *New Zealand Journal of Forestry Science*, 25(1), 73-90.
- Maclaren, P. (2005). Realistic alternatives to radiata pine in New Zealand - A critical review. *New Zealand Journal of Forestry*, 50(1), 3-10.
- Mäkelä, A. (2003). Process-based modelling of tree and stand growth: towards a hierarchical treatment of multiscale processes. *Canadian Journal of Forest Research*, 33(3), 398-409.
- Mäkelä, A., Landsberg, J., Ek, A. R., Burk, T. E., Ter-Mikaelian, M., Ågren, G. I., . . . Puttonen, P. (2000). Process-based models for forest ecosystem management: current state of the art and challenges for practical implementation. *Tree Physiology*, 20(5-6), 289-298.

- Margolis, H. A., & Brand, D. G. (1990). An ecophysiological basis for understanding plantation establishment. *Canadian Journal of Forest Research*, 20(4), 375-390.
- Martín-Alcón, S., Coll, L., & Salekin, S. (2015). Stand-level drivers of tree-species diversification in Mediterranean pine forests after abandonment of traditional practices. *Forest Ecology and Management*, 353(0), 107-117. doi:http://dx.doi.org/10.1016/j.foreco.2015.05.022
- Mason, E., Rose, R., & Rosner, L. (2007). Time vs. light: a potentially useable light sum hybrid model to represent the juvenile growth of Douglas-fir subject to varying levels of competition. *Canadian Journal of Forest Research*, 37(4), 795-805.
- Mason, E. G. (1985). Causes of juvenile instability of *Pinus radiata* in New Zealand. *New Zealand Journal of Forestry Science*, 15(3), 263-280.
- Mason, E. G. (1992). *Decision-support systems for establishing Radiata pine plantations in the central North Island of New Zealand*. (Doctor of Philosophy in Forestry), University of Canterbury.
- Mason, E. G. (2001). A model of the juvenile growth and survival of *Pinus radiata* D. Don; adding the effects of initial seedling diameter and plant handling. *New Forests*, 22(1-2), 133-158. doi:10.1023/A:1012393130118
- Mason, E. G. (2004). Effects of soil cultivation, fertilisation, initial seedling diameter and plant handling on the development of maturing *Pinus radiata* D. Don on Kaingaroa gravelly sand in the central North Island of New Zealand. *Bosque*, 25(2), 43-55.
- Mason, E. G. (2013). Linking hybrid mensurational/eco-physiological growth and yield models with crop establishment: a replacement for time gain analysis. *New Forests*, 44(6), 951-959. doi:10.1007/s11056-013-9387-3
- Mason, E. G., Methol, R., & Cochrane, H. (2011). Hybrid mensurational and physiological modelling of growth and yield of *Pinus radiata* D. Don. using potentially useable radiation sums. *Forestry*, 84(2), 99-108. doi:10.1093/forestry/cpq048
- Mason, E. G., South, D. B., & Weizhong, Z. (1996). Performance of *Pinus radiata* in relation to seedling grade, weed control, and soil cultivation in the central North Island of New Zealand. *New Zealand Journal of Forestry Science*, 26(1/2), 173-183.
- Mason, E. G., & Whyte, A. G. D. (1997). Modelling initial survival and growth of radiata pine in New Zealand. *Acta Forestalia Fennica*, 2, 1-38.
- Mason, E. G., Whyte, A. G. D., Woollons, R. C., & Richardson, B. (1997). A model of the growth of juvenile radiata pine in the central North Island of New Zealand: links with older models

- and rotation-length analyses of the effects of site preparation. *Forest Ecology and Management*, 97(2), 187-195. doi:[http://dx.doi.org/10.1016/S0378-1127\(97\)00099-6](http://dx.doi.org/10.1016/S0378-1127(97)00099-6)
- Mátyás, C., Bozic, G., Gömöry, D., Ivankovic, M., & Rasztoivits, E. (2009). Juvenile growth response of European beech (*Fagus sylvatica* L.) to sudden change of climatic environment in SE European trials. *iForest - Biogeosciences and Forestry*, 2(6), 213-220. doi:10.3832/for0519-002
- McMurtrie, R. E., Rook, D. A., & Kelliher, F. M. (1990). Modelling the yield of *Pinus radiata* on a site limited by water and nitrogen. *Forest Ecology and Management*, 30(1-4), 381-413. doi:[http://dx.doi.org/10.1016/0378-1127\(90\)90150-A](http://dx.doi.org/10.1016/0378-1127(90)90150-A)
- Menzies, H. (1995). Eucalypts Show Potential. *Farm Forestry Review*, 33-34.
- Millen, P. (2006). Ground durable Eucalypts for vineyard posts. *New Zealand Tree Grower*.
- Millner, J., & Kemp, P. (2012). Seasonal growth of *Eucalyptus* species in New Zealand hill country. *New Forests*, 43(1), 31-44.
- Millner, J. P. (2006). *The Performance of Eucalyptus Species in Hill Country*. (Doctor of Philosophy in Plant Science), Massey University.
- Minteer, B. A., & Collins, J. P. (2010). Move it or lose it? The ecological ethics of relocating species under climate change. *Ecological Applications*, 20(7), 1801-1804.
- Mohren, G. M. J., & Burkhardt, H. E. (1994). Preface. *Forest Ecology and Management*, 69(1-3), 1-5. doi:[http://dx.doi.org/10.1016/0378-1127\(94\)90215-1](http://dx.doi.org/10.1016/0378-1127(94)90215-1)
- Monserud, R. A. (1984). Height growth and site index curves for inland Douglas-fir based on stem analysis data and forest habitat type. *Forest Science*, 30(4), 943-965.
- Monserud, R. A. (2003). Evaluating forest models in a sustainable forest management context. *Forest Biometry, Modelling and Information Sciences*, 1(1), 35-47.
- Monserud, R. A., & Sterba, H. (1996). A basal area increment model for individual trees growing in even- and uneven-aged forest stands in Austria. *Forest Ecology and Management*, 80(1), 57-80.
- Monteith, J. L., & Moss, C. J. (1977). Climate and the efficiency of crop production in Britain and discussion. *Philosophical Transactions of the Royal Society of London B: Biological Sciences*, 281(980), 277-294.
- Montgomery, R., & Chazdon, R. (2002). Light gradient partitioning by tropical tree seedlings in the absence of canopy gaps. *Oecologia*, 131(2), 165-174. doi:10.1007/s00442-002-0872-1

- Mooney, H. A., Vitousek, P. M., & Matson, P. A. (1987). Exchange of materials between terrestrial ecosystems and the atmosphere. *Science*, 238(4829), 926-932.
- Morgan, M. G., MacLean, D. A., & Piene, H. (1983). Variation in Balsam Fir needle length due to crown position, foliage age, and intertree differences. *Forest Science*, 29(2), 412-422.
- Munro, D. D. (1974). Forest growth models—a prognosis *Growth models for tree and stand simulation* (Vol. 30, pp. 7-21): Research Note 30. Department of Forest Yield Research, Royal College of Forestry, Stockholm.
- Nagel, L. M., & O'Hara, K. L. (2001). The influence of stand structure on ecophysiological leaf characteristics of *Pinus ponderosa* in western Montana. *Canadian Journal of Forest Research*, 31(12), 2173-2182. doi:10.1139/x01-156
- Nambiar, E. K. S. (1996). Sustained productivity of forests is a continuing challenge to soil science. *Soil Science Society of America Journal*, 60(6), 1629-1642. doi:10.2136/sssaj1996.03615995006000060006x
- Narukawa, Y., & Yamamoto, S. I. (2001). Gap formation, microsite variation and the conifer seedling occurrence in a subalpine old-growth forest, central Japan. *Ecological Research*, 16(4), 617-625.
- Navarro-Cerrillo, R. M., del Campo, A. D., Ceacero, C. J., Quero, J. L., & Hermoso de Mena, J. (2014). On the importance of topography, site quality, stock quality and planting date in a semiarid plantation: feasibility of using low-density LiDAR. *Ecological Engineering*, 67(0), 25-38. doi:http://dx.doi.org/10.1016/j.ecoleng.2014.03.011
- Nicholas, I., & Millen, P. (2012). Durable Eucalypt leaflet Series: *Eucalyptus globoidea* In New Zealand Dryland Forest Initiative (Ed.).
- Nicotra, A. B., Chazdon, R. L., & Iriarte, S. V. B. (1999). Spatial Heterogeneity of light and woody seedling regeneration in tropical wet forests. *Ecology*, 80(6), 1908-1926. doi:10.1890/0012-9658(1999)080[1908:SHOLAW]2.0.CO;2
- Nippert, J. B., & Marshall, J. D. (2003). Sources of variation in ecophysiological parameters in Douglas-fir and grand fir canopies. *Tree Physiology*, 23(9), 591-601. doi:10.1093/treephys/23.9.591
- Nouvellon, Y., Laclau, J.-P., Epron, D., Kinana, A., Mabiála, A., Roupsard, O., . . . Saint-André, L. (2010). Within-stand and seasonal variations of specific leaf area in a clonal *Eucalyptus* plantation in the Republic of Congo. *Forest Ecology and Management*, 259(9), 1796-1807. doi:http://dx.doi.org/10.1016/j.foreco.2009.05.023

- Nyström, K., & Kexi, M. (1997). Individual tree basal area growth models for young stands of Norway spruce in Sweden. *Forest Ecology and Management*, 97(2), 173-185.
- Onyekwelu, J., Stimm, B., & Evans, J. (2011). Review plantation forestry. In S. Günter, M. Weber, B. Stimm, & R. Mosandl (Eds.), *Silviculture in the Tropics* (Vol. 8, pp. 399-454): Springer Berlin Heidelberg.
- Owens, J. N., & Lund, H. G. (2009). Forest plantations. In J. N. Owens & H. G. Lund (Eds.), *Forests and forest Plants* (Vol. 1, pp. 301). Oxford, United Kingdom: Eolss.
- Paquette, A., & Messier, C. (2009). The role of plantations in managing the world's forests in the anthropocene. *Frontiers in Ecology and the Environment*, 8(1), 27-34.
- Parton, W. J., Schimel, D. S., Cole, C. V., & Ojima, D. S. (1987). Analysis of factors controlling soil organic matter levels in great plains grasslands. *Soil Science Society of America Journal*, 51(5), 1173-1179. doi:10.2136/sssaj1987.03615995005100050015x
- Peng, C. (2000). Growth and yield models for uneven-aged stands: past, present and future. *Forest Ecology and Management*, 132(2-3), 259-279. doi:http://dx.doi.org/10.1016/S0378-1127(99)00229-7
- Peng, C., Liu, J., Dang, Q., Apps, M. J., & Jiang, H. (2002). TRIPLEX: a generic hybrid model for predicting forest growth and carbon and nitrogen dynamics. *Ecological Modelling*, 153(1), 109-130.
- Perry, D. (1985). The competition process in forest stands. *Attributes of trees as crop plants*, 481-506.
- Peterson, C. J., & Pickett, S. T. A. (1990). Microsite and elevational influences on early forest regeneration after catastrophic windthrow. *Journal of Vegetation Science*, 1(5), 657-662. doi:10.2307/3235572
- Pinjuv, G., Mason, E. G., & Watt, M. (2006). Quantitative validation and comparison of a range of forest growth model types. *Forest Ecology and Management*, 236(1), 37-46. doi:http://dx.doi.org/10.1016/j.foreco.2006.06.025
- Pinjuv, G. L. (2006). *Hybrid forest modelling of Pinus Radiata D. Don in Canterbury, New Zealand*. (Doctor of Philosophy in Forestry), University of Canterbury. Retrieved from <http://hdl.handle.net/10092/1102>
- Pretzsch, H. (2009). *Forest dynamics, growth and yield: from measurement to model*: Springer.

- Radcliffe, J. E., & Lefever, K. (1981). Aspect influences on pasture microclimate at Coopers creek, North Canterbury. *New Zealand Journal of Agricultural Research*, 24(1), 55-56.
- Radford, I. J., Nicholas, M., Tiver, F., Brown, J., & Kriticos, D. (2002). Seedling establishment, mortality, tree growth rates and vigour of *Acacia nilotica* in different *Astrebla* grassland habitats: implications for invasion. *Austral Ecology*, 27(3), 258-268. doi:10.1046/j.1442-9993.2002.01176.x
- Ralston, C. W. (1964). Evaluation of forest site productivity. *International Review of Forestry Research*, 1, 171-200.
- Rauscher, H., Isebrands, J., Host, G., Dickson, R., Dickmann, D., Crow, T., & Michael, D. (1990). ECOPHYS: an ecophysiological growth process model for juvenile poplar. *Tree Physiology*, 7(1-2-3-4), 255-281.
- Richardson, B., Watt, M. S., Mason, E. G., & Kriticos, D. J. (2006). Advances in modelling and decision support systems for vegetation management in young forest plantations. *Forestry*, 79(1), 29-42. doi:10.1093/forestry/cpi059
- Robertson, G. P., Hutson, M. A., Evans, F. C., & Tiedje, J. M. (1988). Spatial variability in a successional plant community: patterns of nitrogen availability. *Ecology*, 69(5), 1517-1524.
- Runkle, J. R. (1981). Gap regeneration in some old-growth forests of the eastern United States. *Ecology*, 62(4), 1041-1051. doi:10.2307/1937003
- Runkle, J. R., & Yetter, T. C. (1987). Treefalls revisited: gap dynamics in the southern Appalachians. *Ecology*, 68(2), 417-424. doi:10.2307/1939273
- Sax, D. F., Smith, K. F., & Thompson, A. R. (2009). Managed relocation: a nuanced evaluation is needed. *Trends in Ecology & Evolution*, 24(9), 472-473.
- Schimel, D. S. (2010). Drylands in the earth system. *Science*, 327(5964), 418-419. doi:10.1126/science.1184946
- Schönau, A. P. G., & Herbert, M. A. (1989). Fertilizing eucalypts at plantation establishment. *Forest Ecology and Management*, 29(4), 221-244. doi:http://dx.doi.org/10.1016/0378-1127(89)90096-0
- Sedjo, R. A. (1999). The potential of high-yield plantation forestry for meeting timber needs *Planted forests: contributions to the quest for sustainable societies* (pp. 339-359): Springer.

- Sedjo, R. A., & Botkin, D. (1997). Using forest plantations to spare natural forests. *Environment: Science and Policy for Sustainable Development*, 39(10), 14-30.
- Seynave, I., Gégout, J. C., Hervé, J. C., & Dhôte, J. F. (2008). Is the spatial distribution of European beech (*Fagus sylvatica* L.) limited by its potential height growth? *Journal of Biogeography*, 35(10), 1851-1862.
- Shugart, H., Smith, T., & Post, W. (1992). The potential for application of individual-based simulation models for assessing the effects of global change. *Annual Review of Ecology and Systematics*, 15-38.
- Sinclair, T. R., & Muchow, R. C. (1999). Radiation use efficiency. *Advances in Agronomy*, 65(21), 5-265.
- Skovsgaard, J. P., & Vanclay, J. K. (2008). Forest site productivity: a review of the evolution of dendrometric concepts for even-aged stands. *Forestry*, 81(1), 13-31.
- Skovsgaard, J. P., & Vanclay, J. K. (2013). Forest site productivity: a review of spatial and temporal variability in natural site conditions. *Forestry*, 86(3), 305-315. doi:10.1093/forestry/cpt010
- Snowdon, P. (2002). Modeling Type 1 and Type 2 growth responses in plantations after application of fertilizer or other silvicultural treatments. *Forest Ecology and Management*, 163(1), 229-244.
- Snowdon, P., Jovanovic, T., & Booth, T. H. (1999). Incorporation of indices of annual climatic variation into growth models for *Pinus radiata*. *Forest Ecology and Management*, 117(1), 187-197.
- Spiecker, H., Mieläikinen, K., Köhl, M., & Skovsgaard, J. P. (1996). Discussion. In H. Spiecker, K. Mieläikinen, M. Köhl, & J. Skovsgaard (Eds.), *Growth trends in European forests* (pp. 355-367): Springer Berlin Heidelberg.
- Spurr, S. H. (1951). Forest inventory. *Forest Inventory*.
- Stephens, S., & Wagner, M. R. (2007). Forest plantations and biodiversity: a fresh perspective. *Journal of Forestry*, 105(6), 307-313.
- Tennent, R. B. (1982). Individual-tree growth model for *Pinus radiata*. *New Zealand Journal of Forestry Science*.

- Tesch, S. D. (1980). The evolution of forest yield determination and site classification. *Forest Ecology and Management*, 3(0), 169-182. doi:http://dx.doi.org/10.1016/0378-1127(80)90014-6
- Van Ballekom, S., & Millen, P. (2017). *NZDFI: Achievements, constraints and opportunities*. Paper presented at the Durable eucalypts on drylands: Protecting enhancing value, Blenheim, New Zealand.
- Vanclay, J. K. (1992). Assessing site productivity in tropical moist forests: a review. *Forest Ecology and Management*, 54(1-4), 257-287. doi:http://dx.doi.org/10.1016/0378-1127(92)90017-4
- Vanclay, J. K. (1994). Modeling forest growth and yield. *Applications to Mixed Tropical Forests*. CAB International, Wallingford.
- Vanclay, J. K. (2006). Forest growth and yield modeling. *Encyclopedia of Environmetrics*: John Wiley & Sons, Ltd.
- Vanclay, J. K., & Henry, N. B. (1988). Assessing site productivity of indigenous Cypress Pine forest in southern Queensland. *The Commonwealth Forestry Review*, 67(1 (210)), 53-64. doi:10.2307/42608428
- Vanclay, J. K., & Skovsgaard, J. P. (1997). Evaluating forest growth models. *Ecological Modelling*, 98(1), 1-12. doi:http://dx.doi.org/10.1016/S0304-3800(96)01932-1
- Vitt, P., Havens, K., Kramer, A. T., Sollenberger, D., & Yates, E. (2010). Assisted migration of plants: changes in latitudes, changes in attitudes. *Biological Conservation*, 143(1), 18-27.
- Voelker, S. L., Muzika, R.-M., & Guyette, R. P. (2008). Individual tree and stand level influences on the growth, vigor, and decline of Red Oaks in the Ozarks. *Forest Science*, 54(1), 8-20.
- Vuokila, Y. (1965). Functions for variable density yield tables of pine based on temporary sample plots.
- Watt, M. S., Palmer, D. J., Kimberley, M. O., Höck, B. K., Payn, T. W., & Lowe, D. J. (2010). Development of models to predict *Pinus radiata* productivity throughout New Zealand. *Canadian Journal of Forest Research*, 40(3), 488-499. doi:10.1139/X09-207
- Weiskittel, A., Temesgen, H., Wilson, D., & Maguire, D. (2008). Sources of within- and between-stand variability in specific leaf area of three ecologically distinct conifer species. *Annals of Forest Science*, 65(1), 103-103. doi:10.1051/forest:2007075

- Weiskittel, A. R., Hann, D. W., Kershaw, J. A., & Vanclay, J. K. (2011). *Forest Growth and Yield Modeling*: Wiley.
- West, G. G. (1984). Establishment requirements of *Pinus Radiata* cuttings and seedlings compared. *New Zealand Journal of Forest Science*, 14(1), 41-52.
- Wiens, J. A. (1989). Spatial scaling in ecology. *Functional Ecology*, 3(4), 385-397. doi:10.2307/2389612
- Williams, J., & Woinarski, J. (1997). *Eucalypt ecology: individuals to ecosystems*: Cambridge University Press.
- Woollons, R. C., Snowdon, P., & Mitchell, N. D. (1997). Augmenting empirical stand projection equations with edaphic and climatic variables. *Forest Ecology and Management*, 98(3), 267-275. doi:http://dx.doi.org/10.1016/S0378-1127(97)00090-X
- Yamamoto, S. I. (2000). Forest gap dynamics and tree regeneration. *Journal of Forest Research*, 5(4), 223-229.
- Zhang, S., Burkhart, H. E., & Amateis, R. L. (1996). Modeling individual tree growth for juvenile loblolly pine plantations. *Forest Ecology and Management*, 89(1-3), 157-172. doi:http://dx.doi.org/10.1016/S0378-1127(96)03851-0
- Zhao, W. (1999). *Growth and yield modelling of Pinus radiata in Canterbury, New Zealand*. (Doctor of Philosophy in Forestry), University of Canterbury.

2

A comparative study of three non-geostatistical methods to optimise digital elevation model interpolation*

*This chapter has been published in International Journal of Geo-information (2018), 7(8),300.

2. A comparative study of three non-geostatistical methods to optimise digital elevation model interpolation.

2.1 Introduction

A digital elevation model (DEM) is a mathematically derived representation of the Earth's surface. It is produced by collecting elevation point data and then interpolating those points to a surface. There are several methods to capture the data for DEM interpolation. For example, field surveys, photogrammetry techniques, radar, and aerial laser scanning (ALS) (Peralvo & Maidment, 2004) have all been proposed. This latter method, also known as LiDAR (Light Detection and Ranging) using unmanned airborne systems (UAS) or fixed-wing aircraft has become the de facto standard for producing high-resolution DEMs (Koci et al., 2017; Liu, 2008; Traganos et al., 2018; Vaze & Teng, 2007). This is because other data capture methods (i.e. the field survey) have several limitations, for instances, the coverage, time constraints and accessibility. Whereas, ALS enables accurate measurement of elevation for a dense set of points on the Earth's surface for a large area in a short time period. Moreover, LiDAR point elevations can have +/- 0.5cm (vertical) and +/- 0.5cm (horizontal) accuracy and point densities typically between 0.5 - 50 points per square meter (Kodors, 2017). LiDAR point data are interpolated into a DEM, with typical spatial resolutions of $< 1\text{m}$.

Despite their accuracy, coverage, and efficient data capture, LiDAR acquisitions are costly and require expertise to analyse (Morgenroth & Visser, 2013). As such, LiDAR data are commonly only acquired for specialist land-based applications including forestry (Morgenroth & Visser, 2013), mining (Kurz et al., 2009), agriculture (Tagarakis et al., 2018), and urban planning (Yu et al., 2010). However, even within these industries, the drawbacks of LiDAR acquisition and analysis can preclude their common use (Baltsavias, 1999). As such, there remains a need to

explore less costly, simple alternatives to DEM generation for many small-scale applications. Such alternatives would be especially useful in developing regions and small-scale areas which for which LiDAR acquisitions are uncommon.

One such alternative, field surveying, can be used to describe topography. Field surveys using a global navigation satellite system (GNSS) receiver are methodologically simple. Since the initial launch of the global positioning system (GPS) in 1973 (Parkinson et al., 1996), GNSS has developed progressively, resulting in increased use by scientific communities and the general public. Improvements include a reduction in costs (Pick, 2006), improved positional accuracy and precision (Hofmann-Wellenhof et al., 2012). Moreover, since GPS became fully operational in 1995, worldwide coverage has helped to ensure that GNSS surveying and mapping are possible in the world's developing regions (Groves, 2013). Point elevations are acquired across a landscape by a GNSS receiver and subsequently interpolated to a DEM, in much the same way as LiDAR data are interpolated into a DEM. GNSS (e.g. GPS, GLONASS, Beidou-2 Navigation Satellite System, and Galileo) and regional navigation satellite systems (e.g. Navigation with Indian Constellation (NAVIC)) are designed to estimate the geographic coordinates of a receiver by trilateration with three or more satellites. GNSS data are now commonly used for numerous applications requiring accurate positioning, including precision agriculture (Neményi et al., 2003) and forestry (Olivera et al., 2016), and surveying (Gao, 2007). If GNSS elevation points are to be used to generate accurate DEMs, there remains a need to optimise various aspects of the process to minimise the error reported in previous studies (Yao & Clark, 2000).

Errors in digital elevation models are undesirable, especially because they can be perpetuated through derived topographic surfaces, including aspect, slope, hillshade, and surface curvature. Moreover, DEMs are critical in their role for normalising digital surface models, such

that errors in a DEM will result in corresponding errors in digital surface models and canopy height models. Gong et al. (2000) grouped the factors which could influence the DEM quality into three classes: i) accuracy, density, and distribution of the source data; ii) characteristics of the surface; and iii) the interpolation process. The accuracy of the source data varies with technique, such as LiDAR acquisition or field surveying. Density and sampling interval of the data can be modulated by experimental design, data collection decisions and available time (Chaplot et al., 2006). Besides these, the nature of the terrain also influences the quality of a DEM through natural uncertainty, as irregular surfaces can be more error-prone.

The third source of error is interpolation. Interpolation from elevation points to a surface can be achieved in many ways (see, Li & Heap, 2008), thus introducing potential error into modelled elevation surfaces. The processes of creating a surface from either initial measured points (e.g. IDW) or the degree of similarity of the smoothed surfaces (e.g. Splines) are called non-geostatistical, or deterministic, methods. In contrast, geostatistical methods are based on statistics and probability (Erdogan, 2009; Gong et al., 2000; Li & Heap, 2011). A number of studies have been conducted to compare different interpolation methods based on their use for different disciplines (Li & Heap, 2008; Mitas & Mitasova, 1999; Robinson & Metternicht, 2006; Zimmerman et al., 1999). Previous studies also include a comparison of accuracy based on different spatial attributes such as slope, aspect, curvature and hydrologic process (Amjad et al., 2016; Chaplot et al., 2006; Erdogan, 2009; Habtezion et al., 2016)

The main objective of this study was to evaluate the potential for generating a high-resolution DEM from data collected via a GNSS receiver during a field survey. This objective was achieved by: i) comparing DEM accuracy for a range of spatial resolutions, ii) comparing three

different non-geostatistical interpolations, iii) examining the impact of data density on DEM quality.

2.2 Materials and methods

2.2.1 Study sites

A hilly broken landscape, covered by young *Eucalyptus* spp. plantation, in the southern area of the Marlborough region, New Zealand was selected for this study (Figure 2.1). The site (-41.7364606452187 latitude, 174.1221316582747 longitude) ranges in elevation from 10m to 82m above sea level (asl), has slope ranging from 13° to 32° and covers 4.7 hectares. It has predominantly warm, dry and settled weather during the summer months, with daytime maximum air temperature ranging from 20°C to 26°C, but occasionally rising above 30°C. Winter days often start with a frost, but are usually mild overall, with daytime maximum air temperature ranging from 10°C to 15°C (NIWA, 2015a).

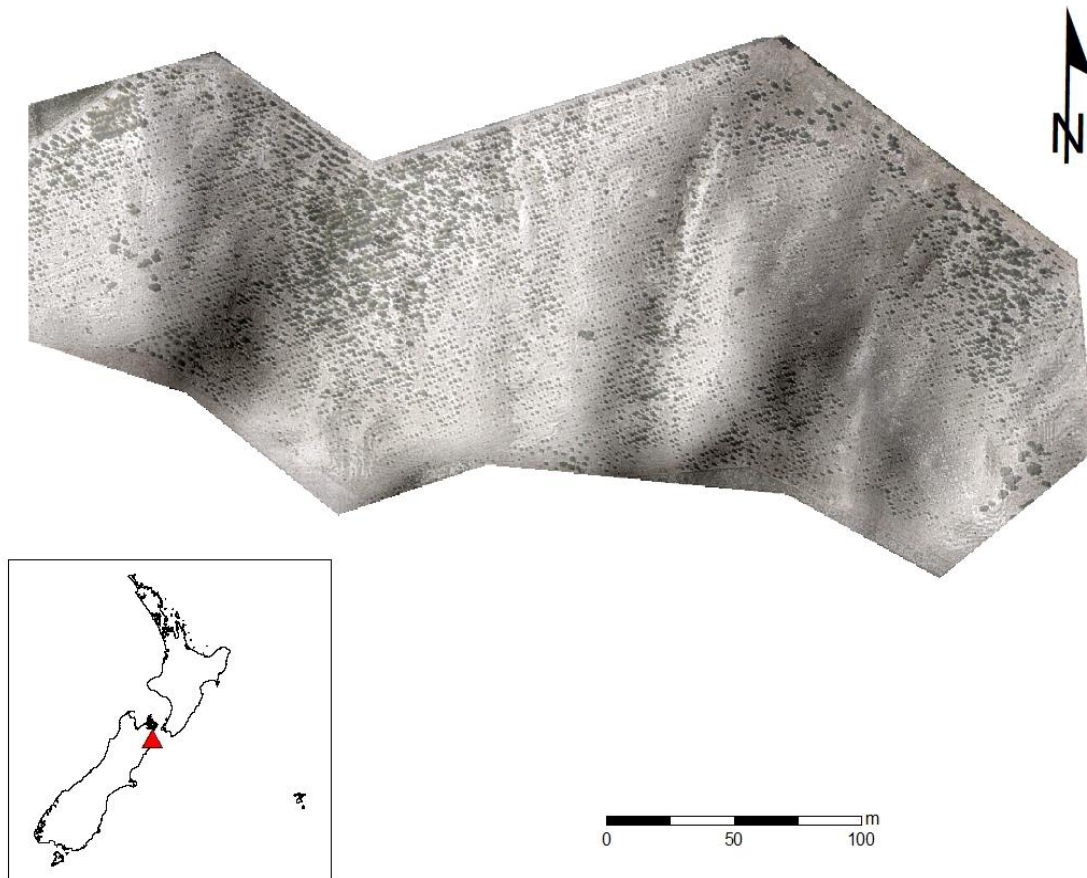


Figure 2.1 Location of the experimental site. Aerial imagery overlaid on a hillshade model.

Positional data points were collected with Trimble® R8s real-time kinetic geo-positioning system (RTK-GPS) by carrying a handheld receiver (‘rover’) and establishing a base station for differential correction (Hofmann-Wellenhof et al., 2012). According to the manufacturer, the RTK-GPS has a theoretical horizontal accuracy of $\pm 0.008\text{m} + 1\text{ppm RMS}$ and vertical accuracy of $\pm 0.015\text{m} + 1\text{ppm RMS}$ (Trimble, 2017). However, a mean horizontal error of 0.014m with standard deviation (SD) of 0.004m, and a mean vertical error of 0.030m with SD of 0.010m were found under field conditions (Koci et al., 2017). A total of 2722 data points were collected, over six hours, by walking transects across the site in a general East-West direction, at roughly five-meter intervals. The data collection was done on a clear sunny day to ensure minimum satellite

distortion. At each point, coordinates (eastings, northings, and elevation) were recorded. All coordinates were georeferenced to the New Zealand Geodetic Datum 2000.

The train and test approach (Miller, 2005) was applied for quantitative evaluation of the GPS points. The collected data points were randomly partitioned into training (90 percent, n=2440) and validation (10% , n=282) datasets (Figure 2.2). The training dataset was randomly thinned by 25% (n=1779), 50% (n=1220), and 75% (n=561) of its original point density (Figure 2.3 and Table 2.1), which ranged from 0.519 points m^{-2} to 0.129 points m^{-2} (Table 2.1).

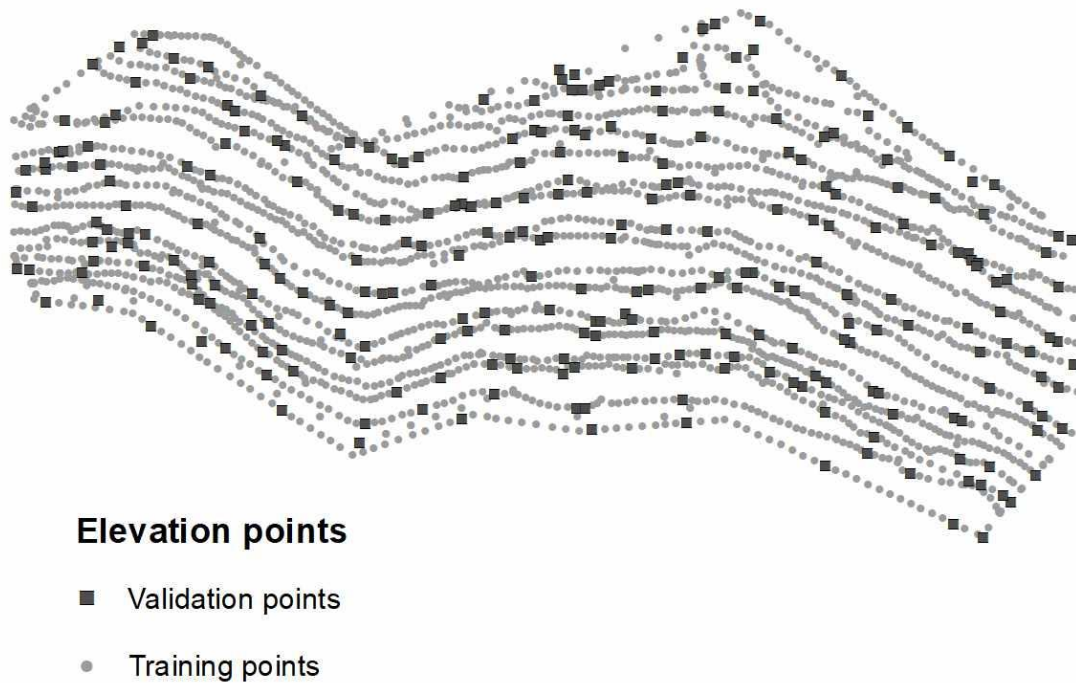


Figure 2.2 Layout of the collected data points.

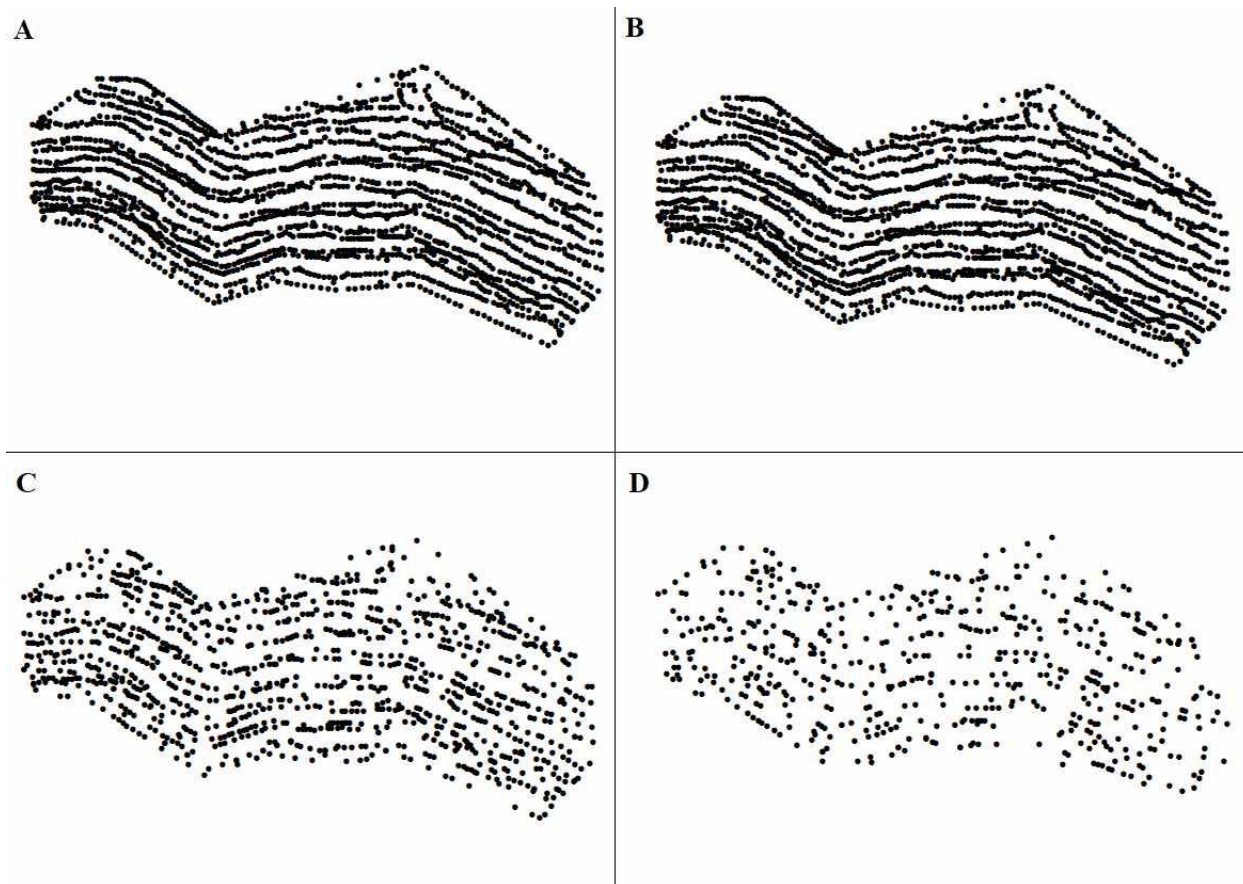


Figure 2.3 Training points were thinned by A) 0%, B) 25%, C) 50%, and D) 75%.

Table 2.1 Summary of elevations resulting from different training data thinning intensities.

Thinning (%)	Points	Elevation (m asl)				Point density m ⁻²
		Min.	Max.	Mean	SD	
0	2440	9.749	82.139	44.316	18.516	0.0519
25	1830	9.748	82.139	44.580	18.295	0.0389
50	1220	9.748	82.139	44.962	18.236	0.0259
75	610	9.765	79.495	44.442	18.336	0.0129

2.2.3 Interpolation methods and parameters

Interpolation methods have been intensively studied for producing DEMs. Kidner (2003) and Torlegård et al. (1986) reported two major research areas: (1) developing new interpolation

methods, and (2) optimising the selection of existing interpolation methods. There are a number of existing geographic data interpolation methods with various approaches and uses (Li & Heap, 2008; Li & Heap, 2011). Lam (1983) categorised interpolation as either point or aerial methods, Shi and Tian (2006) suggested linear, non-linear and hybrid methods, while other authors have suggested various physically-based interpolation methods (Grimaldi et al., 2004; Grimaldi et al., 2005; Niemann et al., 2003; Sandmeier & Itten, 1997). However, Li and Heap (2014) broadly classified all interpolation methods into two main forms, namely deterministic and stochastic methods. Stochastic methods integrate the concept of randomness and provide both estimations and associated variances and uncertainties. In a broad sense, stochastic methods are based on statistical properties of the data. Deterministic interpolation methods create surfaces from measured points based on either similarity or a degree of smoothing (Li & Heap, 2008). As such, deterministic methods are considered the simplest and easiest to apply. Here, three deterministic methods were compared for their potential to interpolate an accurate digital elevation model from different intensities of thinned training data.

The selected interpolation methods, as described below, were applied across all training datasets to create DEMs with spatial resolutions ranging from 0.5m to 10m, increasing in 0.5m increments. In total, 20 DEMs were interpolated. All the interpolation were carried out with the default setting in ArcGIS 10.4.1 (ESRI, 2012). The training DEMs were then evaluated against the validation dataset to assess the degree of agreement between each DEM and measured elevation.

2.2.3.1 Inverse Distance Weighted (IDW)

Inverse distance weighted (IDW) interpolation is an automated technique (Philip & Watson, 1982), requiring very few parameters from the operators (Hessl et al., 2007). It is specifically suitable where the dataset range is narrow and other fitting techniques are heavily

affected by errors. The process is highly flexible and allows estimation of datasets with a trend or anisotropy (Garnero & Godone, 2013).

IDW estimates cell values through a linearly weighted combination of sample points, where the weight assigned to each sample point is the inverse of its distance from the cell being estimated (Philip & Watson, 1982). The underlying assumption of IDW is that an unsampled cell's value is a weighted average of known cells' data in the local neighbourhood (Garnero & Godone, 2013). The surface being interpolated should be that of a locally dependent variable, and each cell's value is estimated as (Equation 3):

$$Z_j = \frac{\sum_{i=1}^n \frac{Z_i}{(h_{ijk} + \delta)^\beta}}{\sum_{i=1}^n \frac{1}{(h_{ijk} + \delta)^\beta}} \quad (3)$$

Where Z_j is the unsampled location value, Z_i is the known cells value, β is the weight and δ is the parameter. The separation distance h_{ijk} is measured by a three-dimensional Euclidian distance (Equation 4):

$$h_{ijk} = \sqrt{(\Delta x)^2 + (\Delta y)^2 + (\Delta z)^2} \quad (4)$$

Where, Δx , Δy and are the distances between the unknown and known point according to the reference axes, and Δz refer to the height as the third point of measure.

2.2.3.2 Topo to Raster (ANUDEM)

Topo to raster (ANUDEM) interpolation is a morphological approach designed for scattered surface-specific point elevation data and streamline data. The input data may include point elevations, elevation contours, streamlines, sink data points, cliff lines, boundary polygons, lake boundaries and data mask polygons. It attempts to take into account the special nature of the terrain surfaces, and the surface specific points that can be used for the sample terrain (Hutchinson,

1989). Topo to raster model is considered by many studies to produce hydrologically correct DEMs (eg., Curebal et al., 2016; Salari et al., 2014)

2.2.3.3 Natural Neighbours (NaN)

The natural neighbours (NaN) interpolation method was introduced by Sibson (1981). The model works by finding the nearest subset of samples for a given cell without a measured value, and then applies weights to the samples based on the proportional area they occupy (Sibson, 1981). In other words, it combines features from both Nearest neighbours (NN) and Triangular irregular network (TIN) interpolation methods. It starts with a triangulation of the data by Delaunay's method and then finds adjacent samples by Thiessen polygons. The value of an unknown cell is estimated by inserting and determining the point within a polygon. For each neighbour, the area of the portion of its original polygon that becomes incorporated in the tile of the new point is calculated (Webster & Oliver, 2001). This method is well known for its ability to interpolate scattered and unevenly distributed data (Ledoux & Gold, 2005).

2.2.4 Analysis

For evaluation purposes, a set of statistical calculations was carried out (Table 2.2), following Willmott (1981), Vicente-Serrano et al. (2003), and Li and Heap (2014) in R statistical environment by using base packages (R Core Team, 2017). These include the coefficient of determination (r^2) from the ordinary least square (OLS) model, the bias of the model as indicated by the intercept–slope pair, the mean bias error (MBE), the mean absolute error (MAE) and the root mean square error (RMSE). MAE and RMSE are the best overall measures for evaluating agreement between observed and predicted data (Li & Heap, 2014; Vicente-Serrano et al., 2003; Willmott, 1982). Both are similar metrics, except the RMSE is more sensitive to extreme outliers, whereas MAE is less sensitive. To overcome that, we include model efficiency (EF), which is

based on the relationship between observed and predicted mean deviations (Greenwood et al., 1985). EF values closer to 1 specify model reliability.

In addition to statistical metrics, a subjective evaluation was also undertaken to evaluate the different interpolations. As Daly et al. (2002) highlighted, empirical knowledge can help to determine which method best reflects reality, as long as those methods produce reasonable statistical values. So, following the statistical evaluation, DEMs were visually assessed for their agreement with the original landscape.

Table 2.2 Statistical metrics to assess interpolation quality.

Statistical features	Definitions
	N =Number of observation
	O =Observed value
	\bar{O} =mean of observed value
	P =Predicted value
	$P'_i = P_i - \bar{O}$
	$O'_i = O_i - \bar{O}$
Ordinary least square regression	Slope
	Intercept
	r^2 =coefficient of determination
Mean bias error (MBE)	$MBE = \frac{\sum_{i=1}^N (P_i - O_i)}{N}$
Root mean square error (RMSE)	$RMSE = \sqrt{\frac{\sum_{i=1}^N (P_i - O_i)^2}{N}}$
Mean absolute error (MAE)	$MAE = \frac{\sum_{i=1}^N P_i - O_i }{N}$
Model efficiency (EF)	$EF = 1 - \frac{\sum_{i=1}^N (P_i - O_i)^2}{\sum_{i=1}^N (\bar{O} - O_i)^2}$

2.3 Results

2.3.1 DEM resolution analysis

All DEM resolutions yielded very high r^2 values, ranging from 0.9946 – 0.9995 (Table 2.3). The 0.5m resolution produced the DEM surface with the highest r^2 value (0.9995), and r^2 values decreased with a reduction in resolution, reaching 0.9946 at 10m resolution. This result was reinforced by the RMSE and MAE being lowest for the 0.5m resolution DEM (Table 2.3 and Figure 2.4), and increasing steadily from 0.429m to 1.38m and 0.274m to 1.088m for RMSE and MAE, respectively at 10m resolution. The MBE, which indicates the bias of the prediction, showed that at or below resolutions of 5m the DEMs underestimated elevation slightly, whereas, at coarser resolutions (specifically at 5.5m, 8m, 8.5m, 9m, and 10m), the DEMs generally overestimated elevation. Moreover, the EF (0.999>0.994) for 0.5 m resolution found more close to 1 compared to lower resolutions which indicate in line with other findings irrespective of any of the three selected methods.

Table 2.3 Results of statistical analysis for different DEM resolutions.

Resolution	r^2	Slope	Intercept	RMSE (m)	MAE (m)	MBE (m)	EF
0.5	0.9995	1.0042	-0.2155	0.428	0.274	0.029	0.999
1	0.9994	1.0051	-0.2604	0.450	0.308	0.036	0.999
1.5	0.9994	1.0042	-0.2114	0.455	0.325	0.024	0.999
2	0.9993	1.0039	-0.2213	0.488	0.363	0.049	0.999
2.5	0.9992	1.0053	-0.2654	0.532	0.409	0.029	0.998
3	0.9991	1.0049	-0.2438	0.571	0.447	0.024	0.998
3.5	0.9989	1.0027	-0.1715	0.616	0.484	0.051	0.998
4	0.9989	1.0048	-0.2549	0.615	0.485	0.040	0.998
4.5	0.9987	1.0077	-0.3825	0.697	0.548	0.044	0.998
5	0.9984	1.0064	-0.3156	0.758	0.600	0.033	0.998
5.5	0.9982	1.0077	-0.3316	0.804	0.648	-0.009	0.997
6	0.998	1.0020	-0.1096	0.830	0.656	0.021	0.997
6.5	0.9976	1.0056	-0.2718	0.91	0.744	0.024	0.997
7	0.9974	1.0057	-0.3005	0.968	0.789	0.050	0.996
7.5	0.9966	1.0094	-0.4256	1.103	0.889	0.011	0.996
8	0.9965	1.0049	-0.1730	1.108	0.877	-0.044	0.995
8.5	0.9957	1.0032	-0.1151	1.228	0.991	-0.026	0.995
9	0.9953	1.0034	-0.0916	1.276	1.030	-0.060	0.994
9.5	0.9945	1.0030	-0.1725	1.384	1.107	0.040	0.994
10	0.9946	1.0062	-0.1957	1.380	1.088	-0.077	0.994

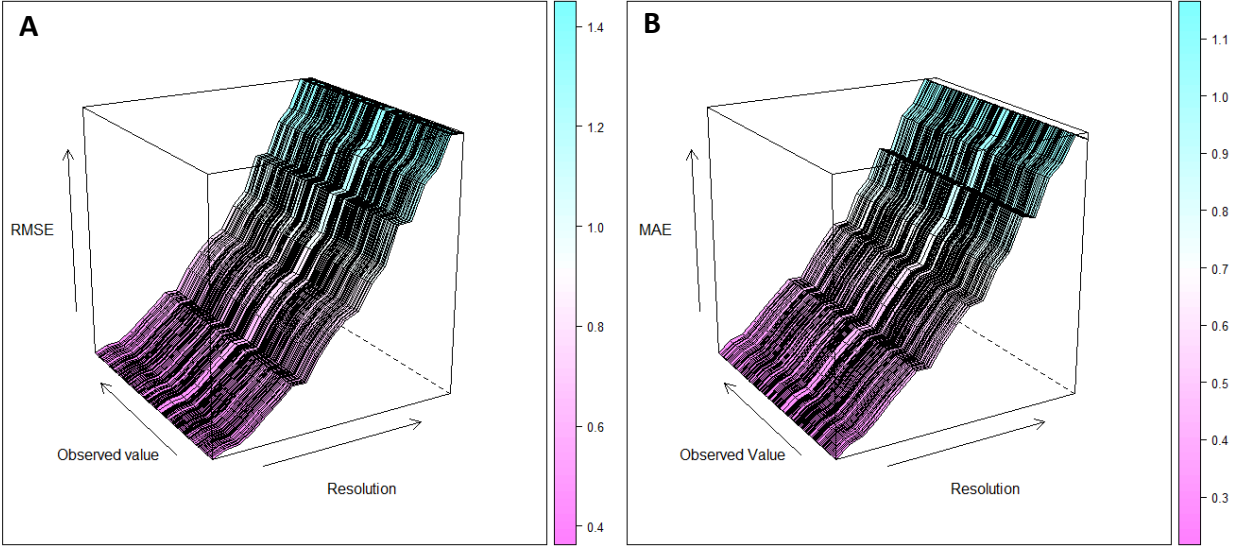


Figure 2.4 Effect of resolution at each observation point by A) RMSE (root mean square error) and B) MAE (mean absolute error).

2.3.2 Interpolation methods and data density

GPS points were thinned by 25%, 50%, and 75% and interpolated into three DEMs with 0.5 m resolution, using each of the three different interpolation methods. Thinning had little effect on r^2 relative to the DEM produced from the complete set of data points (0% thinned) (Table 2.4). Even with 75% thinning, the r^2 values only decreased to 0.999, 0.9952 and 0.9984 for Natural neighbour (NaN), Inverse distance weighting (IDW) and Topo to raster (ANUDEM), respectively. NaN had the lowest levels of bias at 25% (MBE = 0.004m) and 50% (MBE = -0.015m), while at 75% thinning, IDW exhibited the least bias (MBE = 0.029m).

Table 2.4 Comparison of the three methods at 0.5m resolution with different data density.

Method	Thinning (%)	r ²	Slope	Intercept	MBE
<i>Natural Neighbour (NaN)</i>	0	0.9995	1.004	-0.216	0.004
	25	0.9998	1.001	-0.090	0.004
	50	0.9997	1.003	-0.140	-0.015
	75	0.999	1.009	-0.370	-0.059
<i>Inverse Distance Weighting (IDW)</i>	0	0.9989	1.004	-0.269	0.059
	25	0.9989	1.004	-0.269	0.059
	50	0.9982	1.014	-0.730	0.116
	75	0.9952	1.027	-1.238	0.029
<i>Topo to Raster (ANUDEM)</i>	0	0.9998	1.005	-0.284	0.024
	25	0.9998	1.005	-0.282	0.022
	50	0.9996	1.010	-0.489	0.028
	75	0.9984	1.024	-1.046	-0.044

Given the high r² values, it is unsurprising that generally the observed and predicted were in agreement (Figure 2.5). The observed and predicted values of the data points were slightly more scattered in the DEM interpolated using IDW. Figure 2.5 also shows that the spread of the residuals increased when elevation data were thinned by 75% prior to DEM interpolation.

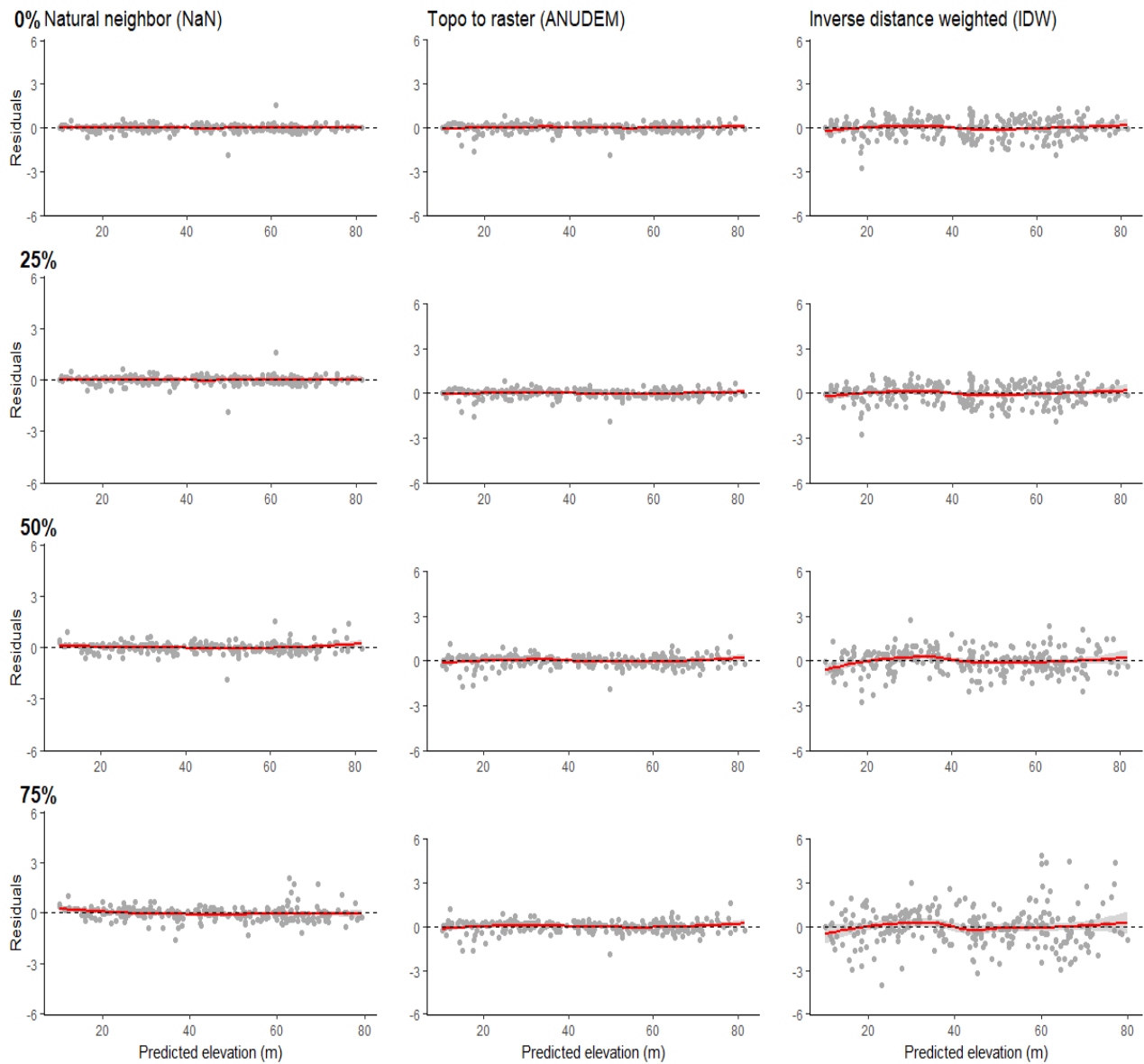


Figure 2.5 Residuals plotted against predicted elevation (m) for different models and levels of data thinning. Red line shows the model prediction trend.

RMSE and MAE data provide a better opportunity to discriminate between different interpolation algorithms with thinned data. IDW yielded the highest RMSE and MAE irrespective of the level of data thinning applied (Figure 2.6). RMSE ranged between 0.631m and 1.388m and MAE ranged between 0.471m and 0.984m for IDW. In contrast, NaN and ANUDEM

interpolations resulted in lower RMSE and MAE values at all thinning intensities. RMSE ranged between 0.239m and 0.614m and 0.305m and 0.877m for NaN and ANUDEM, respectively, while MAE ranged between 0.152m and 0.301m and 0.197m and 0.526m. Irrespective of interpolation algorithm, RMSE and MAE remained reasonably consistent until 75% thinning, when there was a large increase in both metrics. At 75% thinning the density of points used to interpolate the DEM was only 0.129 points m⁻², compared with 0.519 points m⁻² in the unthinned data.

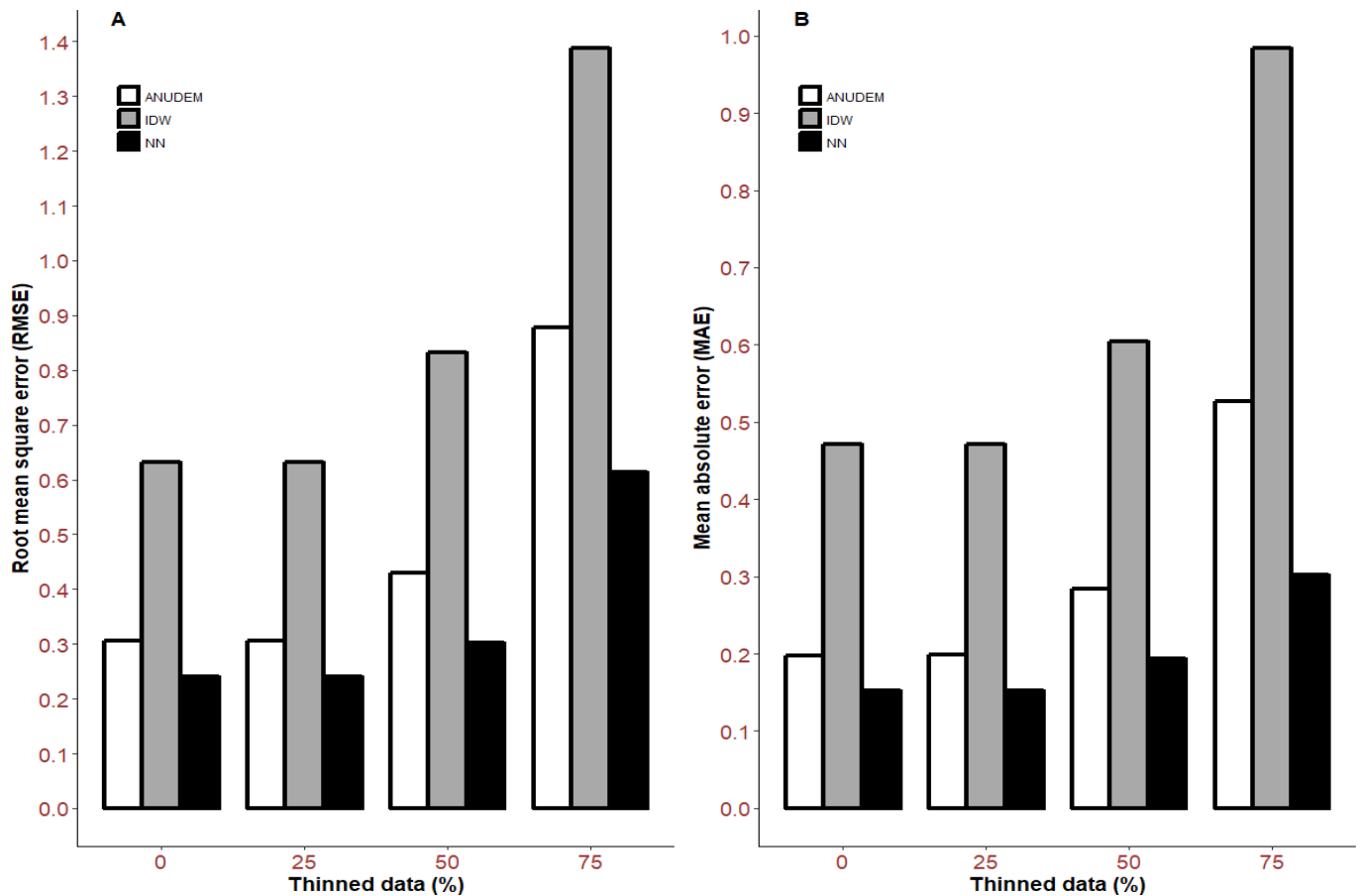


Figure 2.6 Comparison of three interpolation method in regards to different data density A) Root mean square error (RMSE) and B) Mean absolute error (MAE).

In addition to quantitative analyses, a visual inspection was carried out on the DEMs produced by the three interpolation methods. It was found that the IDW produced a less reliable surface with a lot of abnormalities (Figure 2.7(C0-3)). In contrast to that, the NaN and ANUDEM

produced more consistent and representative DEM surfaces. Moreover, among the two, ANUDEM interpolated the DEM surface, both with consistency and reliability in relation to the original surface (Figure 2.7(B0-3)). It resembled reality more closely, where NaN produced a surface that was overly smooth and unrealistic (Figure 2.7(A0-3)). With greater elevation data density, the surface better resembled the original natural surface, showing features like mounds or gullies. Whereas, with the reduction of elevation data points through thinning, the surface was rendered relatively smoothly and obscured topographic features that were visible with higher data densities. For example, a gully on the site was virtually invisible with the lowest data density (i.e. 75% thinning) (Figure 2.7(A3, B3, C3)).

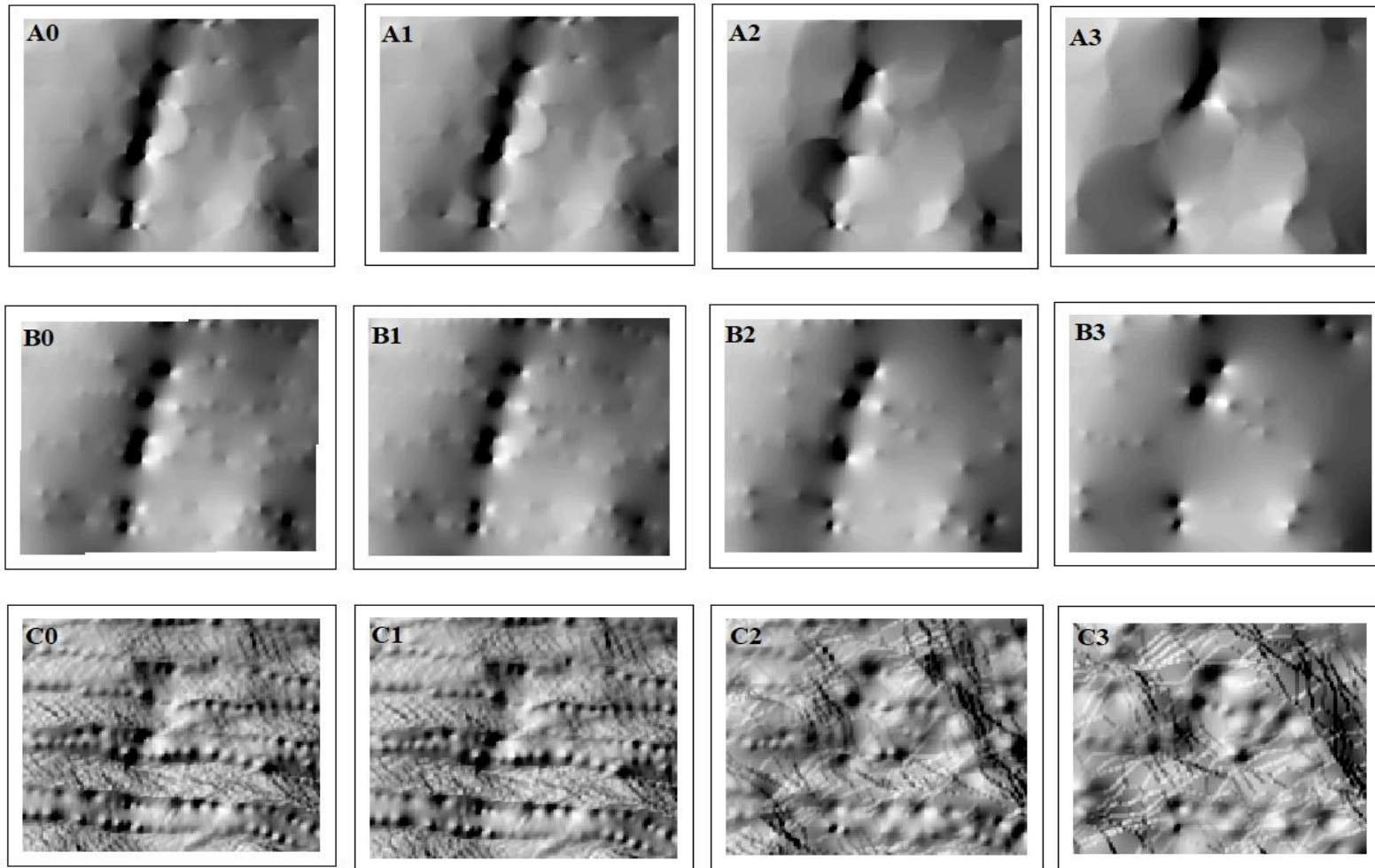


Figure 2.7 Hillshade surfaces produced from DEMs interpolated by: A) Nearest neighbour, B) ANUDEM and C) IDW. Numbers 0 to 3 represent 0%, 25%, 50%, and 75% elevation data thinning prior to DEM interpolation.

2.4 Discussion

2.4.1 An alternate data source

The GNSS surveyed elevation point data can be used to produce high-resolution DEM. Though aerial laser scanning data are commonly used for this purpose, its shortcomings may preclude its use in some instances. In contrast, collecting elevation data via GNSS surveys is inexpensive, easy to undertake, often with little or no specialist skill. The data density of ALS yields high accuracy and resolution (Anderson et al., 2006; Liu et al., 2007). However, depending on the desired DEM resolution, high point density associated with ALS data may not be needed (Anderson et al., 2006), suggesting that the relatively low elevation data density achievable with a GNSS approach may be appropriate under some conditions; however, this will depend on the required resolution, and the interpolation used to generate the DEM.

2.4.2 Optimal resolution

Spatial resolution is important for DEMs as many other surfaces can be derived from it. Errors in a DEM are perpetuated through to derived aspect, slope, hill-shade, and surface curvature surfaces, amongst many others. Moreover, DEMs are critical in their role for normalising digital surface models. In this study, errors in the DEM were minimised by increasing spatial resolution from 10m to 0.5m. This finding is in line with previous research showing that DEMs interpolated from LiDAR point clouds had accuracy proportional to spatial resolution (Kienzle, 2004; Ouma, 2016; Thomas et al., 2017). Although those results were based on LiDAR data, which typically has much greater point density than the point density achieved with the GNSS approach in this study, the underlying theory remains the same.

2.4.3 Influencers of DEM quality

The question of resolution and DEM accuracy is also dependent on the characteristics of the surface being modelled (Arun, 2013; Kienzle, 2004; Zimmerman et al., 1999). Flat surfaces can be interpolated accurately even with relatively few elevation points due to topographic homogeneity. In contrast, surfaces that are topographically heterogeneous are likely to require greater point density and higher resolution to capture small undulations or other features in the landscape.

Data density and distribution have also been shown to influence interpolation quality (Erdogan, 2009; Guo et al., 2010). The present study clearly showed that elevation point density influenced DEM quality. At low densities, a small number of data points are used for interpolation, creating a generalised surface; this is because most the deterministic approaches are mainly based on some simple mathematical functions (Erdogan, 2009). Li and Heap (2011) reported that data distribution had a greater effect, relative to data density, on the quality of the DEM produced.

On the contrary, it is not suitable to produce high-resolution DEM from sparse data as the surface will be shaped by the interpolator and interpolation artefacts will proliferate (Albani* et al., 2004; Florinsky, 2002; Liu et al., 2007) and the resolution constraints by the data density (Florinsky, 1998). For this study the all the data were collected in a way that was assumed to give an evenly distributed dataset. Hence, the effect of distribution was not tested explicitly. Moreover, the selection of validation points, thinning and study site characteristics would have resulted in some spatial variation in point distribution. Firstly, the validation points had a high positive spatial correlation with the training dataset as they were not independently collected and lying in line with each other. Secondly, even though the thinning routine was performed in a randomised manner, minor clustering may have influenced the results. Thirdly, the study site was relatively small.

Hence, it is expected that the results are site specific and could vary with changes in site or surface structure. For example, if the site was more rugged than this one, a higher error could be expected.

2.4.4 Deterministic interpolation method

The interpolation method is important for the accuracy of the interpolated digital elevation model because interpolation can vary with the nature of the surface terrain and spatial structure (Arun, 2013; Tan & Xu, 2014; Zimmerman et al., 1999). In the present study, though ANUDEM and NaN had similar quantitative metrics, ANUDEM produced a more realistic and consistent DEM, relative the NaN interpolation. NaN is mostly used in cases where there is a need to have a geo-morphologically smooth surface (Bobach & Umlauf, 2008), whereas ANUDEM tends to be useful where well-defined drainage and major topographic features exist (Hutchinson., 1989). It is important to note that there is no single optimal interpolation method, but rather many methods optimised by matching with particular end uses of the DEM (Li et al., 2000). This is further supported by Arun (2013) and Kienzle (2004), who stated that the interpolation method is mostly chosen based on the purpose and focus of the research. The implication of this research and previous studies is the importance of testing various interpolation algorithms for individual sites to guide through the process to get an optimised one.

2.5 Summary and conclusions

This study evaluated the quality of digital elevation models interpolated from elevation data acquired from a differentially corrected GNSS (RTK-GPS) receiver. Three interpolation methods (NaN, IDW, ANUDEM) were compared, as was the influence of different spatial resolutions and data density. With dense and regularly distributed data, a high-resolution DEM (0.5m) was interpolated with RMSE as low as 0.428m and MSE as low as 0.274m. Thinning the elevation point data by 25% or even 50% had minimal effect on the DEM quality. Despite similar

quality from a quantitative perspective, ANUDEM performed better than NaN and IDW interpolated DEMs from a qualitative perspective. In this study, the use of quantitative and qualitative approaches for judging DEM quality resulted in a better decision.

LiDAR data acquisition has become the standard approach for collecting point data to interpolate high-resolution ground and above-ground surfaces (e.g. canopy height model). LiDAR acquisition is generally only cost effective over large contiguous areas of land. The present results are promising for applications where it is unfeasible to acquire LiDAR data. The RMSE and MAE values are higher than those from LiDAR studies (Hodgson & Bresnahan, 2004), but are within an order of magnitude, and therefore comparable. In conclusion, the interpolation of data collected via GNSS surveys can yield accurate digital elevation models. This method should be considered alongside LiDAR data interpolation as a viable means of generating topographic surfaces, especially in cases where study areas are small and easily accessible. In these areas, the GNSS approach can provide a low cost, efficient, and effective solution to DEM creation.

2.6 References

- Albani*, M., Klinkenberg, B., Andison, D. W., & Kimmins, J. P. (2004). The choice of window size in approximating topographic surfaces from Digital Elevation Models. *International Journal of Geographical Information Science*, 18(6), 577-593. doi:10.1080/13658810410001701987
- Amjad, M., Ali, M. Z., & Shafique, M. (2016). Impact of DEM resolution and accuracy on remote sensing and topographic DEM derived topographic attributes and drainage pattern. *Journal of Himalayan Earth Science*, 49(2), 109-117.
- Anderson, E. S., Thompson, J. A., Crouse, D. A., & Austin, R. E. (2006). Horizontal resolution and data density effects on remotely sensed LiDAR-based DEM. *Geoderma*, 132(3), 406-415. doi:https://doi.org/10.1016/j.geoderma.2005.06.004
- Arun, P. V. (2013). A comparative analysis of different DEM interpolation methods. *The Egyptian Journal of Remote Sensing and Space Science*, 16(2), 133-139. doi:http://dx.doi.org/10.1016/j.ejrs.2013.09.001
- Bobach, T., & Umlauf, G. (2008). Natural neighbor concepts in scattered data interpolation and discrete function approximation. *Visualization of large and unstructured data sets*.
- Chaplot, V., Darboux, F., Bourennane, H., Legu dois, S., Silvera, N., & Phachomphon, K. (2006). Accuracy of interpolation techniques for the derivation of digital elevation models in relation to landform types and data density. *Geomorphology*, 77(1), 126-141.
- Curebal, I., Efe, R., Ozdemir, H., Soykan, A., & S nmez, S. (2016). GIS-based approach for flood analysis: case study of Ke idere flash flood event (Turkey). *Geocarto International*, 31(4), 355-366. doi:10.1080/10106049.2015.1047411
- Daly, C., Gibson, W. P., Taylor, G. H., Johnson, G. L., & Pasteris, P. (2002). A knowledge-based approach to the statistical mapping of climate. *Climate Research*, 22(2), 99-113.
- Erdogan, S. (2009). A comparison of interpolation methods for producing digital elevation models at the field scale. *Earth Surface Processes and Landforms*, 34(3), 366-376.
- ESRI. (2012). ArcGIS Release 10.1. Redlands, CA.
- Florinsky, I. V. (1998). Combined analysis of digital terrain models and remotely sensed data in landscape investigations. *Progress in Physical Geography: Earth and Environment*, 22(1), 33-60. doi:10.1177/030913339802200102

- Florinsky, I. V. (2002). Errors of signal processing in digital terrain modelling. *International Journal of Geographical Information Science*, 16(5), 475-501. doi:10.1080/13658810210129139
- Gao, J. (2007). Towards accurate determination of surface height using modern geoinformatic methods: possibilities and limitations. *Progress in Physical Geography: Earth and Environment*, 31(6), 591-605. doi:10.1177/0309133307087084
- Garnero, G., & Godone, D. (2013). Comparisons between different interpolation techniques. *Proceedings of the international archives of the photogrammetry, remote sensing and spatial information sciences XL-5 W, 3*, 27-28.
- Gong, J., Li, Z., Zhu, Q., Sui, H., & Zhou, Y. (2000). Effects of various factors on the accuracy of DEMs: An intensive experimental investigation. *Photogrammetric Engineering and Remote Sensing*, 66(9), 1113-1117.
- Greenwood, D. J., Neeteson, J. J., & Draycott, A. (1985). Response of potatoes to N fertilizer: dynamic model. *Plant and Soil*, 85(2), 185-203. doi:10.1007/bf02139623
- Grimaldi, S., Teles, V., & Bras, R. L. (2004). Sensitivity of a physically based method for terrain interpolation to initial conditions and its conditioning on stream location. *Earth Surface Processes and Landforms*, 29(5), 587-597. doi:doi:10.1002/esp.1053
- Grimaldi, S., Teles, V., & Bras, R. L. (2005). Preserving first and second moments of the slope area relationship during the interpolation of digital elevation models. *Advances in Water Resources*, 28(6), 583-588. doi:https://doi.org/10.1016/j.advwatres.2004.11.014
- Groves, P. D. (2013). *Principles of GNSS, inertial, and multisensor integrated navigation systems*: Artech house.
- Guo, Q., Li, W., Yu, H., & Alvarez, O. (2010). Effects of topographic variability and LiDAR sampling density on several DEM interpolation methods. *Photogrammetric Engineering & Remote Sensing*, 76(6), 701-712.
- Habtezion, N., Tahmasebi Nasab, M., & Chu, X. (2016). How does DEM resolution affect microtopographic characteristics, hydrologic connectivity, and modelling of hydrologic processes? *Hydrological Processes*, 30(25), 4870-4892. doi:10.1002/hyp.10967
- Hessl, A., Miller, J., Kernan, J., Kenum, D., & McKenzie, D. (2007). Mapping paleo-fire boundaries from binary point data: comparing interpolation methods. *The Professional Geographer*, 59(1), 87-104.

- Hodgson, M. E., & Bresnahan, P. (2004). Accuracy of airborne LiDAR-derived elevation. *Photogrammetric Engineering & Remote Sensing*, 70(3), 331-339. doi:10.14358/PERS.70.3.331
- Hofmann-Wellenhof, B., Lichtenegger, H., & Collins, J. (2012). *Global positioning system: theory and practice*: Springer Science & Business Media.
- Hutchinson, M. (1989). A new procedure for gridding elevation and stream line data with automatic removal of spurious pits. *Journal of Hydrology*, 106(3-4), 211-232.
- Hutchinson., M. F. (1989). A new procedure for gridding elevation and stream line data with automatic removal of spurious pits. *Journal of Hydrology*, 106(3), 211-232. doi:https://doi.org/10.1016/0022-1694(89)90073-5
- Kidner, D. B. (2003). Higher-order interpolation of regular grid digital elevation models. *International Journal of Remote Sensing*, 24(14), 2981-2987. doi:10.1080/0143116031000086835
- Kienzle, S. (2004). The effect of DEM raster resolution on first order, second order and compound terrain derivatives. *Transactions in GIS*, 8(1), 83-111. doi:10.1111/j.1467-9671.2004.00169.x
- Koci, J., Jarihani, B., Leon, J. X., Sidle, R., Wilkinson, S., & Bartley, R. (2017). Assessment of UAV and ground-based structure from motion with multi-view stereo photogrammetry in a gullied savanna catchment. *ISPRS International Journal of Geo-Information*, 6(11), 328.
- Kodors, S. (2017). Point distribution as true quality of LiDAR point cloud. *Baltic Journal of Modern Computing*, 5(4), 362-378.
- Kurz, T. H., Buckley, S. J., Howell, J. A., & Schneider, D. (2009, 26-28 Aug. 2009). *Close range hyperspectral and lidar data integration for geological outcrop analysis*. Paper presented at the 2009 First Workshop on Hyperspectral Image and Signal Processing: Evolution in Remote Sensing.
- Lam, N. S.-N. (1983). Spatial interpolation methods: a review. *The American Cartographer*, 10(2), 129-150. doi:10.1559/152304083783914958
- Ledoux, H., & Gold, C. (2005). *An efficient natural neighbour interpolation algorithm for geoscientific modelling*, Berlin, Heidelberg.
- Li, J., & Heap, A. D. (2008). A review of spatial interpolation methods for environmental scientists. *Geoscience Australia, Canberra* (No. Record 200/23).

- Li, J., & Heap, A. D. (2011). A review of comparative studies of spatial interpolation methods in environmental sciences: performance and impact factors. *Ecological Informatics*, 6(3), 228-241. doi:<http://dx.doi.org/10.1016/j.ecoinf.2010.12.003>
- Li, J., & Heap, A. D. (2014). Spatial interpolation methods applied in the environmental sciences: a review. *Environmental Modelling & Software*, 53, 173-189. doi:<http://dx.doi.org/10.1016/j.envsoft.2013.12.008>
- Li, X., Cheng, G., & Lu, L. (2000). Comparison of spatial interpolation methods. *Advance in Earth sciences*, 3, 003.
- Liu, X. (2008). Airborne LiDAR for DEM generation: some critical issues. *Progress in Physical Geography: Earth and Environment*, 32(1), 31-49. doi:10.1177/0309133308089496
- Liu, X., Zhang, Z., Peterson, J., & Chandra, S. (2007). *The effect of LiDAR data density on DEM accuracy*. Paper presented at the Proceedings of the International Congress on Modelling and Simulation (MODSIM07).
- Miller, J. (2005). Incorporating spatial dependence in predictive vegetation models: residual interpolation methods. *The Professional Geographer*, 57(2), 169-184. doi:10.1111/j.0033-0124.2005.00470.x
- Mitas, L., & Mitasova, H. (1999). Spatial interpolation. *Geographical information systems: principles, techniques, management and applications*, 1, 481-492.
- Morgenroth, J., & Visser, R. (2013). Uptake and barriers to the use of geospatial technologies in forest management. *New Zealand Journal of Forestry Science*, 43(1), 16. doi:10.1186/1179-5395-43-16
- Neményi, M., Mesterházi, P. Á., Pecze, Z., & Stépán, Z. (2003). The role of GIS and GPS in precision farming. *Computers and Electronics in Agriculture*, 40(1), 45-55. doi:[https://doi.org/10.1016/S0168-1699\(03\)00010-3](https://doi.org/10.1016/S0168-1699(03)00010-3)
- Niemann, J. D., Bras, R. L., & Veneziano, D. (2003). A physically based interpolation method for fluvially eroded topography. *Water Resources Research*, 39(1). doi:doi:10.1029/2001WR001050
- NIWA. (2015). Overview of New Zealand climate. Retrieved from <https://www.niwa.co.nz/education-and-training/schools/resources/climate/overview>
- Olivera, A., Visser, R., Acuna, M., & Morgenroth, J. (2016). Automatic GNSS-enabled harvester data collection as a tool to evaluate factors affecting harvester productivity in a *Eucalyptus*

- spp. harvesting operation in Uruguay. *International Journal of Forest Engineering*, 27(1), 15-28. doi:10.1080/14942119.2015.1099775
- Ouma, Y. (2016). Evaluation of multiresolution Digital Elevation Model (DEM) from real-time kinematic GPS and ancillary data for reservoir storage capacity estimation. *Hydrology*, 3(4). doi:10.3390/hydrology3020016
- Parkinson, B. W., Enge, P., Axelrad, P., & Spilker Jr, J. J. (1996). *Global positioning system: Theory and applications, Volume II*: American Institute of Aeronautics and Astronautics.
- Peralvo, M., & Maidment, D. (2004). Influence of DEM interpolation methods in drainage analysis. *Gis Hydro*, 4.
- Philip, G., & Watson, D. F. (1982). A precise method for determining contoured surfaces. *The APPEA Journal*, 22(1), 205-212.
- Pick, J. (2006). A case-study analysis of costs and benefits of geographic information systems: relationships to firm size and strategy. *AMCIS 2006 Proceedings*, 207.
- R Core Team. (2015). R: A language and environment for statistical computing. Vienna, Austria; 2014. URL <http://www.R-project.org>.
- Robinson, T. P., & Metternicht, G. (2006). Testing the performance of spatial interpolation techniques for mapping soil properties. *Computers and Electronics in Agriculture*, 50(2), 97-108. doi:<http://dx.doi.org/10.1016/j.compag.2005.07.003>
- Salari, A., Zakaria, M., Nielsen, C. C., & Boyce, M. S. (2014). Quantifying tropical wetlands using field surveys, spatial statistics and remote sensing. *Wetlands*, 34(3), 565-574. doi:10.1007/s13157-014-0524-3
- Sandmeier, S., & Itten, K. I. (1997). A physically-based model to correct atmospheric and illumination effects in optical satellite data of rugged terrain. *IEEE Transactions on Geoscience and Remote Sensing*, 35(3), 708-717. doi:10.1109/36.581991
- Shi, W. Z., & Tian, Y. (2006). A hybrid interpolation method for the refinement of a regular grid digital elevation model. *International Journal of Geographical Information Science*, 20(1), 53-67. doi:10.1080/13658810500286943
- Sibson, R. (1981). A brief description of natural neighbor interpolation. *Interpreting Multivariate Data*, 21-36.

- Tagarakis, A. C., Koundouras, S., Fountas, S., & Gemtos, T. (2018). Evaluation of the use of LiDAR laser scanner to map pruning wood in vineyards and its potential for management zones delineation. *Precision Agriculture*, *19*(2), 334-347. doi:10.1007/s11119-017-9519-4
- Tan, Q., & Xu, X. (2014). Comparative analysis of spatial interpolation methods: an experimental study. *Sensors & Transducers*, *165*(2), 155-163.
- Thomas, I. A., Jordan, P., Shine, O., Fenton, O., Mellander, P. E., Dunlop, P., & Murphy, P. N. C. (2017). Defining optimal DEM resolutions and point densities for modelling hydrologically sensitive areas in agricultural catchments dominated by microtopography. *International Journal of Applied Earth Observation and Geoinformation*, *54*, 38-52. doi:<https://doi.org/10.1016/j.jag.2016.08.012>
- Torlegård, K., Östman, A., & Lindgren, R. (1986). A comparative test of photogrammetrically sampled digital elevation models. *Photogrammetria*, *41*(1), 1-16. doi:[https://doi.org/10.1016/0031-8663\(86\)90002-5](https://doi.org/10.1016/0031-8663(86)90002-5)
- Traganos, D., Poursanidis, D., Aggarwal, B., Chrysoulakis, N., & Reinartz, P. (2018). Estimating Satellite-Derived Bathymetry (SDB) with the Google earth engine and Sentinel-2. *Remote Sensing*, *10*(6), 859.
- Trimble. (2017). Trimble R8s GNSS system. In Trimble Inc. (Ed.), <https://geospatial.trimble.com/products-and-solutions>. USA.
- Vaze, J., & Teng, J. (2007). *High resolution LiDAR DEM—how good is it?* Paper presented at the Modelling and Simulation.
- Vicente-Serrano, S. M., Saz-Sánchez, M. A., Cuadrat, J. M. (2003). Comparative analysis of interpolation methods in the middle Ebro Valley (Spain): application to annual precipitation and temperature. *Climate Research*, *24*(2), 161-180.
- Webster, R., & Oliver, M. (2001). *Geostatistics for Environmental Scientists (Statistics in Practice)*: Wiley.
- Willmott, C. J. (1981). On the validation of models. *Physical Geography*, *2*(2), 184-194. doi:10.1080/02723646.1981.10642213
- Willmott, C. J. (1982). Some comments on the evaluation of model performance. *Bulletin of the American Meteorological Society*, *63*(11), 1309-1313. doi:10.1175/1520-0477(1982)063<1309:scoteo>2.0.co;2

- Yao, H., & Clark, R. L. (2000). Evaluation of sub-meter and 2 to 5 meter accuracy GPS receivers to develop digital elevation models. *Precision Agriculture*, 2(2), 189-200. doi:10.1023/a:1011429815226
- Yu, B., Liu, H., Wu, J., Hu, Y., & Zhang, L. (2010). Automated derivation of urban building density information using airborne LiDAR data and object-based method. *Landscape and Urban Planning*, 98(3), 210-219. doi:https://doi.org/10.1016/j.landurbplan.2010.08.004
- Zimmerman, D., Pavlik, C., Ruggles, A., & Armstrong, M. P. (1999). An experimental comparison of ordinary and universal kriging and inverse distance weighting. *Mathematical Geology*, 31(4), 375-390. doi:10.1023/a:1007586507433

3

Modelling the effect of environmental micro-site influences on the growth of juvenile *Eucalyptus globoidea* and *Eucalyptus bosistoana* in New Zealand

3. Modelling the effect of environmental micro-site influences on the growth of juvenile *Eucalyptus globoidea* and *Eucalyptus bosistoana* in New Zealand.

3.1 Introduction

The term “site”, used as a primary ecological unit, plays an important role as one of the principal factors in the survival and growth of trees at different scales (Radford et al., 2002). It refers to a geographical location with a homogenous physical and biological environment (Bailey et al., 1978; Grey, 1980). In a forestry context, plantation forest sites, typically called stands, are specific bounded areas that receive similar silvicultural treatments (Louw, 1999; Skovsgaard & Vanclay, 2008). However, although plantation forests are homogenised through silviculture, their growth shows considerable spatial and temporal variability (Skovsgaard & Vanclay, 2013).

The two main components of a site that control its productivity are its soil and associated climate. They developed over time through plant-soil interactions involving soil moisture, nutrients and gas-exchange (Bohlen et al., 2001; Koch et al., 2004; Mooney et al., 1987). Koch et al. (2004) reported a direct relationship between soil moisture and plant height growth, while Parton et al. (1987) documented meteorological effects on soil properties. Skovsgaard and Vanclay (2008) defined site productivity as the potential of a particular stand to produce aboveground biomass. Variation in site productivity has long been a subject of interest to researchers, forest managers and owners. Normally, it depends on soil, climate and management regimes. In many cases, it is assumed to change gradually and predictably. Previously, large-scale site variation has been extensively researched (e.g., Berrill & O'Hara, 2015; Bravo-Oviedo et al., 2008; Landsberg, 2003). However, forests can be organised on different scales (Wiens, 1989) including small scales that directly affect forest productivity (Chen et al., 1999). Small scale or micro-site variation has been recently explored in both mature natural forests (Coates, 2002; Kuuluvainen, 2002; Martín-

Alcón et al., 2015; Narukawa & Yamamoto, 2001) and plantation forests (Mummery & Battaglia, 2002; Weiskittel et al., 2008). The topic of micro-site variation in plantation forests merits further attention.

Forest growth models are mostly developed for established trees (Spiecker et al., 1996) that have undergone canopy closure, when competition among trees is active (Zhang et al., 1996). Stand and individual tree-level growth models, and simulators have been well researched (Burkhart & Tomé, 2012; Clutter, 1963; Daniels & Burkhart, 1988; Ek, 1974; Garcia, 1984; Goulding, 1979; Weiskittel et al., 2011). Juvenile growth models for the period prior to canopy closure and competition are rare (Avila, 1993). However, such juvenile growth models could explain the unique features of young stands, as listed by Mason and Whyte (1997). Also, juvenile growth models can provide information about the whole stand development process, and therefore assist in scheduling silvicultural treatments (Mason & Whyte, 1997; Zhang et al., 1996). Moreover, juvenile growth is often more complex than mature stand growth, as both inter- and intra-specific competition occurs among the trees.

Information produced by traditional time-based mensurational growth models from inventory data can guide the decision making process in forest management. Such models are robust and simple, but sacrifice the explanatory ability of ecophysiological process of tree growth. For this reason, the addition of tree growth factors (e.g., edaphic and biotic) into models can improve precision and accuracy, and enhance understanding of the modelled system (Casnati, 2016). Models explanatory ability can be improved by several approaches. Among them, integrating growth factors into the mathematical environment is the most common procedure for both juvenile (Mason, 2001; Mason & Whyte, 1997) and mature stand models (Weiskittel et al., 2011; Woollons et al., 1997). Another approach used is to replace the stand age with structural

explanatory indices (Snowdon et al., 1999). These hybrid approaches give a physiological understanding of traditional mensurational models, yet do not require a high number of parameters like ecophysiological models (Mäkelä et al., 2000). So, the usefulness of hybrid models has been considered as an improvement over mensurational and ecophysiological models (Mäkelä et al., 2000; Watt et al., 2004).

Like the agricultural sector, production forestry is moving towards a precision approach (Dyck, 2003), which requires measurement of individual tree growth and response to fine-scale environmental conditions and silvicultural treatments. Precision agriculture and forestry rely on multi-scalar data collection techniques, e.g. remote sensing (Adão et al., 2017; Akay et al., 2009) and geostatistical techniques, e.g. surface interpolation (Salekin et al., 2018). The challenge for precision forestry is to adapt traditional growth modelling to take advantage of relatively new abilities to describe environmental conditions at a fine spatial scale.

This study explores a comprehensive set of topographic, edaphic and climatic explanatory variable effects at the micro-site level on the growth and survival of small plots of trees in juvenile plantations. Hence, the main research objectives were,

- i) To identify micro-site level topographic, edaphic and climatic variables that influence the height growth of juvenile *Eucalyptus globoides* and *Eucalyptus bosistoana*, and to include these in a height growth model.
- ii) To identify micro-site level topographic, edaphic and climatic variables that influence the survival of juvenile *E. globoides* and *E. bosistoana*, and to include these in a survival model.

3.2 Materials and methods

3.2.1 Experimental sites

The study was conducted in a subhumid climate zone of the South Island of New Zealand. The three experimental sites for this study were situated close to Blenheim, New Zealand (Figure 3.1). Site A, B, and C have areas 4.7, 3.7 and 2.2 hectares, respectively and are planted with *E. globoidea* (Site A) and *E. bosistoana* (Sites B and C) (Table 3.1).

The region in which the trial sites are located is sheltered by high country to the west, south and in some areas to the east, and it is one of the sunniest regions of New Zealand (NIWA, 2015). Warm, dry and settled weather predominates during summer, while winter days often begin with a frost, but are usually mild overall. Typical summer daytime maximum air temperatures range from 20°C to 26°C, but occasionally rise above 30°C. Typical winter daytime maximum air temperatures range from 10°C to 15°C (NIWA, 2015). Northeast winds prevail in Nelson, while south-westerlies prevail in Blenheim. High temperatures are frequent in Blenheim and may be accompanied by dry Foehn winds from the northwest (NIWA, 2015).

The soils at these sites are formed from loess and classified as Pallic Argillic soils (New Zealand Department of Scientific and Industrial Research, 1968) commonly categorised as Flaxbourne soils. Pallic Argillic soils have clay accumulations found as thin subsoil bands and occur predominantly in the seasonally dry eastern parts of the North and South Islands and in the Manawatu region of New Zealand. Parent materials in the region are commonly loess derived from schist or greywacke, which cover approximately 12% of New Zealand. According to Land Resource Information System (2015), the trial sites are considered to have very low productivity. Detail soil classification information of three study sites presented in Table 3.5.

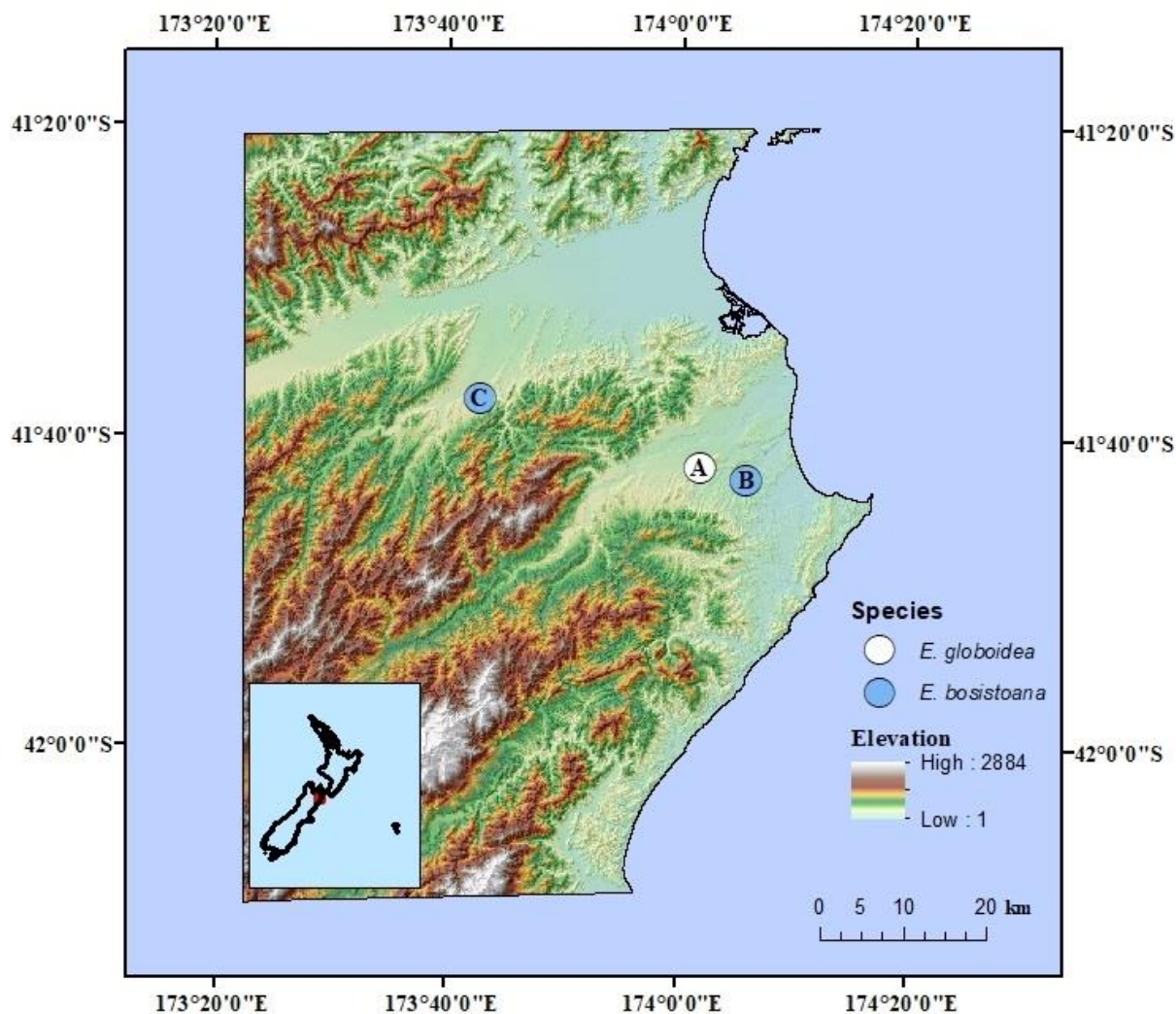


Figure 3.1 Study site locations.

3.2.2 Data collection and preparation

Data related to stands, climate and soils were collected for both species from all three experimental sites. The data collection and preparation procedures are described below.

3.2.2.1 Tree data

Sites A, B and C were established respectively in 2011, 2009 and 2012. Site A and C have 282, and 108 plots, respectively with each plot measuring 14.4m x 10.8m, and site B have

150 plots measuring 12m x 10.8m (Table 3.1). Trees were planted in regular rows and columns within plots with spacing equal to 2.4m x 1.8m in all sites.

There were approximately 25,000 trees at the three sites. The height (h), diameter at breast height at 1.4m (DBH), and tree status (dead or alive) were measured for all trees. All tree measurements were undertaken during November-January 2015-2016 and again in June-August 2017 (Table 3.1). Prior to these measurements, the New Zealand Dryland Forest Initiative (NZDFI) conducted a tree inventory by measuring the height and tree status at age 1.2 years.

Individual tree height and survival data were averaged at each plot. Due to the small height and stem diameter of the trees, there were not enough DBH measurements to use or calculate basal area. Even, the root collar diameter measurement was not available. The survival proportion (S) was calculated for each plot from the average number of surviving trees.

Height data from all three sites were used to create the juvenile height model. For survival data, only the A and C sites survival proportion (S) were used to create the juvenile survival model, as there was a thinning trial in the B site prior to completion of field measurements for this study.

Table 3.1 Summary of the plantation inventory data.

Site	A				B				C			
<i>Variable</i>	<i>Height</i>		<i>Survival</i>		<i>Height</i>		<i>Survival</i>		<i>Height</i>		<i>Survival</i>	
	<i>Fit.</i>	<i>Vald.</i>	<i>Fit.</i>	<i>Vald.</i>	<i>Fit.</i>	<i>Vald.</i>	<i>Fit.</i>	<i>Vald.</i>	<i>Fit.</i>	<i>Vald.</i>	<i>Fit.</i>	<i>Vald.</i>
Est. (Year)	2011				2009				2012			
Area (ha)	4.7				3.7				2.2			
Trees	12,000				8,000				5,000			
Age (year)	6				8				5			
Plots (n)	217	65	217	65	112	38	-	-	81	27	81	27
Ht(m)												
<i>Mean</i>	1.54	1.48	-	-	4.88	4.99	-	-	2.11	2.04	-	-
<i>Min</i>	0.33	0.46	-	-	0.98	1.07	-	-	1.29	1.26	-	-
<i>Max</i>	4.58	3.67	-	-	13.47	13.66	-	-	3.74	2.93	-	-
<i>SD</i>	0.84	0.73	-	-	2.60	2.69	-	-	0.52	0.44	-	-
S												
<i>Mean</i>	-	-	0.75	0.74	-	-	-	-	-	-	0.99	0.99
<i>Min</i>	-	-	0.19	0.33	-	-	-	-	-	-	0.89	0.92
<i>Max</i>	-	-	1.00	1.00	-	-	-	-	-	-	1.00	1.00
<i>SD</i>	-	-	0.18	0.19	-	-	-	-	-	-	0.02	0.02

3.2.2.2 Topographic data

The digital elevation model (DEM) for all the sites was produced by using a real-time kinetic geo-positioning system (RTK-GPS). The unit was carried on transect lines across the sites, with coordinates and elevation collected at five-metre intervals along the transects. The final digital elevation model (DEM) was produced by the process described in “Chapter 2”.

Next, primary and secondary surface attributes were derived from the DEM. The primary attributes include elevation, aspect, and slope (Travis et al., 1975). From these, the following secondary indices were calculated: total, profile and plan curvature (Heerdegen & Beran, 1982; Zevenbergen & Thorne, 1987); topographic ruggedness (TRI) (Riley et al., 1999); topographic position (TPI) (Weiss, 2001); topographic wetness (WTI) (Beven & Kirkby, 1979; Moore et al., 1991); wind exposure (WEI) (Gerlitz et al., 2015); and morphometric protection (MPI) index (Yokoyama et al., 2005) (details of these indices are described in Table 3.2). Table 3.3 represents the summary statistics of these indices. All surfaces were interpolated or derived using ArcMap v.10.4 (ESRI, 2012) and the System For Automated Geoscientific Analysis (SAGA) (Conrad et al., 2015).

1 Table 3.2 Description of the topographic attributes.

Type	Equation	Properties	Reference	
<i>Primary attributes</i>	<i>Elevation</i>	Value at each point of the DEM	Above sea level (a.s.l) in meters.	(Speight, 1980; Travis et al., 1975)
	<i>Slope</i>	$\arctan[(G^2 + H^2)^{\frac{1}{2}}]$	Steepness in degrees.	(Moore et al., 1991; Speight, 1980; Travis et al., 1975)
<i>Secondary attributes</i>	<i>Curvature</i>	$CV = 2E - 2D$	Higher value = convex surface Lower value = concave surface <i>Can take negative value.</i>	(Heerdegen & Beran, 1982; Zaslavsky & Sinai, 1981; Zevenbergen & Thorne, 1987)
	<i>Profile curvature</i>	$CVPRO = -2 \frac{DH^2 + EH^2 + FGH}{G^2 + H^2}$	Higher value = vertical surface convexity Lower value = vertical surface concavity <i>Can take negative value.</i>	(Heerdegen & Beran, 1982; Zaslavsky & Sinai, 1981; Zevenbergen & Thorne, 1987)
	<i>Plan curvature</i>	$CVPLA = 2 \frac{DH^2 + EH^2 - FGH}{G^2 + H^2}$	Higher value = horizontal surface convexity Lower value = horizontal surface concavity <i>Can take negative value.</i>	(Heerdegen & Beran, 1982; Zaslavsky & Sinai, 1981; Zevenbergen & Thorne, 1987)
	<i>Ruggedness index</i>	$TRI = Y \left[\sum (X_{ij} - X_{00})^2 \right]^{1/2}$	Terrain heterogeneity. Higher values represent the more heterogeneous surface.	(Riley et al., 1999)
	<i>Position index</i>	$TPI<scalefactor> = \text{int}(\text{DEM} - \text{focalmean}(\text{DEM}, \text{annulus}, \text{irad}, \text{orad}) + 0.5)$	Higher value = overall convexity Lower value = overall concavity	(Weiss, 2001)

		<i>Can take negative value.</i>	
<i>Wetness index</i>	$TWI = W = qa/bT \sin \theta$	Values can be >0. Greater values correspond to increasing surface wetness.	(Beven & Kirkby, 1979; Montgomery & Dietrich, 1994)
<i>Wind exposure index</i>	$WEI = \frac{\sum_{i=1}^n \frac{1}{d_{WHi}} \cdot \tan^{-1} \left(\frac{d_{WZi}}{d_{WHi}} \right)}{\sum_{i=1}^n \frac{1}{d_{LHi}} + \frac{\sum_{i=1}^n \frac{1}{d_{LHi}} \cdot \tan^{-1} \left(\frac{d_{LZi}}{d_{LHi}} \right)}{\sum_{i=1}^n \frac{1}{d_{LHi}}}}$	<p>Higher value = High wind exposed</p> <p>Lower value = Low wind exposed</p>	(Böhner & AntoniĆ, 2009; Gerlitz et al., 2015)
<i>Morphometric protection index (MPI)</i>	$D\phi L = 90 - D\beta L$ $D\psi L = 90 + D\delta L$ $\phi_L = (0\phi L + 45\phi L + \dots + 315\phi L)/8$ $\psi_L = (0\psi L + 45\psi L + \dots + 315\psi L)/8$	<p>Higher value = Less protected by surroundings</p> <p>Lower value = More protected from surroundings.</p>	(Yokoyama et al., 2005)
<i>Distance from the top ridge (DIST)</i>	<i>Linear distance to every plot centre from the top ridgeline.</i>	Value increases with distance from the nearest ridgeline	

Table 3.3 Summary of the topographic attributes for study sites.

Attributes	A				B				C			
	<i>Min</i>	<i>Max</i>	<i>Mean</i>	<i>SD</i>	<i>Min</i>	<i>Max</i>	<i>Mean</i>	<i>SD</i>	<i>Min</i>	<i>Max</i>	<i>Mean</i>	<i>SD</i>
<i>Aspect (°)</i>	5	356	127	137	56	346	125	84	209	330	266	26
<i>Slope(°)</i>	14	32	24	4	12	30	21	3	9	29	22	5
<i>Elevation (m)</i>	13	79	45	17	134	168	149	10	233	278	257	12
<i>Curvature</i>	-2	4	0.1	1	-2	5	0.2	1	-3	3	0.3	1
<i>Profile curvature</i>	-3	2	-0.01	0.7	-2	1	-0.1	0.6	-2	3	0.00	1
<i>Plan curvature</i>	-2	2	0.10	1	-1	3	0.1	1	-2	2	0.30	1
<i>TRI</i>	0.5	1	1	0.2	0.1	0.2	0.1	0.0	0.1	0.2	0.1	0.0
<i>TPI</i>	-2	4	0.1	1	-14	13	-1	7	-14	10	-1	7
<i>WTI</i>	0	4	1	1	-0.1	3	1	1	0	7	3	4
<i>WEI</i>	0.5	1	1	0.1	0.8	1	1	0.1	0.5	1	1	0.1
<i>MPI</i>	0.1	0.2	0.1	0.1	0.1	0.2	0.1	0.0	0.1	0.2	0.1	0.0

3.2.2.3 Soil data

Each of the three experimental sites was stratified by a combination of aspect and slope. Soil pits (n = 31) were excavated to one-metre depth within the different strata to collect soil samples. The physical properties of the soil samples and pits were described according to Gradwell (1972). In addition, soil profile depth, rooting depth, and soil penetrability were measured for each pit (Table 3.4). A set of randomly chosen subsamples (n = 30) from these pits were tested for their moisture retention characteristics. There were no visual signs for limited nutrition.

Table 3.4 Summary statistics of soil pits with rooting depth.

Variables	A				B				C			
	<i>Min</i>	<i>Max</i>	<i>Mean</i>	<i>SD</i>	<i>Min</i>	<i>Max</i>	<i>Mean</i>	<i>SD</i>	<i>Min</i>	<i>Max</i>	<i>Mean</i>	<i>SD</i>
<i>Total pits</i>	12				11				8			
<i>Rooting depth (cm)</i>	48.00	100.0*	74.92	17.8	50.0	100.0	81.36	18.56	90	100	93.75	3.15
<i>Elevation (m)</i>	13.19	60.89	33.43	11.9	128	159.7	141.56	9.93	233	269.5	251.37	12.83
<i>Slope (°)</i>	12.50	26.31	22.01	4.31	11.2	24.61	19.05	3.69	10.8	25.57	18.20	4.61
<i>Aspect (°)</i>	4.91	357.1	79.01	129	46.1	345.3	230.91	139.01	266	315.4	292.04	16.49

*1 meter/100cm was the maximum depth of soil pits.

Table 3.5 Soil description of three sites according to Hewitt (2010).

<i>Site</i>	<i>Soil series</i>	<i>Dominant soil type</i>	<i>Soil class</i>	<i>Class name</i>	<i>Comments</i>
A	Flaxbourne	Hill soils	PJT	Typic argillic pallic	Argillic pallic soils have a clay accumulation in the sub-soils
B	Flaxbourne	Hill soils	PJT	Typic argillic pallic	
C	Wither	Hills soils	PXJN	Argillic-sodic fragic pallic	Fragic pallic soils are predominantly silty and severely restrict root movement.

3.2.2.4 Climatic data

Each site had an independent meteorological station established in close proximity. Each station was equipped with radiation, temperature and moisture loggers, and wind and rain sensors. There were 20 additional air temperature loggers installed in the A and B sites at one meter above ground to measure the air temperature variation within the sites. All the loggers, including the meteorological stations, collected data at 30-minute intervals from 2015 to 2017.

The independent temperature logger data were summarised by average daily and maximum monthly temperatures for the whole period (Table 3.6 and Figure 3.2 (A, B)). The temperature differences between these loggers and the temperature logger within the meteorological stations were calculated (Figure 3.2(C, D)).

Table 3.6 Summary of the average daily maximum monthly temperature.

Sites	Total number	logger	Summary statistics			
			<i>Min</i>	<i>Max</i>	<i>Mean</i>	<i>SD</i>
A	10		13.23	34.34	22.45	4.50
B	10		12.66	45.59	21.25	5.42

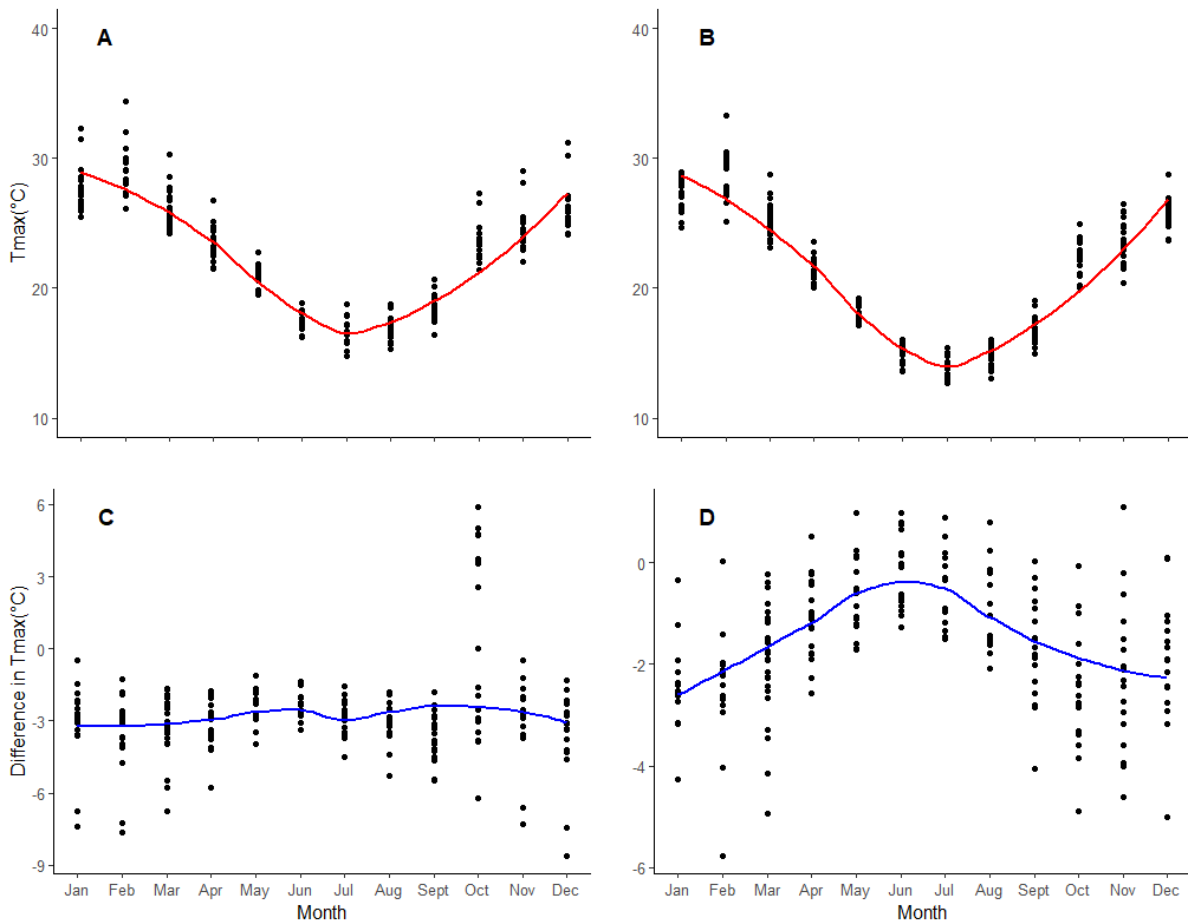


Figure 3.2 Daily maximum temperature by month at A) A, and B) B sites (red line showed the general monthly temperature trend); C) and D) represents the temperature difference at A and B sites from the independent weather station temperature (blue line showed the general trend).

3.2.3 Modelling approach

3.2.3.1 Soil rooting depth model

Soil moisture availability is important for tree growth, but it is crucial at the seedling stage, and it often relates to seedling growth and survival. Padilla and Pugnaire (2007) found a positive relationship with soil moisture availability in dryland areas with rooting depth. Seedlings experiencing deeper rooting depth can have better growth and survival rates as they have the opportunity to access more moisture and nutrients available in the soil. Because of this, gaining knowledge about soil rooting depth is desirable for growth and survival modelling. Unfortunately, it is hard to measure soil rooting depth over large areas, due to soil heterogeneity. However, it may be possible to estimate soil rooting depth for large areas based on topographic attributes (Burke et al., 1999; Chen et al., 1997; Lexer & Hönninger, 1998). To explore the soil rooting depth relationship with different primary topographic attributes, i.e., elevation, aspect and slope, simple Pearson correlation (Benesty et al., 2009) and ordinary least square (OLS) regression (Hutcheson, 1999) were applied.

3.2.3.2 Temperature model

Pearson correlation test was performed to check the degree of association between the temperature difference with primary topographic attributes. As the temperature differences were captured for different strata through a repeated time series measurement, a linear mixed-effect regression model (Verbeke & Lesaffre, 1996) was applied to explain these differences by using random and fixed effects. The general structure of a linear mixed-effect model is represented by Equation 5. In this case, the primary topographic attributes were the fixed effects, whereas the loggers, site and different months were placed random effects. Once, the relationship was established, it was used to simulate the temperature at each plot with respect to the base weather station.

$$Y_{ij} = b_0 + b_1 X_{ij} + V_{i0} + V_{i1} X_{ij} + \varepsilon_{ij} \quad (5)$$

where, Y_{ij} = the response variables, b_0 = fixed intercept, b_1 = fixed slope, X_{ij} = predictor variable of j -th measurement of the i -th subject, V_{i0} = random intercept of the i -th subject, V_{i1} = random slope of the i -th subject, ε_{ij} = error term.

3.2.3.3 Juvenile height model

In young plantations prior to canopy closure, one might expect that growth should be exponential, with larger trees having greater leaf and root surface areas than smaller trees.

Mason and Whyte (1997) expressed this growth function as,

$$\frac{d\bar{h}}{dT} = \gamma \bar{h}^{-\delta} \quad (6)$$

by solving this,

$$\bar{h} = \bar{h}_0 + \alpha T^\beta \quad (7)$$

where,

$$\alpha = ((1 - \delta)\gamma)^{\frac{1}{1-\delta}} \quad \beta = \frac{1}{1-\delta} \quad (8)$$

So, equation 6 can be written as,

$$\bar{h}_T = \bar{h}_0 + \alpha T^\beta \quad (9)$$

Here, \bar{h}_0 = mean height immediately after planting, in this case 0.25 m, which is the estimated height for *Pinus radiata* seedlings planted in plantations in New Zealand. Also, \bar{h}_T = mean height at stand age T.

Equation 9 has been widely used for modelling juvenile crops (Belli & Ek, 1988; Mason & Whyte, 1997). Furthermore, Mason and Whyte (1997) showed that the coefficients of

Equation 9 can be extended as a linear function (Equation 10 and 11) to independent variables and their interactions by inserting them into linear functions.

$$\alpha = \alpha_0 + \alpha_1 V_1 + \dots + \alpha_n V_n \quad (10)$$

$$\beta = \beta_0 + \beta_1 V_1 + \dots + \beta_n V_n \quad (11)$$

3.2.3.4 Survival model

It is rare to have specific information about each tree in young plantations. The mortality of trees in young plantations is not due to competition among them, but rather water stress or other site-specific factors. According to Mason and Whyte (1997) juvenile mortality should be considered as a random process over time and, therefore, should follow a Poisson probability distribution, where, N represents stems per unit area, T is crop age in years, and K is a constant that varies with crop and conditions.

$$\frac{dN/dT}{N} = K \quad (12)$$

The numerical value of K changes with time and location (Eq. 13)

$$\frac{dN/dT}{N} = \alpha T^\beta \quad K = \alpha T^\beta \quad (13)$$

When solved, the derivative expression results in a form of the well known Weibull probability density function (Mason & Whyte 1997). The functional form should be anamorphic, as the percentage of deaths would be independent of the stocking.

The survival function used by Belli and Ek (1988) was one of exponential decay, which converted to mortality by taking the same Weibull probability density functions derivatives given by Mason (1992). Other modellers have used similar approaches (Amateis et al., 1997; Belli & Ek, 1988; Zhang et al., 1996). In this case, the survival proportion function (Equation 14) fitted a yield form described in Mason and Whyte (1997) (Equation 14).

$$S_T = -e^{\alpha T^\beta} \quad (14)$$

where, S_T = survival at stand age T, and α and β represent model coefficients.

It is expected that the coefficients should vary with independent explanatory variables, which can be extended linearly by following the same approach as the height model (Equations 10 and 11).

3.2.4 Model testing and validation

Model validation is a procedure in which the model is tested for agreement with an independent dataset of those observations used to structure the model and estimate its parameters (Shugart, 1984). There are many types of model validation in use, where both quantitative and qualitative assessments are taken into consideration (Sargent, 2013). However, using only statistical tests for validation has resulted in strong debate (Sale et al., 2002; Wright, 1972). This is because there are many criteria for assessing the suitability of models (Mayer et al., 1994). As each model is unique, there is no single validation process or method, so Kozak and Kozak (2003) advised a combination of techniques. In consequence, the goals of model validation and testing are important, as they are not designed to prove that a model is accurate (Popper, 2014), but rather to see how well the model performs and agrees with the independent observations. Also, the model predictions should be sufficiently statistically and biologically similar to independent observations that the model choices can be defensible (Yang et al., 2004). In this circumstance, a mixed approach was applied to evaluate the model, by performing a full set of residual analyses. Validation included a visual analysis of graphs of the residuals, the calculation of root mean square error (RMSE) (Equation 15), mean absolute error (MAE) (Equation 16), bias (Equation 17), coefficient of determination (r^2) (Equation 19) and corrected Akaike information criterion (AICc) (Equation 18) (Akaike, 1981).

$$\text{RMSE} = \sqrt{\frac{\sum_{i=1}^N (P_i - O_i)^2}{N}} \quad (15)$$

$$\text{MAE} = \frac{\sum_{i=1}^N |P_i - O_i|}{N} \quad (16)$$

$$\text{bias} = \frac{\sum_{i=1}^N (P_i - O_i)}{N} \quad (17)$$

$$\text{AICc} = \text{AIC} + \frac{2K^2 + 2K}{N - K - 1} \quad (18)$$

$$r^2 = \frac{\sum P'_i{}^2}{\sum O'_i{}^2} \quad (19)$$

where N = Number of observation, O = Observed value, \bar{O} = mean of observed value, P = Predicted value, $P'_i = P_i - \bar{O}$, $O'_i = O_i - \bar{O}$. K denotes the is the number of estimated parameters.

There are many established procedures to perform model validation (Uzoh & Mori, 2012). Among them, independent datasets are often not available; as a result, splitting data sets is a commonly accepted practice for model testing and validation if the dataset is sufficiently large (Kozak & Kozak, 2003). Dobbin and Simon (2011) suggested a data splitting ratio of 75:25 (model fitting: validation), which was applied in this study.

3.2.5 Statistical analysis

All statistical analyses were performed in the R statistical environment (R Core Team, 2017). The Pearson correlation was applied to soil rooting depth and temperature difference by “cor” function. Also, ordinary least square (OLS) for soil rooting depth was performed with the “lm” function. All these were performed through the base package in R. The temperature difference within sites was explored with “lme4” package (Bates et al., 2014) by applying the “lmer” function through the selected random and fixed effects.

The nonlinear regression model coefficients were fitted and separated by running the “nls” function. Then an assessment for potential multicollinearity was performed for all explanatory variables by using the variation inflation factor (VIF) with the “vif.mer” function of the car package in R (Fox & Weisberg, 2011). Elevation, slope, and topographic ruggedness

index (TRI), total curvature were shown to have high multicollinearity, hence were excluded from the model building procedure.

Following multicollinearity analysis, model coefficients were fitted against the explanatory variables by using the “lm” function. Finally, the height and survival models were fitted using the “nls” function with only the significant variables. The height and survival models were validated against the validation datasets by using “Rsqa.ad”, “AICc” function in “qpcR” package (Spiess & Ritz, 2014), and “rmse”, “mae”, “bias” functions from the “metrics” package (Hamner & Frasco, 2018). Besides this, residuals were visually inspected for their normality and variance homogeneity.

3.3 Results

3.3.1 Soil rooting depth

At all the three sites, soil rooting depths showed weak correlation with all primary topographic parameters. Moreover, rooting depth did not vary significantly among the three sites. Besides, none of the primary topographic attributes had a significant relationship with rooting depth. Elevation was slightly and negatively correlated to soil rooting depth at the A and C sites, whereas in the B site there was a positive correlation. The correlation coefficients, R , were respectively -0.28, -0.33 and 0.26. Slope had a positive association at the B and C sites, and a negative association at the A site (Table 3.7).

Table 3.7 Results of rooting depth analysis.

Sites	A			B			C		
<i>Stat.</i>	Aspect	Slope	Elev.	Aspect	Slope	Elev.	Aspect	Slope	Elev.
<i>R</i>	0.41	-0.23	-0.28	-0.096	0.32	0.26	-0.39	0.049	-0.33
<i>p</i>	0.19	0.47	0.38	0.79	0.37	0.46	0.34	0.91	0.43
<i>Sig.</i>	NS	NS	NS	NS	NS	NS	NS	NS	NS

Note: Correlation coefficient *R*, *p*-value indicates the significant level at >0.05 and significant level (*Sig.*) *NS* stands for not significant.

3.3.2 Temperature variation at Avery and Lawson sites

The full temperature difference mixed-effect model indicated that primary topographic attributes (aspect, slope and elevation) had a significant effect on air temperature difference within sites (p -value=2.306e-09 and AICc=1506.06). Aspect had a negative effect. This indicated that the temperature difference increased significantly from South to North. Slope also affected the air temperature differences negatively, indicated that the temperature differences lowered with a higher slope. On the other hand, elevation had a positive effect which means temperature difference increased with increasing elevation (Table 3. 8).

Table 3. 8 Coefficients for final full linear mixed models for air temperature difference within site.

Fixed effects	Est.	SE	t	Sig
<i>Intercept</i>	-1.870177	1.145	-1.633	NS
<i>Aspect</i>	-0.321877	0.162	-1.984	*
<i>Slope</i>	-0.108914	0.024	-4.400	***
<i>Elevation</i>	0.026662	0.006	3.964	***
Random effect	Var.	SD		
<i>Months</i>	0.328	0.573		
<i>Site</i>	0.800	0.894		
<i>Logger</i>	0.720	0.8488		
<i>Residual</i>	1.500	1.225		

Note: Est. = Estimate; SE = Standard error; Sig. = Significance level, Var. = Variance, SD = Standard deviation (*** = p<0.001, ** = p<0.05; NS = p≥0.05)

3.3.3 Juvenile height model

All of the juvenile height models for both species (Equation 20, 21 and 22) had low and stable error statistics (Table 3.9). For *E. globoidea*, bias was found at low and high predicted height values (Figure 3.3), where the model overpredicted the height. With the exception of bias, all calculated statistics were lower for the fitting dataset than for the validation dataset (see Table 3.9).

$$h_{EGT_A} = h_{EG0} + (\alpha_0 + \alpha_1 * WEI + \alpha_2 * DIST) * T_{EGT}^{(\beta_0 + \beta_1 * DIST + \beta_2 * WEI + \beta_3 * MPI)} \quad (20)$$

$$h_{EBT_B} = h_{EB0} + (\alpha_0 + \alpha_1 * CVPLA + \alpha_2 * TPI + \alpha_3 * WEI + \alpha_4 * MPI) * T_{EBT}^{(\beta_0 + \beta_1 * CVPLA + \beta_2 * WEI + \beta_3 * MPI + \beta_4 * TPI + \beta_5 * DIST + \beta_6 * WEI : DIST)} \quad (21)$$

$$h_{EBT_C} = h_{EB0} + (\alpha_0 + \alpha_1 * WEI + \alpha_2 * WTI + \alpha_3 * TPI + \alpha_4 * MPI + \alpha_5 * DIST) * T_{EBT}^{(\beta_0 + \beta_1 * TPI + \beta_2 * DIST)} \quad (22)$$

where h_{EGT_A} is the *E. globoidea* height at time T in site A; h_{EBT_B} and h_{EBT_C} are the *E. bosistoana* height at time T respectively in site B and C. h_{EG0} and h_{EB0} are the initial height of

E. globoidea and *E. bosistoana*. T_{EGT} and T_{EBT} are the age of *E. globoidea* and *E. bosistoana*.

Others are as defined earlier in Section 3.2.2.2.

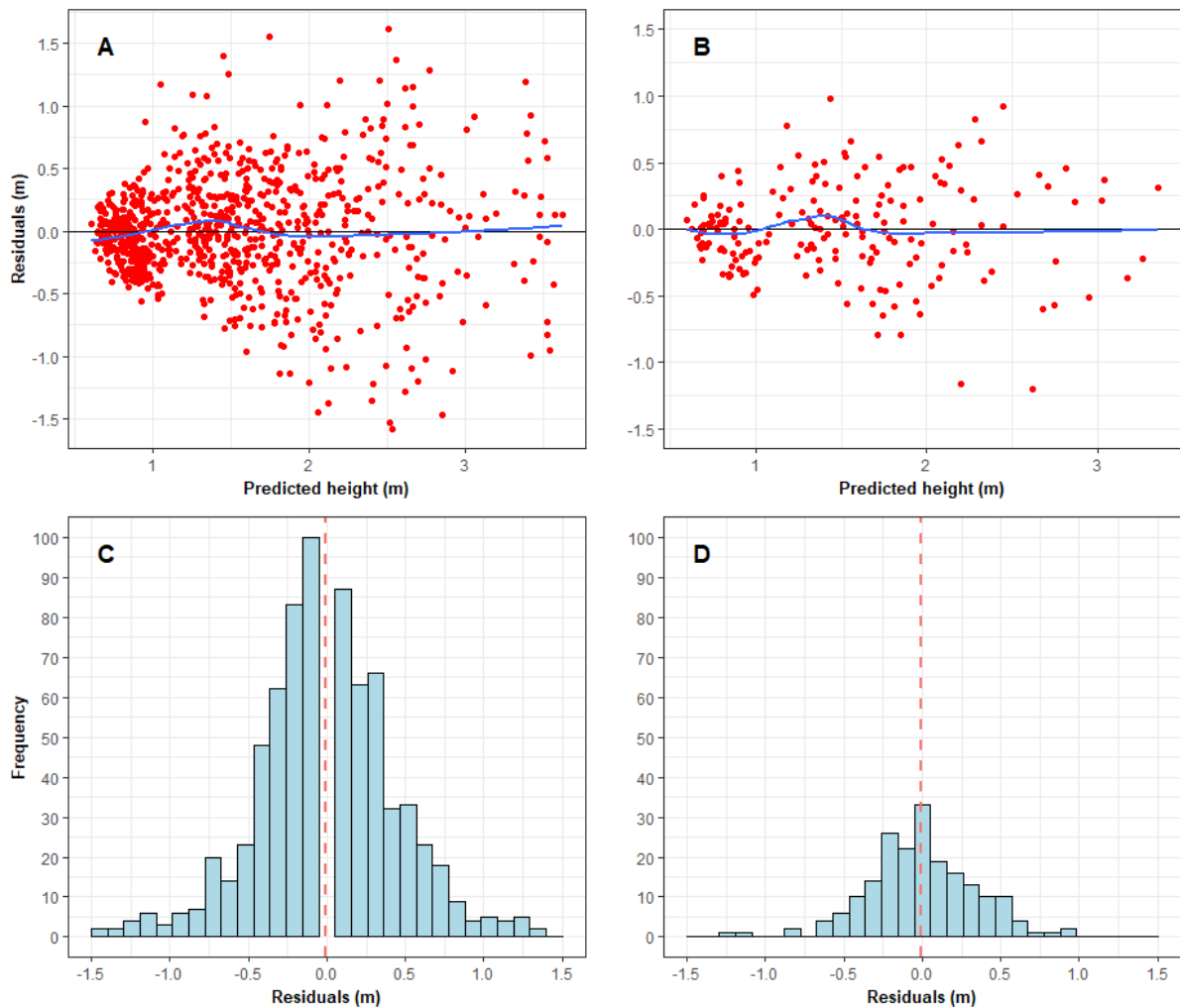


Figure 3.3 *E. globoidea* juvenile height model residual plots: A) final model residuals and B) validation residuals with loess line (blue); C) and D) respectively final model and validation residuals distribution.

The *E. bosistoana* height model behaved differently at different sites. At site B, the model underpredicted moderate height values (Figure 3.4), while at site C, the model followed *E. globoidea*'s residual distribution pattern (Figure 3.5). At the site B, RMSE, MAE and SE increased respectively to 0.603, 0.429 and 0.615 from the fit statistics, while BIAS and AICc reversed in turn to 0.024 and 645.847 from the fitting statistics. In contrast to that, at the site C, all the fitting statistics features were reduced during validation (Table 3.9).

Table 3.9 Fitting and validation statistics of the final height growth equations.

Species	Site	Action	RMSE	MAE	BIAS	AICc	SE
<i>E. globoidea</i>	A	Fitting	0.453	0.338	0.009	1000.842	0.455
		Validation	0.348	0.273	0.011	154.103	0.354
<i>E. bosistoana</i>	B	Fitting	0.518	0.385	0.032	1502.06	0.521
		Validation	0.603	0.429	0.024	637.045	0.614
	C	Fitting	0.342	0.274	0.001	247.399	0.347
		Validation	0.322	0.251	0.001	77.077	0.339

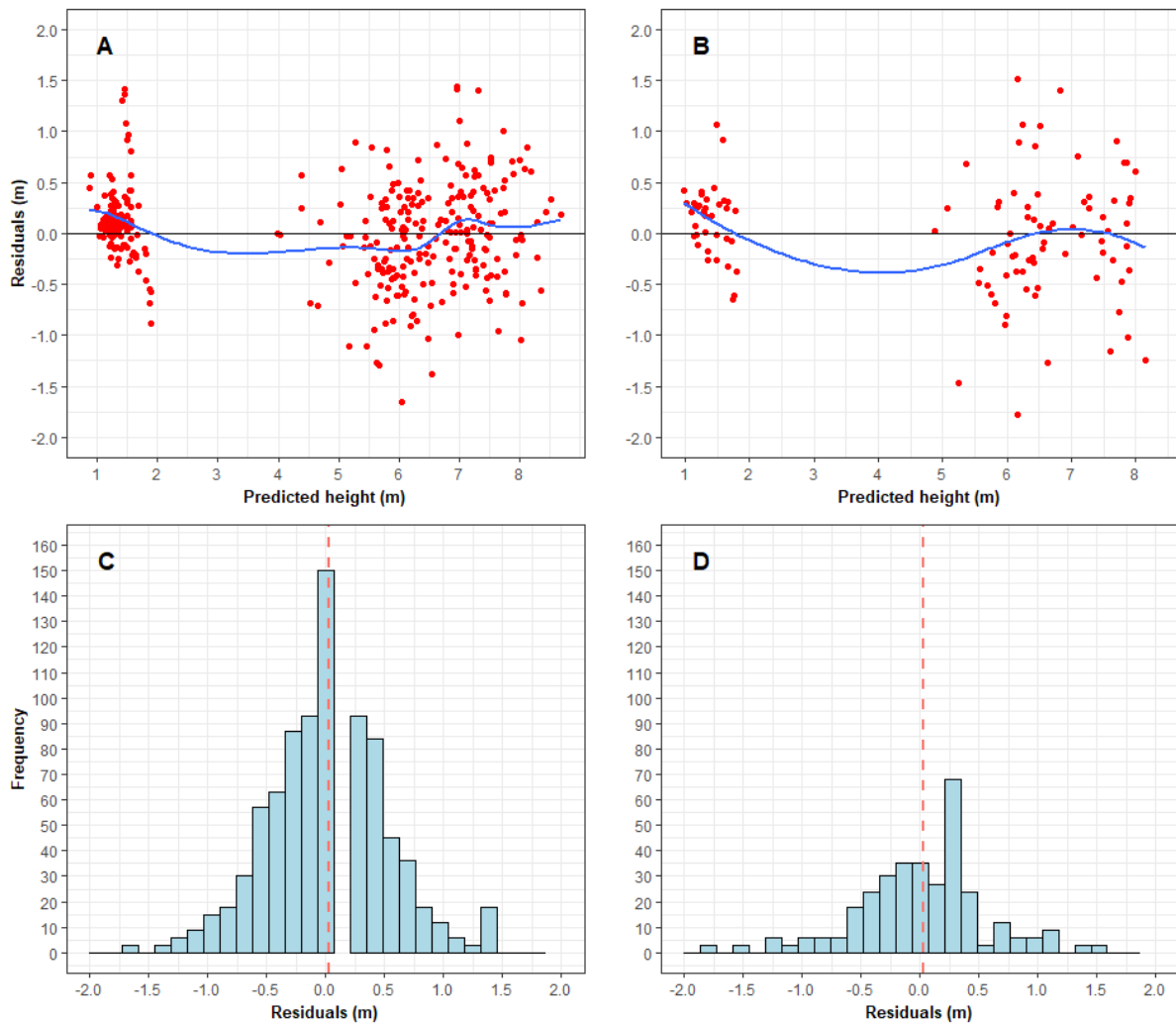


Figure 3.4 *E. bosistoana* juvenile height models residuals (m) plot for site B; A) Final model residuals and B) validation residuals representation with loess line (blue); C) and D) represents the residuals distribution of model fit and validation dataset.

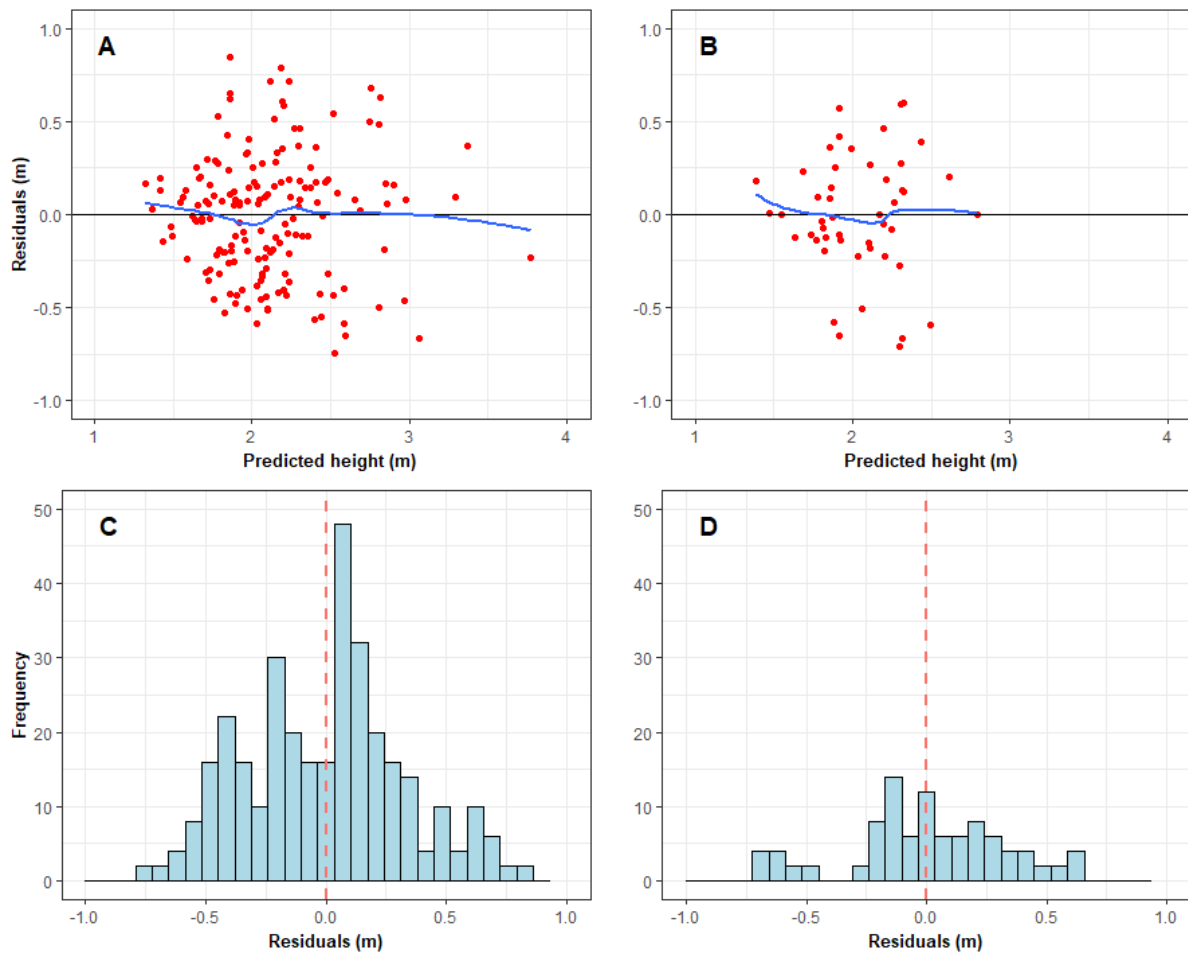


Figure 3.5 *E. bosistoana* juvenile height models residuals (m) plot for site C; A) Final model residuals and B) validation residuals representation with loess line (blue); C) and D) represents the residuals distribution of model fit and validation dataset.

3.3.4 Key variables for micro-site height growth

Juvenile *E. globoidea* height was significantly correlated with WEI, MPI and plot distance from the top ridge (DIST) (Table 3.10 and Figure 3.6). Therefore, these variables were added to the final height yield model represented by Equation 18. All three had large effects on height growth. The micro-sites highly exposed to wind had the lowest height growth, and tree height decreased with reduced morphometric protection (MPI). Trees close to the top ridge had the lowest height growth, while the height increased with distance proportionally until the age of 4.5 years. From then, trees at the mid-distance from the top ridge grew taller.

Table 3.10 Tested variables and their significance on juvenile height growth.

Variables	Significance code		
	A	B	C
Maximum daily temperature	NS	NS	NS
Profile curvature	NS	NS	NS
Plan curvature	NS	***	NS
Topographic position index (TPI)	NS	***	***
Wind exposure index (WEI)	***	***	**
Wetness index (TWI)	NS	***	*
Morphometric protection index (MPI)	***	***	***
Distance from the top ridge (DIST)	***	***	***

Signif. Codes: *** = $p < 0.001$, ** = $p < 0.05$; NS = $p \geq 0.05$

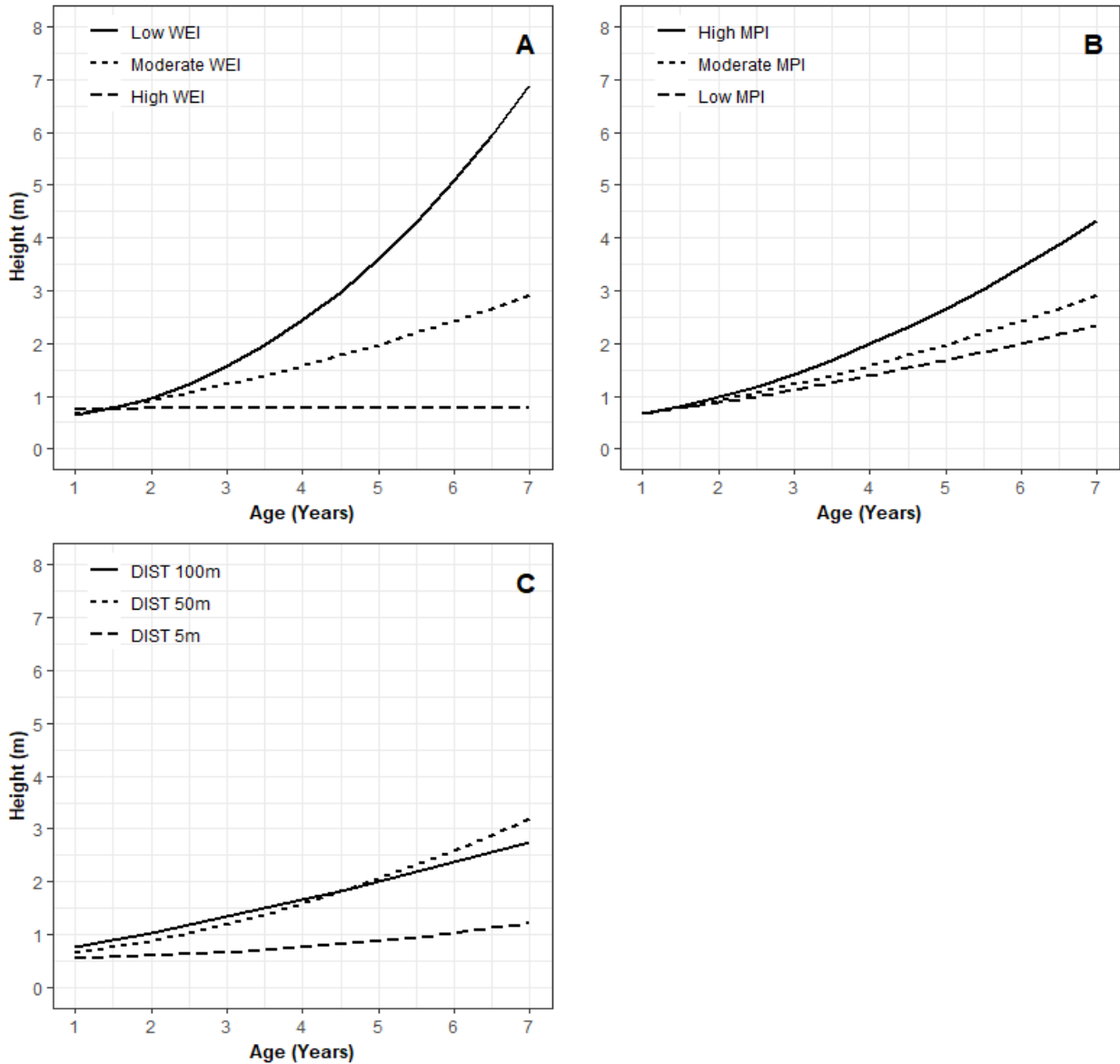


Figure 3.6 Micro-topographic effect of *E. globoidea* height growth: (A) Wind exposure effect, (B) Morphometric protection effect, and (C) Distance from the top ridge effect.

E. bosistoana height growth was influenced by different factors at different sites (Table 3.10). At the site B, plan curvature (CVPLA), MPI, distance from the top ridge (DIST), TPI, WEI, and interaction between wind exposure and distance from the top ridge influenced tree height (Figure 3.7). In sites with local horizontal concave surfaces, trees were taller than the trees on horizontal flat or convex surfaces. TPI also showed a similar pattern: trees were taller in valleys than on ridges. Until age 4.5 years, trees nearer the ridge experienced faster height growth than trees in the valley. After age 4.5 years, the converse was true (Figure 3.7 (D)).

Higher MPI and lower WEI resulted in greater height growth. Distance from the ridge top showed that the distant trees were growing faster than the trees closest to the ridge top. However, the lowest WEI with distant micro-site had the highest height growth compare to low WEI and a position close to the ridge. On the other hand, high WEI with farthest micro-site which means close to the valley floor was the worst for tree height at the B site.

In the case of the site C, *E. bosistoana* height was affected by WEI, WTI, TPI, MPI and distance from the ridge top (DIST) (Figure 3.8). The MPI and WEI effects were similar to other results, with high MPI and low WEI resulting in increased tree height (Figure 3.8(A) & (E)). An increase of TPI affected the tree height, but at age 2.5 years the effect reversed, with trees in valleys having greater height growth, relative to trees on midslopes or ridges. The trees situated at mid-distance from the ridge top grew taller than those closest to, and furthest from, the ridge top. Interestingly, the surface wetness minimally influenced the tree height (Figure 3.8 .B).

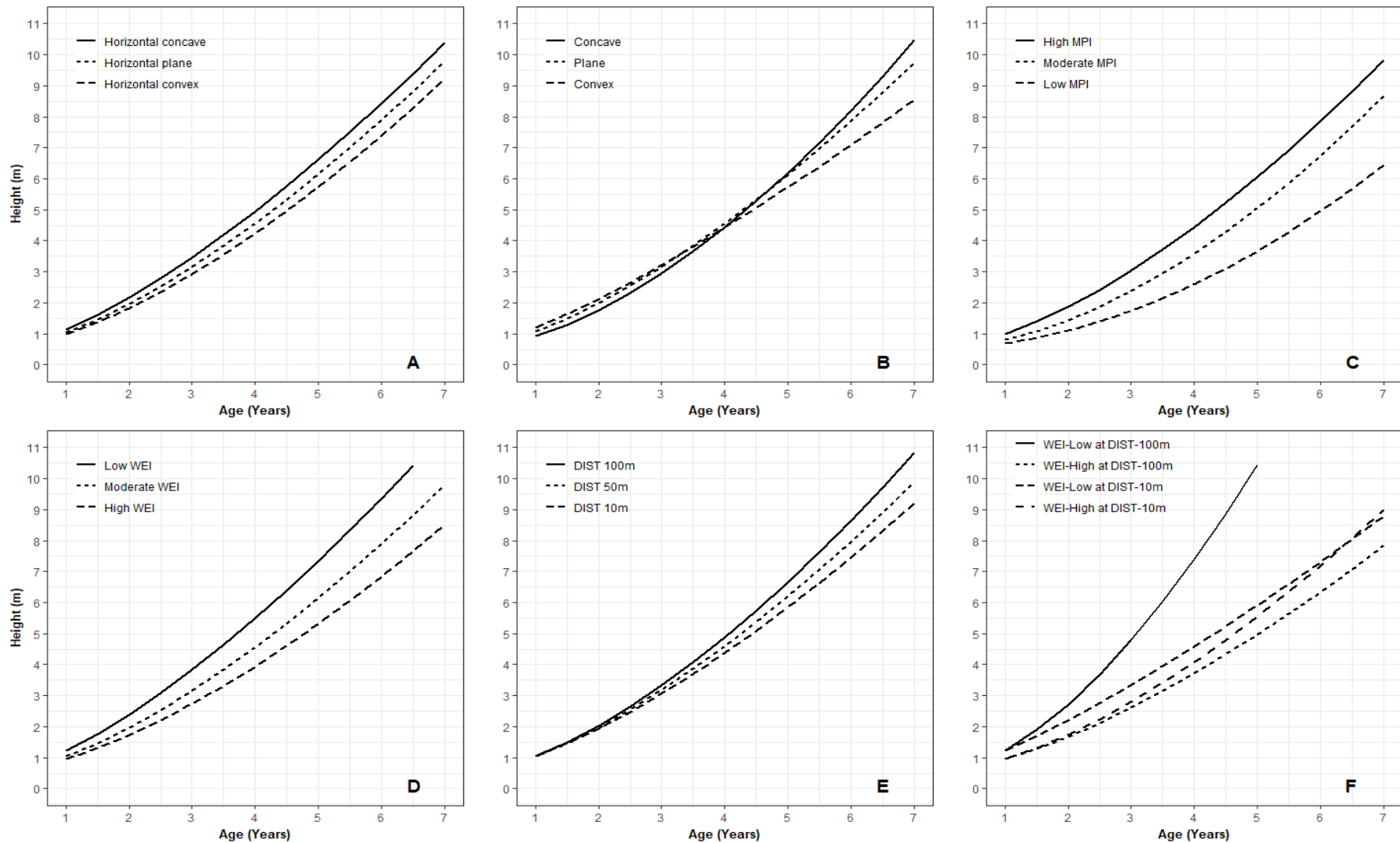


Figure 3.7 Micro-topographic effects on *E. bosistoana* height growth at site B; (A) Plan curvature, (B) Morphometric protection effect, (C) Distance from the top ridge effect, (D) Topographic position effect, (E) Wind exposure effect and (F) WEI and DIST interaction effect.

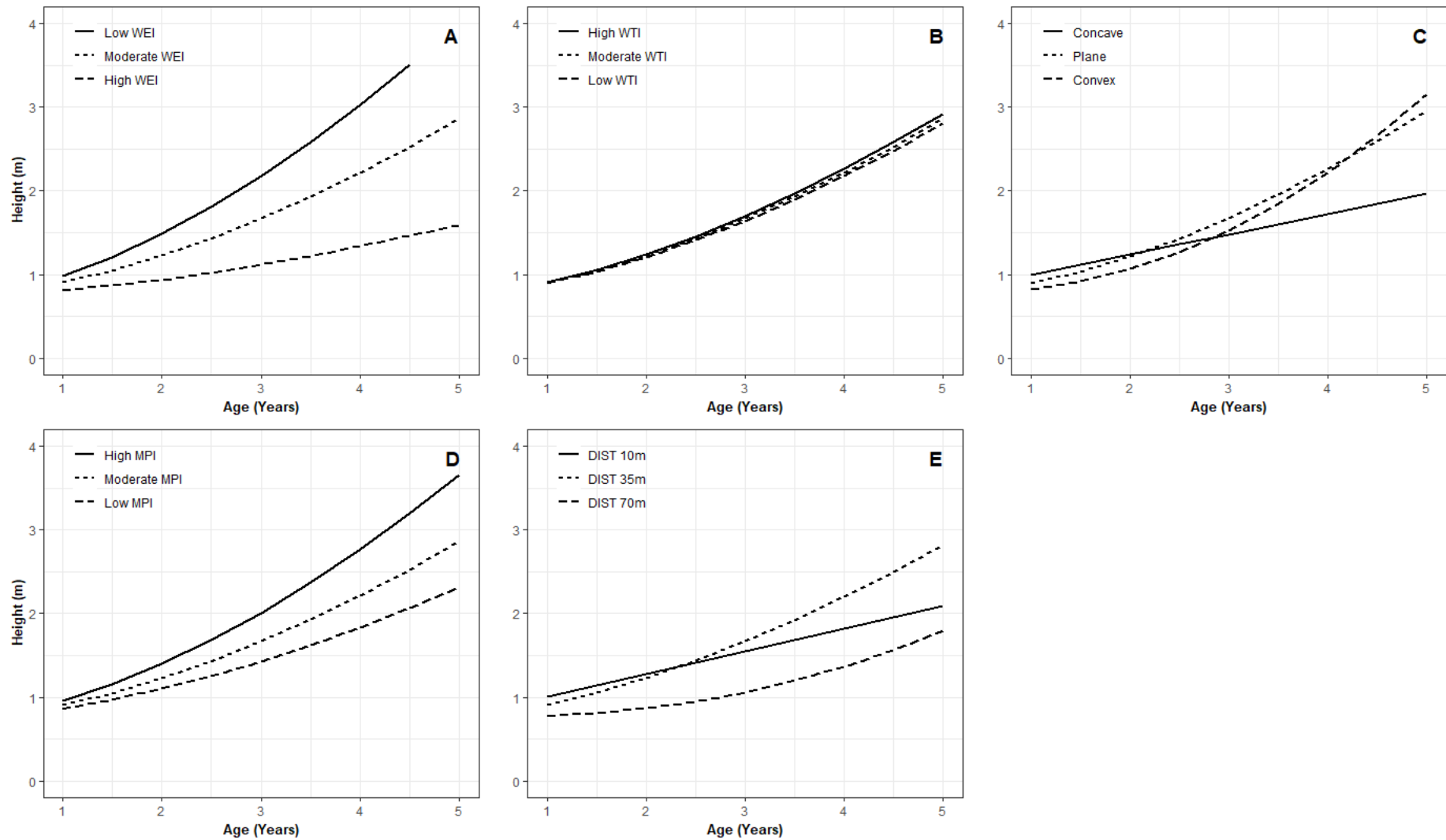


Figure 3.8 micro-topographic effect of *E. bosistoana* height growth at site C: (A) Wind exposure, (B) Wetness effect, (C) Distance from the top ridge effect, (D) Topographic position effect, and (E) Morphometric protection effect.

3.3.5 Juvenile survival model

Analyses revealed that the smallest residual mean squares and the least biased residuals were produced by augmenting survival models (Equation 23 and 24) with topographic attributes. The rate of mortality diminished with time in most plots, but mortality was higher during later years than during the early years.

$$S_{EGT_A} = -e^{(\alpha_0 + \alpha_1 * CVPLA + \alpha_2 * CVPRO) * T^{(\beta_0 + \beta_1 * DIST + \beta_2 * CVPLA)}} \quad (23)$$

$$S_{EBT_C} = -e^{\alpha_0 * T^{(\beta_0 + \beta_1 * CVPRO)}} \quad (24)$$

where, S_{EGT_A} and S_{EBT_C} are the survival proportion of *E.globoidea* and *E. bosistoana* at time T in site A and C; others are defined earlier in section 3.2.2.2.

The residual distribution against predicted and independent datasets was normally distributed with minor distortions for all species and sites (Figure 3.9 and Figure 3.10). Validation for both species was undertaken and the survival proportion model reported with a minimal increase in precision and bias (Table 3.11, and Figure 3.9 and Figure 3.10). In the case of *E. globoidea*, the RMSE and MAE reduced during validation while they increased slightly with *E. bosistoana* model validation.

Table 3.11 Juvenile survival proportion model fitting statistics.

Species	Site	Action	RMSE	MAE	BIAS	AICc	SE
<i>E. globoidea</i>	Avery	Fitting	0.108	0.076	-0.001	-1224.5	0.109
		Validation	0.097	0.068	-2.08617e-06	-411.26	0.099
<i>E. bosistoana</i>	Dillon	Fitting	0.019	0.013	-7.951e-06	-1234.4	0.020
		Validation	0.021	0.015	2.980e-05	-339.42	0.022

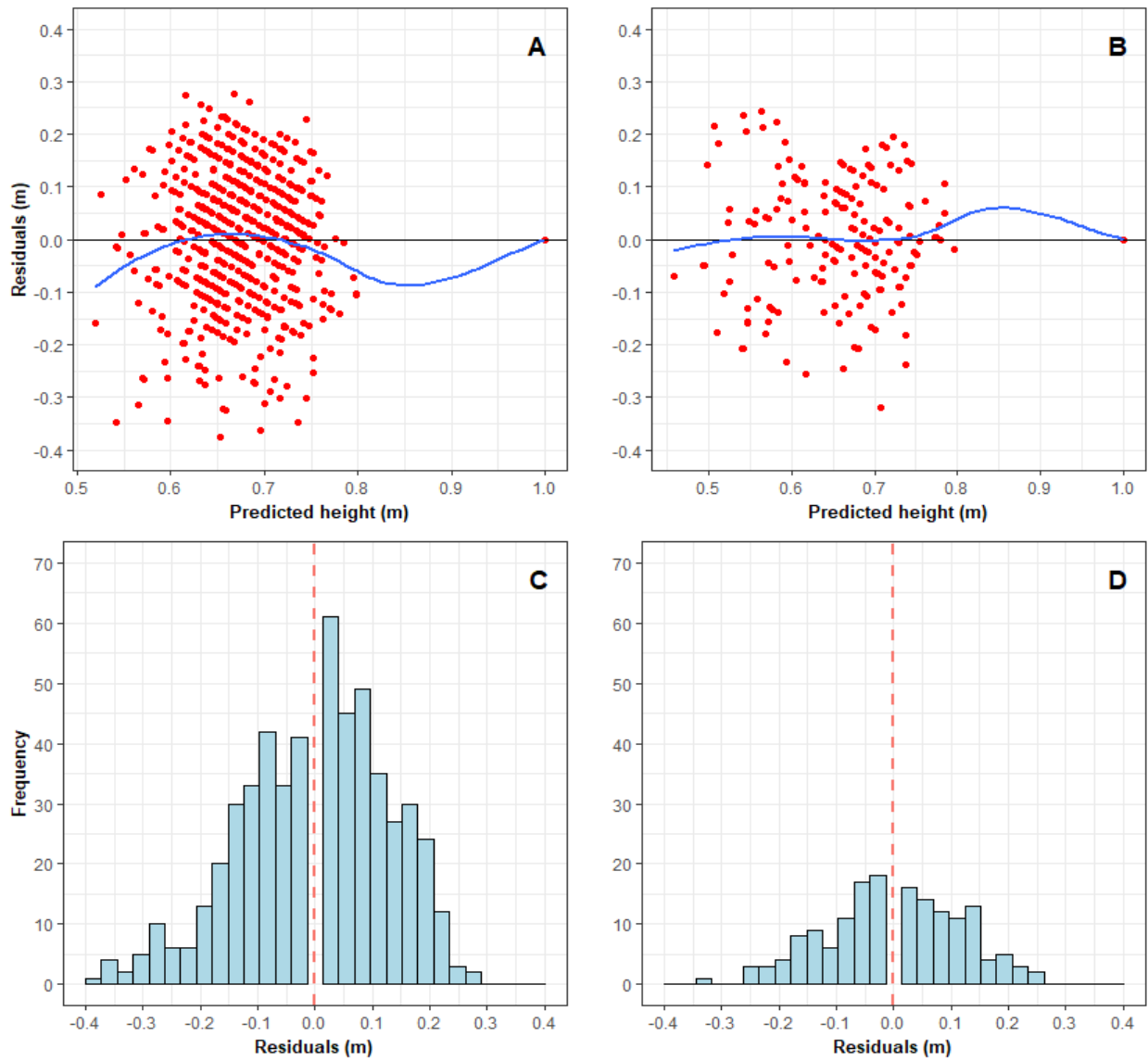


Figure 3.9 *E. globoidea* juvenile survival models residuals (m) plot for site A; A) Final model residuals and B) validation residuals representation with loess line (blue); C) and D) represents the residuals distribution of model fit and validation dataset.

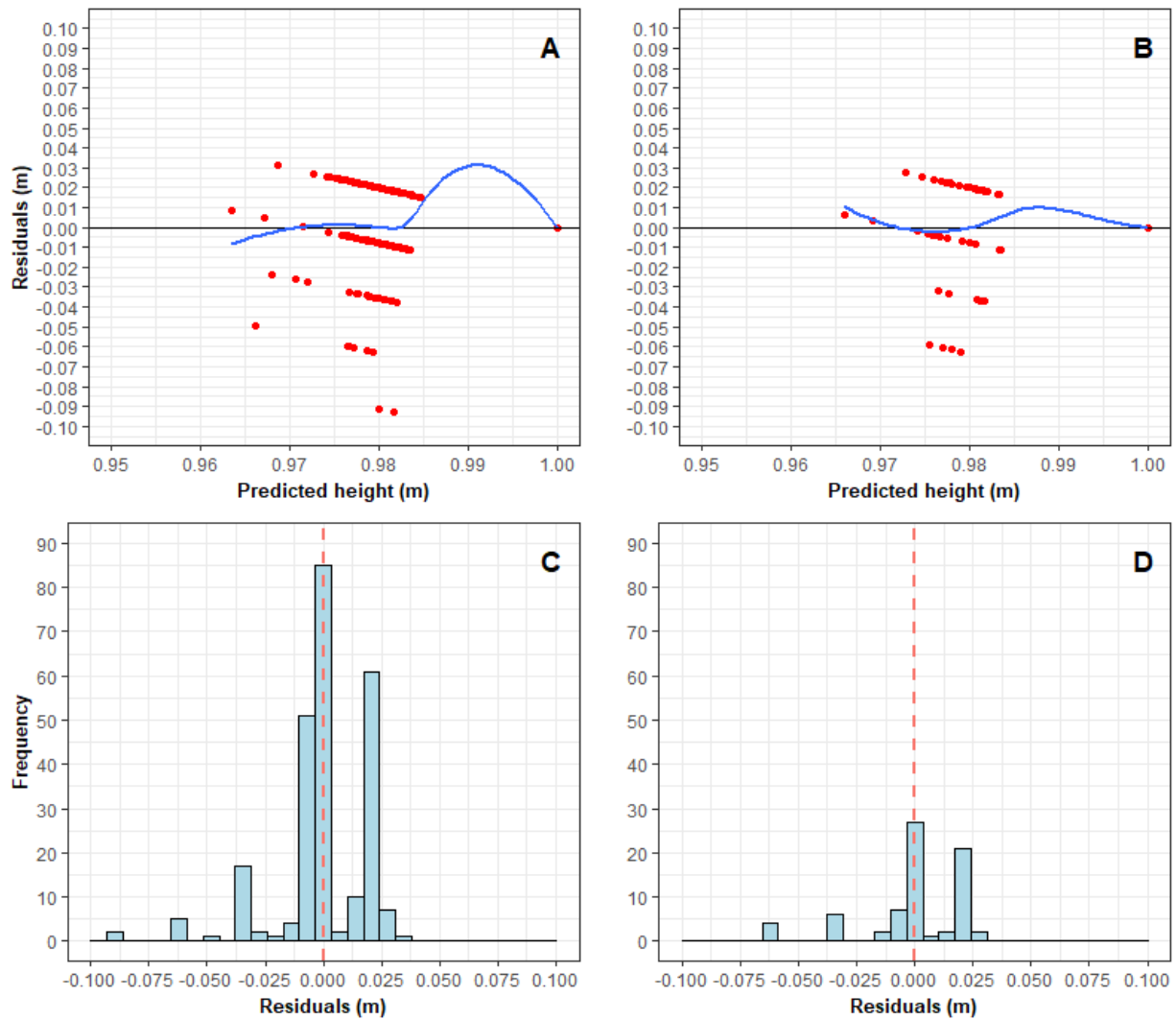


Figure 3.10 *E. bosistoana* juvenile survival models residuals (m) plot for site C; A) Final model residuals and B) validation residuals representation with loess line (blue); C) and D) represents the residuals distribution of model fit and validation dataset.

3.3.6 Key factors to juvenile micro-site survival

E. globoidea survival was influenced by plan and profile curvature, WEI and distance from the ridge top (Table 3.12 and Figure 3.11). In concave and flat areas, the mortality rate was steady whereas in convex areas mortality reduced with time. This result was repeated for profile curvature, where on the raised surfaces trees survived in higher proportions than on hollow or flat surfaces. The micro-site highly exposed to wind had a lower survival rate than the areas less exposed to the wind. Moreover, plots a long distance from the ridge top showed lower survival rates than the ones close to it.

Table 3.12 Tested variables and their significance on juvenile *Eucalyptus* survival proportion.

Variables	Significance code for different sites	
	A	C
Maximum daily temperature	NS	NS
Profile curvature	***	*
Plan curvature	*	NS
Topographic position index (TPI)	NS	NS
Wind exposure index (WEI)	**	NS
Wetness index (TWI)	NS	NS
Morphometric protection index (MPI)	NS	NS
Distance from the top ridge (DIST)	***	NS

Signif. Codes: *** = $p < 0.001$, ** = $p < 0.05$; NS = $p \geq 0.05$

E. bosistoana survival was influenced only by profile curvature (Figure 3.11 (E)). It showed that, in gullies, higher proportions of trees survived than on flat surfaces or ridges. However, it had a very narrow effect in size and pattern.

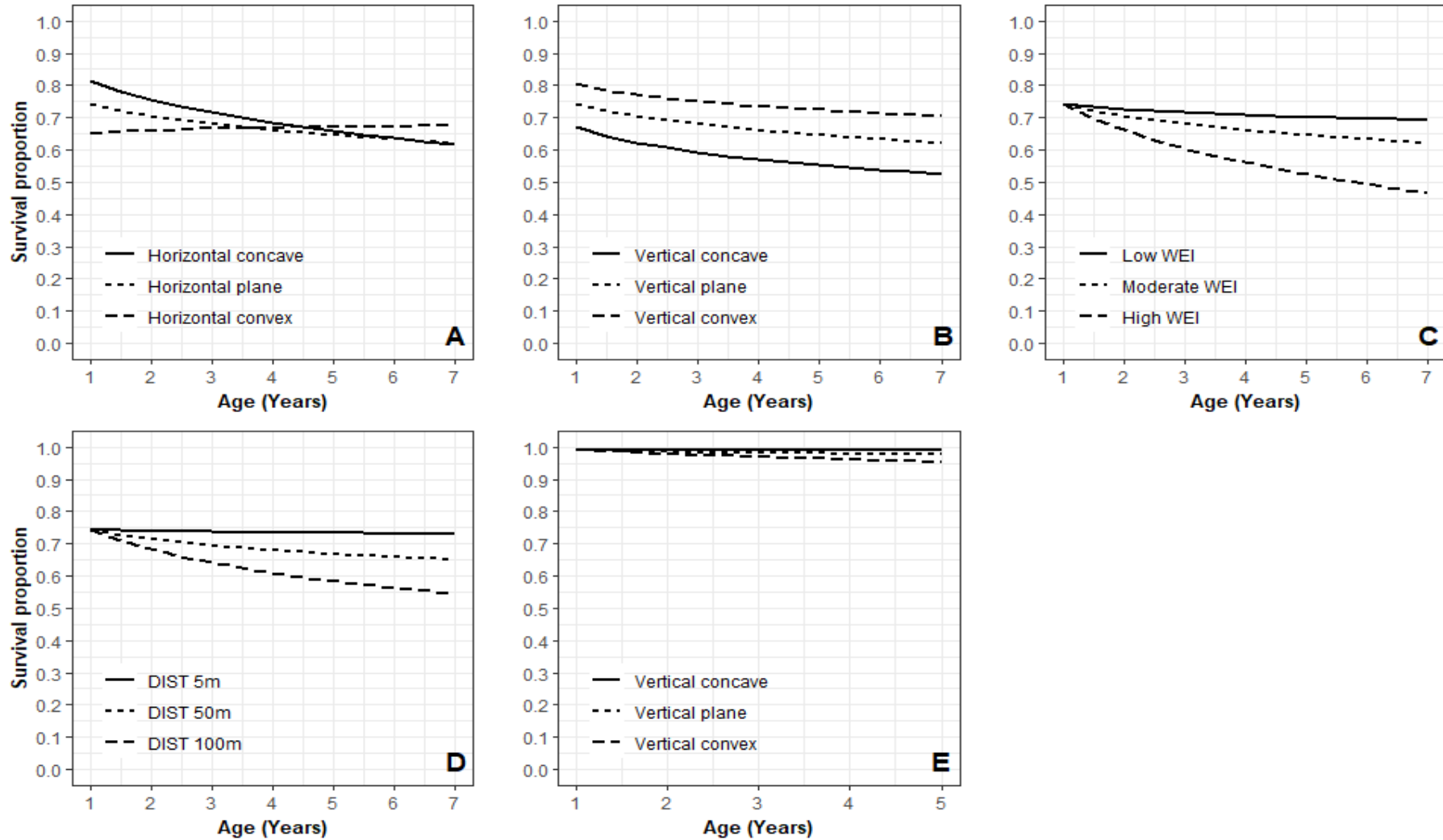


Figure 3.11 Topographic effect of *E. globoidea* survival at Site A: (A) Plan curvature, (B) Profile curvature effect, (C) Wind exposure effect, and (D) Distance from the ridge top effect; E) *E. bosistoana* survival with profile curvature effect at the site C.

3.4 Discussion

3.4.1 Juvenile micro-site models

While earlier work has modelled juvenile trees on a broad scale (e.g., Avila, 1993; Mason & Whyte, 1997), the juvenile micro-site models described here have shown that it is possible to model juvenile crops at a finer scale. Individual juvenile trees have also been modelled by applying mathematical equations (Nyström & Kexi, 1997; Ritchie & Hamann, 2006; Zhang et al., 1996) and explaining different competing variables (Nyström & Kexi, 1997; Preece et al., 2015; Richardson et al., 2006). Kohama et al. (2006) and Weiskittel et al. (2008) studied juvenile and mature stand tree growth on a micro-scale, and Weiskittel et al. (2008) proposed a modelling framework but only for mature stand trees. Although, juvenile and mature stand trees have different growth requirements and competition indices. The model presented in this study for juvenile trees has field applicability, which could be incorporated into a decision support system for silviculture at the site with similar characteristics.

3.4.2 Micro-site variables affect juvenile tree height growth

This study showed that juvenile tree height growth and survival were affected by micro-site related variables. Zhang et al. (1996) found the same but at a broader scale with loblolly pine in the northern USA. Topographic variables are major drivers of tree growth in many hilly regions (Ares & Marlats, 1995), as they relate to both climatic and edaphic factors (Adams et al., 2014). For both of the species in this study, the sheltered micro-sites resulted in greater height growth. For instance, distance from the ridge top means that the trees in the bottom of the valleys could experience less wind load than trees on the ridges. Similar results were found by Brüchert and Gardiner (2006) who showed that wind could influence the aerial architecture of the trees. Both morphometric protection and wind exposure index influence supported this result. Valley floors are expected to have greater rooting depth, meaning the trees are more stable and better physiologically supported in terms of nutrients and moisture. However, this

study found that middle distance from the ridge top was the best for *E. globoidea*, which may relate to the optimum range of moisture availability to this species and sensitivity to higher soil moisture.

E. bosistoana grew taller in concave, depressed (valley) surfaces, and in locations farthest from ridges, which had relatively low WEI. This can be explained in a similar way to *E. globoidea*, but suggests that this species is more water-demanding than *E. globoidea* at young ages. Rohner et al. (2018) and Monserud and Sterba (1996) reported that the high slope results in shallow soil and less moisture availability due to lateral moisture flow. This is in line with the TPI effect, as it described each micro-site with respect to the slope.

3.4.3 Micro-site variability on juvenile tree survival

This study reported that *E. globoidea* was sensitive to higher moisture levels, but could withstand harsher conditions means can survive limited resources such as moisture, than *E. bosistoana*. Results suggested that *E. globoidea* may experience sub-optimal optimal levels of soil moisture for tree health in valleys and hollows. Conversely, *E. bosistoana* survived better in gullies, where there is presumably a chance to access higher moisture availability. Bathgate et al. (1993) reported conditions similar to the above for *E. regnans* in the North Island of New Zealand. Moreover, Ares and Marlats (1995) found and concluded that in mountain regions of Argentina coniferous trees died on north facing slopes due to overheating, as this aspect receives more radiative heat than other aspects, which may increase the water stress. Distance from the ridge top represents the sites' flatness. The further a site is from the ridge top, the flatter it is. In this situation, Mason and Whyte (1997) reported that frost negatively influences juvenile tree survival, which could be an alternative or additional reason for increased mortality of *E. globoidea* in hollows.

3.4.4 Data constraints

The initial height for the young *Eucalyptus* plantations was not recorded immediately after planting. For that reason, the initial height model was fitted by assuming *Eucalyptus* seedlings met the *Pinus radiata* plantation standard, which was 0.25 m in height at time of planting (Mason & Whyte, 1997). The use of this standard height value might have influenced model stability at the early ages because the model extrapolated the height values for that age. Therefore, these models should be used cautiously over the period from planting to first measurement age.

High-resolution soil data was not available for these sites: the plantations were not established on a single soil type. Unfortunately, the sampling strategy applied was not sufficiently comprehensive to characterise soil variability, probably because the number of soil sampling points was low compared to standard soil studies (Brocca et al., 2007; Padilla & Pugnaire, 2007). Though the soil data appeared variable during preliminary data assessment (e.g., SD, Min, and Max), they did not have a statistically significant effect on height growth, nor on survival. Including higher-resolution soil data may improve model precision in future studies.

Including climatic variables into the models may give greater explanatory power and understanding about causal processes (Jame & Cutforth, 1996; Michael et al., 2017). However, in this study, it was not statistically significant to incorporate temperature into the final model. This is because no data existed at a sufficiently fine resolution.

3.5 Conclusion

This study successfully demonstrated a statistically and biologically logical framework to model juvenile tree growth at micro-site levels. It also identified and explained height and survival variation of two dryland *Eucalyptus* species. For both species, topographically sheltered surfaces yielded greater height growth and survival. Furthermore, it was also shown

that *E. globoidea* thrived with lower available moisture, while *E. bosistoana* preferred moister soil conditions.

This study and models can help the decision making process about site preparation when establishing new plantation sites, as well as helping to decide about silvicultural regimes for new plantations. It also indicated about within-stand resource partitioning by juvenile plants and reinforced the importance of matching species to sites.

3.6 References

- Adams, H. R., Barnard, H. R., & Loomis, A. K. (2014). Topography alters tree growth-climate relationships in a semi-arid forested catchment. *Ecosphere*, 5(11), 148. doi:doi:10.1890/ES14-00296.1
- Adão, T., Hruška, J., Pádua, L., Bessa, J., Peres, E., Morais, R., & Sousa, J. (2017). Hyperspectral imaging: a review on UAV-based sensors, data processing and applications for agriculture and forestry. *Remote Sensing*, 9(11), 1110.
- Akaike, H. (1981). Likelihood of a model and information criteria. *Journal of Econometrics*, 16(1), 3-14. doi:https://doi.org/10.1016/0304-4076(81)90071-3
- Akay, A. E., Oğuz, H., Karas, I. R., & Aruga, K. (2009). Using LiDAR technology in forestry activities. *Environmental Monitoring and Assessment*, 151. doi:10.1007/s10661-008-0254-1
- Amateis, R. L., Burkhart, H. E., & Liu, J. (1997). Modeling survival in juvenile and mature loblolly pine plantations. *Forest Ecology and Management*, 90(1), 51-58. doi:http://dx.doi.org/10.1016/S0378-1127(96)03833-9
- Ares, A., & Marlats, R. M. (1995). Site factors related to growth of coniferous plantations in a temperate, hilly zone of Argentina. *Australian Forestry*, 58(3), 118-128.
- Avila, O. B. (1993). *Modeling growth dynamics of juvenile loblolly pine plantations*. (PhD), Virginia Polytechnic Institute and State University, Blacksburg.
- Bailey, R. G., Pfister, R. D., & Henderson, J. A. (1978). Nature of land and resource classification-a review. *Journal of Forestry*, 76(10), 650-655.
- Bates, D., Mächler, M., Bolker, B., & Walker, S. (2014). Fitting linear mixed-effects models using lme4. *arXiv preprint arXiv:1406.5823*.
- Bathgate, J. L., Guo, L. B., Allbrook, R. F., & Payn, T. W. (1993). Microsite effect on *Eucalyptus regnans* growth. *New Zealand Journal of Forestry Science*, 23, 154-162.
- Belli, K. L., & Ek, A. R. (1988). Growth and survival modeling for planted conifers in the Great Lakes region. *Forest Science*, 34(2), 458-473.
- Benesty, J., Chen, J., Huang, Y., & Cohen, I. (2009). Pearson correlation coefficient *Noise reduction in speech processing* (pp. 1-4): Springer.
- Berrill, J.-P., & O'Hara, K. L. (2015). How do biophysical factors contribute to height and basal area development in a mixed multiaged coast redwood stand? *Forestry*. doi:10.1093/forestry/cpv049

- Beven, K. J., & Kirkby, M. J. (1979). A physically based, variable contributing area model of basin hydrology. *Hydrological Sciences Bulletin*, 24(1), 43-69. doi:10.1080/02626667909491834
- Bohlen, P. J., Groffman, P. M., Driscoll, C. T., Fahey, T. J., & Siccama, T. G. (2001). Plant-soil-microbial interactions in a northern hardwood forest. *Ecology*, 82(4), 965-978.
- Böhner, J., & Antonić, O. (2009). Land-surface parameters specific to topo-climatology. *Developments in Soil Science*, 33, 195-226.
- Bravo-Oviedo, A., Tomé, M., Bravo, F., Montero, G., & del Río, M. (2008). Dominant height growth equations including site attributes in the generalized algebraic difference approach. *Canadian Journal of Forest Research*, 38(9), 2348-2358. doi:10.1139/X08-077
- Brocca, L., Morbidelli, R., Melone, F., & Moramarco, T. (2007). Soil moisture spatial variability in experimental areas of central Italy. *Journal of Hydrology*, 333(2), 356-373. doi:https://doi.org/10.1016/j.jhydrol.2006.09.004
- Brüchert, F., & Gardiner, B. (2006). The effect of wind exposure on the tree aerial architecture and biomechanics of Sitka spruce (*Picea sitchensis*, Pinaceae). *American Journal of Botany*, 93(10), 1512-1521. doi:doi:10.3732/ajb.93.10.1512
- Burke, I. C., Lauenroth, W. K., Riggle, R., Brannen, P., Madigan, B., & Beard, S. (1999). Spatial variability of soil properties in the shortgrass steppe: the relative importance of topography, grazing, microsite, and plant species in controlling spatial patterns. *Ecosystems*, 2(5), 422-438. doi:10.1007/s100219900091
- Burkhart, H. E., & Tomé, M. (2012). *Modeling Forest Trees and Stands*: Springer.
- Casnati, A. C. R. (2016). *Hybrid mensurational-physiological models for Pinus taeda and Eucalyptus grandis in Uruguay*. (PhD), University of Canterbury, Christchurch, New Zealand.
- Chen, J., Saunders, S. C., Crow, T. R., Naiman, R. J., Broszofski, K. D., Mroz, G. D., . . . Franklin, J. F. (1999). Microclimate in forest ecosystem and landscape ecology variations in local climate can be used to monitor and compare the effects of different management regimes. *BioScience*, 49(4), 288-297.
- Chen, Z.-S., Hsieh, C.-F., Jiang, F.-Y., Hsieh, T.-H., & Sun, I. F. (1997). Relations of soil properties to topography and vegetation in a subtropical rain forest in southern Taiwan. *Plant Ecology*, 132(2), 229-241. doi:10.1023/A:1009762704553
- Clutter, J. L. (1963). Compatible growth and yield models for Loblolly Pine. *Forest Science*, 9(3), 354-371.

- Coates, K. D. (2002). Tree recruitment in gaps of various size, clearcuts and undisturbed mixed forest of interior British Columbia, Canada. *Forest Ecology and Management*, 155(1), 387-398.
- Conrad, O., Bechtel, B., Bock, M., Dietrich, H., Fischer, E., Gerlitz, L., . . . Böhner, J. (2015). System for automated geoscientific analyses (SAGA) v. 2.1.4. *Geosci. Model Dev.*, 8(7), 1991-2007. doi:10.5194/gmd-8-1991-2015
- Daniels, R. F., & Burkhart, H. E. (1988). An integrated system of forest stand models. *Forest Ecology and Management*, 23(2), 159-177.
- Dobbin, K. K., & Simon, R. M. (2011). Optimally splitting cases for training and testing high dimensional classifiers. *BMC Medical Genomics*, 4(1), 31.
- Dyck, B. (2003). *Precision forestry—The path to increased profitability*. Paper presented at the Proceedings, The 2nd International Precision Forestry Symposium.
- Ek, A. R. (1974). Nonlinear models for stand table projection in northern hardwood stands. *Canadian Journal of Forest Research*, 4(1), 23-27.
- ESRI. (2012). ArcGIS Release 10.1. Redlands, CA.
- Fox, J. A., & Weisberg, S. (2011). *An R companion to applied regression*.
- Garcia, O. (1984). New class of growth models for even-aged stands: Pinus radiata in Golden Downs Forest. *New Zealand Journal of Forest Science*, 14(1), 65-88.
- Gerlitz, L., Conrad, O., & Böhner, J. (2015). Large-scale atmospheric forcing and topographic modification of precipitation rates over high Asia - a neural-network-based approach. *Earth System Dynamics*, 6(1), 61-81. doi:10.5194/esd-6-61-2015
- Goulding, C. J. (1979). Validation of growth models used in forest management. *New Zealand Journal of Forestry*, 24(1), 108-124.
- Gradwell, M. W. (1972). *Methods for physical analysis of soils*. New Zealand Soil Bureau Scientific Report No. 10C. Retrieved from Wellington, New Zealand:
- Grey, D. (1980). On the concept of site in forestry. *South African Forestry Journal*, 113(1), 81-83.
- Hamner, B., & Frasco, M. (2018). *Metrics: evaluation metrics for machine Learning*. R package version 0.1.4.
- Heerdegen, R. G., & Beran, M. A. (1982). Quantifying source areas through land surface curvature and shape. *Journal of Hydrology*, 57(3), 359-373. doi:https://doi.org/10.1016/0022-1694(82)90155-X

- Hutcheson, G. D. (1999). Ordinary Least-Squares Regression. In G. D. Hutcheson (Ed.), *The Multivariate Social Scientist*: SAGE Publications, Ltd.
- Jame, Y., & Cutforth, H. (1996). Crop growth models for decision support systems. *Canadian Journal of Plant Science*, 76(1), 9-19.
- Koch, G. W., Sillett, S. C., Jennings, G. M., & Davis, S. D. (2004). The limits to tree height. *Nature*, 428(6985), 851-854.
- Kohama, T., Mizoue, N., Ito, S., Inoue, A., Sakuta, K., & Okada, H. (2006). Effects of light and microsite conditions on tree size of 6-year-old *Cryptomeria japonica* planted in a group selection opening. *Journal of Forest Research*, 11(4), 235-242. doi:10.1007/s10310-005-0202-7
- Kozak, A., & Kozak, R. (2003). Does cross validation provide additional information in the evaluation of regression models? *Canadian Journal of Forest Research*, 33(6), 976-987. doi:10.1139/x03-022
- Kuuluvainen, T. (2002). Natural variability of forests as a reference for restoring and managing biological diversity in boreal Fennoscandia. *Silva Fennica*, 36(1), 97-125.
- Land Resource Information System. (2015). Fundamental soil layer (All attributes). Retrieved from <https://lris.scinfo.org.nz/search/?q=FSL+all+atributes>
- Landsberg, J. (2003). Physiology in forest models: history and the future. *FBMIS*, 1, 49-63.
- Lexer, M. J., & Hönninger, K. (1998). Estimating physical soil parameters for sample plots of large-scale forest inventories. *Forest Ecology and Management*, 111(2), 231-247.
- Louw, J. H. (1999). A review of site-growth studies in South Africa. *Southern African forestry journal*, 185(1), 57-65. doi:10.1080/10295925.1999.9631228
- Mäkelä, A., Landsberg, J., Ek, A. R., Burk, T. E., Ter-Mikaelian, M., Ågren, G. I., . . . Puttonen, P. (2000). Process-based models for forest ecosystem management: current state of the art and challenges for practical implementation. *Tree Physiology*, 20(5-6), 289-298.
- Martín-Alcón, S., Coll, L., & Salekin, S. (2015). Stand-level drivers of tree-species diversification in Mediterranean pine forests after abandonment of traditional practices. *Forest Ecology and Management*, 353(0), 107-117. doi:http://dx.doi.org/10.1016/j.foreco.2015.05.022
- Mason, E. G. (1992). *Decision-support systems for establishing Radiata pine plantations in the central North Island of New Zealand*. (Doctor of Philosophy in Forestry), University of Canterbury.

- Mason, E. G. (2001). A model of the juvenile growth and survival of *Pinus radiata* D. Don; adding the effects of initial seedling diameter and plant handling. *New Forests*, 22(1-2), 133-158. doi:10.1023/A:1012393130118
- Mason, E. G., & Whyte, A. G. D. (1997). Modelling initial survival and growth of Radiata pine in New Zealand. *Acta Forestalia Fennica*, 2, 1-38.
- Mayer, D., Stuart, M., & Swain, A. (1994). Regression of real-world data on model output: an appropriate overall test of validity. *Agricultural Systems*, 45(1), 93-104.
- Michael, J. R., Noah, O. B., Thomas, R. S., David, B. L., & Wolfram, S. (2017). Comparing and combining process-based crop models and statistical models with some implications for climate change. *Environmental Research Letters*, 12(9), 095010.
- Monserud, R. A., & Sterba, H. (1996). A basal area increment model for individual trees growing in even-and uneven-aged forest stands in Austria. *Forest Ecology and Management*, 80(1), 57-80.
- Montgomery, D. R., & Dietrich, W. E. (1994). A physically based model for the topographic control on shallow landsliding. *Water Resources Research*, 30(4), 1153-1171. doi:doi:10.1029/93WR02979
- Mooney, H. A., Vitousek, P. M., & Matson, P. A. (1987). Exchange of materials between terrestrial ecosystems and the atmosphere. *Science*, 238(4829), 926-932.
- Moore, I. D., Grayson, R. B., & Ladson, A. R. (1991). Digital terrain modelling: a review of hydrological, geomorphological, and biological applications. *Hydrological Processes*, 5(1), 3-30. doi:doi:10.1002/hyp.3360050103
- Mummery, D., & Battaglia, M. (2002). Data input quality and resolution effects on regional and local scale *Eucalyptus globulus* productivity predictions in north-east Tasmania. *Ecological Modelling*, 156(1), 13-25. doi:https://doi.org/10.1016/S0304-3800(02)00042-X
- Narukawa, Y., & Yamamoto, S. I. (2001). Gap formation, microsite variation and the conifer seedling occurrence in a subalpine old-growth forest, central Japan. *Ecological Research*, 16(4), 617-625.
- New Zealand Department of Scientific and Industrial Research. (1968). *General survey of the soils of South Island New Zealand, Soil Bureau Bulletin 27*. Retrieved from
- NIWA. (2015). Overview of New Zealand climate. Retrieved from <https://www.niwa.co.nz/education-and-training/schools/resources/climate/overview>
- Nyström, K., & Kexi, M. (1997). Individual tree basal area growth models for young stands of Norway spruce in Sweden. *Forest Ecology and Management*, 97(2), 173-185.

- Padilla, F. M., & Pugnaire, F. I. (2007). Rooting depth and soil moisture control Mediterranean woody seedling survival during drought. *Functional Ecology*, 21(3), 489-495. doi:10.1111/j.1365-2435.2007.01267.x
- Parton, W. J., Schimel, D. S., Cole, C. V., & Ojima, D. S. (1987). Analysis of factors controlling soil organic matter levels in great plains grasslands. *Soil Science Society of America Journal*, 51(5), 1173-1179. doi:10.2136/sssaj1987.03615995005100050015x
- Popper, K. (2014). *Conjectures and refutations: The growth of scientific knowledge*: Routledge.
- Preece, N. D., Lawes, M. J., Rossman, A. K., Curran, T. J., & van Oosterzee, P. (2015). Modelling the growth of young rainforest trees for biomass estimates and carbon sequestration accounting. *Forest Ecology and Management*, 351(0), 57-66. doi:http://dx.doi.org/10.1016/j.foreco.2015.05.003
- R Core Team. (2017). R: A language and environment for statistical computing. Vienna, Austria: R Foundation for Statistical Computing; 2016. URL <http://www.R-project.org>.
- Radford, I. J., Nicholas, M., Tiver, F., Brown, J., & Kriticos, D. (2002). Seedling establishment, mortality, tree growth rates and vigour of *Acacia nilotica* in different *Astrebla* grassland habitats: implications for invasion. *Austral Ecology*, 27(3), 258-268. doi:10.1046/j.1442-9993.2002.01176.x
- Richardson, B., Watt, M. S., Mason, E. G., & Kriticos, D. J. (2006). Advances in modelling and decision support systems for vegetation management in young forest plantations. *Forestry*, 79(1), 29-42. doi:10.1093/forestry/cpi059
- Riley, S. J., DeGloria, S. D., & Elliot, R. (1999). A terrain ruggedness index that quantifies topographic heterogeneity. *Intermountain Journal of Sciences*, 5(1-4), 23-27.
- Ritchie, M. W., & Hamann, J. D. (2006). Modeling dynamics of competing vegetation in young conifer plantations of northern California and southern Oregon, USA. *Canadian Journal of Forest Research*, 36(10), 2523-2532. doi:10.1139/x06-124
- Rohner, B., Waldner, P., Lischke, H., Ferretti, M., & Thürig, E. (2018). Predicting individual-tree growth of central European tree species as a function of site, stand, management, nutrient, and climate effects. *European Journal of Forest Research*, 137(1), 29-44. doi:10.1007/s10342-017-1087-7
- Sale, J. E. M., Lohfeld, L. H., & Brazil, K. (2002). Revisiting the quantitative-qualitative debate: implications for mixed methods research. *Quality and Quantity*, 36(1), 43-53. doi:10.1023/a:1014301607592

- Salekin, S., Burgess, J., Morgenroth, J., Mason, E., & Meason, D. (2018). A comparative study of three non-geostatistical methods for optimising Digital Elevation Model interpolation. *ISPRS International Journal of Geo-Information*, 7(8), 300.
- Sargent, R. G. (2013). Verification and validation of simulation models. *Journal of Simulation*, 7(1), 12-24. doi:10.1057/jos.2012.20
- Shugart, H. H. (1984). *A theory of forest dynamics. The ecological implications of forest succession models*: Springer-Verlag.
- Skovsgaard, J. P., & Vanclay, J. K. (2008). Forest site productivity: a review of the evolution of dendrometric concepts for even-aged stands. *Forestry*, 81(1), 13-31.
- Skovsgaard, J. P., & Vanclay, J. K. (2013). Forest site productivity: a review of spatial and temporal variability in natural site conditions. *Forestry*, 86(3), 305-315. doi:10.1093/forestry/cpt010
- Snowdon, P., Jovanovic, T., & Booth, T. H. (1999). Incorporation of indices of annual climatic variation into growth models for *Pinus radiata*. *Forest Ecology and Management*, 117(1), 187-197.
- Speight, J. G. (1980). The role of topography in controlling throughflow generation: a discussion. *Earth Surface Processes*, 5(2), 187-191. doi:doi:10.1002/esp.3760050209
- Spiecker, H., Mieläkinen, K., Köhl, M., & Skovsgaard, J. P. (1996). Discussion. In H. Spiecker, K. Mieläkinen, M. Köhl, & J. Skovsgaard (Eds.), *Growth Trends in European Forests* (pp. 355-367): Springer Berlin Heidelberg.
- Spieß, A., & Ritz, C. (2014). qpcR: modelling and analysis of real-time PCR data. *R package version*, 1.4-0.
- Travis, M. R., Elsner, G. H., Iverson, W. D., & Johnson, C. G. (1975). VIEWIT: computation of seen areas, slope, and aspect for land-use planning. *Gen. Tech. Rep. PSW-GTR-11*. Berkeley, CA: Pacific Southwest Research Station, Forest Service, US Department of Agriculture: 70 p, 11.
- Uzoh, F. C. C., & Mori, S. R. (2012). Applying survival analysis to managed even-aged stands of ponderosa pine for assessment of tree mortality in the western United States. *Forest Ecology and Management*, 285, 101-122. doi:10.1016/j.foreco.2012.08.006
- Verbeke, G., & Lesaffre, E. (1996). A linear mixed-effects model with heterogeneity in the random-effects population. *Journal of the American Statistical Association*, 91(433), 217-221. doi:10.1080/01621459.1996.10476679
- Watt, M. S., Kimberley, M. O., Richardson, B., Whitehead, D., & Mason, E. G. (2004). Testing a juvenile tree growth model sensitive to competition from weeds, using *Pinus radiata*

- at two contrasting sites in New Zealand. *Canadian Journal of Forest Research*, 34(10), 1985-1992. doi:10.1139/x04-072
- Weiskittel, A., Temesgen, H., Wilson, D., & Maguire, D. (2008). Sources of within- and between-stand variability in specific leaf area of three ecologically distinct conifer species. *Annals of Forest Science*, 65(1), 103-103. doi:10.1051/forest:2007075
- Weiskittel, A. R., Hann, D. W., Kershaw, J. A., & Vanclay, J. K. (2011). *Forest Growth and Yield Modeling*: Wiley.
- Weiss, A. (2001). *Topographic position and landforms analysis*. Paper presented at the Poster presentation, ESRI user conference, San Diego, CA.
- Wiens, J. A. (1989). Spatial scaling in ecology. *Functional Ecology*, 3(4), 385-397. doi:10.2307/2389612
- Woollons, R. C., Snowdon, P., & Mitchell, N. D. (1997). Augmenting empirical stand projection equations with edaphic and climatic variables. *Forest Ecology and Management*, 98(3), 267-275. doi:http://dx.doi.org/10.1016/S0378-1127(97)00090-X
- Wright, R. D. (1972). *Validating dynamic models: an evaluation of tests of predictive power*. Paper presented at the Proceedings of 1972 Summer Computer Simulation Conference.
- Yang, Y., Monserud, R. A., & Huang, S. (2004). An evaluation of diagnostic tests and their roles in validating forest biometric models. *Canadian Journal of Forest Research*, 34(3), 619-629. doi:10.1139/x03-230
- Yokoyama, R., Shlrasawa, M., & Richard, I. P. (2005). Visualizing topography by openness : a new application of image processing to Digital Elevation Models. *Photogrammetric Engineering and Remote Sensing*, 68(3), 257-266.
- Zaslavsky, D., & Sinai, G. (1981). Surface hydrology: I—explanation of phenomena. *Journal of the Hydraulics Division*, 107(1), 1-16.
- Zevenbergen, L. W., & Thorne, C. R. (1987). Quantitative analysis of land surface topography. *Earth Surface Processes and Landforms*, 12(1), 47-56. doi:doi:10.1002/esp.3290120107
- Zhang, S., Burkhart, H. E., & Amateis, R. L. (1996). Modeling individual tree growth for juvenile loblolly pine plantations. *Forest Ecology and Management*, 89(1-3), 157-172. doi:http://dx.doi.org/10.1016/S0378-1127(96)03851-0

4

Modelling the growth and survival of juvenile *Eucalyptus globoidea* and *Eucalyptus bosistoana* in New Zealand

4. Modelling the growth and survival of juvenile *Eucalyptus globoidea* and *Eucalyptus bosistoana* in New Zealand.

4.1 Introduction

Tree growth and development are complex processes (Rauscher et al., 1990), and greatly influenced by a stand's resource conditions e.g. climatic and edaphic conditions (Toledo et al., 2011; Yang et al., 2006). However, it is essential to predict future forest growth and development to practice proper forest management (Ritchie & Hamann, 2008), which for commercial forestry, leads ideally to high stem growth and financial returns. For good growth prediction, it is necessary to have proper information from the early stages of establishment before canopy closure (Mason & Whyte, 1997; Zhao, 1999). Consequently, growth dynamics at the juvenile stage of a plantation are crucial as this will generate site-specific information to assist with modelling later developmental stages (Avila, 1993). The growth and survival of the juvenile stage are often more complex than the mature stages as both inter and intra-specific competition occur, but intra-specific competition dominates mature stands where only one species was planted.

Stand models for mature trees have been well explored from several different perspectives (Burkhart & Tomé, 2012; Weiskittel et al., 2011) and implemented in practice by both researchers and forest managers. Also, different mature stand-level modelling approaches have been applied to increase the level of understanding (Clutter, 1963; Mäkelä et al., 2000; Peng et al., 2002a) and applicability in the field (Battaglia & Sands, 1998). Conversely, since their inception (Belli & Ek, 1988; Payandeh, 1987), growth and yield models of juvenile plantations are less common than mature stand models (Zhang et al., 1996). Several studies do exist, describing influences on young stands due to site preparation and seedling handling (Mason, 2001; Mason et al., 1997; Westfall et al., 2004), various levels of stand density (Zhang et al., 1996) and competition with weed and surrounding vegetation (Comeau & Rose, 2006;

Tesch & Hobbs, 1989; Watt et al., 2004; Watt et al., 2003). Also, the ecophysiological processes of juvenile plantation growth were also modelled by Rauscher et al. (1990) for young poplar plantations at an individual tree level.

Considering the above, there have been recent advancements in juvenile growth and yield modelling, but such models are seldom used by forest managers to make decisions because of their associated complexity and uncertainty (Richardson et al., 2006). Mäkelä et al. (2000) reported that incorporating the most desired elements from both models, which rationalise the biological realism in traditional mathematical models, could be a way to make the models more useful. However, to be truly useful, models also need to be simple and developed in close collaboration with the end users with readily available data (Sands et al., 2000).

Furthermore, most of the stand-level or individual tree juvenile models use competition indices or correlated variables as surrogates for other variables. For instance, Villalba et al. (1992) explained tree growth variations in terms of spatial patterns of climate change. Additionally, it gives extra confidence to the users to input directly measured values, thus reducing risks from overestimation or assumption. So, to develop field compatible stand-level models, it is crucial to test and identify the essential predictors from a comprehensive set of site variables directly determined from topography, soil and climate. Then, these variables must be included in the modelling framework to predict and explain at the same time.

The overall goals of this study were to test and identify the essential variables that drive the height growth and survival of juvenile plantations and to add them into a modelling framework. The specific objectives were :

- i) to identify site-specific topographic, edaphic and climatic variables that influence the height growth of juvenile *E. globoidea* and *E. bosistoana*, and to include these in a height growth model;

- ii) to identify site-specific topographic, edaphic and climatic variables that influence the survival of juvenile *E. globoidea* and *E. bosistoana*, and to include these in a survival model.

4.2 Materials and methods

4.2.1 Experimental sites

The study covers all the plantation sites managed by the New Zealand Dryland Forest Initiative (NZDFI). Twenty-five sites were planted with *E. bosistoana* and *E. globoidea*, located in the northern South Island and the North Island, mostly on retired pastures. They were situated between 38° 24' 41.94" S and 43° 11' 46.80" S Latitude, and 177° 41' 34.97" E and 172° 39' 08.15" E Longitude (Figure 4.1). The altitudes of these sites ranged from 53 - 640 meters above sea level (MASL). They experienced cool, dry sub-humid to humid climates with total annual precipitation of 840 - 7935mm and mean annual temperatures of 6 - 20°C (summary of 2009 - 2016). However, both temperature and precipitation had a spatial variation across the planting sites due to their proximity to the coast and changes in topography (Mason et al., 2017). The growing season in New Zealand is typically from October to April, but the duration of the growing period varies due to climate and elevation gradients (Wardle, 1991). The sites covered most of the New Zealand soil classes (Hewitt, 2010), but were dominated by different types of pallic soils. A comprehensive soil classification list is presented in Appendix II.

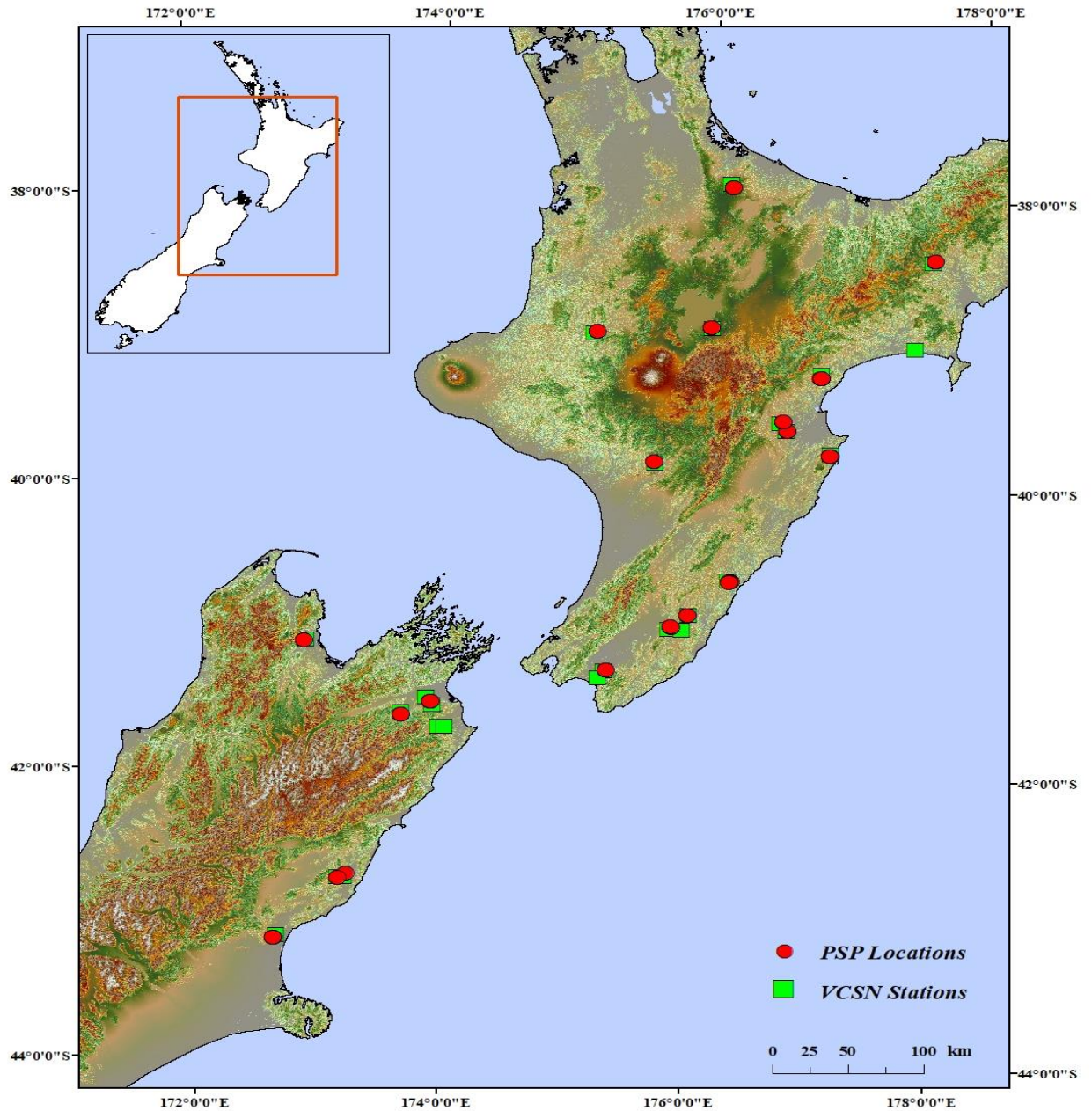


Figure 4.1 Locations of permanent sample plots (PSPs) and virtual climatic stations (VCSN).

4.2.2 Data collection and preparation

All the data related to plantations, topography, climate and soils were collected for both species from all 25 NZDFI plantation sites. The data collection and preparation procedures are described below.

4.2.2.1 Tree data

NZDFI sites had a total of 84 permanent sample plots (PSPs), planted with the study species (*E. bosistoana* and *E. globoidea*) from the year 2009 to 2014. They were of varying sizes (384 - 784m²) and shapes (e.g., circular, square and rectangular). NZDFI conducted a tree inventory during some of their growing seasons and recorded height (h), and status (dead or alive) of all trees for all PSPs. However, trees were not measured immediately after planting. In this study, the inventory data for the period 2010 - 2016 were used.

Individual tree height and survival data were averaged at each plot at each measurement time. Due to the small sizes of trees, there were insufficient measurements of diameter at breast height (DBH) to calculate DBH or basal area. The survival proportion (S) was calculated for each plot from the number of trees that survived per plot (Table 4.1).

Table 4.1 Summary of plantation inventory data.

<i>Total sites</i>	<i>Species</i>	<i>Total PSPs</i>	<i>Measurement periods (Year)</i>	<i>Age (Years)</i>		<i>Plot size (m²)</i>		<i>Height (m)</i>				<i>Survival</i>			
				Min	Max	Min	Max	Min.	Max.	Mean	SD	Min.	Max.	Mean	SD
25	<i>E. bosistoana</i>	42	2010 - 2016	1.1	6.4	384.2	784.0	0.60	7.08	2.78	1.50	0.18	1.00	0.92	0.11
		42	2012 - 2016	1.1	6.4	384.2	784.0	0.51	7.62	3.04	1.67	0.14	1.00	0.78	0.23

4.2.2.2 Topographic data

Land Information New Zealand (LINZ) hosts the most up-to-date nationwide set of topographic data and maps. In the case of topography, these data are well defined and have a planimetric average of $\pm 22\text{m}$ and a vertical average of $\pm 0\text{m}$ accuracy (LINZ, 2017). Therefore, nationwide 15m x 15m digital elevation model (DEM) tiles (Barringer et al., 2002; Columbus et al., 2011) were downloaded through the LINZ data service (LINZ, 2017). In total 30 tiles were processed by using ArcMap 10.4.1 (ESRI, 2012) for the final analyses.

A list of primary and secondary surface attributes was derived from the DEM by the procedure described in Chapter 3. The values of those attributes were presented in Table 4.2.

Table 4.2 Summary of estimated topographic attributes.

Attributes	<i>E. bosistoana</i>				<i>E. globoidea</i>			
	<i>Min</i>	<i>Max</i>	<i>Mean</i>	<i>SD</i>	<i>Min</i>	<i>Max</i>	<i>Mean</i>	<i>SD</i>
<i>Aspect (°)</i>	0	352.87	142.52	124.52	0	350.84	154.14	124.24
<i>Slope (°)</i>	0	23.57	10.37	6.55	0	27.18	12.29	7.35
<i>Elevation (m)</i>	53	640	218.54	152.41	53	637	218.62	151.11
<i>Curvature</i>	-1.33	3.11	0.27	0.94	-0.89	2.67	0.23	0.89
<i>Profile curvature</i>	-2	1.32	-0.15	0.62	-2.32	0.75	-0.24	0.70
<i>Plan curvature</i>	-1.04	1.31	0.13	0.46	-0.56	0.75	0.0	0.33
<i>TRI</i>	0	16.09	7.21	4.33	0.0	19.90	8.48	5.04
<i>TPI</i>	-1.12	2.25	0.21	0.67	-0.75	2.12	0.23	0.65
<i>WTI</i>	2.15	13.37	8.21	4.00	2.18	13.36	8.58	3.75
<i>WEI</i>	0.87	1.19	1.02	0.09	0.87	1.16	1.02	0.08
<i>MPI</i>	0.01	0.23	0.09	0.05	0.02	0.20	0.10	0.08

4.2.2.3 Soil data

The NZLRI System comprises several physical resource themes. These themes are based on the NZLRI with a polygon layer with national coverage. This layer is also supplemented with soil survey layers. Fundamental soil layers (FSL) are part of the NZLRI, describe and characterise soils of New Zealand (Newsome et al., 2008). FSL layers are freely available as georeferenced vector layers through the Land Resource Information System portal (LRIS, 2017).

The most recent FSL layers were downloaded from the NZLRI portal and processed in ArcMap 10.4.1 (ESRI, 2012) to extract values corresponding to the centre point at each PSP location. The soil data included both physical and chemical attributes. All the data were then linked to the final dataset (Table 4.3).

Table 4.3 Summary statistics of soil data.

Variables	Unit	<i>E. bosistoana</i>				<i>E. globoidea</i>			
		<i>Min</i>	<i>Max</i>	<i>Mean</i>	<i>SD</i>	<i>Min</i>	<i>Max</i>	<i>Mean</i>	<i>SD</i>
<i>Potential rooting depth (PRD)</i>	<i>m</i>	0.10	1	0.41	0.29	0.10	1	0.43	0.30
<i>Potentially available water (PAW)</i>	<i>mm</i>	1	10	6.36	3.10	1	9	5.38	3.04
<i>Potential readily available water (PRAW)</i>	<i>mm</i>	1	9	5.28	2.83	1	10	6.32	2.90
<i>Top soil gravel content (GARV)</i>	<i>%</i>	1	3	2.45	0.88	1	4	2.44	0.91
<i>Rock outcrops and surface boulder (ROCK)</i>	<i>%</i>	0	1	0.10	0.30	0	1	0.11	0.32
<i>Drainage class (DRAIN)</i>	<i>%</i>	0	5	2.88	2.01	0	5	2.99	2.12
<i>Permeability (PRM)</i>	<i>Ratio</i>	1	4	2.02	0.79	1	4	2.11	0.93
<i>pH</i>	<i>-</i>	1	9	4.69	2.52	1	9	4.73	2.66
<i>Salinity (SAL)</i>	<i>%</i>	0	0	0.01	0.01	0	0	0.01	0.01
<i>Cation exchange capacity (CEC)</i>	<i>cmoles/kg</i>	1	8	4.60	2.44	1	8	4.48	2.45
<i>Phosphorus retention (PRET)</i>	<i>%</i>	1	9	3.97	2.11	1	9	3.99	2.19
<i>Carbon (C)</i>	<i>%</i>	0	9	4.63	3.38	0	9	4.45	3.53

4.2.2.4 Climatic data

The National Institute of Water and Atmospheric (NIWA) Research operates meteorological stations throughout New Zealand, with higher spatial frequency for the same type of measurements than other similar types of measurements. Those measurements are interpolated daily for the whole country on a regular (~5km) grid (NIWA, 2015b), and the system is called the Virtual Climatic Station Network (VCSN). The closest VCSN points to the experimental sites were selected from the NIWA website. Locations of the VCSN points are shown in Figure 4.1.

From the VCSN, temperature, precipitation, radiation, and potential evapotranspiration (PET) data were extracted. PET was estimated by NIWA using the Penman-Monteith equation, as described by Burman and Pochop (1994). Temperature data were separated based on daily maxima (Tmax) and minima (Tmin), then summarised by year and month, and averaged for each PSP. Radiation data were summarised by summing for the whole period. Besides these, precipitation and PET were summed for the whole period for each PSP. Finally, total PET subtracted from total precipitation to get net moisture yield (NMY) for the whole experimental period. Detailed summary statistics of all climatic information are presented in Table 4.4.

Table 4.4 Summary of climatic data from VCSN points.

Species	Data period (Year)	Temperature monthly mean daily maximum (°C)				Temperature monthly mean daily minimum (°C)				Total annual rainfall (mm)				Radiation (MJ m ⁻² day ⁻¹)			
		Min	Max	Mean	Sd	Min	Max	Mean	Sd	Min	Max	Mean	Sd	Min	Max	Mean	Sd
		<i>E. bosistoana</i>	2009-2017	15.78	20.17	17.86	0.96	5.69	10.20	8.41	0.79	840	7930	2950	1370	10.79	17.01
<i>E. globoidea</i>	2009-2017	16.25	20.17	18.04	0.98	6.57	10.20	8.50	0.84	840	7930	1650	2950	10.79	15.97	13.82	1.34

4.2.3 Modelling approach

Juvenile plantation height before canopy closure is expected to grow exponentially. The modelling approach for juvenile forest plantations was explained in Chapter 3. In this study, the same modelling approach was applied by adding the influence of site-specific variables.

The height yield growth models were fitted with Equation 9, and the survival proportion was modelled using Equation 14. The coefficients were separated and linearly expanded by following Equations 10 and 11 with explanatory variables.

4.2.4 Model testing and validation

Model validation is a vital part of model development. It does not only test the sensitivity of the model but also informs the user about the necessary precautions that need to be taken before final application. The background and procedure of model testing and validation were reported in Chapter 3.

This study followed the same sensitivity metrics described in Chapter 3. Besides those, the predictive ability of the models was evaluated using prediction errors or predictive residual error sum square (PRESS) statistics. These residuals were calculated by omitting each observation in turn from the data, fitting the model to the remaining observations, predicting the response for the omitted observation, and comparing the prediction with the observed value (Equation 26),

$$O_i - P_{i,-i} = e_{i,-i} \quad (i = 1, 2, \dots, n) \quad (25)$$

where O_i is the observed value, $P_{i,-i}$ is the estimated value for observation i (where the latter is absent from the model fitting) and n is the number of observations. Each model has n PRESS residuals associated with it, and the PRESS (Prediction sum of square/P-square) statistic is defined as (Myers & Myers, 1990):

$$\text{PRESS} = \sum_{i=1}^n O_i - (P_{i,-i})^2 = \sum_{i=1}^n (e_{i,-i})^2 \quad (26)$$

The bias and precision of models were analysed by computing means of the PRESS residuals and P-square values.

For validation there was no independent dataset available for this study, nor was the dataset large enough to be subdivided into fit and validation datasets. Therefore, model validation was carried out by ‘leaving-one-out’ method of cross-validations (LOOCV), a method which is also called “Jackknife” (Arlot & Celisse, 2010). Thus, the models were fitted n times, leaving out each sample plot once, so that the number of fittings was equal to the number of plots (Sánchez-González et al., 2005), and residuals of predictions for the plots left out were compared with those of the overall model fit.

For model evaluation, the metrics described in equations 15, 16, 17 and 18 were considered. In this case, the overall estimation of these metrics was carried out by averaging as the prediction errors were calculated for each observation.

4.2.5 Statistical analysis

Neither the NZDFI plantations nor the PSPs therein were established in a single year. The PSPs were re-measured at different time intervals. Hence, the frequency of measurement was not equal for all the PSPs. Also, a high number of explanatory variables were taken into account from soil, climatic and edaphic variables. Consequently, to avoid any kind of vague extrapolation by the final model, the most frequently measured points were separated and modelled by using base model Equation 9 and 14. Then by separating the coefficients, a hierarchical clustering through recursive partitioning analysis was carried out to identify the most important variables. Next, those important variables and their interactions were modelled against coefficients by using multilinear least square (MLS) regression (Equations 10 and 11). Finally, the significant variables and their interactions were included and modelled against height yield and survival through nonlinear least square regression (NLS) (Equations 9 and 14).

All statistical analysis was performed in the R statistical environment (R Core Team, 2017). An assessment for potential multi-collinearity was performed for all the explanatory variables at the beginning by using variance inflation factor (VIF) with “vif.mer” function of car package in R (Fox & Weisberg, 2011). Elevation, slope, topographic ruggedness, total curvature and PET were correlated with variables chosen for use in models. Hence they were left out from the model building procedure. Then the hierarchical clustering was executed through recursive partitioning, based on analysis of variance (ANOVA), by using packages “rpart” and “rpart.plot” and their corresponding functions for this analysis (Therneau et al., 2010). Model coefficients were fitted and separated by running the “lm” function in the base package. Finally, the height and survival models were fitted using the “nls” function in the base package with the significant variables. Models were validated by following the previously explained procedure. “rmse”, “mae”, and “bias” functions were used from the “Metrics” package (Hamner & Frasco, 2018), while the “Rsq.ad” and “AICc” function were used from the “qpcR” package (Spiess & Ritz, 2014). Besides this, residuals were visually inspected for their normality and variance homogeneity. All the graphical analyses and presentations were performed with the “ggplot2” (Wickham, 2016) package.

4.3 Results

4.3.1 Site-specific juvenile height yield models

Final height growth models (Equations 25 and 26) demonstrated the site effect on juvenile tree height yield. Model residual plots (Figure 4.2) and fitting statistics (Table 4. 5) showed that for both species the models were reasonably precise. The residual plots were well distributed, with little or no heteroscedasticity. The model evaluation residuals were also well distributed and followed a similar pattern to the fitted models.

Evaluation statistic values were reasonably reliable with a minor negative bias (Table 4. 5), which indicated that the models slightly underpredicted the tree heights. For *E. bosistoana*, the presence of bias was more visible than for *E. globoidea* (Figure 4.2). Model mean and predicted residual sum of squares (MPRESS and MAPRESS) statistics for two *Eucalyptus* species showed (Table 4. 5) minimal scores in both mean and absolute form. However, a large increase of RMSE, MAE and SE in the validation statistics can be seen. The corrected AIC values for both of the models were small enough to confirm their accuracy (Table 4.5).

$$h_{EGT} = h_0 + (\alpha_0 + \alpha_1 * Tmax)T^{(\beta_0 + \beta_1 * Radiation)} \quad (25)$$

$$h_{EBT} = h_0 + (\alpha_0 + \alpha_1 * WEI)T^{(\beta_0 + \beta_1 * TWI + \beta_2 * WEI)} \quad (26)$$

In these equations, h_{EGT} and h_{EBT} are the height of *E. globoidea* and *E. bosistoana* at time T, h_0 is the initial height immediately after planting (0.25cm in this study case), Tmax is the average daily maximum temperature, Radiation is the total amount of radiation, WEI is the wind exposure index, TWI is topographic wetness index, and α and β are the model coefficients.

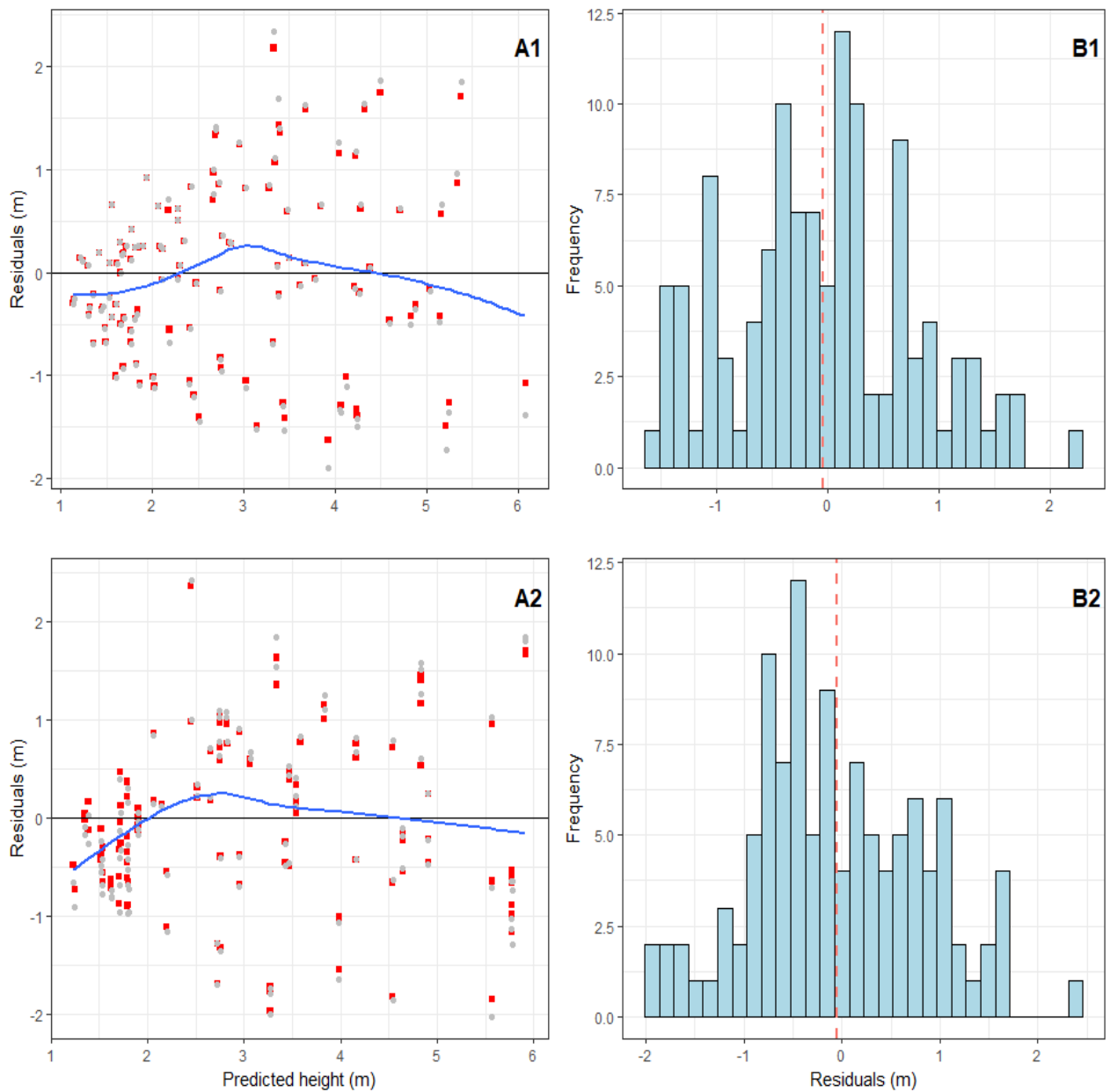


Figure 4.2 Height yield model prediction and residual plot: A1) predicted height yield against model residuals (blue points-model fitting, grey points-model validation residuals and blue line-loess line); B1) model fitting residuals distribution for *E. bosistoana*; A2) predicted height yield against models residuals (red points-model fitting, grey points-model validation residuals and red line shows the loess fit); and B2) model fitting residuals distribution for *E. globoidea*.

Table 4. 5 Height growth model fitting and validation statistics.

Species	Action	RMSE	MAE	BIAS	SE	AICc	R² adj.	MPRESS	MAPRESS
<i>E. globoidea</i>	Fitting	0.864	0.697	-0.031	0.880	295.54	0.6858	-	-
	Validation	1.9666	1.5799	-0.2341	3.983	300.50	-	-0.047	0.630
<i>E. bosistoana</i>	Fitting	0.822	0.660	-0.037	0.840	301.16	0.650	-	-
	Validation	1.8831	1.5469	-0.3152	3.670	301.16	-	-0.040	0.620

4.3.2 Key juvenile height growth factors

The recursive partitioning analyses showed that *E. globoidea* height was influenced by maximum temperature (Tmax) and radiation, whereas, *E. bosistoana* height was influenced by the wind exposure index (WEI) and topographic wetness index (TWI) (Figure 4.3). Both Tmax and radiation were significant in the final model (Equation 25) for *E. globoidea*. Conversely, only WEI and TWI were significant on *E. globoidea* height in the final model (Equation 28). The results showed that, with increasing temperature and radiation, *E. globoidea* attained greater height (Figure 4.4 (A2 and B2)). *E. bosistoana* height growth was positively influenced by TWI, and negatively influenced by WEI (Figure 4.4 A1). Topographic wetness index (TWI) indicates the water availability at certain spatial points, with higher values indicating better water availability. On the other hand, WEI describes exposure to wind for a specified location, and it showed that with less exposure *E. bosistoana* grew taller (Figure 4.4 (A1 and B1)).

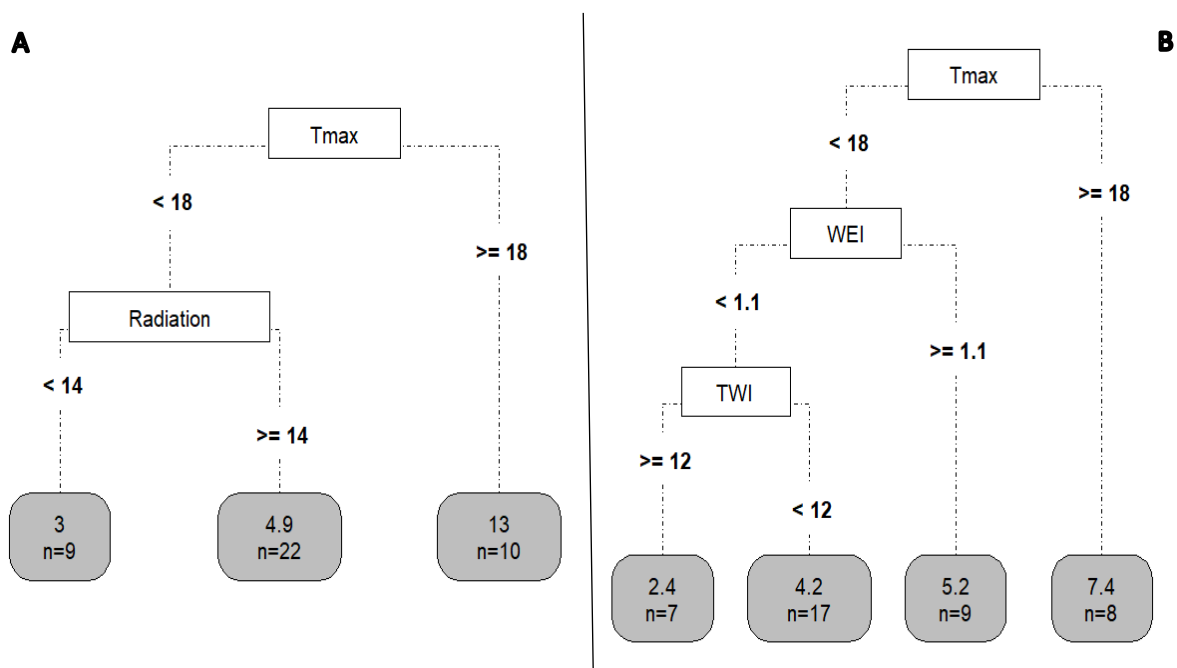


Figure 4.3 Decision trees from the recursive partitioning of independent variables against height yield at a single age. Each factor presents with a threshold value, and each node represents with its splitting values and a number of observations of predicted class. A) represents *E. globoidea*, and B) *E. bosistoana*.

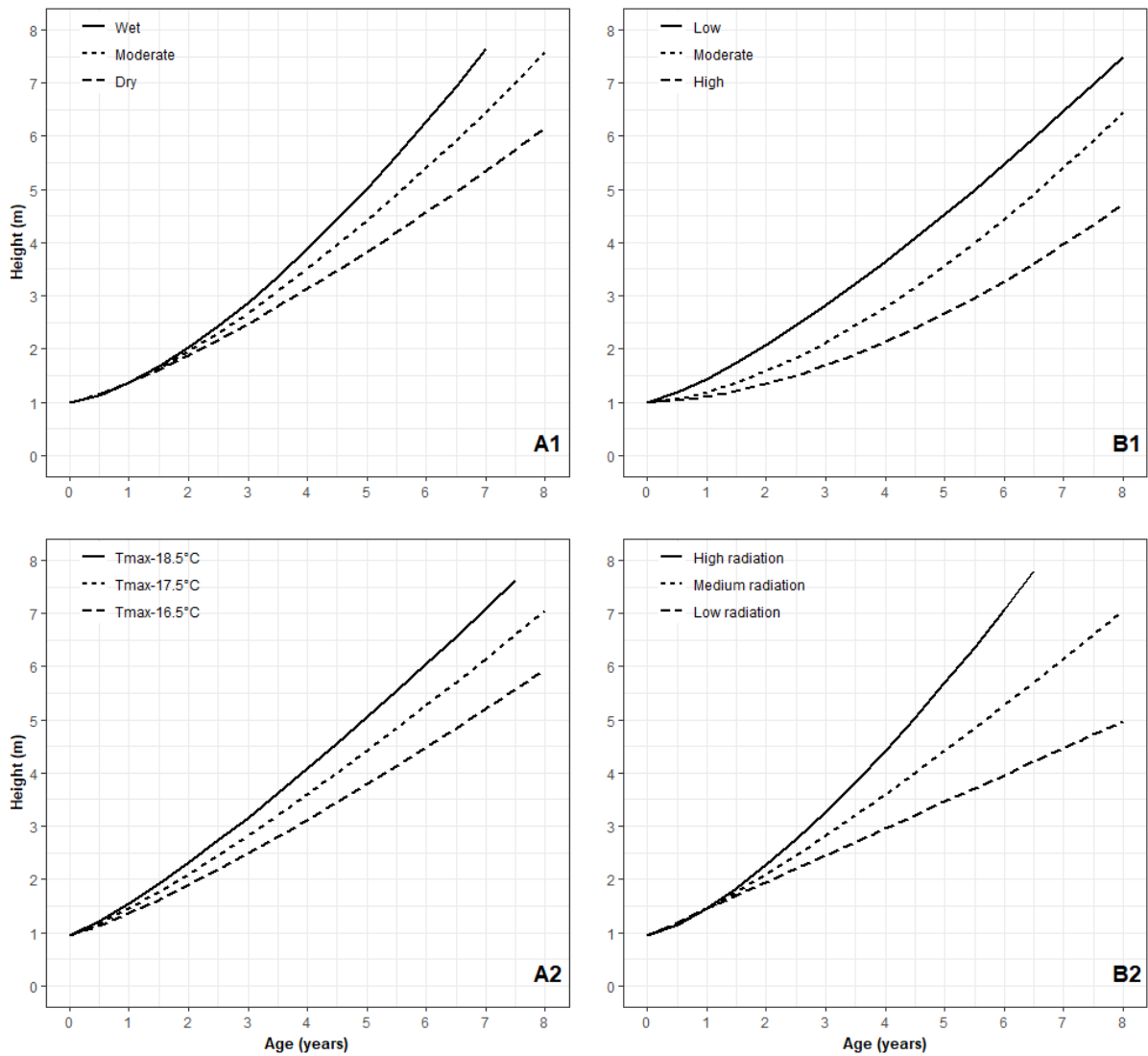


Figure 4.4 Effect of A1) topographic wetness index (TWI), B1) wind exposure index (WEI) on *E. bosistoana*; A2) maximum temperature, and B2) radiation on *E. globoidea* height growth.

4.3.3 Site-specific survival model

The site-specific survival models (Equations 27 and 28) represented a logical framework. Both models were relatively precise in their predictions of survival proportion. The residuals plots for both fitted and evaluation models were homogeneously distributed. Ranges for residuals were small, although, in the case of *E. globoidea*, the model was unstable at the beginning of the period (Figure 4.5 (A2)). For both species, there were a few outliers (Figure 4.5). The *E. bosistoana* survival model was comparatively more stable and precise than that for *E. globoidea*, except for one extreme outlier.

$$S_{EGT} = e^{((\alpha_0 + \alpha_1 * T_{min} + \alpha_2 * TPI) * T^{\beta_0})} \quad (27)$$

$$S_{EBT} = e^{((\alpha_0 + \alpha_1 * T_{min} + \alpha_2 * Radiation) * T^{\beta_0})} \quad (28)$$

In these equations, S_{EGT} and S_{EBT} are the survival proportions for *E. globoidea* and *E. bosistoana* at time T, where T_{min} is minimum temperature, TPI is the topographic position index, and Radiation is the total amount of intercepted radiation for the study period at each PSP position. α and β variables with subscripts are model coefficients.

From the fitted and validation statistics (Table 4.6), models had reasonable goodness-of-fit statistics. RMSE, MAE and SE were small, though they increased by a small amount during validation. MPRESS and MAPRESS were fairly small. Bias for fitting statistics was negative, but for validation it was positive for *E. globoidea*. Furthermore, the AICc values for both species were fairly small, which reconfirmed the accuracy of the models (Table 4.6).

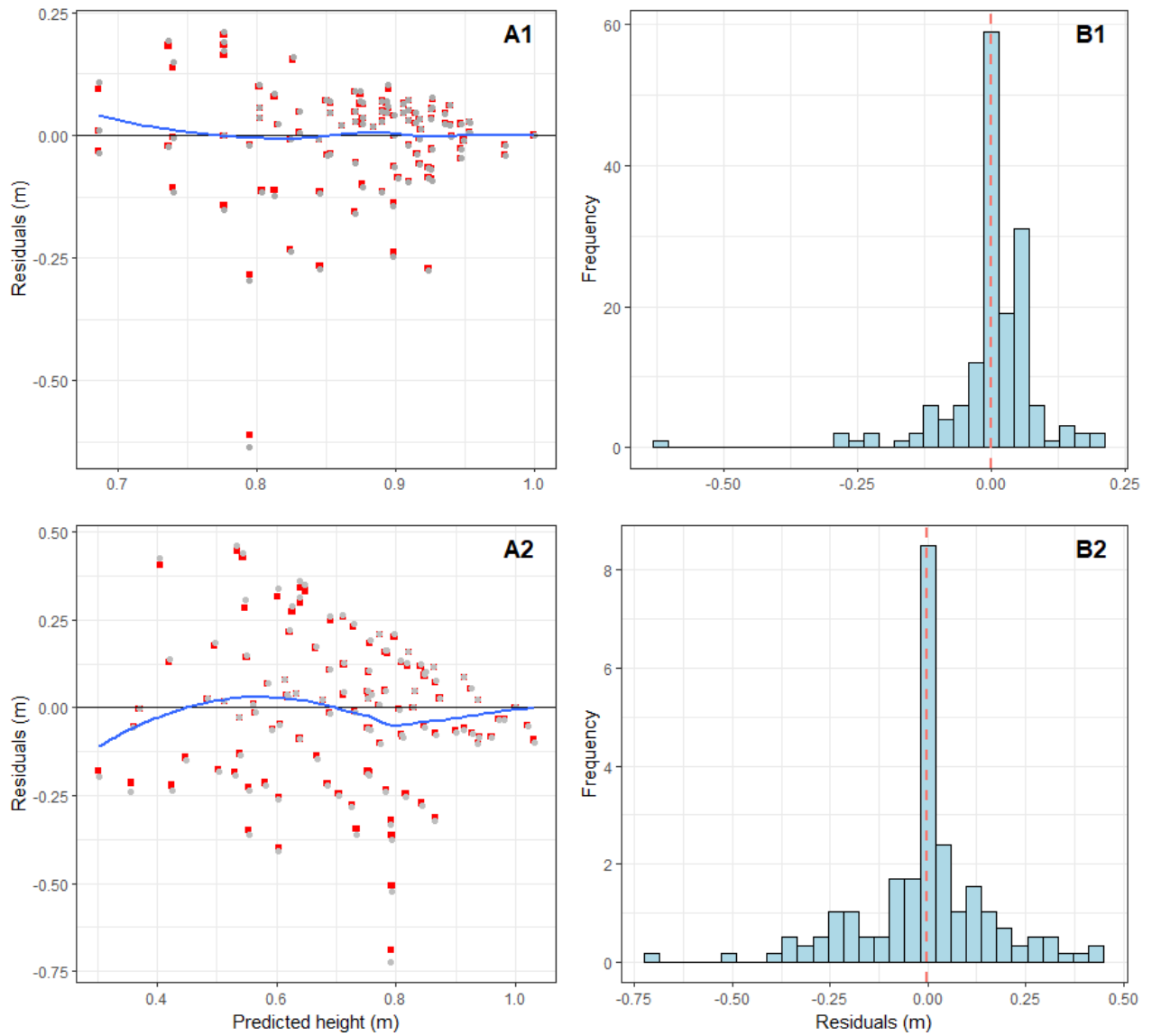


Figure 4.5 Survival models predicted, and residuals plots: A1) predicted survival against model residuals (red points-model fitting, grey points-model validation residuals and blue line-loess line); B1) model fitting residuals distribution for *E. bosistoana* (red dashed line shows the mean); A2) predicted survival proportion against model residuals; and B2) model fitting residuals distribution for *E. globoidea* (the red dashed line shows the mean).

Table 4.6 Survival model fitting and validation statistics.

Species	Action	RMSE	MAE	BIAS	SE	AICc	R² adj.	MPRESS	MAPRESS
<i>E. globoidea</i>	Fitting	0.167	0.109	-0.006	0.17	-99.636	0.561	-	-
	Validation	0.291	0.237	0.0001	0.092	-99.636	-	-0.0068	0.382
<i>E. bosistoana</i>	Fitting	0.089	0.051	-0.007	0.090	-308.715	0.431	-	-
	Validation	0.130	0.103	-0.003	0.021	-308.716	-	-0.00101	0.381

4.3.4 Key site-specific factors for juvenile survival

The initial analyses from recursive partitioning showed that minimum temperature (Tmin) and topographic position index (TPI) were the two most important factors for *E. globoidea* survival. The same analyses found that Tmin and total radiation (Radiation) were important for *E. bosistoana* survival (Figure 4.6).

During linear expansion of the coefficients and final model building, the above variables were found to correlate significantly with the α coefficients, but not with the β coefficients. However, the final model showed that, with increasing radiation and Tmin, the survival proportion increased for *E. bosistoana* (Figure 4.7 (A1 and B1)). The pattern was similar for *E. globoidea*, so sites with higher Tmin and TPI had higher survival proportions for *E. globoidea* than other sites, where *E. globoidea* experienced lower Tmin and TPI (Figure 4.7 (A2 and B2)).

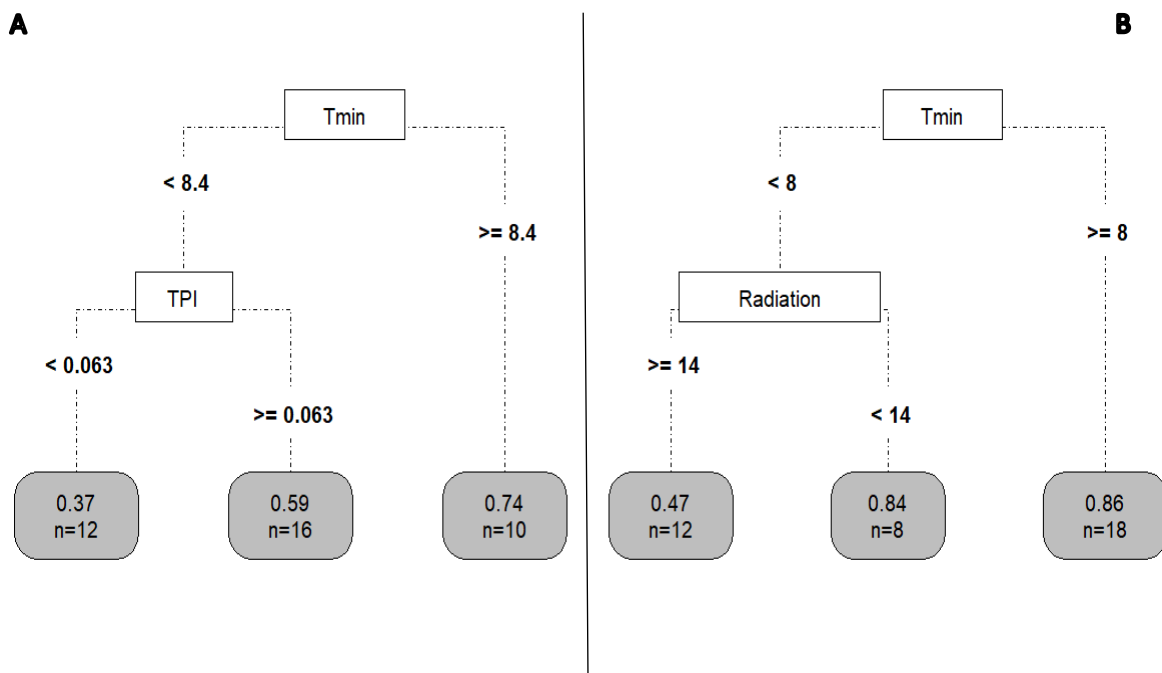


Figure 4.6 Decision trees from the recursive partitioning of independent variables against survival proportion at a single age. Each factor presents a threshold value, and each node represents its splitting values and a number of observations of the predicted class: A) *E. globoidea* and B) *E. bosistoana*.

E. globoidea survival was significantly influenced by WEI. A site more exposed to wind had lower survival rates and vice-versa. This effect was more pronounced immediately after planting and throughout the first year. In the case of *E. bosistoana*, MPI influenced survival. The site with higher protection also had the highest rate of survival. However, influences of MPI on *E. bosistoana* were milder than the WEI effect on *E. globoidea*.

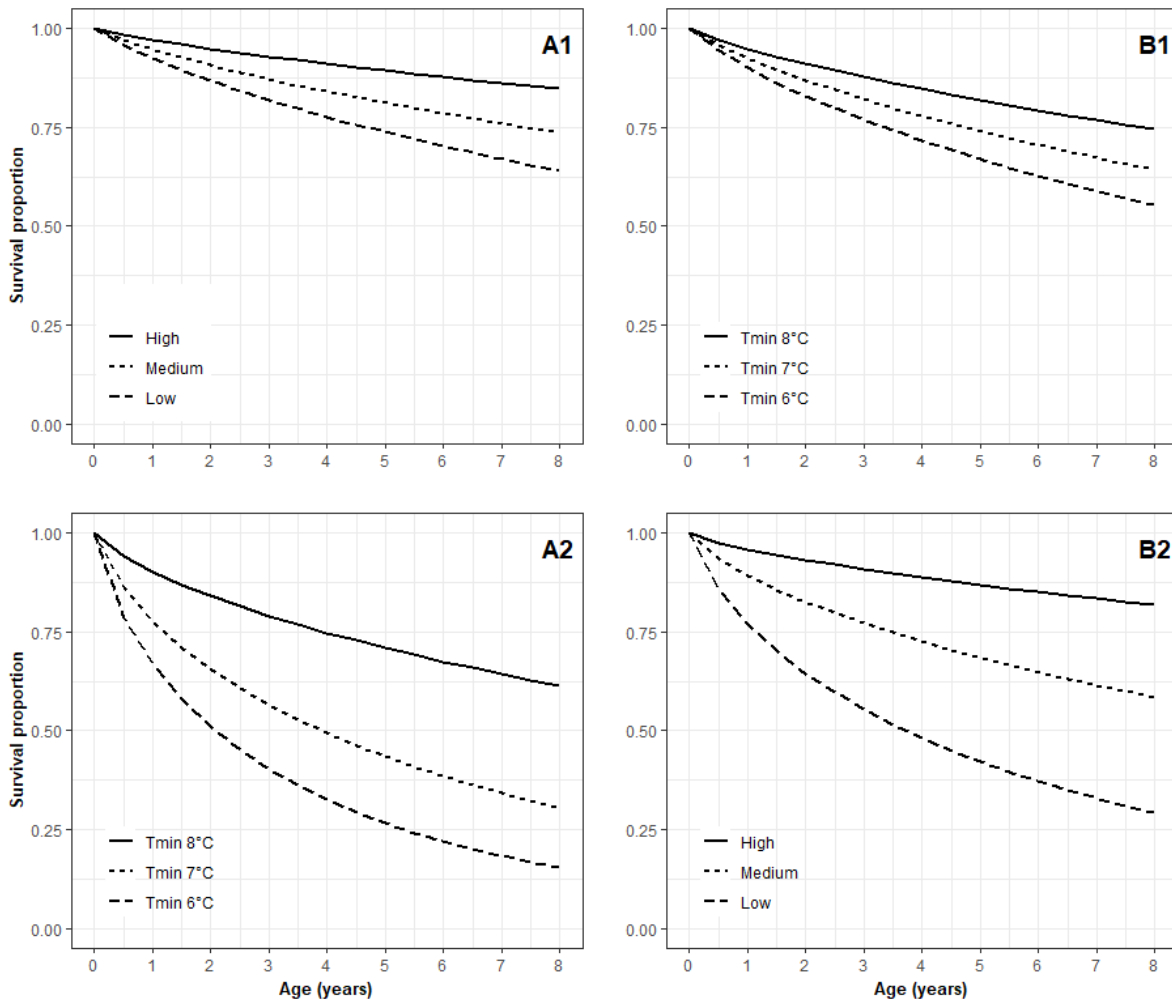


Figure 4.7 Effect of A1) topographic wetness index (TPI), B1) minimum temperature (Tmin) on *E. bosistoana*, A2) minimum temperature (Tmin), and B2) radiation on *E. globoidea* survival.

4.4. Discussion

Fitting height and survival proportion models by identifying and including site-specific factors added more model complexity as well as improving understanding of juvenile stands. The

augmenting process with different explanatory variables was not directly comparable for the two species. Juvenile plantation experiments need careful planning and organisation from the initial stage. This is because those initial steps can easily influence data and thus produce unexpected variations. Also, it is crucial to address the model distortions caused by repeated measurements.

Simple models for the two species tested and considered edaphic and climatic information, which is a spatial scale evaluation. The two studied species seemed to be influenced by climatic and topographic variables, but not by soil variables. This may be due to the quality of the soil data available through FSL layers: their resolution was coarse and predicted values from the FSL layers were found to be highly inaccurate when compared with field observations from soil pits, as reported by Pearse et al. (2015). The climatic data were relatively precise, except for precipitation was likely imprecise (Mason et al., 2017), and potentially by a large margin at some sites.

4.4.1. Site-specific growth and survival models

This study successfully demonstrated a modelling framework for juvenile *Eucalyptus* plantations, which behaves in both a biologically and a methodologically rational way. The results here showed some differences between the two species. The height model for *E. globoidea* was less precise than that for *E. bosistoana*. This inconsistency may arise from the lack of initial height measurements. Zhang et al. (1996) reported that the model could be influenced by the initial measurements, which is an essential feature for juvenile plantation modelling. Additionally, the sample size for this study was small, and that may have influenced the results. For both species, the models were negatively biased which means that some under-prediction occurred. These underpredictions may be caused by the site conditions, as all the sites in this study are collectively known as dryland sites of New Zealand. Also, there is a significant lack of information about the seedling quality as well as the site conditions when these species were planted.

The mortality models were considerably more precise than the height models because they had better initial data and a robust dataset compared with the height dataset, for example, the initial number of seedlings per plot and the size of the plots, though needed to be taken into account at the time of model application.

Although LOOCV or jack-knifing is a widely used model evaluation method, the confidence limit was very narrow in this study. Moreover, the height model performed poorly during validation. Some errors may have arisen from repeated measurements and an unbalanced dataset. For example, the age classes distribution were not homogenous for all the study sites. This limitation was addressed by using a two-step procedure: first a recursive partitioning and then final model fitting. However, height yield models still showed poor fits during validation. Those errors may be reduced by taking more measurements in future and making the dataset more orthogonal, as data quality significantly influences tree growth model building (Aubry et al., 2017; McRoberts & Westfall, 2014).

4.4.2. Juvenile height growth factors

Height growth of *E. bosistoana* and *E. globoidea* was significantly influenced by climatic and topographic variables. Ares and Marlats (1995) reported topographic features as the most significant influencers of tree growth in hilly regions, and they are simultaneously coupled with climatic and edaphic variables (Adams et al., 2014). All the NZDFI plantation sites are in comparatively dry hilly regions of New Zealand. Moreover, Brunori et al. (1995) found that topographical features significantly affect *Eucalyptus* height growth in deserts in Israel. Furthermore, Bullock and Burkhart (2005) reported a spatial dependency in juvenile *Pinus taeda* stands, which is in line with these findings. The overall findings were in line with Davis et al. (1999) for seedling growth in central North America.

Wind exposure index indicates the amount of wind loading at a single spatial location. The WEI influenced the height growth of *E. bosistoana*. The results show that with low wind exposure, juvenile *E. bosistoana* trees grew taller. Brüchert and Gardiner (2006) reported similar results for *Picea sitchensis* in western Scotland and concluded that wind exposure can change the aerial architecture and biomechanics of planted trees. It also influences evapotranspiration, as well as provoking topsoil erosion (Berg et al., 2017; Fremme & Sodemann, 2018; Shukla & Mintz, 1982; Zhou et al., 2015). This finding was also similar to the *E. bosistoana* micro-site study results (Chapter 3). Moreover, Watt et al. (2008) reported that wind is likely to affect the abiotic and biotic factors of New Zealand plantation forests, and the effect can be greater with a modest increase of WEI (Moore & Watt, 2015). Though this research considered only mature *Pinus radiata* plantations, it can be equally applicable to young plantations in New Zealand.

Topographic wetness index represents the water availability at any given spatial location. TWI also significantly affected *E. bosistoana* height growth. TWI calculation involves measuring flow direction and accumulation point from the elevation and slope. The plots with a higher wetness index grew taller, whereas the opposite occurred for the low wetness index plots. Water availability is one of the most important factors in tree growth (Beedlow et al., 2013) and trees adapt different strategies based on moisture conditions (McDowell et al., 2008). Mason (2001) reported that water supply is a critical factor for newly established plantations, and Watt et al. (2004) tested the effects of weeds on the juvenile growth of *Pinus radiata*, based on competition for available water.

Eucalyptus globoidea height was significantly influenced by maximum temperature and radiation. Apart from water, these two are the most important tree growth modulators at any stage (Campillo et al., 2012; Richards, 2000; Ryan, 2010). Most of the plantation sites were in the dry

regions of New Zealand, and it is expected that the trees were limited by edaphic resources, for example, soil water and nutrients, though it was not explicitly proved in this study.

The findings of other researchers were all in line with this study. For example, Olesen and Grevsen (1997) reported that the vegetative growth of plants under such conditions was highly modulated by the temperature and intercepted radiation, which was consistent with these results. Prior and Bowman (2014) found that *Eucalyptus* species are sensitive to temperature and that they grow best within the temperature ranges 15°C - 24°C. Temperature effects are prominent at the mature stage though they can gain up to 20% total growth at the juvenile stage within the mentioned temperature range. Also, Way and Oren (2010) noticed that increasing temperature influenced tree growth positively, except in the tropical biome, which means that others biomes are maintained under their optimum temperature (Ryan, 2010). Also, Yang et al. (2006) found a growth increase with increasing temperature.

The productivity of a plantation forest crop directly relates to its ability to intercept radiation (Campillo et al., 2012). Although it largely depends on the leaf architecture, generally trees with a high leaf area index (LAI) can intercept more light. However, the LAI of a juvenile tree can be influenced by several different factors, e.g., initial seedling morphology, handling and preparation (Mason, 2001). These features were not extensively recorded for this study, which made these variables mechanistically complex to explain.

4.4.3. Factors affecting juvenile survival

Both of the study species were influenced by the minimum temperature (T_{min}), which was also the most important variable amongst all the tested variables. This result was in line with Prior and Bowman (2014), where 11°C was reported as the minimum threshold T_{min} for *Eucalyptus*. However, the sites in this study were experiencing much lower T_{min} than 11°C. The study species

are known as dryland species (NZDFI, 2013), but their resistance to frost conditions and minimum temperature is still unknown. Paton (1981) reported that most of the *Eucalyptus* species have very low resistance to frost conditions.

Other than T_{min} , *E. bosistoana* was significantly influenced by intercepted radiation. The survival proportion increased with increasing radiation. This may be possible that under some circumstances the trees simply run out of energy, and higher radiation level offers greater photosynthesis (Evans, 2013). The radiative heat may increase the air temperature (Caldwell et al., 1998) as well as the photosynthetic capacity of the trees (Richards, 2000). *Eucalyptus globoidea* was also affected by the topographic position index (TPI), which describes the spatial concavity and convexity in relation to the surroundings. A higher TPI indicates that the surface is more convex, and a lower TPI indicates that it is more concave. The survival proportion was higher on convex surfaces than on concave surfaces. Again, the frost conditions of the sites may be the reason behind this, as mounding is a common practice for other plantation forest species to save seedlings from frost effects (Mason et al., 1996). Another reason could be that saturated soil around the tree roots is not suitable for this species. However, these findings need further validation as there is not much research available regarding the ecophysiology of dryland *Eucalyptus* species.

4.5 Conclusion

The principal aim of this study was to develop models for two durable *Eucalyptus* species by identifying the most influential site-specific factors and including them in juvenile growth models. This study explicitly tested a comprehensive set of site-specific edaphic and biotic variables for two juvenile dryland *Eucalyptus* species. It identified and integrated the most important variables into a hybrid height growth yield and survival models.

This study found that topographic and climatic features were the most important factors for juvenile plantation height growth and survival. The study findings show that *E. bosistoana* needed optimal wind shelter and available water, and *E. globoidea* demanded more light and optimal maximum temperature to grow taller at the juvenile stage. Furthermore, *E. bosistoana* survival was influenced by minimum temperature with light availability, but *E. globoidea* needed a more convex surface, along with high minimum temperature. As all the soil data was somewhat coarser than other data, it may be worth conducting an intensive soil investigation before adding soil variables to any modelling framework, though in this study they were not significant.

The models and results here for the two dryland *Eucalyptus* species are useful for forest managers to decide on species and site selection as well as silvicultural regime.

4.6 References

- Adams, H. R., Barnard, H. R., & Loomis, A. K. (2014). Topography alters tree growth-climate relationships in a semi-arid forested catchment. *Ecosphere*, 5(11), 148. doi:doi:10.1890/ES14-00296.1
- Ares, A., & Marlats, R. M. (1995). Site factors related to growth of coniferous plantations in a temperate, hilly zone of Argentina. *Australian Forestry*, 58(3), 118-128.
- Arlot, S., & Celisse, A. (2010). A survey of cross-validation procedures for model selection. *Statistics Surveys*, 4(0), 40-79. doi:10.1214/09-ss054
- Aubry, K. B., Raley, C. M., & McKelvey, K. S. (2017). The importance of data quality for generating reliable distribution models for rare, elusive, and cryptic species. *PLoS ONE*, 12(6), e0179152. doi:10.1371/journal.pone.0179152
- Avila, O. B. (1993). *Modeling growth dynamics of juvenile loblolly pine plantations*. (PhD), Virginia Polytechnic Institute and State University, Blacksburg.
- Barringer, J. R. F., Pairman, D., & McNeill, S. J. (2002). *Development of a high-resolution digital elevation model for New Zealand*. (Contract Report LC0102/170.). Retrieved from Landcare Research, Lincoln, New Zealand:
- Battaglia, M., & Sands, P. J. (1998). Process-based forest productivity models and their application in forest management. *Forest Ecology and Management*, 102(1), 13-32. doi:[http://dx.doi.org/10.1016/S0378-1127\(97\)00112-6](http://dx.doi.org/10.1016/S0378-1127(97)00112-6)
- Beedlow, P. A., Lee, E. H., Tingey, D. T., Waschmann, R. S., & Burdick, C. A. (2013). The importance of seasonal temperature and moisture patterns on growth of Douglas-fir in western Oregon, USA. *Agricultural and Forest Meteorology*, 169, 174-185. doi:<https://doi.org/10.1016/j.agrformet.2012.10.010>
- Belli, K. L., & Ek, A. R. (1988). Growth and survival modeling for planted conifers in the Great Lakes region. *Forest Science*, 34(2), 458-473. doi:10.1093/forestscience/34.2.458
- Berg, A., Lintner, B., Findell, K., & Giannini, A. (2017). Soil moisture influence on seasonality and large-scale circulation in simulations of the west African monsoon. *Journal of Climate*, 30(7), 2295-2317.
- Brüchert, F., & Gardiner, B. (2006). The effect of wind exposure on the tree aerial architecture and biomechanics of Sitka spruce (*Picea sitchensis*, Pinaceae). *American Journal of Botany*, 93(10), 1512-1521. doi:doi:10.3732/ajb.93.10.1512
- Brunori, A., Nair, P. K. R., & Rockwood, D. L. (1995). Performance of two *Eucalyptus* species at different slope positions and aspects in a contour-ridge planting system in the Negev desert of Israel. *Forest Ecology and Management*, 75(1-3), 41-48. doi:[http://dx.doi.org/10.1016/0378-1127\(95\)03540-Q](http://dx.doi.org/10.1016/0378-1127(95)03540-Q)
- Bullock, B. P., & Burkhart, H. E. (2005). An evaluation of spatial dependency in juvenile loblolly pine stands using stem diameter. *Forest Science*, 51(2), 102-108.
- Burkhart, H. E., & Tomé, M. (2012). *Modeling forest trees and stands*: Springer.

- Burman, R., & Pochop, L. O. (1994). Evaporation, evapotranspiration and climatic data.
- Caldwell, M. M., Björn, L. O., Bornman, J. F., Flint, S. D., Kulandaivelu, G., Teramura, A. H., & Tevini, M. (1998). Effects of increased solar ultraviolet radiation on terrestrial ecosystems. *Journal of Photochemistry and Photobiology B: Biology*, 46(1), 40-52. doi:[https://doi.org/10.1016/S1011-1344\(98\)00184-5](https://doi.org/10.1016/S1011-1344(98)00184-5)
- Campillo, C., Fortes, R., & del Henar Prieto, M. (2012). Solar radiation effect on crop production *Solar Radiation*: InTech.
- Clutter, J. L. (1963). Compatible growth and yield models for Loblolly Pine. *Forest Science*, 9(3), 354-371.
- Columbus, J., Sirguey, P., & Tenzer, R. (2011). A free fully assessed 15-m digital elevation model for New Zealand. *Survey Quarterly*(66), 16-19.
- Comeau, P., & Rose, R. W. (2006). Proceedings of the fifth international conference on forest vegetation management: useable science, practical outcomes, and future needs *Canadian Journal of Forest Research*, 36(10). doi:10.1139/x06-905
- Davis, M. A., Wrage, K. J., Reich, P. B., Tjoelker, M. G., Schaeffer, T., & Muermann, C. (1999). Survival, growth, and photosynthesis of tree seedlings competing with herbaceous vegetation along a water-light-nitrogen gradient. *Plant Ecology*, 145(2), 341-350. doi:10.1023/a:1009802211896
- ESRI. (2012). ArcGIS Release 10.1. Redlands, CA.
- Evans, J. R. (2013). Improving photosynthesis. *Plant Physiology*.162(4), 1780-1793. doi:10.1104/pp.113.219006
- Fox, J. A., & Weisberg, S. (2011). *An R companion to applied regression*.
- Fremme, A., & Sodemann, H. (2018). *The influence of wind and land evapotranspiration on monsoon precipitation intensity and timing*. Paper presented at the EGU General Assembly Conference Abstracts.
- Hamner, B., & Frasco, M. (2018). *Metrics: evaluation metrics for machine learning*. R package version 0.1.4.
- Hewitt, A. E. (2010). *New Zealand soil classification* (3rd ed.). Lincoln, New Zealand: Manaaki Whenua Press.
- Land resources information system LRIS. (2017). Fundamental soil layers (all attributes). Retrieved June 2017, from Landcare Research New Zealand Ltd <https://lris.scinfo.org.nz/>
- LINZ. (2017). NZSoSDEM v1.0. Retrieved 19 Jul 2017, from National School of Surveying, University of Otago <https://data.linz.govt.nz/>
- Mäkelä, A., Landsberg, J., Ek, A. R., Burk, T. E., Ter-Mikaelian, M., Ågren, G. I., . . . Puttonen, P. (2000). Process-based models for forest ecosystem management: current state of the art and challenges for practical implementation. *Tree Physiology*, 20(5-6), 289-298.

- Mason, E. G. (2001). A model of the juvenile growth and survival of *Pinus radiata* D. Don; Adding the effects of initial seedling diameter and plant handling. *New Forests*, 22(1-2), 133-158. doi:10.1023/A:1012393130118
- Mason, E. G., Salekin, S., & Morgenroth, J. A. (2017). Comparison between meteorological data from the New Zealand National Institute of Water and Atmospheric Research (NIWA) and data from independent meteorological stations. *New Zealand Journal of Forestry Science*, 47(1), 7. doi:10.1186/s40490-017-0088-0
- Mason, E. G., South, D. B., & Weizhong, Z. (1996). Performance of *Pinus radiata* in relation to seedling grade, weed control, and soil cultivation in the central North Island of New Zealand. *New Zealand Journal of Forestry Science*, 26(1/2), 173-183.
- Mason, E. G., & Whyte, A. G. D. (1997). Modelling initial survival and growth of radiata pine in New Zealand. *Acta Forestalia Fennica*, 2, 1-38.
- Mason, E. G., Whyte, A. G. D., Woollons, R. C., & Richardson, B. (1997). A model of the growth of juvenile radiata pine in the central North Island of New Zealand: links with older models and rotation-length analyses of the effects of site preparation. *Forest Ecology and Management*, 97(2), 187-195. doi:[http://dx.doi.org/10.1016/S0378-1127\(97\)00099-6](http://dx.doi.org/10.1016/S0378-1127(97)00099-6)
- McDowell, N., Pockman, W. T., Allen, C. D., Breshears, D. D., Cobb, N., Kolb, T., . . . Yezpez, E. A. (2008). Mechanisms of plant survival and mortality during drought: why do some plants survive while others succumb to drought? *New Phytologist*, 178(4), 719-739. doi:doi:10.1111/j.1469-8137.2008.02436.x
- McRoberts, R. E., & Westfall, J. A. (2014). Effects of uncertainty in model predictions of individual tree volume on large area volume estimates. *Forest Science*, 60(1), 34-42. doi:10.5849/forsci.12-141
- Moore, J. R., & Watt, M. S. (2015). Modelling the influence of predicted future climate change on the risk of wind damage within New Zealand's planted forests. *Global Change Biology*, 21(8), 3021-3035. doi:doi:10.1111/gcb.12900
- Myers, R. H., & Myers, R. H. (1990). *Classical and modern regression with applications* (Vol. 2): Duxbury press Belmont, CA.
- Newsome, P. F. J. N., Wilde, R. H. W., & Willoughby, E. J. W. (2008). Land resource information system spatial data layers: *Data dictionary*. Retrieved from Palmerston North, New Zealand.
- NIWA. (2015). Virtual climate station data and products. Retrieved from <https://www.niwa.co.nz/climate/our-services/virtual-climate-stations>
- NZDFI. (2013). New Zealand Dryland Forest Initiative introductory brochure. In Marlborough Research Centre (Ed.). Blenheim, New Zealand.
- Olesen, J. E., & Grevsen, K. (1997). Effects of temperature and irradiance on vegetative growth of cauliflower (*Brassica oleracea* L. botrytis) and broccoli (*Brassica oleracea* L. Italica). *Journal of Experimental Botany*, 48(8), 1591-1598. doi:10.1093/jxb/48.8.1591

- Paton, D. (1981). *Eucalyptus* Physiology. III. frost resistance. *Australian Journal of Botany*, 29(6), 675-688. doi:<https://doi.org/10.1071/BT9810675>
- Payandeh, B. (1987). Plant: a model for artificial forest regeneration in Ontario. *USDA Forest Service general technical report NC-North Central Forest Experiment Station (USA)*.
- Pearse, G., Moltchanova, E., & Bloomberg, M. (2015). Assessment of the accuracy of profile available water and potential rooting depth estimates held within New Zealand's fundamental soil layers geo-database. *Soil Research*, 53(7), 737-744. doi:<https://doi.org/10.1071/SR14012>
- Peng, C., Liu, J., Dang, Q., Apps, M. J., & Jiang, H. (2002). TRIPLEX: a generic hybrid model for predicting forest growth and carbon and nitrogen dynamics. *Ecological Modelling*, 153(1), 109-130.
- Prior, L. D., & Bowman, D. M. J. S. (2014). Big eucalypts grow more slowly in a warm climate: evidence of an interaction between tree size and temperature. *Global Change Biology*, 20(9), 2793-2799. doi:doi:10.1111/gcb.12540
- R Core Team. (2017). R: A language and environment for statistical computing. Vienna, Austria: R Foundation for Statistical Computing; 2016. URL <http://www.R-project.org>.
- Rauscher, H., Isebrands, J., Host, G., Dickson, R., Dickmann, D., Crow, T., & Michael, D. (1990). ECOPHYS: an ecophysiological growth process model for juvenile poplar. *Tree Physiology*, 7(1-2-3-4), 255-281.
- Richards, R. A. (2000). Selectable traits to increase crop photosynthesis and yield of grain crops. *Journal of Experimental Botany*, 51(suppl_1), 447-458. doi:10.1093/jexbot/51.suppl_1.447
- Richardson, B., Watt, M. S., Mason, E. G., & Kriticos, D. J. (2006). Advances in modelling and decision support systems for vegetation management in young forest plantations. *Forestry*, 79(1), 29-42. doi:10.1093/forestry/cpi059
- Ritchie, M., & Hamann, J. (2008). Individual-tree height-, diameter- and crown-width increment equations for young Douglas-fir plantations. *New Forests*, 35(2), 173-186. doi:10.1007/s11056-007-9070-7
- Ryan, M. G. (2010). Temperature and tree growth. *Tree Physiology*, 30(6), 667-668. doi:10.1093/treephys/tpq033
- Sánchez-González, M., Tomé, M., & Montero, G. (2005). Modelling height and diameter growth of dominant cork oak trees in Spain. *Annals of Forest Science*, 62(7), 633-643.
- Sands, P. J., Battaglia, M., & Mummery, D. (2000). Application of process-based models to forest management: experience with PROMOD, a simple plantation productivity model. *Tree Physiology*, 20(5-6), 383-392. doi:10.1093/treephys/20.5-6.383
- Shukla, J., & Mintz, Y. (1982). Influence of land-surface evapotranspiration on the earth's climate. *Science*, 215(4539), 1498-1501. doi:10.1126/science.215.4539.1498

- Spiess, A., & Ritz, C. (2014). qpcR: Modelling and analysis of real-time PCR data. *R package version*, 1.4-0.
- Tesch, S. D., & Hobbs, S. D. (1989). Impact of shrub sprout competition on Douglas-fir seedling development. *Western Journal of Applied Forestry*, 4(3), 89-92. doi:10.1093/wjaf/4.3.89
- Therneau, T. M., Atkinson, B., & Ripley, M. B. (2010). The rpart package: Chicago.
- Toledo, M., Poorter, L., Peña-Claros, M., Alarcón, A., Balcázar, J., Leño, C., . . . Bongers, F. (2011). Climate is a stronger driver of tree and forest growth rates than soil and disturbance. *Journal of Ecology*, 99(1), 254-264. doi:doi:10.1111/j.1365-2745.2010.01741.x
- Villalba, R., Holmes, R. L., & Boninsegna, J. A. (1992). Spatial patterns of climate and tree growth variations in subtropical northwestern Argentina. *Journal of Biogeography*, 19(6), 631-649. doi:10.2307/2845706
- Wardle, P. (1991). *Vegetation of New Zealand*: CUP Archive.
- Watt, M., Kirschbaum, M., Paul, T., Tait, A., Pearce, H., Brockerhoff, E., . . . Kriticos, D. (2008). The effect of climate change on New Zealand's planted forests. *Impacts, risks and opportunities. Contract report by Scion for Ministry of Agriculture and Forestry, Wellington*.
- Watt, M. S., Kimberley, M. O., Richardson, B., Whitehead, D., & Mason, E. G. (2004). Testing a juvenile tree growth model sensitive to competition from weeds, using *Pinus radiata* at two contrasting sites in New Zealand. *Canadian Journal of Forest Research*, 34(10), 1985-1992. doi:10.1139/x04-072
- Watt, M. S., Whitehead, D., Richardson, B., Mason, E. G., & Leckie, A. C. (2003). Modelling the influence of weed competition on the growth of young *Pinus radiata* at a dryland site. *Forest Ecology and Management*, 178(3), 271-286. doi:[https://doi.org/10.1016/S0378-1127\(02\)00520-0](https://doi.org/10.1016/S0378-1127(02)00520-0)
- Way, D. A., & Oren, R. (2010). Differential responses to changes in growth temperature between trees from different functional groups and biomes: a review and synthesis of data. *Tree Physiology*, 30(6), 669-688. doi:10.1093/treephys/tpq015
- Weiskittel, A. R., Hann, D. W., Kershaw, J. A., & Vanclay, J. K. (2011). *Forest Growth and Yield Modeling*: Wiley.
- Westfall, J. A., Burkhart, H. E., & Allen, H. L. (2004). Young stand growth modelling for intensively-manged loblolly pine plantations in southeastern US. *Forest Science*, 50(6), 823-835.
- Wickham, H. (2016). *ggplot2: Elegant graphics for data analysis*: Springer.
- Yang, Y., Watanabe, M., Li, F., Zhang, J., Zhang, W., & Zhai, J. (2006). Factors affecting forest growth and possible effects of climate change in the Taihang mountains, northern China. *Forestry*, 79(1), 135-147. doi:10.1093/forestry/cpi062

- Zhang, S., Burkhart, H. E., & Amateis, R. L. (1996). Modeling individual tree growth for juvenile loblolly pine plantations. *Forest Ecology and Management*, 89(1–3), 157-172. doi:[http://dx.doi.org/10.1016/S0378-1127\(96\)03851-0](http://dx.doi.org/10.1016/S0378-1127(96)03851-0)
- Zhao, W. (1999). *Growth and yield modelling of Pinus Radiata in Canterbury, New Zealand*. (Doctor of Philosophy in Forestry), University of Canterbury.
- Zhou, Y., Guo, B., Wang, S., & Tao, H. (2015). An estimation method of soil wind erosion in inner Mongolia of China based on geographic information system and remote sensing. *Journal of Arid Land*, 7(3), 304-317.

5

Modelling juvenile growth and survival using a hybrid ecophysiological approach

5. Modelling juvenile growth and survival using a hybrid ecophysiological approach.

5.1. Introduction

Hybrid ecophysiological components have the potential to enhance the capability of the models by surmounting the shortcomings of either mensurational or purely ecophysiological models (Landsberg, 2003; Mäkelä et al., 2000; Monserud, 2003; Weiskittel et al., 2011). Hybrid models simplify and combine the best features of each approach. Those features are carefully chosen based on their ability to explain the process, enhancing model precision and, more importantly, a drastic simplification of growth processes (Weiskittel, 2007; Weiskittel et al., 2011). Hybrid models have received less attention than strictly mensurational or ecophysiological models, but are currently a focus of attention from researchers as well as forest managers (Mason et al., 2018). This results from a combination of increasing awareness of both natural and anthropogenic changes in climate, and advancement in precise and automated data collection. Hybrid models typically operate at the stand level and on a monthly time step, although a few runs at the individual tree level and on a daily time step (Weiskittel, 2007).

Weiskittel et al. (2011) classified hybrid modelling frameworks into two classes: 1) linked mensurational equations with external or internal ecophysiological growth modifiers or submodels (Almeida et al., 2004; Battaglia et al., 2004; Peng et al., 2002), and 2) theoretical assumption based equations of ecophysiological processes (Mason et al., 2011; Pinkard & Battaglia, 2001; Snowdon et al., 1999). The degree of hybridisation varies within each class, so it is hard to define a clear line for each approach (Weiskittel et al., 2011). Monteith (1977) observed a linear relationship between productivity and absorbed photosynthetically active radiation (APAR), which slope is a term known as radiation or light use efficiency (RUE/LUE), which is widely used, with differing levels of refinement, in hybrid modelling.

The 3-PG (Physiological Principles for Predicting Growth) model (Landsberg and Waring (1997), is widely used for predicting productivity around the world. It explicitly considers the LUE principle for forests by estimating the use of intercepted photosynthetically active radiation modified by available soil water (ASW), vapour pressure deficit (VPD), air temperature and soil fertility. The 3-PG model can be expressed as (Mason et al., 2007):

$$NPP = \varepsilon \sum_{m=1}^M APAR_m \min\{f_{\theta} f_D\} f_T f_S \quad (24)$$

where m is the time interval (months), $APAR$ is the absorbed photosynthetically active radiation, ε is the maximum quantum efficiency for a species, f_{θ} is the soil water modifier (0-1), f_D is the vapour pressure deficit modifier (0-1), f_T is the air temperature modifier (0-1), and f_S is the senescence modifier (0-1). However, it has some limitations from the mensurational perspective of a growth and yield model. The 3-PG model is not path invariant (Clutter, 1963; Clutter et al., 1983) and it can be calibrated for a single dataset in a variety of ways by changing one or more of a large number of modelling parameters. Moreover, the 3-PG model is highly recursive so that errors can be propagated over prediction time (Mason et al., 2007).

Potentially usable light sum equations (PULSE) represent a hybrid modelling approach proposed by Mason et al. (2007), which combines the LUE principle with mensurational models to overcome the shortcomings of 3-PG. Also, it gives more plausibility from both the ecophysiological and mensurational perspectives of growth modelling. The LUE components of this model are formulated following modified 3-PG methods, and the mensurational growth equations complement the base growth equations. More simply, potentially usable light sum (PULS) approaches replace time in mensurational models with intercepted accumulations of radiation over given periods. The accumulated radiation sum over the period can be restricted by

3-PG modifiers. The PULSE model suggests that potentially useable radiation can be represented as

$$R_T = \sum_{i=1}^T R_t \min(f_\theta f_D) f_T \quad (25)$$

where R_T is the total radiation sum from month 1 to T (MJ), and f_θ , f_D , and f_T are the soil water balance, vapour pressure deficit (VPD), and temperature modifiers calculated for month t_m .

The PULSE modelling approach was first applied in a controlled experiment on a juvenile *Pseudotsuga menziesii* plantation near Portland, Oregon in the United States to model ground line diameter (GLD), and it proved to be stable in all cases, suggesting that environmental changes were explained by the modifiers (Mason et al., 2007). Since then it has been tested for mature *Pinus radiata* in New Zealand (Mason et al., 2011), *Pinus taeda* and *Eucalyptus grandis* in Uruguay (Casnati, 2016), and a site index (SI) model of *Pinus sylvestris* in Sweden (Mason et al., 2018). A similar approach was applied by Montes (2012) to model height increments, basal area and mortality as a function of APAR, using a state-space approach (Garcia, 1984). Interestingly, after its early development, the PULSE modelling approach had not been re-tested for juvenile growth. Therefore, there were grounds to test this approach, especially to model height yield and survival, in order to make the PULSE modelling approach more compatible with the establishment phase of a plantation.

Stand nutrition is an important regulator of NPP, yet current understanding seems insufficient to bring it into a modelling framework (Landsberg & Waring, 1997). Hence, this is another limitation of 3-PG (Bown et al., 2013; Landsberg, 2003), which also has been a limitation for the PULSE modelling approach (Casnati, 2016). Moreover, radiation interception and tree growth can be modulated by the topography (Böhner & Antonić, 2009; Gerlitz et al., 2015), but relevant modifiers have not yet been presented in 3-PG or PULSE. Casnati (2016) resolved this

problem by augmenting aspect and slope directly into the equation as a linear expansion of the coefficients, an approach which merits further exploration.

So far, the results of applying the PULSE model seems promising with respect to precision and outputs for predicting tree growth. Nevertheless, open questions remain, especially in PULSE for modelling juvenile growth and survival, along with the influence of different topographic metrics.

The main questions addressed in this chapter are,

1. How much does the PULSE model contribute to explaining variability in juvenile growth of *Eucalyptus bosistoana* and *Eucalyptus globoidea*?
2. Can models be improved by adding topographic indices?

In this chapter, PULSE equations were adjusted at the site level for *E. bosistoana* and *E. globoidea*, to model height yield and survival. Detailed topographic information was also tested for its potential to improve estimations, and hence be included in the hybrid modelling system.

5.2. Methods

To develop the models, modified light sums were computed through PULSE models, then height yield (h_T) and survival proportion (S) were fitted directly as a function of the modified light sums. The detailed modelling procedure is presented below.

5.2.1 Data description

Geo-referenced NZDFI permanent sample plot (PSP) measurements were used to model height yield (h_T) and survival proportion (S). For computing, the radiation sums and the modifiers, monthly solar radiation, mean air temperature, vapour pressure deficit (VPD), and rainfall were downloaded from the virtual climatic station network (VCSN) dataset (NIWA, 2015). Location of

the closest VCSN points showed in Chapter 4 (Figure 4.1). Soil water balance was computed based on soil texture, potential rooting depth, available soil water (ASW), potentially available soil water (SWPA), with data sourced through the fundamental soil layers (FSL) (Land Resource Information System, 2015). All the data used here are described in detail in Chapter 4.

5.2.2 Calculation of modifiers

The modifier applicable to vapour pressure deficit (VPD) describes a relationship where the modifier declines exponentially when VPD increases. It is computed as follows (Landsberg & Waring, 1997):

$$f_D = e^{-k_g VPD} \quad (29)$$

where k_g is a coefficient based on the relationship between stomatal conductance and VPD. In addition, VPD is calculated as follows:

$$VPD = \frac{DT_{max} - DT_{min}}{2} \quad (30)$$

where DT_{max} and DT_{min} represent saturated vapour pressure when temperature = T_{max} and T_{min} . Those variables are calculated using minimum or maximum temperatures each month (T_i) using the equation:

$$DT_i = 0.61078e^{17.269T_i/(T_i+237.3)} \quad (31)$$

The soil water-dependent modifier was calculated as follows (Landsberg & Waring, 1997):

$$f_\theta = \frac{1}{1 + \left[\frac{(1+r_\theta)}{C_\theta}\right]^{n_\theta}} \quad (32)$$

where C_θ and n_θ take different values for different soil types and r_θ is the moisture ratio, calculated as follows:

$$r_\theta = \frac{\theta_T}{SWPA} \quad (31)$$

θ_T is the soil water balance, and SWPA is the soil water potentially available. SWPA information was obtained from the FSL layers (Chapter 4, Soil data).

Soil water balance was estimated through the following equation:

$$\theta_T = \theta_{T-1} + R - I - E - D \quad (32)$$

where θ_{T-1} is the root zone water balance in the previous month; R is rainfall; I is canopy interception; E is evapotranspiration from the soil and D is soil drainage. When, $\theta_{T-1} + P - I - E > \text{SWPA}$, it confirms the existence of excess water. Although in this case, it is assumed to be drained.

The 3-PG model estimates evapotranspiration using the Penman-Monteith “big-leaf” model (Monteith, 1981):

$$\lambda E = \frac{SR_n + \lambda g_b \rho_a \text{VPD}}{S + \gamma \left(1 + \frac{g_b}{g_c}\right)} \quad (33)$$

where λ is the latent heat of water vaporisation (JKg); S is the slope of saturation vapour pressure curve for water (kPa°C⁻¹); R_n is net radiation absorbed by the canopy (Jm⁻²month⁻¹); ρ_a is air density (kg m⁻³); VPD is vapour pressure deficit (mbar); γ is the psychometric parameter (kPa°C⁻¹); g_b is boundary layer conductance (ms⁻¹); and g_c is canopy conductance (ms⁻¹). The values used are given in Table 5.1.

Boundary layer conductance depends on wind speed as well as size and shape of leaves, and density of foliage (Landsberg & Sands, 2011). However fixed values are commonly used for practical purposes, and a fixed value of 0.2 ms⁻¹ was assumed by following the work of Mielke et al. (1999). Mielke et al. (1999) also found wind speeds around 2 ms⁻¹ leading to canopy conductance values of 0.2 ms⁻¹ for *E. grandis*. According to Martin et al. (1999), boundary layer conductance did not increase markedly when wind velocity ranged from 1 to 2 ms⁻¹. Therefore, it

was assumed that wind speed was spatially and temporally uniform, and boundary layer conductance values assumed in this study did not seem to lead to significant error. The specific values are presented in Table 5.1.

Canopy conductance was calculated as follows:

$$g_{cx} = g_{sx} \min \left\{ 1, \frac{L}{L_{gc}} \right\} \min \{ f_{\theta}, f_D \} \quad (34)$$

where g_{cx} is maximum stomatal conductance, assumed as 0.02 ms^{-1} (Almeida et al., 2004; Sands, 2004). L is leaf area index (LAI), L_{gc} is leaf area index at maximum conductance, and other terms are as specified before. LAI was required for both trees and competing vegetation in each month to run the water balance, but no measured data were available. Consequently, generic exponential LAI models were built for juvenile trees and competing vegetation (e.g. weeds) at monthly time steps by following Dodd et al. (2005) and Mason (In Prep.), by assuming that individual competing vegetation would reach maximum LAI values similar to those reported in Breuer et al. (2003). The plantation sites were initially sprayed with herbicide so, both trees and weeds were assumed to start with a LAI value of 0 (Figure 5.1). The models are as follows:

$$\text{LAI}_p = e^{\left(1.5 - \frac{2}{\left(\frac{K}{12} \right)^{1.5}} \right)} + 0.1 \quad (35)$$

$$\text{LAI}_g = e^{\left(1 - \frac{1.5}{\left(\frac{K}{12} \right)^{3.5}} \right)} \quad (36)$$

where LAI_p is tree LAI, and LAI_g is weed LAI; K stands for the month. Weighted means of juvenile trees and competing vegetation (L) were used in the final water balance model.

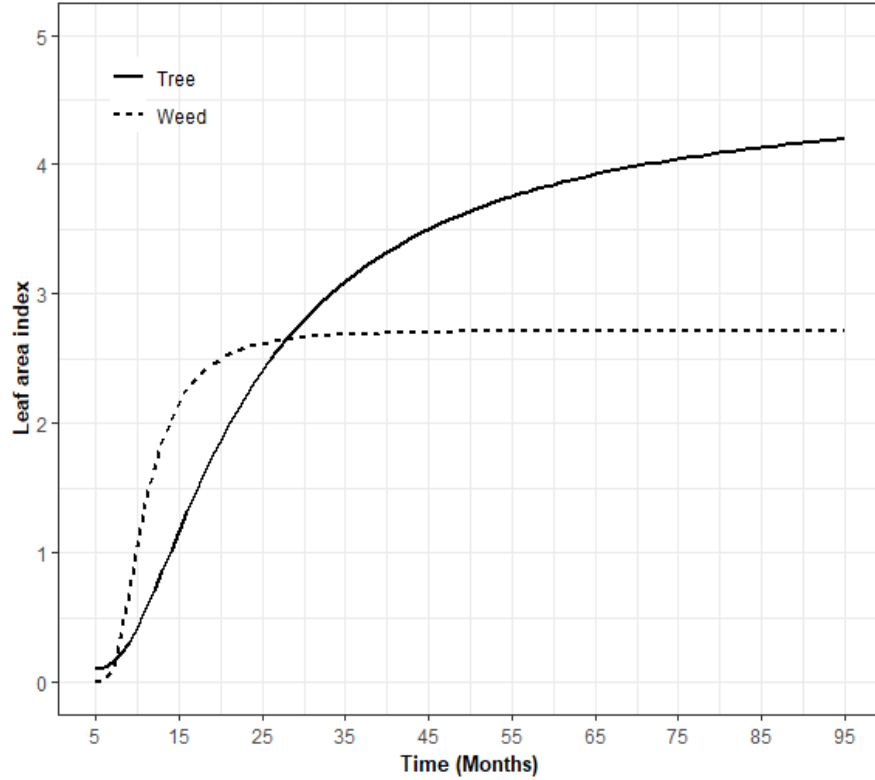


Figure 5.1 Generic leaf area index (LAI) estimation models.

Net radiation was estimated using a linear relationship with radiation as follows:

$$R_n = q_a + q_b H_s \quad (37)$$

where q_a (Wm^{-2}) and q_b are the intercept and the slope parameters. The values applied were the ones used in 3-PG by Sands (2004).

The temperature dependent growth modifier is based on the assumption that production increases with increasing temperature and starts declining after an optimum is reached (Mason et al., 2007):

$$f_T(\bar{T}) = \left(\frac{\bar{T} - T_{min}}{T_{opt} - T_{min}} \right) \left(\frac{T_{max} - \bar{T}}{T_{max} - T_{opt}} \right)^{\frac{(T_{max} - T_{opt})}{(T_{opt} - T_{min})}} \quad (38)$$

where $f_T = 0$ if $\bar{T} \leq T_{min}$ or $T_{max} \leq \bar{T}$; T_{max} , T_{min} and T_{opt} are the maximum, minimum and optimum temperatures for net photosynthetic production; and \bar{T} is the mean temperature for each

month. In this case, the mean daytime temperature was employed instead of mean temperature because Mason et al. (2011) found that this modification gave better precision than daily mean temperature. The mean daytime temperature defined in Mason et al. (2011) by:

$$\bar{T} = \Delta T_{\max} 0.7575 + \Delta T_{\min} 0.2425 \quad (39)$$

where \bar{T} is mean daytime temperature; ΔT_{\max} is mean daily maximum temperature; and ΔT_{\min} is mean daily minimum temperature.

Competition for light was estimated using the ratio of squares for competing vegetation and crop mean heights multiplied by the percentage cover of competing vegetation as a competition index, and the following equations were used to estimate light transmission to crop plants (Richardson et al., 1999):

$$CI = \frac{H_{\text{weeds}}^2}{H_{\text{crop}}^2} C \quad (40)$$

$$f_{CI} = 1 - (1 - e^{M_1 \times CI})^{M_2} \quad (41)$$

where f_{CI} is the light competition modifier, CI is the competition index, H is the height of competing vegetation or crops as noted, C is the percentage cover of competing vegetation, and M_1 and M_2 are parameters estimated in competition experiments (Richardson et al., 1999), with values given in Table 5.1.

Table 5.1 List of parameters used in PULSE.

Modifier	Parameter	Unit	Value	Reference
Water balance	Maximum stomatal conductance of trees	ms ⁻¹	0.02	(Coops & Waring, 2001)
	Maximum stomatal conductance of weeds	ms ⁻¹	0.02	(Mason et al., 2007)
	LAI for maximum canopy conductance		3.33	(Sands, 2004)
	Boundary layer conductance of trees	ms ⁻¹	0.2	(Landsberg & Waring, 1997)
	Boundary layer conductance of weeds	ms ⁻¹	0.25	(Mason et al., 2007)
	Intercept of net radiation relation for trees	Wm ⁻²	-90	(Sands, 2004)
	Slope of net radiation relation for trees		0.8	(Sands, 2004)
	Intercept of net radiation relation for weeds	Wm ⁻²	-90	(Sands, 2004)
	Slope of net radiation relation for weeds		0.65	(McNaughton & Jarvis, 1983)
	LAI for maximum rainfall interception	mm	4	(Mason et al., 2007)
	Latent heat of water vaporisation	J Kg	2 460 000	(Casnati, 2016)
	Air density	Kgm ⁻³	1.2	
Temperature	Maximum temperature for photosynthesis	°C	45	(Oparah, 2012)
	Optimum temperature for photosynthesis	°C	18	(Oparah, 2012)
	Minimum temperature for photosynthesis	°C	6	(Oparah, 2012)
VPD	Exponential decay parameter		-0.5	(Landsberg & Waring, 1997)
Light competition	M ₁		-0.760	(Richardson et al., 1999)
	M ₂		1.289	(Richardson et al., 1999)

5.2.3 Model building and evaluation

Accumulated radiation for each month was multiplied by a different combination of modifiers for temperature, water balance, and VPD. Each month was summed up from planting date to measurement date. An example including all the modifiers is as follows:

$$R_M = \sum_{m=1}^M R_m \min[f_\theta f_D] f_T f_{CI} \quad (42)$$

where R_m is the radiation in month m , R_M is the potentially useable light sum, f_{CI} is the light competition modifier, and the other variables are as previously defined. This model blends the key submodels with commonly used mensurational equations, which avoids the need to estimate APAR directly, does not require estimates of carbon allocation, and can be both fitted and used without recursion (Mason et al., 2007).

The PULSE equation was used in combination with the previously defined height yield and survival proportion model (Chapter 3), by replacing the time with radiation sum. The equations can be represented as follows:

$$\bar{h}_M = \bar{h}_0 + \alpha R_M^\beta \quad (43)$$

$$S_M = -e^{\alpha R_M^\beta} \quad (44)$$

where \bar{h}_M is the height at month M , S_M is the survival at month M , and α and β are the modelling parameters previously defined in Chapter 3.

To build the final model a two-step procedure was applied. First, height and survival equations were fitted with PULS restricted different modifiers through PULSE model. That means radiation sum for the study period was calculated by applying different modifiers separately for the study period. Therefore, potentially usable light was calculated by applying all modifiers (R_M), temperature (R_T), temperature with ASW (R_{T0}), and temperature with VPD (R_{TVPD}). The best-

fitted PULSE model was identified through a full set of residual analyses. Second, testing was undertaken of the best-fitted PULSE model by augmenting it with secondary topographic variables, as described in Chapters 3 and 4, and comparing it with the version without topographic variables.

The PULSE modelling and PULS calculations were carried out in an R workspace (R Core Team, 2017), through object-oriented programming developed and provided by Prof. Euan G. Mason (Casnati, 2016; Mason et al., 2018; Mason et al., 2011), which was used previously for similar kinds of modelling experiments.

The model evaluation was carried out by following the procedures described in Chapter 4. The model evaluation and comparison for height yield and survival were performed only for the best PULSE model and the improved augmented PULSE model.

5.3. Results

5.3.1. Site-specific height yield PULSE models

The PULSE calculated radiation sum replaced the time from the base mensurational model, and among all four types of modified PULSE models, temperature and VPD restricted radiation sum (R_{TVPD}) calculation gave the best prediction of the height yield for both *E. bosistoana* and *E. globoidea* (Equation 44 and 45). Model statistics are described in Table 5.2, and shown in Figure 5.2, Figure 5.3, Figure 5.4, and Figure 5.5, where the distribution and model fitting trends can be seen. All indications are that the model with R_{TVPD} gave the best fit. In the case of *E. bosistoana*, radiation sum modified only by temperature (R_T) was also statistically sound, with a very slight improvement over the R_{T0} (Table 5.2). However, results were different for *E. globoidea*. The PULS restricted by all modifiers (R_M) and the PULS with available soil water (R_{T0}) were the worst performers (Figure 5.2 and Figure 5.3). The validation statistics showed reasonable values in the

given situation. RMSE, MAE, SE increased somewhat in comparison to fitting statistics, but AICc values reversed (Table 5.3). Visually, plot validation statistics (Figure 5.6) confirmed improvement in goodness-of-fit of the models.

$$\bar{h}_{EBM} = \bar{h}_0 + \alpha R_{TVPD}^\beta \quad (45)$$

$$\bar{h}_{EGM} = \bar{h}_0 + \alpha R_{TVPD}^\beta \quad (46)$$

where \bar{h}_{EBM} and \bar{h}_{EGM} are the height of *E. bosistoana* and *E. globoidea* respectively at month M; α and β are the parameters; the others have been defined previously.

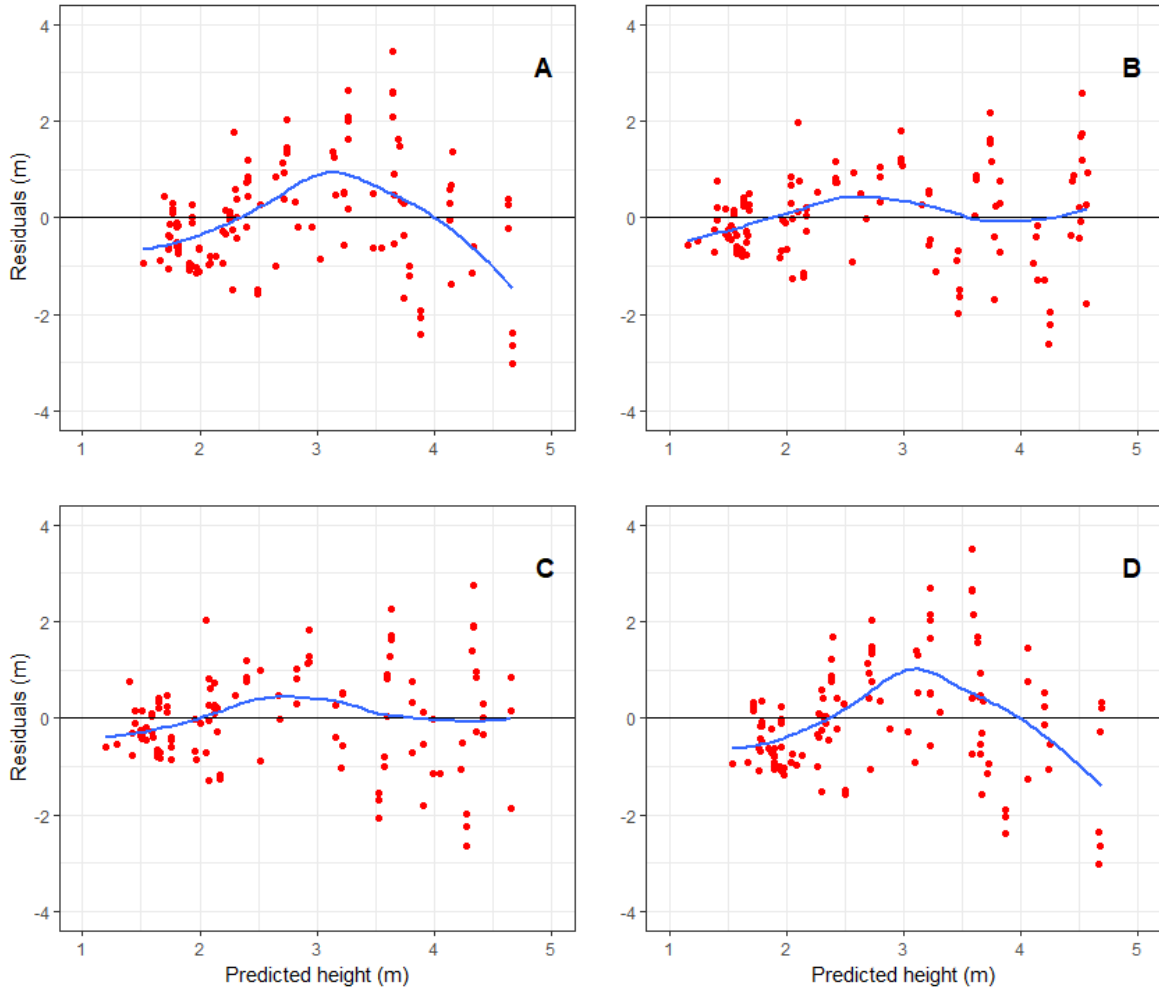


Figure 5.2 Residuals against predicted of *E. bosistoana* PULSE height yield models (blue line indicating the loess fit), with A) All modifiers (R_M); B) temperature (R_T); C) temperature and vapour pressure deficit (R_{TVPD}); D) available soil water ($R_{T\theta}$) modified radiation sum.

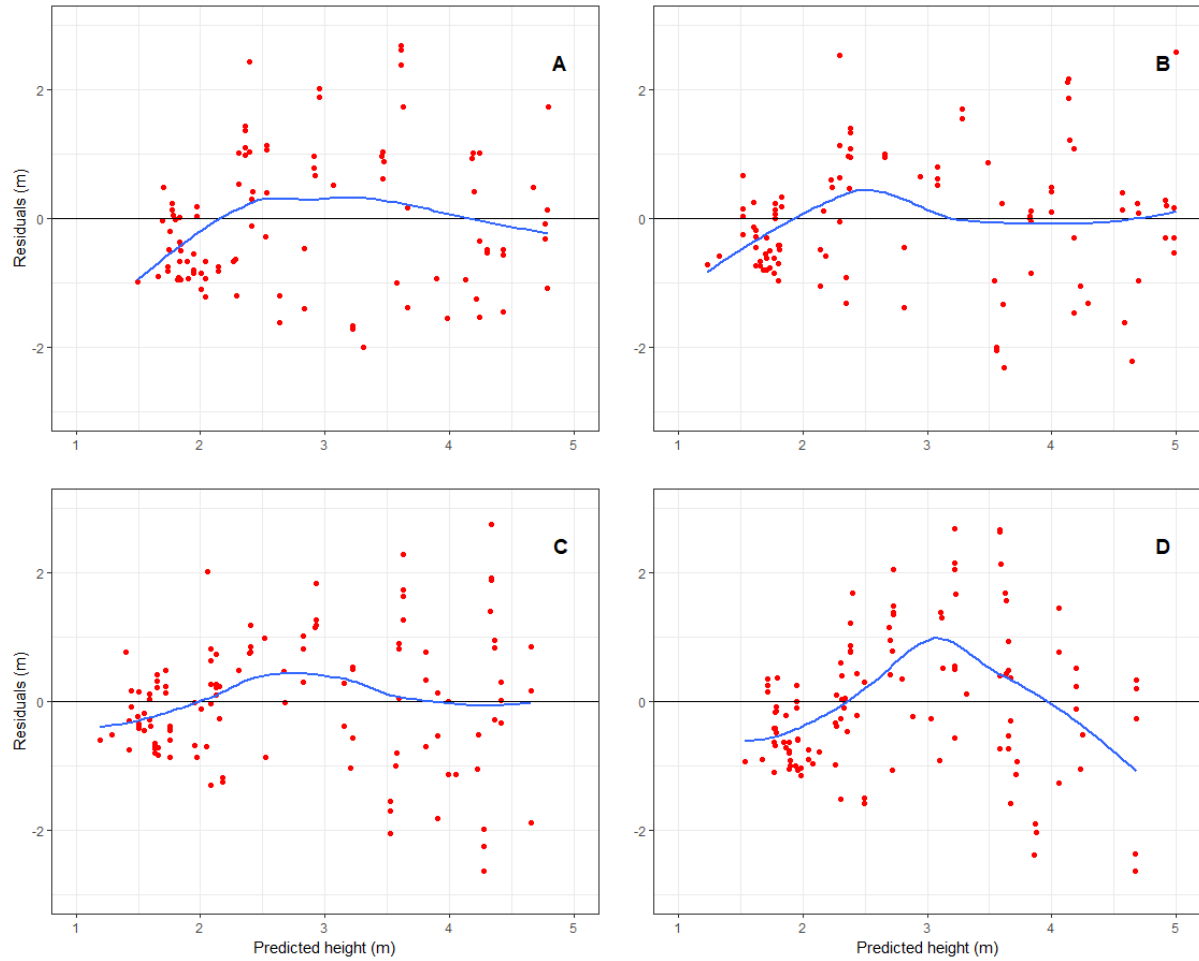


Figure 5.3 Residuals against predicted of *E. globoidea* PULSE height yield models (blue line indicating the loess fit), with A) All modifiers (R_M); B) temperature (R_T); C) temperature and vapour pressure deficit (R_{TVPD}); D) available soil water ($R_{T\theta}$) modified radiation sum.

Table 5.2 Fitting statistics for PULSE height yield models.

Fitting Metrics	PULSE models with different modifiers				Species
	R _M	R _T	R _{TVPD}	R _{T0}	
RMSE	1.143	0.932	0.965	1.152	<i>E. bosistoana</i>
MAE	0.891	0.733	0.752	0.901	
BIAS	-0.0339	-0.018	-0.020	-0.033	
SE	1.153	0.940	0.974	1.162	
AICc	375.64	327.16	335.54	377.63	
R ² adj.	0.321	0.579	0.544	0.310	
RMSE	1.128	0.99	0.965	1.152	<i>E. globoidea</i>
MAE	0.902	0.778	0.752	0.901	
BIAS	-0.031	-0.022	-0.020	-0.033	
SE	1.139	1.009	0.974	1.162	
AICc	341.791	315.314	335.542	377.630	
R ² adj.	0.474	0.602	0.544	0.310	

Table 5.3 Validation statistics for the best PULSE height yield models.

Species	Validation statistics of R _{TVPD}						
	RMSE	MAE	SE	BIAS	AICc	MPRESS	MAPRESS
<i>E. bosistoana</i>	1.414	1.056	2.065	0.005	327.388	-0.0212	0.532
<i>E. globoidea</i>	1.625	1.216	2.692	0.006	311.336	-0.0212	0.532

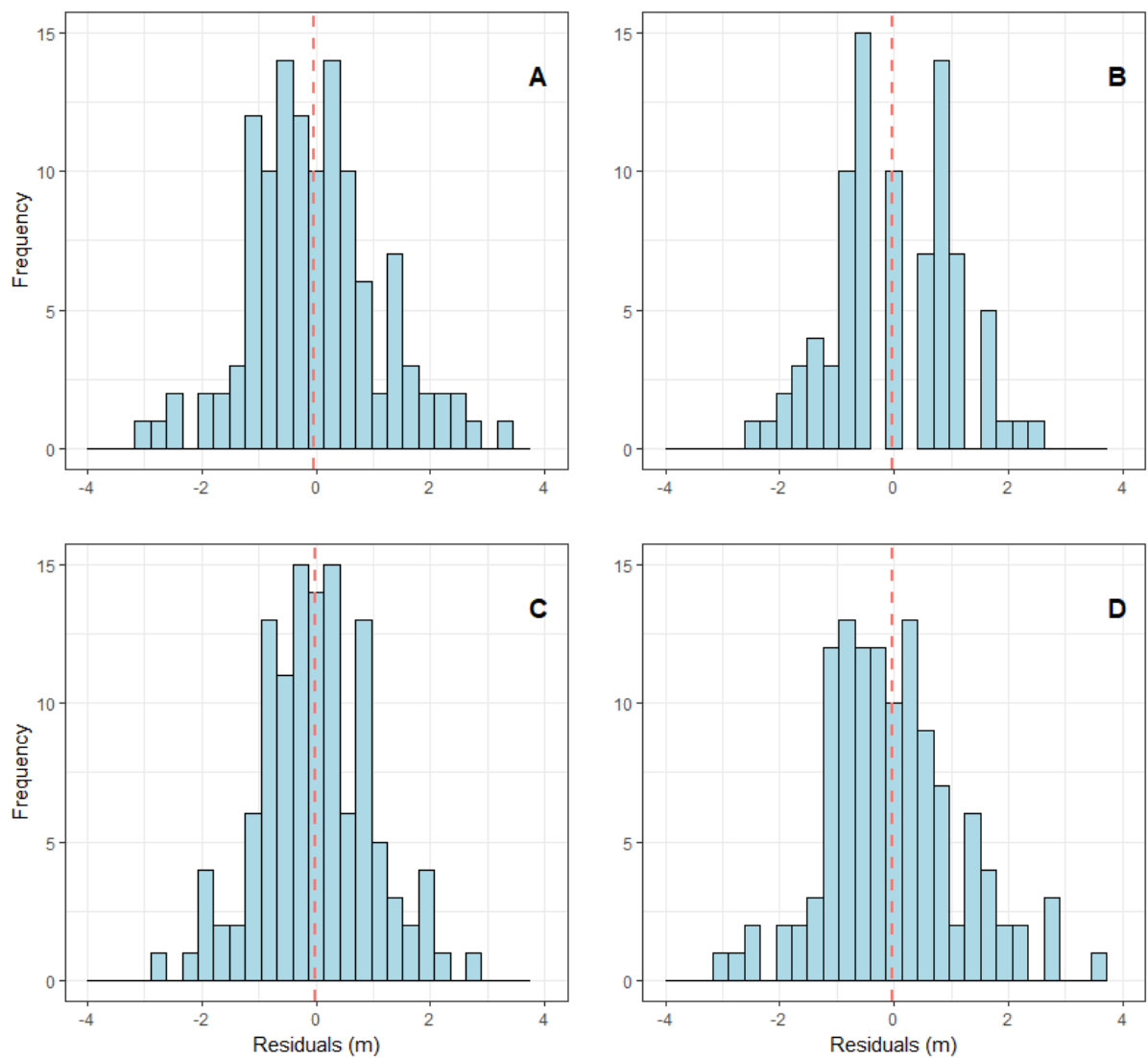


Figure 5.4 Residuals distribution of *E. bosistoana* PULSE height yield models (red dashed line shows the mean), A) All modifiers (R_M); B) temperature (R_T); C) temperature and vapour pressure deficit (R_{TVPD}); D) available soil water ($R_{T\theta}$) modified radiation sum.

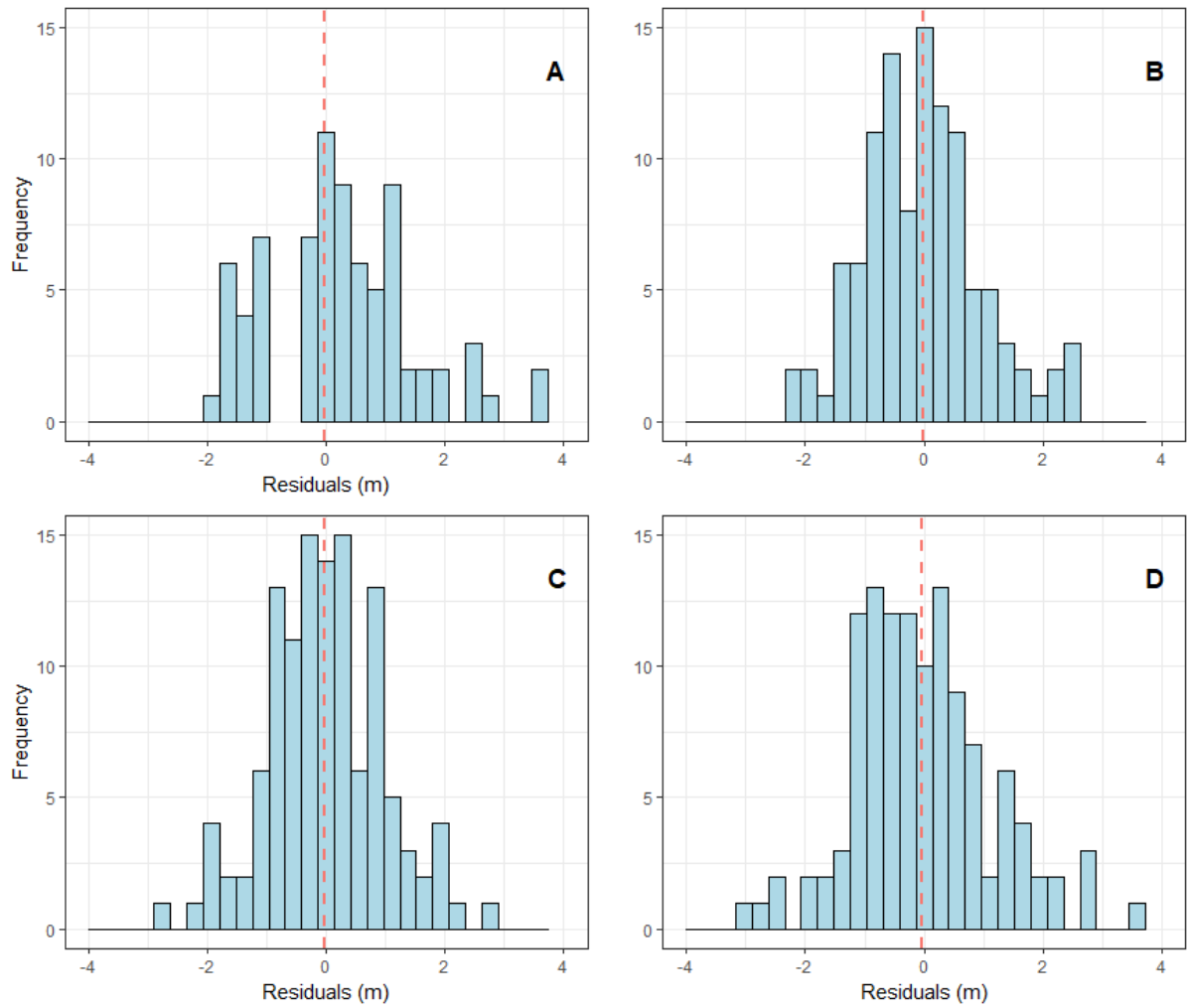


Figure 5.5 Residuals distribution of *E. globoidea* PULSE height yield models (red dashed line showed the mean), A) All modifiers (R_M); B) temperature (R_T); C) temperature and vapour pressure deficit (R_{TVPD}); D) available soil water ($R_{T\theta}$) modified radiation sum.

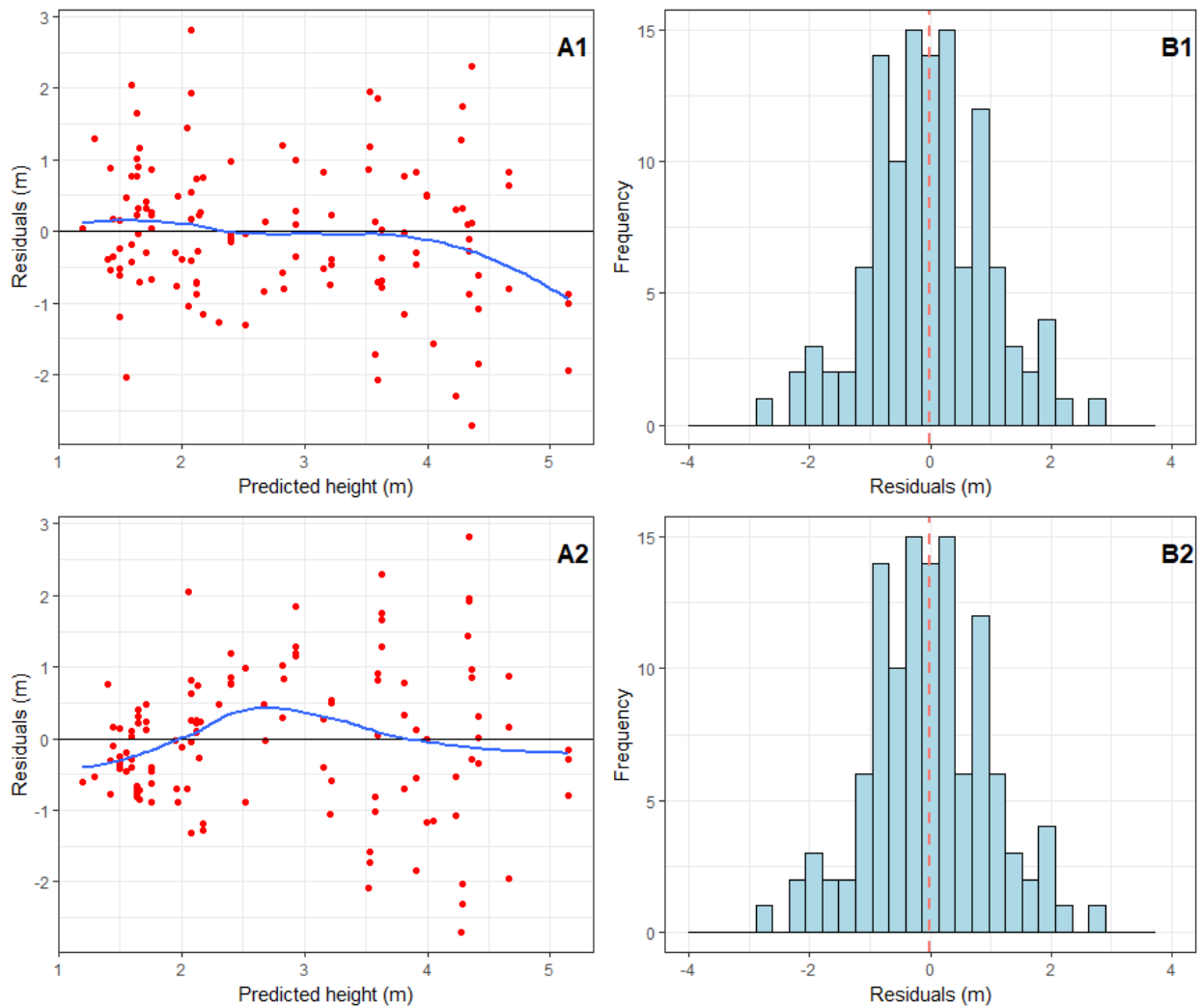


Figure 5.6 Residuals distribution from the model validation, A) predicted against residuals distribution with loess fit line in blue and B) frequency distribution (red dashed line showing the mean). A1 and B1 for *E. bosistoana*; A2 and B2 for *E. globoidea*.

5.3.2 Augmented PULSE model for juvenile height yield

The temperature and VPD modified PULSE model was augmented with secondary topographic variables by linearly expanding the coefficients. A set of variables (Table 5.4) and their interaction terms were augmented, and only statistically significant variables were retained in the final models. For *E. bosistoana*, the morphometric protection index (MPI) and wind exposure index (WEI) were the most significant variables. Only the MPI was significant for *E. globoidea* (Equation 46 and 47).

Table 5.4 Augmented variables and their significant status.

Species	Variables	Sig. Codes
<i>E. bosistoana</i>	Topographic position index (TPI)	NS
	Topographic wetness index (TWI)	NS
	Morphometric protection index (MPI)	***
	Wind exposure index (WEI)	***
	Profile curvature	NS
	Plan curvature	NS
<i>E. globoidea</i>	Topographic position index (TPI)	NS
	Topographic wetness index (TWI)	NS
	Morphometric protection index (MPI)	***
	Wind exposure index (WEI)	NS
	Profile curvature	NS
	Plan curvature	NS

Sig. Codes: 0 ‘***’; 0.001 ‘**’; 0.01 ‘*’; 0.05 ‘.’; 0.1 ‘-’; NS ‘Not Significant’

$$\bar{h}_{EBM} = \bar{h}_0 + \alpha R_{TVPD}^{(\beta_0 + \beta_1 * MPI + \beta_2 * WEI)} \quad (47)$$

$$\bar{h}_{EGM} = \bar{h}_0 + \alpha R_{TVPD}^{(\beta_0 + \beta_1 * MPI)} \quad (48)$$

where \bar{h}_{EBM} and \bar{h}_{EGM} are the height of *E. bosistoana* and *E. globoidea* respectively at month M; α , β_0 , β_1 and β_2 are parameters; MPI is the morphometric protection index, and WEI is the wind exposure index; the others have been defined previously.

Both models (Equations 46 and 47) predicted height with minimal errors, and the errors were normally distributed. The loess line showed the model fit which was reliable in both cases. The fit statistics of the models showed relatively small values, which were desirable characteristics. For both species, the RMSE, MAE and SE increased in validation statistics compared to the fit statistics. BIAS and AICc were reversed from fit to validation statistics (Table 5.5). However, visual comparison suggested that model performance was slightly lowered and there was evidence of positive heteroscedasticity (Figure 5.9).

Including topographic features in the height yield models proved statistically significant. The *E. bosistoana* height yield PULSE model was significantly influenced by the

morphometric protection index (MPI) and the wind exposure index (WEI). Height increased with increasing MPI, whereas height decreased with increasing WEI. The height yield PULSE model of *E. globoidea* was influenced by MPI alone in the same manner as for *E. bosistoana* (Figure 5.7 and Figure 5.8).

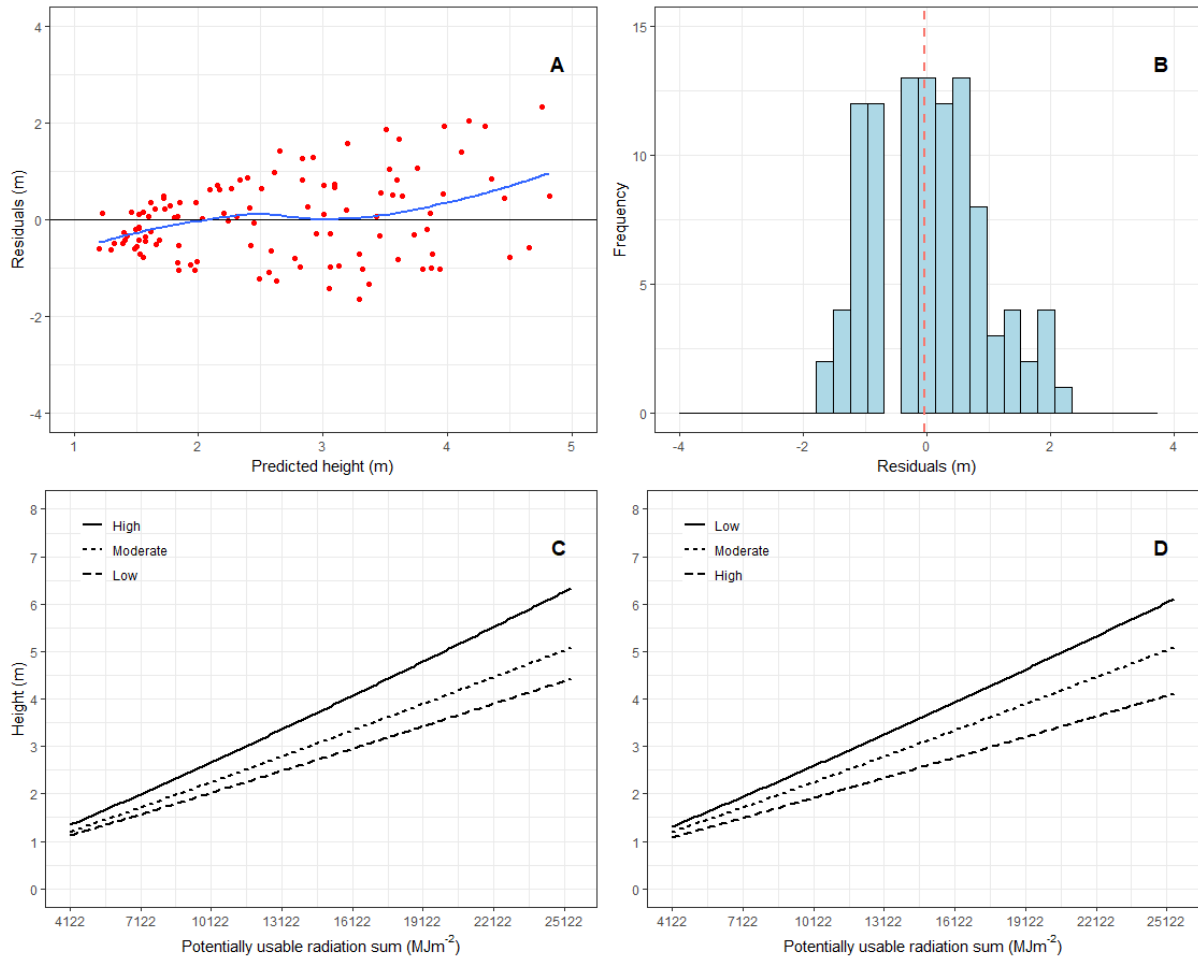


Figure 5.7 Augmented PULSE height model for *E. bosistoana* residuals: A) residuals against predicted plot, the blue line indicating the loess fit; B) residuals distribution; C) morphometric protection index (MPI) effect; and D) wind exposure index (WEI) effect.

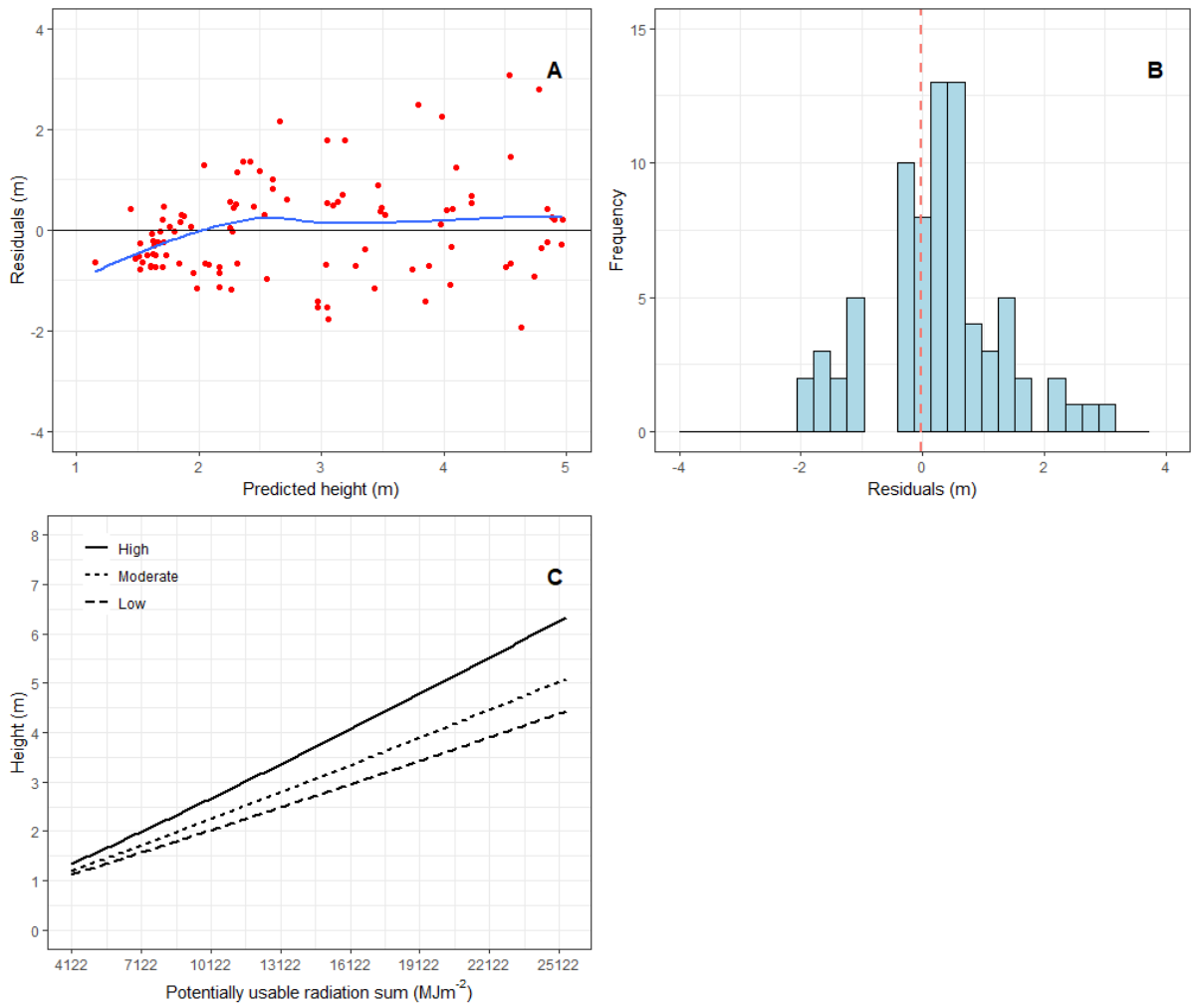


Figure 5.8 Augmented PULSE height model for *E. globoidea* residuals: A) residuals against predicted plot, the blue line indicating the loess fit; B) residuals distribution; C) Morphometric protection index (MPI) effect.

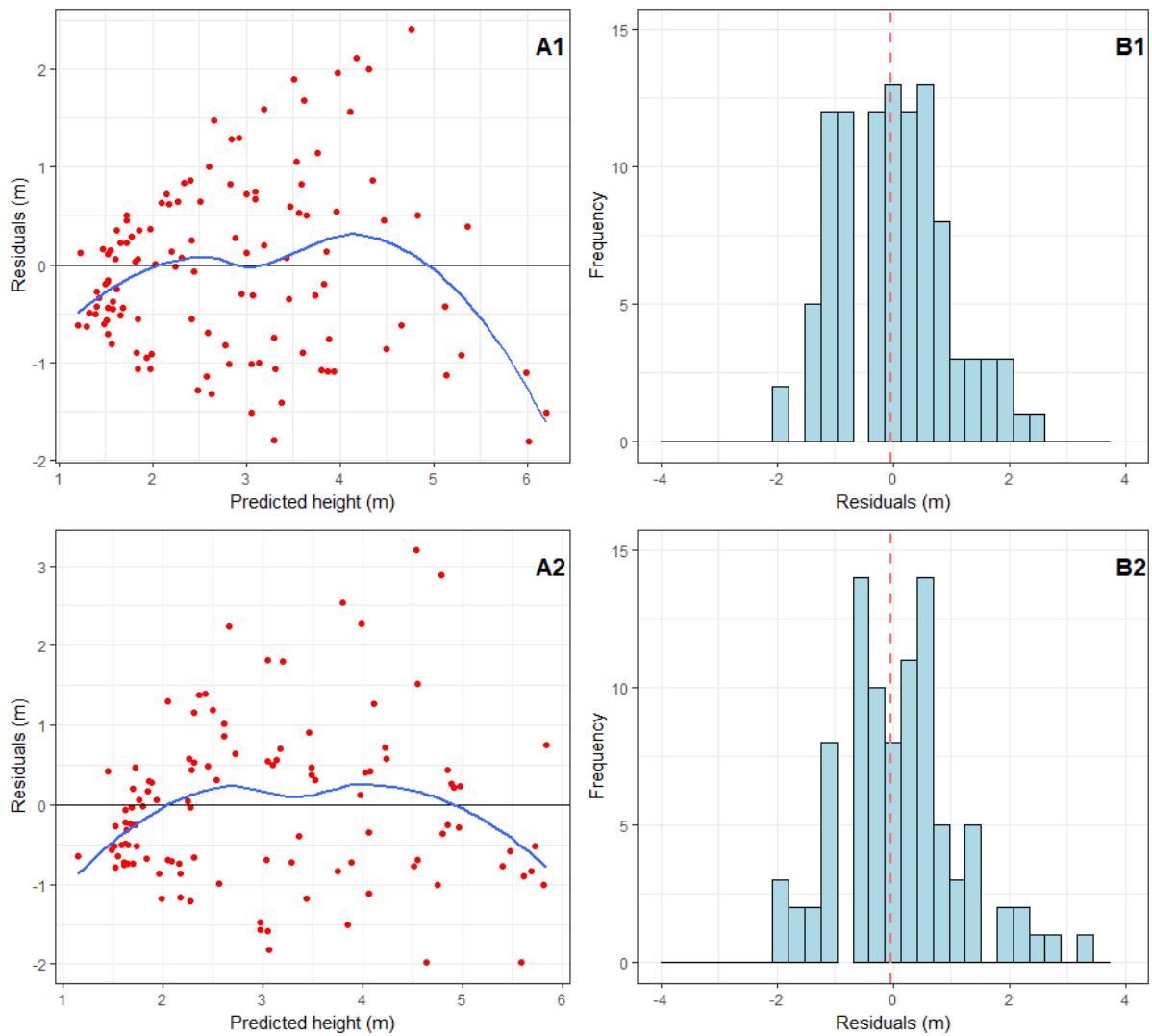


Figure 5.9 Residuals distribution from augmented models validation: A) predicted against residuals distribution with the loess fit line in blue and B) frequency distribution (red dashed showing the mean line). A1 and B1 for *E. bosistoana*; A2 and B2 for *E. globoidea*.

Table 5.5 Fitting and validation statistics for augmented PULSE height yield models.

Species		Fitting and validation statistics of augmented R_{TVPD}							
		RMSE	MAE	SE	BIAS	R^2 adj.	AICc	MPRESS	MAPRESS
<i>E. bosistoana</i>	Fitting	0.8464	0.691	0.861	-0.032	0.623	308.3902	-	-
	Validation	1.330	1.019	1.857	-0.010	-	301.461	-0.041	0.600
<i>E. globoidea</i>	Fitting	0.971	0.771	0.985	-0.030	0.609	311.256	-	-
	Validation	1.586	1.187	2.575	-0.002	-	304.330	-0.034	0.593

5.3.3 Site-specific survival PULSE model

Similarly to the height model, PULSE also performed well for survival proportion. Quantitatively, R_T and R_{TASW} showed the best results (Table 5.6) but, when combining the visual and statistical analyses, R_{TVPD} was the most satisfactory one. R_{TVPD} had very low distortion of residuals against predicted values, as well as being distributed more normally than other models (Figure 5.10, Figure 5.11, Figure 5.12 and Figure 5.13). Therefore, temperature and VPD modified PULS were included in the final modelling framework for both species. The final models are as follows (Equations 49 and 50):

$$S_{EBM} = -e^{\alpha R_{TVPD}^\beta} \quad (49)$$

$$S_{EGM} = -e^{\alpha R_{TVPD}^\beta} \quad (50)$$

where S_{EBM} and S_{EGM} are, respectively, *E. bosistoana* and *E. globoidea* survival proportions at month M and α and β are the modelling parameters.

Moreover, the validation analyses confirmed the models' performance and goodness-of-fit, but with less precision in comparison to the fitting statistics. From the validation statistics (Table 5.7) it can be seen that models performed with little or no distortion in comparison to the model fit. Residual fitting values increased by a negligible amount, which is also apparent in the plots (Figure 5.14).

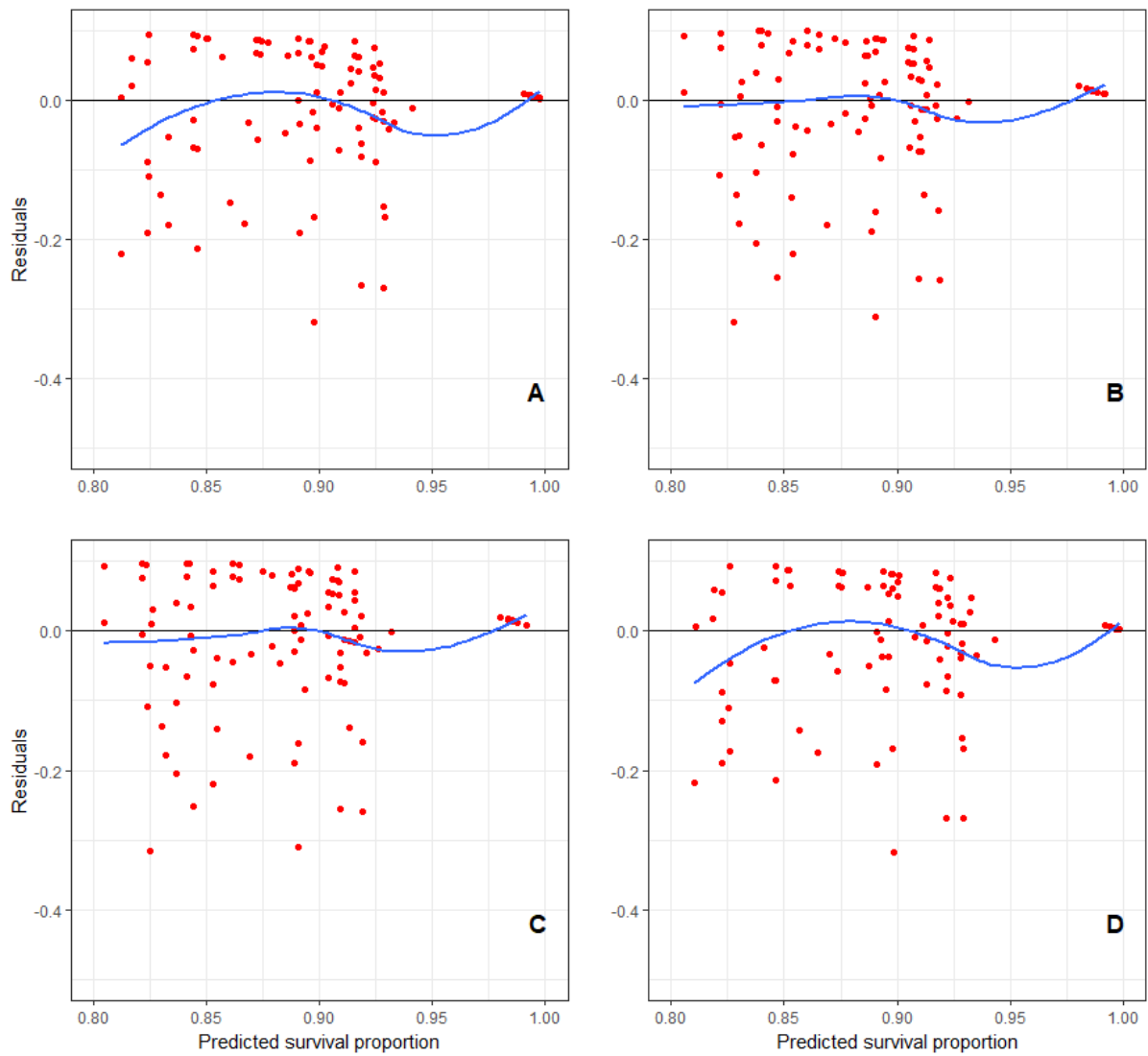


Figure 5.10 Residuals against predicted survival proportion of *E. bosistoana* PULSE survival proportion models (blue line indicating the loess fit): with A) all modifiers (R_M); and PULS modified by B) temperature (R_T); C) temperature and vapour pressure deficit (R_{TVPD}); and D) available soil water ($R_{T\theta}$).

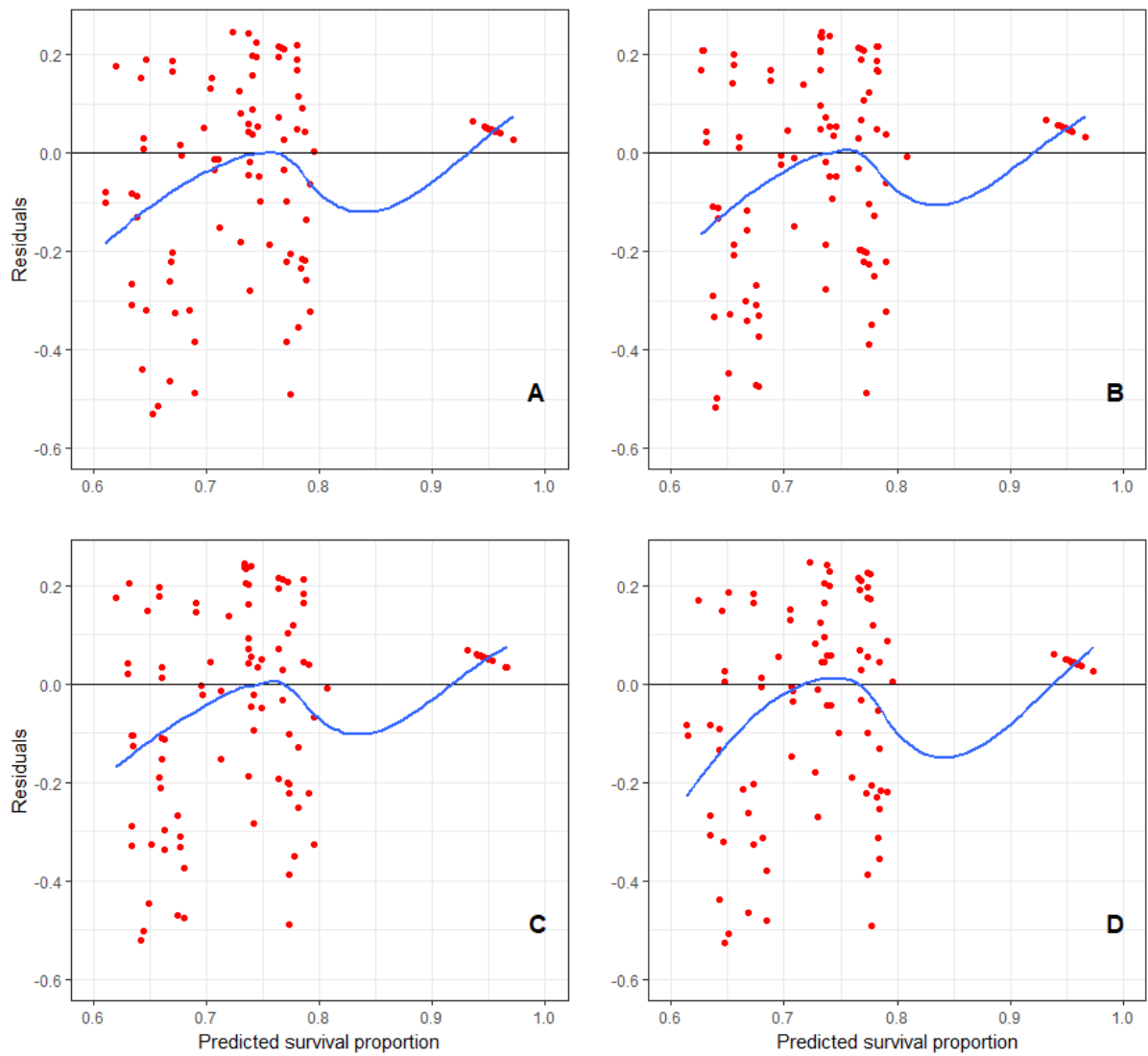


Figure 5.11 Residuals against predicted survival proportion of *E. globoidea* PULSE survival proportion models (blue line indicating the loess fit) and PULS modified by A) all modifiers (R_M); B) temperature (R_T); C) temperature and vapour pressure deficit (R_{TVPD}); D) available soil water ($R_{T\theta}$).

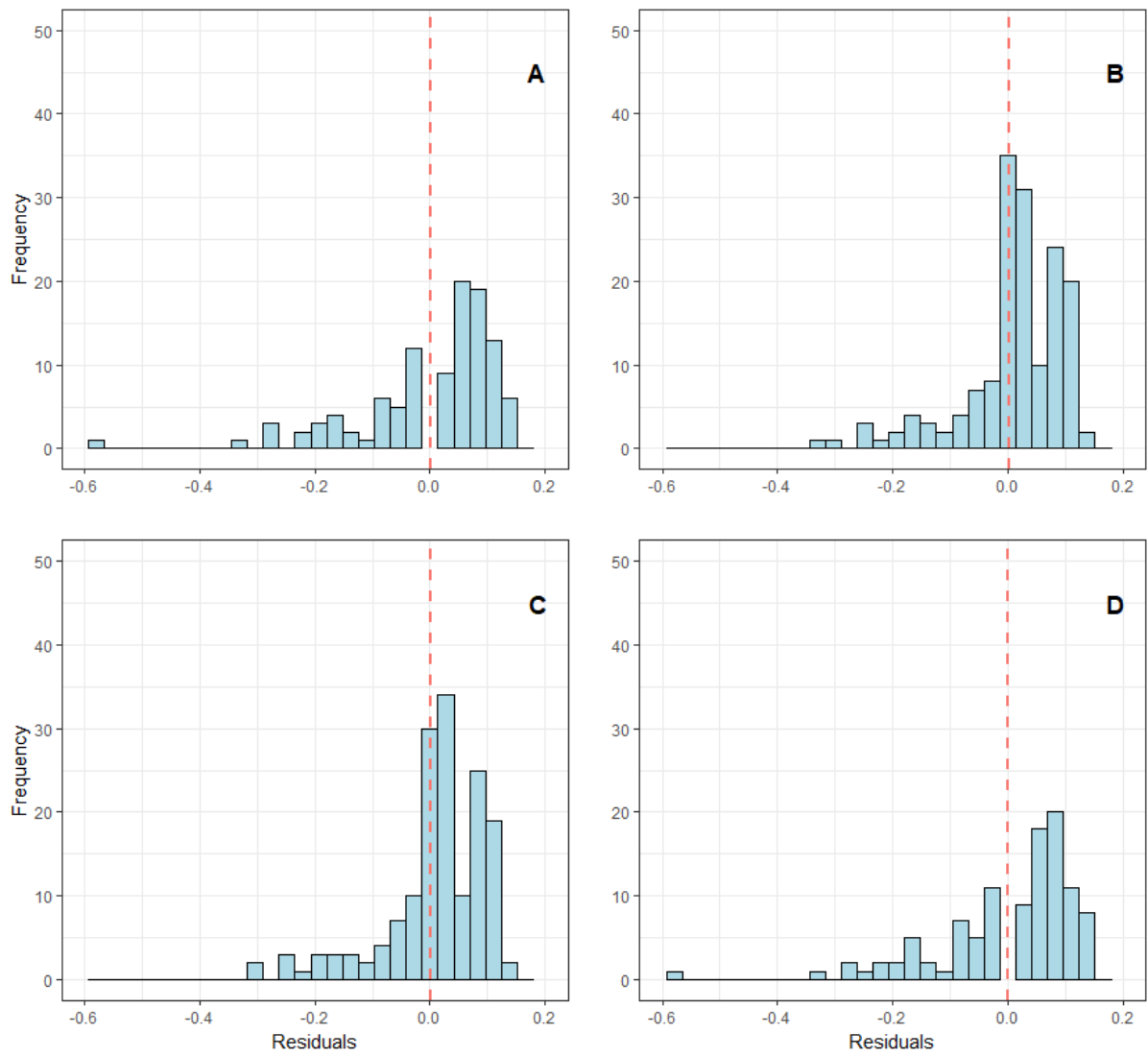


Figure 5.12 Residual distributions of *E. bosistoana* PULSE survival proportion models (red dashed line showing the mean), and PULS modified by A) all modifiers (R_M); B) temperature (R_T); C) temperature and vapour pressure deficit (R_{TVPD}); D) available soil water (R_{T0}) modified radiation sum.

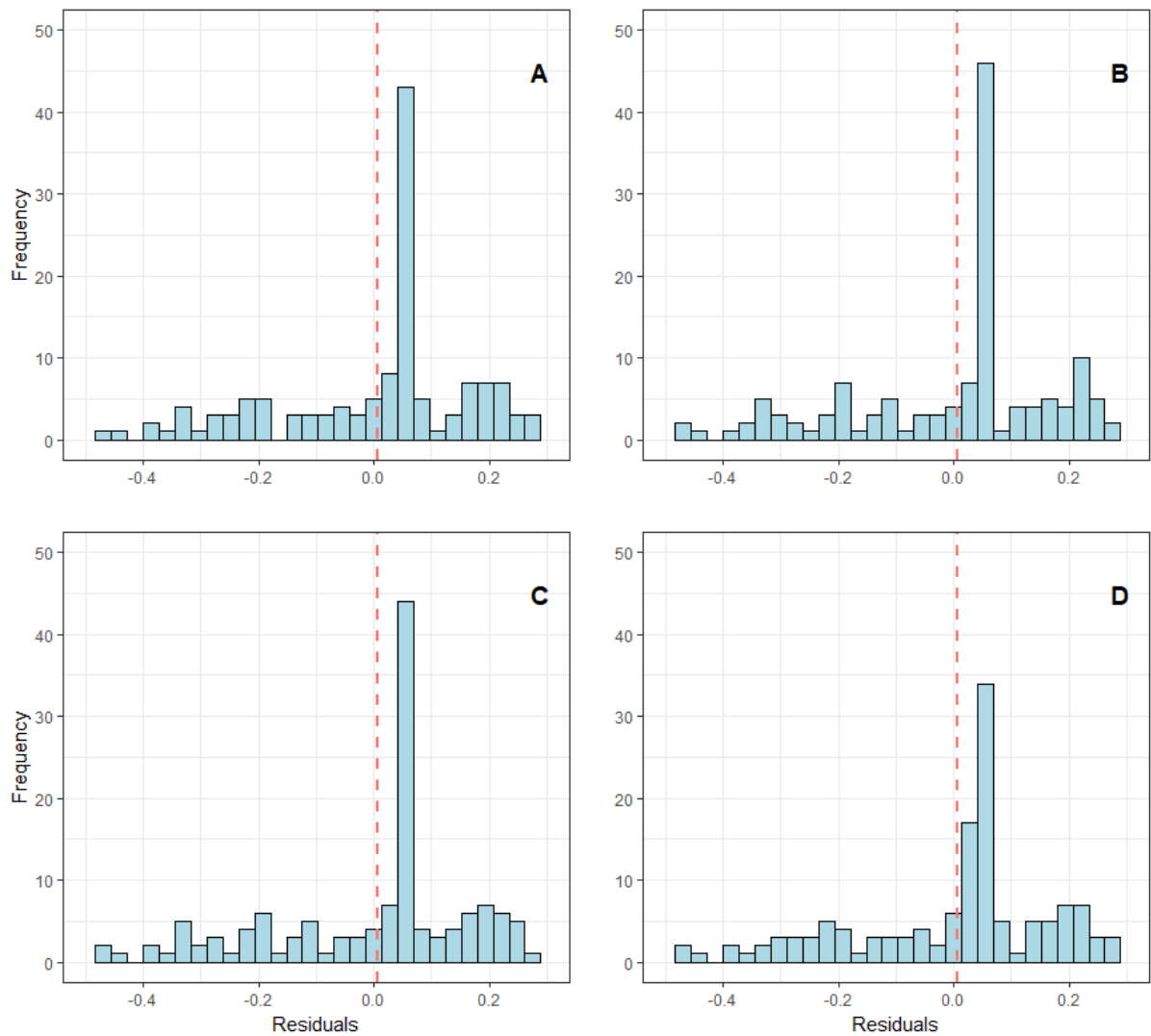


Figure 5.13 Residuals distribution of *E. globoidea* PULSE survival proportion models (red dashed line showing the mean), and PULS modified by A) all modifiers (R_M); B) temperature (R_T); C) temperature and vapour pressure deficit (R_{TVPD}); D) available soil water ($R_{T\theta}$) modified radiation sum.

Table 5.6 Fitting statistics for the PULSE survival proportion models.

Fitting Metric	PULSE models with different modifiers				Species
	R _M	R _T	R _{TVPD}	R _{T0}	
RMSE	0.110	0.114	0.114	0.110	<i>E. bosistoana</i>
MAE	0.069	0.072	0.072	0.069	
BIAS	0.0003	0.002	0.002	-1.299	
SE	0.111	0.115	0.114	0.111	
AICc	-244.082	-233.757	-234.237	-245.426	
R ² adj.	0.266	0.182	0.184	0.278	
RMSE	0.205	0.207	0.207	0.205	<i>E. globoidea</i>
MAE	0.157	0.161	0.161	0.156	
BIAS	0.006	0.007	0.007	0.006	
SE	0.207	0.208	0.209	0.206	
AICc	-42.689	-40.050	-39.875	-43.314	
R ² adj.	0.214	0.196	0.194	0.221	

Table 5.7 Validation statistics for the best PULSE survival proportion models.

Species	Validation statistics of R _{TVPD}						
	RMSE	MAE	SE	BIAS	AICc	MPRESS	MAPRESS
<i>E. bosistoana</i>	0.127	0.082	0.016	0.001	-229.248	0.002	0.164
<i>E. globoidea</i>	0.233	0.185	0.054	0.006	-38.641	0.007	0.177

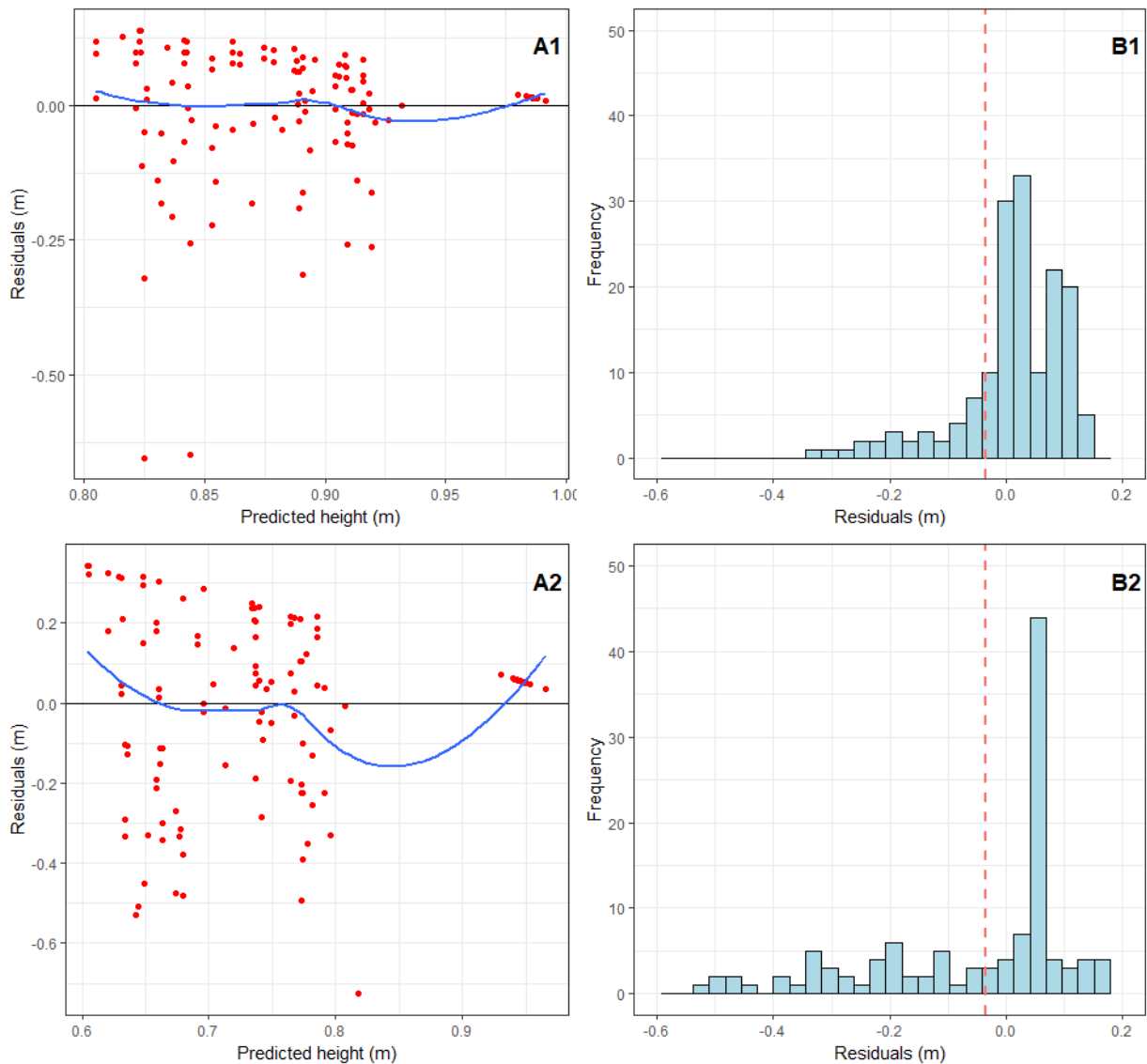


Figure 5.14 Residuals distribution for validation of survival proportion models: A) predicted against residuals distribution with the loess fit line in blue, and B) frequency distribution (red dashed line showing the mean). A1 and B1 for *E. bosistoana*; A2 and B2 for *E. globoidea*.

5.3.4 Augmented PULSE model for juvenile survival proportion

A list of uncorrelated secondary topographic variables (Table 5.8) and their interaction terms were considered to augment the best PULSE model for survival found previously. However, the statistical significance of the various combinations showed that only the topographic wetness index (TWI) for *E. bosistoana* and the wind exposure index (WEI) for *E. globoidea* merited inclusion. Likewise, for height yield models, in both cases topographic features were significant with the β parameter of the models. The equations are as follows:

$$S_{EBM} = -e^{\alpha R_{TVPD}(\beta_0 + \beta_1 * TWI)} \quad (51)$$

$$S_{EGM} = -e^{\alpha R_{TVPD}(\beta_0 + \beta_1 * WEI)} \quad (52)$$

where TWI is the topographic wetness index and WEI is the wind exposure index, and all others as described in earlier sections.

Table 5.8 Augmented variables and their significance status.

Species	Variables	Sig. Codes
<i>E. bosistoana</i>	Topographic position index (TPI)	NS
	Topographic wetness index (TWI)	***
	Morphometric protection index (MPI)	NS
	Wind exposure index (WEI)	NS
	Profile curvature	NS
	Plan curvature	NS
<i>E. globoidea</i>	Topographic position index (TPI)	NS
	Topographic wetness index (TWI)	NS
	Morphometric protection index (MPI)	NS
	Wind exposure index (WEI)	***
	Profile curvature	NS
	Plan curvature	NS

Sig. Codes: 0 ‘****’; 0.001 ‘***’; 0.01 ‘**’; 0.05 ‘.’; 0.1 ‘-’; NS ‘Not Significant’

Both of the augmented survival proportion models (Equations 51 and 52) performed with minimal error and visual distortion. In the frequency distribution plots of residuals, a few extreme outliers can be found, but other than those, the models fit within satisfactory ranges (Figure 5.15 and Figure 5.16). The *E. globoidea* model showed an abnormality in the residual against the predicted survival proportion plot (Figure 5.16 (A)). The model validation statistics and figures showed relatively small BIAS and other goodness-of-fit properties (Figure 5.17), though all of them increased during validation (Table 5.9).

The *E. bosistoana* survival proportion PULSE model was significantly influenced by the TWI, which indicates the wetness status of a certain location. The models showed that with increased wetness the survival proportion decreased. In the case of *E. globoidea*, WEI showed

a similar pattern. WEI indicates the wind load of a certain location. It showed that, with increased WEI, the *E. globoidea* survival proportion decreased (Figure 5.15 and Figure 5.16,(C)).

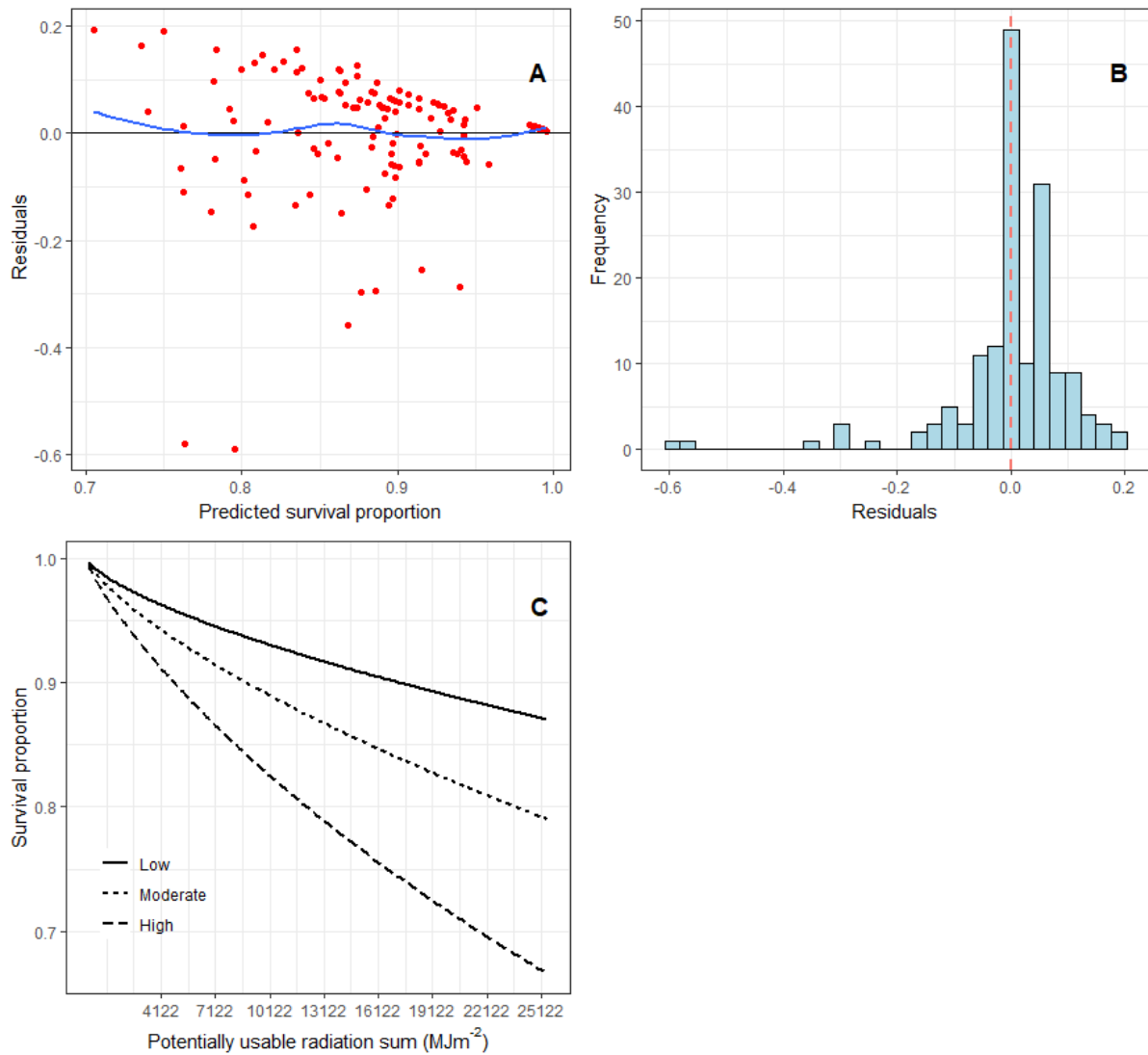


Figure 5.15 Augmented PULSE survival proportion model for *E. bosistoana*: A) residuals against predicted plot, the blue line indicating the loess fit; B) residuals distribution (red dashed line indicating the mean); C) topographic wetness index (TWI) effect.

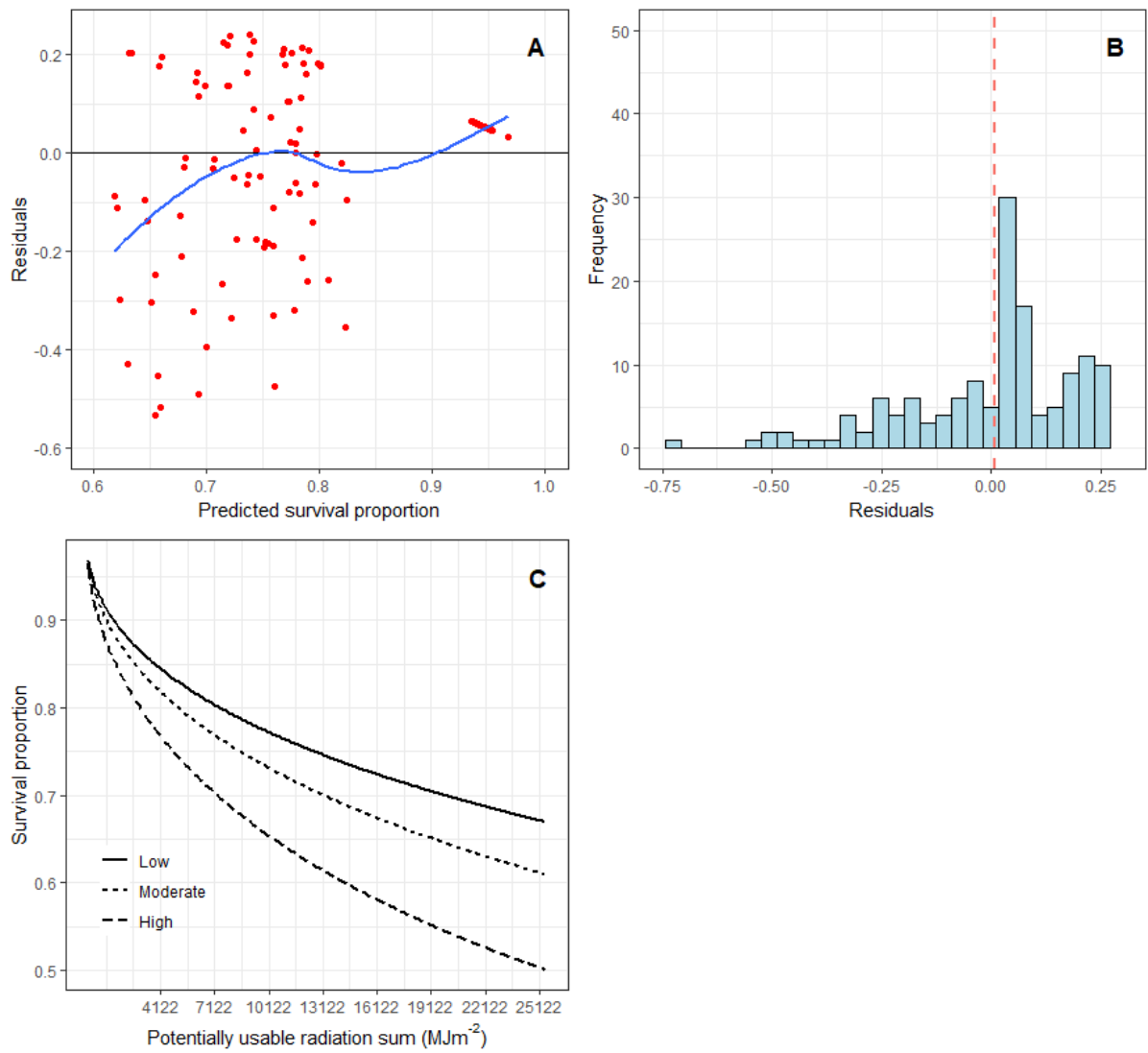


Figure 5.16 Augmented PULSE survival proportion model for *E. globoidea*: A) residuals against predicted plot, blue line indicating the loess fit; B) residuals distribution (red dashed line indicating the mean); C) wind exposure index (WEI) effect.

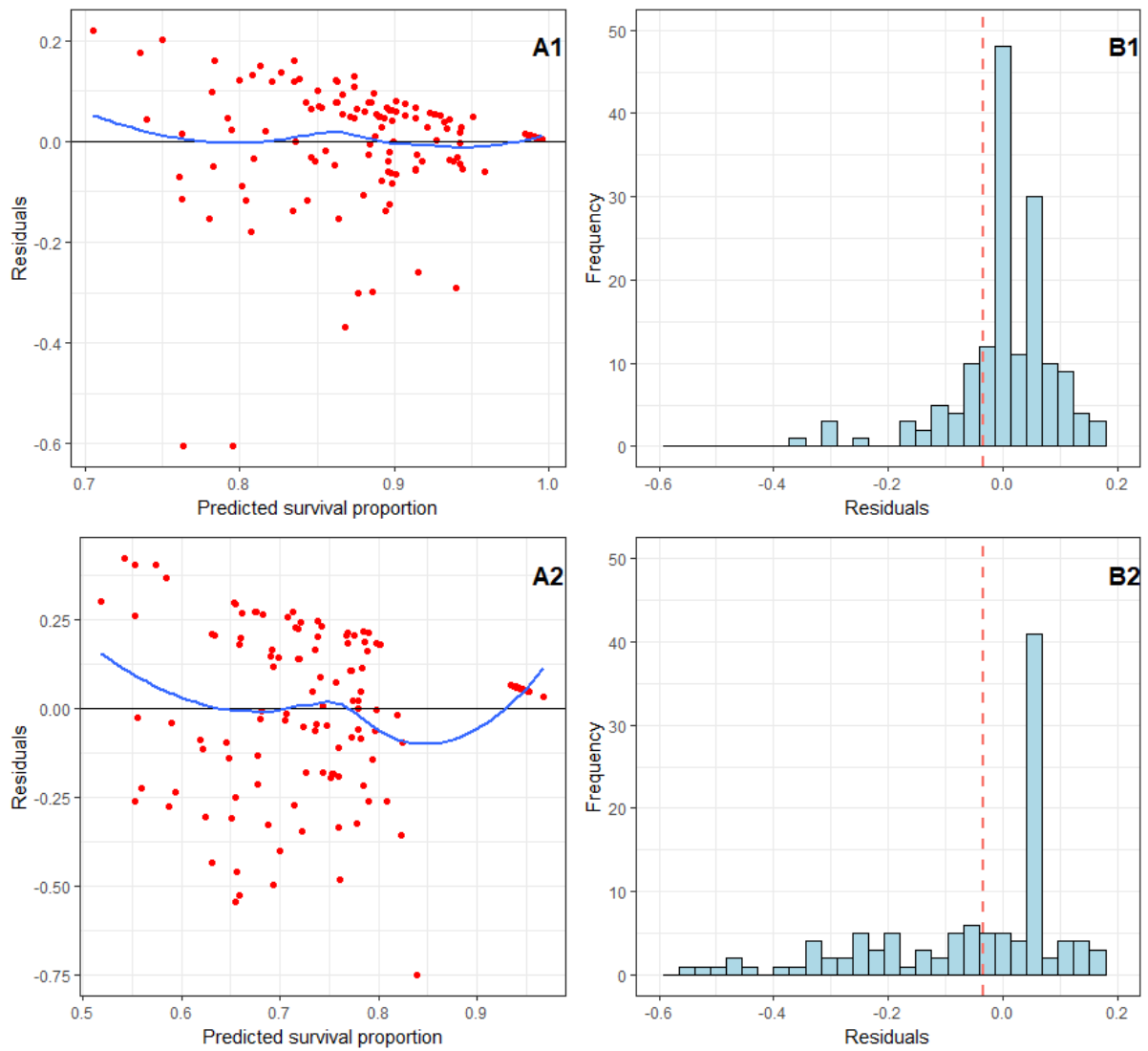


Figure 5.17 Residuals distribution from augmented survival proportion model validation: A) predicted against residuals distribution with the loess fit line (blue line) and B) frequency distribution (red dashed line shows the mean). A1 and B1 for *E. bosistoana*; A2 and B2 for *E. globoidea*.

Table 5.9 Fitting and validation statistics for augmented survival proportion PULSE models.

Species		Fitting and validation statistics of augmented R_{TVPD}							
		RMSE	MAE	SE	BIAS	R ² adj.	AICc	MPRESS	MAPRESS
<i>E. bosistoana</i>	Fitting	0.108	0.066	0.109	0.001	0.282	-249.573	-	-
	Validation	0.133	0.086	0.017	0.0003	-	-242.218	0.001	0.246
<i>E. globoidea</i>	Fitting	0.204	0.158	0.206	0.007	0.213	-42.076	-	-
	Validation	0.231	0.183	0.053	0.006	-	-40.8076	0.008	0.188

5.4 Discussion

Traditional growth and yield models are highly abstract and geographically local. They are likely to be unstable with changes, for example, climate change and change in management regime (Kimmins et al., 2008). These may need to be addressed, either by examining the underlying process, or by avoiding the model complexity. Moreover, models should follow the basic assumptions of traditional growth and yield modelling (Burkhart & Tomé, 2012; Weiskittel et al., 2011). In this study, an ecophysiological hybrid modelling system (PULSE) has been successfully implemented to predict height yield and survival at the site-specific level for juvenile *E. bosistoana* and *E. globoidea*. This framework was first implemented for juvenile *Pinus taeda* ground level diameter (GLD) growth (Mason et al., 2007). Since then it has not been tested on any juvenile forest. Adding topographic features gave extra explanatory power and gave more precision to both the height yield and the survival proportion models.

5.4.1 Juvenile PULSE models

This study included different approaches to cumulative radiation for modelling the height yield and survival proportion, which gave an insight into key growth variables. Models with different modifiers performed well with little residual distortion and desirable statistical properties. All the models were relatively stable with regard to temperature, and the VPD modified radiation sum (R_{TVPD}). Casnati (2016) reported that PULS performed best with multiple modifiers for stand dynamics of *Pinus taeda* and *Eucalyptus grandis* in Uruguay, and that temperature-only modified PULS performed worst. In contrast, Mason et al. (2018) found potentially usable radiation sum was best modified by temperature alone for site index (SI) of *Pinus sylvestris* in Sweden. Both studies were on mature stand growth, whereas this study was carried out on juvenile stands. As the application of PULSE is very much dependent on the input data, with more precise measurements the models presented would likely have included other modifiers. For instance, in this study, the LAI for trees and competing vegetation were

modelled without any site-specific data. Moreover, the information provided by the fundamental soil layers was coarse and potentially erroneous (Pearse et al., 2015). As these two inputs were critical for making the water balance model for PULSE, it is possible that the resultant water balance model was not sufficiently precise to be significant in the final modelling step.

Eucalyptus are highly sensitive to temperature (Bell & Williams, 1997) and atmospheric humidity (Battaglia & Sands, 1998), with both influencing growth and survival. The results of this study support these same findings. Besides, these results were consistent with Chapters 3 and 4. Also, *Eucalyptus* species are well known to be water demanding (Bell & Williams, 1997). That aside, there is very little published information about ecophysiological behaviour of *E. bosistoana* and *E. globoidea*.

In all models, errors increased at the validation step. The survival proportion model had lower validation errors: better initial data of newly planted stock may explain this and reduce the errors (Mason et al., 2007; Mason & Whyte, 1997). In this study, no tree measurements immediately after planting were available. For example, initial seedling height, site preparation and weeding treatments were unknown, which may have influenced final modelling outcomes.

5.4.2 Topographic variables

As the radiation sums used by PULSE were calculated for a flat surface, it is important to modify the models to account for topography. Coops et al. (2000) reported differences in incoming radiation for a variety of slopes and orientations, which are therefore important when estimating incoming radiation as input for hybrid forest growth and yield models. Berg et al. (2017) explained topographic wetness in relation to seasonality, and Fremme and Sodemann (2018) reported wind effects on soil moisture. Casnati (2016) also recommended the inclusion of topography as it played an important role in the PULSE model precision and explanatory

power. The topographic features used in the final models, MPI, WEI and TWI, may potentially influence the radiation sum.

Juvenile *E. bosistoana* height was influenced by the morphometric protection index (MPI) and the wind exposure index (WEI), and *E. globoidea* height was influenced by MPI alone – in line with previous findings in this thesis. Wind actively influences the tree architecture (Brüchert & Gardiner, 2006) and seedlings are more conservative with resources than mature trees, especially in arid regions (Mediavilla & Escudero, 2004).

The survival of *E. bosistoana* was influenced by the topographic wetness index (TWI), whereas WEI influenced *E. globoidea* survival. Interestingly, increasing TWI negatively affected *E. bosistoana* survival. Possibly this dryland species is adversely affected by high soil moisture, or the trend may be caused by winter frosts (Paton, 1981), which presumably appear in cool-air affecting areas that also correlate with high TWI values. For *E. globoidea*, the relationship may be due to the wind influence on evapotranspiration, which is also associated with moisture circulation (Fremme & Sodemann, 2018).

5.5 Conclusion

The results presented in this study suggest that PULSE can be used to predict height yield and survival of juvenile *E. bosistoana* and *E. globoidea* plantations, and can be a basis of forecasting systems. This study explicitly explored a set of different alternatives to estimate the potentially usable radiation sum. Better initial plantation data (e.g., competing vegetation information, initial measurement) will increase the model precision.

Including topographic features into the system not only improved the model precision and bias but also gave some indications on the ecophysiological behaviour of the studied species. The models and results presented here for the two dryland *Eucalyptus* species will give useful information to forest managers for establishing new plantations. In particular, their ecophysiological nature of growth with regards to different factors. This study has also

demonstrated that PULS techniques can avoid the complexity of traditional models while obtaining better predictions of tree performance.

5.6 References

- Almeida, A. C., Landsberg, J. J., & Sands, P. J. (2004). Parameterisation of 3-PG model for fast-growing *Eucalyptus grandis* plantations. *Forest Ecology and Management*, 193(1), 179-195. doi:<https://doi.org/10.1016/j.foreco.2004.01.029>
- Battaglia, M., & Sands, P. (1998). Modelling site productivity of *Eucalyptus globulus* in Response to Climatic and Site Factors. *Functional Plant Biology*, 24(6), 831-850. doi:<https://doi.org/10.1071/PP97065>
- Battaglia, M., Sands, P., White, D., & Mummery, D. (2004). CABALA: a linked carbon, water and nitrogen model of forest growth for silvicultural decision support. *Forest Ecology and Management*, 193(1), 251-282. doi:<https://doi.org/10.1016/j.foreco.2004.01.033>
- Bell, D. T., & Williams, J. E. (1997). Eucalypt ecophysiology. *Eucalypt ecology: individuals to ecosystems*. Cambridge University Press, Cambridge, 168-196.
- Berg, A., Lintner, B., Findell, K., & Giannini, A. (2017). Soil moisture influence on seasonality and large-scale circulation in simulations of the west African monsoon. *Journal of Climate*, 30(7), 2295-2317.
- Böhner, J., & Antonić, O. (2009). Land-surface parameters specific to topo-climatology. *Developments in Soil Science*, 33, 195-226.
- Bown, H. E., Mason, E. G., Watt, M. S., & Clinton, P. W. (2013). A potential nutritional modifier for predicting primary productivity of *Pinus radiata* in New Zealand using a simplified radiation-use efficiency model. *Ciencia e Investigación Agraria*, 40(2), 361-374.
- Breuer, L., Eckhardt, K., & Frede, H.-G. (2003). Plant parameter values for models in temperate climates. *Ecological Modelling*, 169(2), 237-293. doi:[https://doi.org/10.1016/S0304-3800\(03\)00274-6](https://doi.org/10.1016/S0304-3800(03)00274-6)
- Brüchert, F., & Gardiner, B. (2006). The effect of wind exposure on the tree aerial architecture and biomechanics of Sitka spruce (*Picea sitchensis*, Pinaceae). *American Journal of Botany*, 93(10), 1512-1521. doi:[doi:10.3732/ajb.93.10.1512](https://doi.org/10.3732/ajb.93.10.1512)
- Burkhart, H. E., & Tomé, M. (2012). *Modeling Forest Trees and Stands*: Springer.
- Casnati, A. C. R. (2016). *Hybrid mensurational-physiological models for Pinus taeda and Eucalyptus grandis in Uruguay*. (PhD), University of Canterbury, New Zealand.
- Clutter, J. L. (1963). Compatible growth and yield models for Loblolly Pine. *Forest Science*, 9(3), 354-371.

- Clutter, J. L., Fortson, J. C., Pienaar, L. V., Brister, G. H., & Bailey, R. L. (1983). *Timber management: a quantitative approach*: John Wiley & Sons, Inc.
- Coops, N. C., & Waring, R. H. (2001). Estimating forest productivity in the eastern Siskiyou mountains of southwestern Oregon using a satellite driven process model, 3-PGS. *Canadian Journal of Forest Research*, *31*(1), 143-154. doi:10.1139/x00-146
- Coops, N. C., Waring, R. H., & Moncrieff, J. B. (2000). Estimating mean monthly incident solar radiation on horizontal and inclined slopes from mean monthly temperatures extremes. *International Journal of Biometeorology*, *44*(4), 204-211. doi:10.1007/s004840000073
- Dodd, M. B., McGowan, A. W., Power, I. L., & Thorrold, B. S. (2005). Effects of variation in shade level, shade duration and light quality on perennial pastures. *New Zealand Journal of Agricultural Research*, *48*(4), 531-543. doi:10.1080/00288233.2005.9513686
- Fremme, A., & Sodemann, H. (2018). *The influence of wind and land evapotranspiration on monsoon precipitation intensity and timing*. Paper presented at the EGU General Assembly Conference Abstracts.
- Garcia, O. (1984). New class of growth models for even-aged stands: *Pinus radiata* in Golden Downs Forest. *NZJ For. Sci*, *14*(1), 65-88.
- Gerlitz, L., Conrad, O., & Böhner, J. (2015). Large-scale atmospheric forcing and topographic modification of precipitation rates over high Asia - a neural-network-based approach. *Earth System Dynamics*, *6*(1), 61-81. doi:10.5194/esd-6-61-2015
- Kimmins, J. P. H., Blanco, J. A., Seely, B., Welham, C., & Scoullar, K. (2008). Complexity in modelling forest ecosystems: how much is enough? *Forest Ecology and Management*, *256*(10), 1646-1658.
- Land Resource Information System. (2015). Fundamental soil layer (All attributes). Retrieved from <https://lris.scinfo.org.nz/search/?q=FSL+all+atributes>
- Landsberg, J. (2003). Physiology in forest models: history and the future. *FBMIS*, *1*, 49-63.
- Landsberg, J., & Waring, R. (1997). A generalised model of forest productivity using simplified concepts of radiation-use efficiency, carbon balance and partitioning. *Forest Ecology and Management*, *95*(3), 209-228.
- Landsberg, J. J., & Sands, P. J. (2011). *Physiological ecology of forest production: principles, processes and models* (Vol. 4): Elsevier/Academic Press.
- Mäkelä, A., Landsberg, J., Ek, A. R., Burk, T. E., Ter-Mikaelian, M., Ågren, G. I., . . . Puttonen, P. (2000). Process-based models for forest ecosystem management: current state of the art and challenges for practical implementation. *Tree Physiology*, *20*(5-6), 289-298.

- Martin, T. A., Hinckley, T. M., Meinzer, F. C., & Sprugel, D. G. (1999). Boundary layer conductance, leaf temperature and transpiration of *Abies amabilis* branches. *Tree Physiology*, 19(7), 435-443. doi:10.1093/treephys/19.7.435
- Mason, E., Rose, R., & Rosner, L. (2007). Time vs light: a potentially useable light sum hybrid model to represent the juvenile growth of Douglas-fir subject to varying levels of competition. *Canadian Journal of Forest Research*, 37(4), 795-805.
- Mason, E. G. (In Prep.). Using ecophysiological modelling to estimate the influence of variably sized pasture free zones around the trees on *Pinus radiata* D. Don. height growth.
- Mason, E. G., Holmström, E., & Nilsson, U. (2018). Using hybrid physiological/mensurational modelling to predict site index of *Pinus sylvestris* L. in Sweden: a pilot study. *Scandinavian Journal of Forest Research*, 33(2), 147-154. doi:10.1080/02827581.2017.1348539
- Mason, E. G., Methol, R., & Cochrane, H. (2011). Hybrid mensurational and physiological modelling of growth and yield of *Pinus radiata* D. Don. using potentially useable radiation sums. *Forestry*, 84(2), 99-108. doi:10.1093/forestry/cpq048
- Mason, E. G., & Whyte, A. G. D. (1997). Modelling initial survival and growth of radiata pine in New Zealand. *Acta Forestalia Fennica*, 2, 1-38.
- McNaughton, K., & Jarvis, P. (1983). Predicting effects of vegetation changes on transpiration and evaporation. *Water Deficits and Plant Growth*, 7, 1-47.
- Mediavilla, S., & Escudero, A. (2004). Stomatal responses to drought of mature trees and seedlings of two co-occurring Mediterranean oaks. *Forest Ecology and Management*, 187(2), 281-294. doi:https://doi.org/10.1016/j.foreco.2003.07.006
- Mielke, M. S., Oliva, M. A., de Barros, N. F., Penchel, R. M., Martinez, C. A., & de Almeida, A. C. (1999). Stomatal control of transpiration in the canopy of a clonal *Eucalyptus grandis* plantation. *Trees*, 13(3), 152-160. doi:10.1007/pl00009746
- Monserud, R. A. (2003). Evaluating forest models in a sustainable forest management context. *Forest Biometry, Modelling and Information Sciences*, 1(1), 35-47.
- Monteith, J. L. (1981). Evaporation and surface temperature. *Quarterly Journal of the Royal Meteorological Society*, 107(451), 1-27. doi:doi:10.1002/qj.49710745102
- Montes, C. R. (2012). A resource driven growth and yield model for Loblolly Pine plantations. (PhD), North Carolina State University, United States.
- NIWA. (2015). Virtual climate station data and products. Retrieved from <https://www.niwa.co.nz/climate/our-services/virtual-climate-stations>

- Oparah, I. A. (2012). *Photosynthetic acclimation to temperature of four Eucalyptus species and Sequoia sempervirens*. (MSc), University of Canterbury, New Zealand.
- Paton, D. (1981). *Eucalyptus* Physiology. III. frost resistance. *Australian Journal of Botany*, 29(6), 675-688. doi:<https://doi.org/10.1071/BT9810675>
- Pearse, G., Moltchanova, E., & Bloomberg, M. (2015). Assessment of the accuracy of profile available water and potential rooting depth estimates held within New Zealand's fundamental soil layers geo-database. *Soil Research*, 53(7), 737-744. doi:<https://doi.org/10.1071/SR14012>
- Peng, C., Liu, J., Dang, Q., Apps, M. J., & Jiang, H. (2002). TRIPLEX: a generic hybrid model for predicting forest growth and carbon and nitrogen dynamics. *Ecological Modelling*, 153(1-2), 109-130. doi:[http://dx.doi.org/10.1016/S0304-3800\(01\)00505-1](http://dx.doi.org/10.1016/S0304-3800(01)00505-1)
- Pinkard, E. A., & Battaglia, M. (2001). Using hybrid models to develop silvicultural prescriptions for *Eucalyptus nitens*. *Forest Ecology and Management*, 154(1), 337-345. doi:[https://doi.org/10.1016/S0378-1127\(00\)00641-1](https://doi.org/10.1016/S0378-1127(00)00641-1)
- R Core Team. (2017). R: A language and environment for statistical computing. Vienna, Austria: R Foundation for Statistical Computing; 2016. URL <http://www.R-project.org>.
- Richardson, B., Kimberley, M. O., Ray, J. W., & Coker, G. W. (1999). Indices of interspecific plant competition for *Pinus radiata* in the central North Island of New Zealand. *Canadian Journal of Forest Research*, 29(7), 898-905. doi:10.1139/x99-099
- Sands, P. (2004). Adaptation of 3-PG to novel species: guidelines for data collection and parameter assignment. *CRC Sustainable Production Forestry, Hobart*, 34.
- Snowdon, P., Jovanovic, T., & Booth, T. H. (1999). Incorporation of indices of annual climatic variation into growth models for *Pinus radiata*. *Forest Ecology and Management*, 117(1), 187-197.
- Weiskittel, A. R. (2007). *Development of a hybrid modeling framework for intensively managed Douglas-fir plantations in the Pacific Northwest*. Oregon State University, United States.
- Weiskittel, A. R., Hann, D. W., Kershaw, J. A., & Vanclay, J. K. (2011). *Forest Growth and Yield Modeling*: Wiley.

6

Comparison of hybrid ecophysiological modelling approaches between sites

6. Comparison of hybrid ecophysiological modelling approaches between sites.

6.1 Introduction

Several different hybrid modelling approaches have been reported in the literature for both juvenile (Mátyás et al., 2009; Peng et al., 2002; Rauscher et al., 1990) and mature stands (Landsberg & Sands, 2011; Mason et al., 2018; Snowdon et al., 1999). In addition, the advantages of hybrid modelling and its opportunities to aid sustainable forest management have been discussed (Kimmins et al., 1996; Monserud, 2003; Weiskittel et al., 2011). In contrast to these studies, different hybrid ecophysiological approaches have rarely been compared based on the following criteria: i) capability to embody the biological process; ii) coherence between model components and consistency with co-variates; iii) comprehensiveness and shortcomings; iv) application and risk associated to future implementation. However, examples are available: for instance, Pinjuv et al. (2006) quantitatively compared different hybrid ecophysiological models for *Pinus radiata* in New Zealand. Casnati (2016) performed both a quantitative and qualitative comparison for a range of modelling approaches, from pure mensurational to high-resolution hybrid ecophysiological models for *Pinus taeda* and *Eucalyptus grandis* in Uruguay. Interestingly, both of these studies were performed on mature stands, and there has been no further study of this nature to date.

In previous chapters (Chapters 3, 4 and 5), three different hybrid modelling approaches were developed and tested for juvenile height and survival. They were as follows:

- i. The augmented traditional approach (T_A): topographic, edaphic and climatic variables augmented time-based model.
- ii. The PULSE approach (PULSE): a hybrid ecophysiological model, where time was replaced by cumulative light sums from the time of planting, with potential radiation use calculated by modifiers.

- iii. The augmented PULSE approach (PULSE_A): augmented hybrid ecophysiological model with topographic variables.

The aim of this chapter was to compare the three approaches with respect to their suitability for predicting stand dynamics and structure. This comparison was based on model precision and bias, capacity to use initial data in order to explain juvenile stand growth, and survival. The analysis was focused on understanding the effectiveness of the data used by each approach as well as the usefulness of the information provided by models for juvenile growth dynamics. The set of equations were described in Chapter 4 and 5.0

6.2 Methodology

The analysis was based on five basic concepts defined by Casnati (2016), namely i) use of data; ii) assumptions, sources of errors and variations; iii) precision and bias; iv) system integration, and v) data requirements. These ideas were validated through three simple steps that covered both quantitative and qualitative aspects of the models. Step 1 considered the whole between sites dataset described in Chapter 4 in order to obtain an overall picture, whereas Steps 2 and 3 were based only on the validation results. The steps are described below.

Step 1: A comparison of time- versus radiation-based models was established. It was followed by a comparison between the input data used by each approach for each species.

Step 2: Precision and bias of all models were compared in order to understand which formulation provided quality implementation. Precision was assessed through the root mean square error (RMSE) and bias through the mean absolute error (MAE). Both statistics were calculated by the methods described in Chapter 4. Moreover, residuals were plotted against predicted values in order to compare distribution and tendencies.

Step 3: This step involved discussing system integration and how well the components work together, as well as obtaining a deeper understanding of the consequences of using different approaches.

6.3. Results and discussion

6.3.1. Time versus radiation

The substitution of time by modified potentially usable radiation sums (PULS) is the main feature of the PULSE approach. Modelling tree growth as a function of time (age) is traditional practice, and it is mathematically precise. This is because the traditional approach is free from estimation error; however, it provides less information. In particular, traditional approaches cannot give a clear insight into the ecophysiological process. The relationships between PULS and different growth indices (e.g. height and survival) are shown in Figure 6.1 and Figure 6.2. PULS ranged from 130 to 35,000 MJm⁻² for the study period. The overall correlation between PULS with height growth and survival was slightly greater (PULSE=0.776>T_A=0.756) than the time-based model (Figure 6.1 and Figure 6.2). An additional benefit of the PULSE approach is that it can provide a better explanation of stand conditions (Casnati, 2016; Mason et al., 2007) in comparison with T_A. It was also observed that with different modifiers the PULSE approach can produce better results (Figure 6.1 and Figure 6.2); of course, it relies on more elaborate input data. Moreover, by combining data related to growth, the PULSE approach allows inclusion of data that varies spatially and temporarily without interfering with ideal model properties, for instance, the path invariance property of tree growth models.

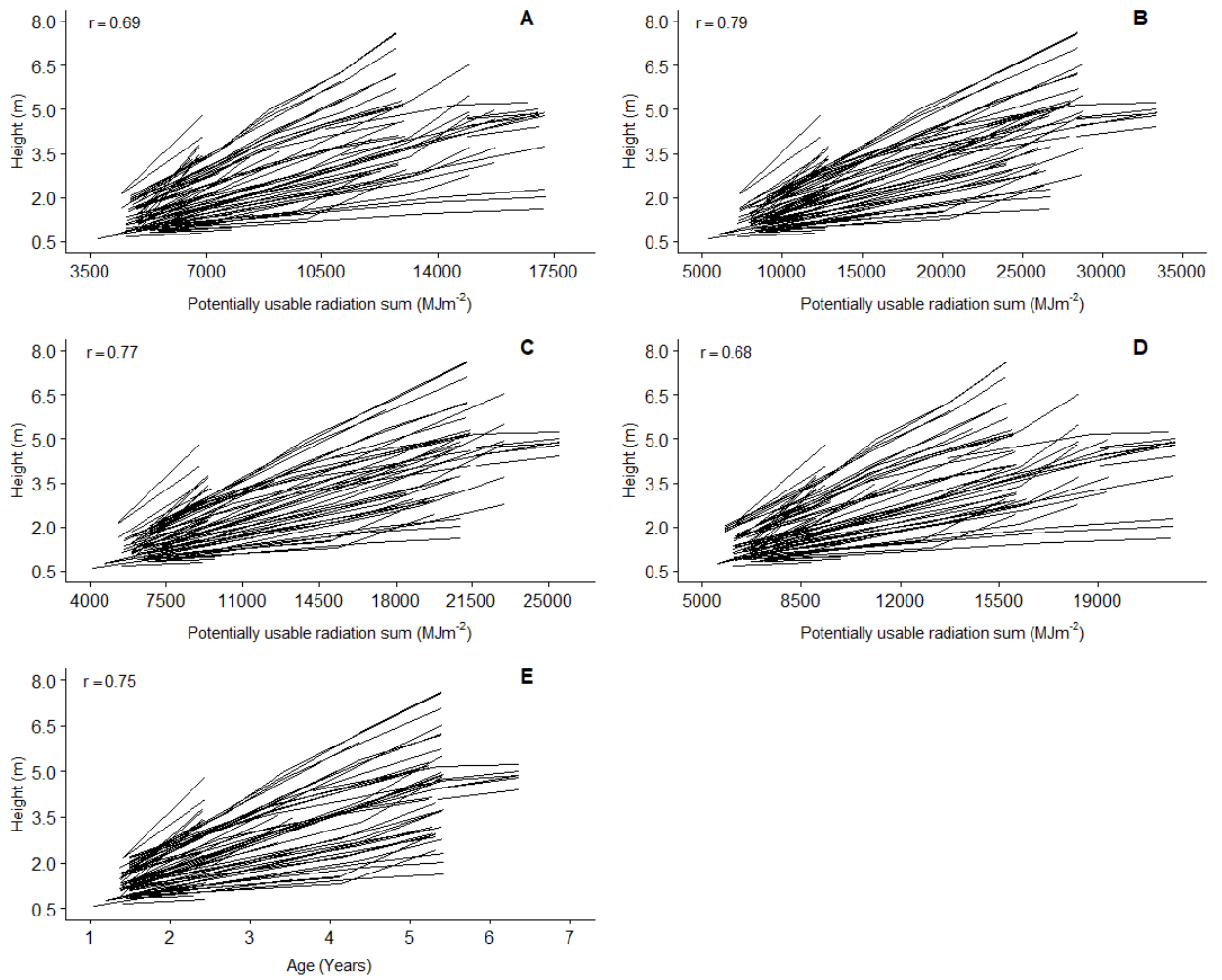


Figure 6.1 Relationship between height (m) with modified PULS and time (age) with correlation coefficients: A) all modifiers; B) temperature modifier; C) temperature and VPD modifiers; D) temperature and ASW modifiers; and E) age in years.

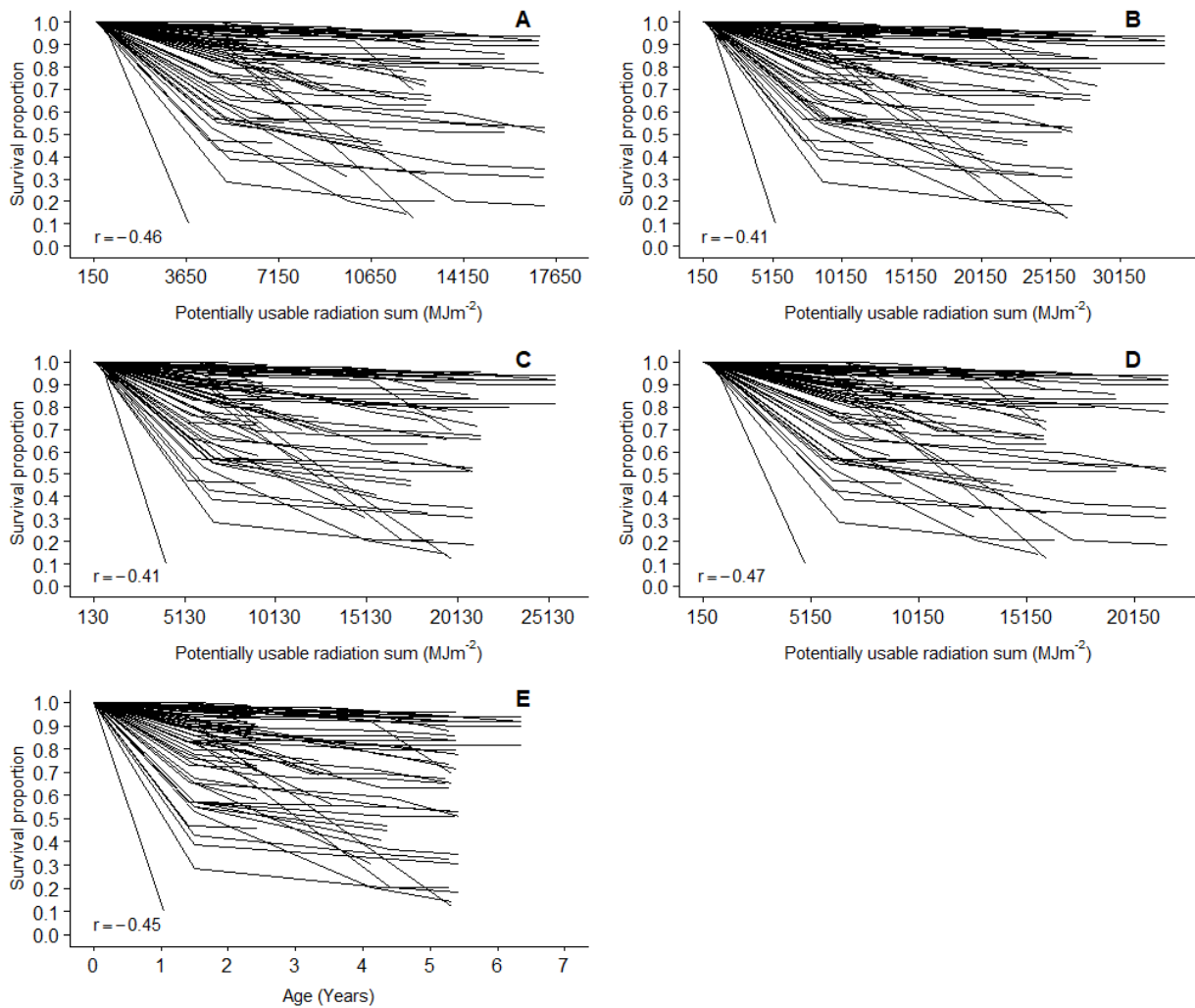


Figure 6.2 Relationship between survival proportion with modified PULS and time (age) with correlation coefficients: A) all modifiers; B) temperature modifier; C) temperature and VPD modifiers; D) temperature and ASW modifiers; and E) age in years.

6.3.2 Information used

A comparison of input data used in this study by each of the approaches is presented in Table 6.1. The simplest approach was PULSE, where the equations calculated the PULS from a few basic inputs, for example, temperature, rainfall and radiation. Next to PULSE was the augmented version of it with topographic variables. By contrast, the time-based approach used a lot more data as input. In terms of complexity and explanatory power, augmented PULSE was more complete and covered different aspects of growth processes. Chapters 3 and 4 indicated that *E. globoidea* and *E. bosistoana* were influenced by different topographic features, soil characteristics, and climatic variables. These factors played a key role in tree

growth. The augmented PULSE approach represented those factors in a single simple equation, which fulfils basic modelling requirements, simplicity and rationality (Gunawardena, 2014). Moreover, Casnati (2016) came to a similar conclusion in the case of mature *Pinus taeda* and *Eucalyptus grandis* in Uruguay.

All the approaches studied require the same data regarding tree characteristics; however, PULSE approaches need geo-referenced plot locations, digital elevation models (DEM) and more detailed soil data. They also need leaf area index (LAI) information for trees as well as the competing vegetation. All these may add complexity to the models.

Beyond potential difficulties regarding input data required, the application of each methodology would depend on the goal of the users by seeking an exact answer based on “what if” type of analyses. It can be helpful for site preparation (Mason, 2013) or projecting future scenarios under climate change, as this approach offers within-year growth changes (Mason et al., 2011).

Table 6.1 Data used in different modelling approaches.

<i>Component</i>	<i>Approach</i>		
	<i>Time-based augmented</i>	<i>PULSE</i>	<i>Augmented PULSE</i>
Height (h_T)	Age	LAI _T	LAI _T
	Climatic variables	LAI _g	LAI _g
	Topographic variables	Soil rooting depth	Soil rooting depth
	Soil variables	PSP position	PSP position
		Intercepted radiation	Intercepted radiation
		Temperature	Temperature
		Rain	Rain
			Topographic variables
Survival proportion (S)	Age	LAI _T	LAI _T
	Climatic variables	LAI _g	LAI _g
	Topographic variables	Soil rooting depth	Soil rooting depth
	Soil variables	PSP position	PSP position
		Intercepted radiation	Intercepted radiation
		Temperature	Temperature
		Rain	Rain
			Topographic variables

6.3.3 Precision and bias

The results from the various approaches differed with respect to precision and bias and were also species dependent (Table 6.2, Figure 6. 3 and Figure 6.4).

Statistically, height (h_T) was best predicted by the augmented PULSE model for both species (Table 6.2). The lowest RMSE, which indicates the precision of models, was reported from the augmented PULSE models. This was also true for bias. However, in Figure 6. 3- B1, it can be shown that the PULSE model residual for *E. bosistoana* height was the best in terms of homogeneity and distribution, although the augmented PULSE model (Figure 6. 3- C1) had a narrower range of distribution. *E. globoidea* height, on the other hand, was best predicted by augmented PULSE, and this was confirmed statistically and graphically (Figure 6. 3- C2).

Survival proportion (S) differed between approaches and species. For *E. bosistoana* survival proportion was statistically best predicted by the PULSE model, whereas for *E. globoidea*, survival was best predicted by the augmented time-based model (Table 6.2). This was also confirmed by the graphical presentation (Figure 6.4).

The magnitude of improvement from augmented PULSE modelling of juvenile height was satisfactory, in terms of precision and bias. On the other hand, survival proportion was not improved much by adding this extra data.

Table 6.2 Comparison of precision, bias and performance of the different approaches. Bold faces show the best values in the group.

Species	Component	Approach					
		Augmented time-based		PULSE		Augmented PULSE	
		RMSE	MAE	RMSE	MAE	RMSE	MAE
<i>E. bosistoana</i>	Height (h_T)	1.966	1.579	1.414	1.056	1.330	1.019
	Survival (S)	0.291	0.237	0.127	0.082	0.133	0.086
<i>E. globoidea</i>	Height (h_T)	1.883	1.546	1.625	1.216	1.586	1.187
	Survival (S)	0.130	0.103	0.233	0.185	0.231	0.183

In previous studies, height growth was not much improved by a hybrid approach (Mason et al., 2011; Pinjuv, 2006; Snowdon et al., 1999), whereas for this study modelled height was improved considerably. This may be influenced by the stand age or species. In this case, it was a juvenile broadleaf plantation stand, whereas all known comparative studies are mature conifer stands, more specifically *Pinus radiata* or *Pinus taeda*. However, a similar method of time-based augmentation was applied and found efficient for *Pinus radiata* in New Zealand (Woollons et al., 1997) and *Eucalyptus grandis* in Uruguay (Casnati, 2016). Smaller gains in precision and bias between different approaches can result from several sources. Casnati (2016) reported that this is most likely related to asymptote modifiers.

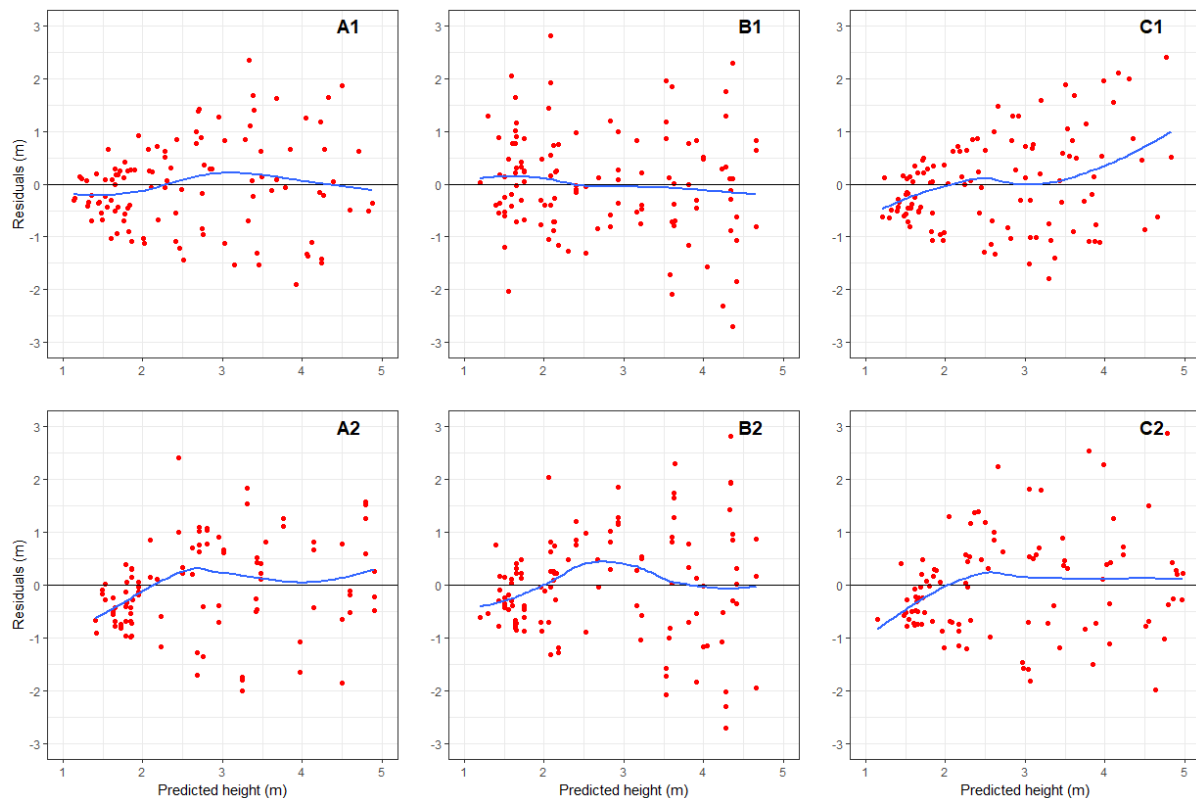


Figure 6. 3 Comparison of three different height model approaches based on residual against predicted values: A) augmented time-based model; B) simple PULSE; and C) augmented PULSE. 1) *E. bosistoana*, and 2) *E. globoidea*.

Modelling survival proportion is complex, especially for juvenile crops. This may be a result of several factors, which include site characteristics. In a study of a similar nature, Mason et al. (2007) collected detailed data about the weeds, different treatments and the nature of

competition that trees experienced. There were no such data for this study, which may have limited the performance of the survival proportion model. In addition, information obtained about soils from the FSL layers was coarse, and Pearse et al. (2015) reported that it could be markedly incorrect in some places, which may affect the water balance model; hence the soil data was not considered to be precise enough. Mason et al. (2011) reported that establishing a fully modified PULSE model can be unreliable without a precise water balance model.

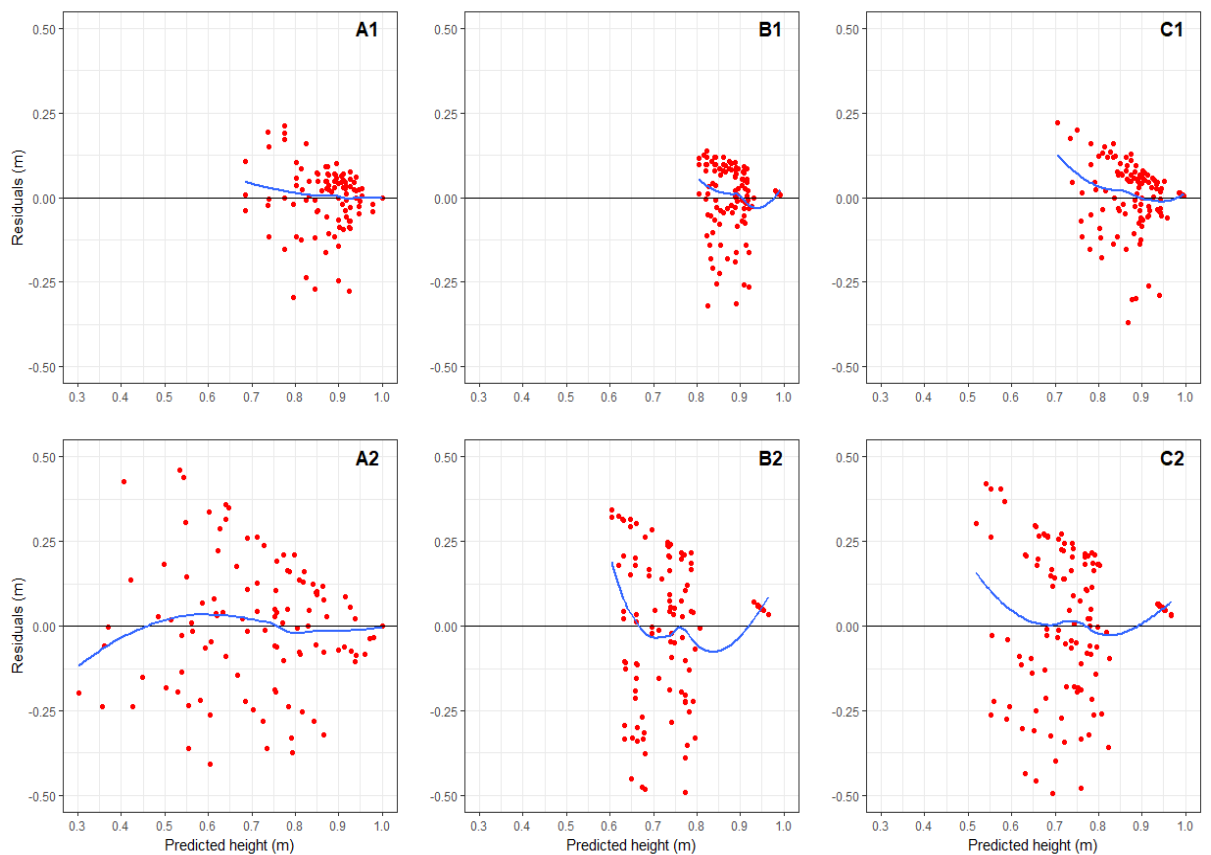


Figure 6.4 Comparison of three different survival proportion model approaches based on residual against predicted values: A) augmented time-based model; B) simple PULSE; and C) augmented PULSE. 1) *E. bosistoana*, and 2) *E. globoidea*.

6.3.4 System integration

Both augmentation processes were well integrated within the system. Furthermore, PULSE and augmented PULSE provided extra information and explanation about growth processes without breaking any mensurational modelling rules. For example, these models

were all path invariant and non-recursive. The PULSE approaches were a coherent synthesis of the traditional approach, but they provided more information at the same time. They also provided a framework for testing climate change within the system and gave an implicit estimation of within-year patterns, as the PULS is estimated in monthly time steps. These findings were in line with previous studies for both mature and juvenile plantations (Casnati, 2016; Mason et al., 2007; Mason et al., 2018; Mason et al., 2011).

6.4 Conclusion

This study explicitly compared three different hybrid modelling approaches and reported each of their pros and cons, based on experimented results. The augmented PULSE approach showed better results for height yield prediction, though it was not better than using time-based models for representing survival proportion.

The precision and bias between models varied within a marginal limit. However, based on the given information and explanatory ability, the PULSE modelling framework stands out from the traditional time-based system. It was simple enough to integrate into the system, and it uses very basic direct input. However, those inputs need to be precise enough to obtain a satisfactory result, which may be a major limitation for the PULSE approach to be applied in the field. Finally, all three approaches can be applied for juvenile plantation in any given site-specific case, based on available data and management demands.

6.5 References

- Casnati, A. C. R. (2016). *Hybrid mensurational-physiological models for Pinus taeda and Eucalyptus grandis in Uruguay*. (PhD), University of Canterbury, New Zealand.
- Gunawardena, J. J. B. B. (2014). Models in biology: 'accurate descriptions of our pathetic thinking'. *12*(1), 29. doi:10.1186/1741-7007-12-29
- Kimmins, J., Brunner, A., & Mailly, D. (1996). *Modeling the sustainability of managed forests: hybrid ecosystem simulation modeling from individual tree to landscape*. Paper presented at the Proceedings of the Society of American Foresters National Convention.
- Landsberg, J. J., & Sands, P. J. (2011). *Physiological ecology of forest production: principles, processes and models* (Vol. 4): Elsevier/Academic Press.
- Mason, E., Rose, R., & Rosner, L. (2007). Time vs. light: a potentially useable light sum hybrid model to represent the juvenile growth of Douglas-fir subject to varying levels of competition. *Canadian Journal of Forest Research*, *37*(4), 795-805.
- Mason, E. G. (2013). Linking hybrid mensurational/eco-physiological growth and yield models with crop establishment: a replacement for time gain analysis. *New Forests*, *44*(6), 951-959. doi:10.1007/s11056-013-9387-3
- Mason, E. G., Holmström, E., & Nilsson, U. (2018). Using hybrid physiological/mensurational modelling to predict site index of *Pinus sylvestris* L. in Sweden: a pilot study. *Scandinavian Journal of Forest Research*, *33*(2), 147-154. doi:10.1080/02827581.2017.1348539
- Mason, E. G., Methol, R., & Cochrane, H. (2011). Hybrid mensurational and physiological modelling of growth and yield of *Pinus radiata* D. Don. using potentially useable radiation sums. *Forestry*, *84*(2), 99-108. doi:10.1093/forestry/cpq048
- Mátyás, C., Bozic, G., Gömöry, D., Ivankovic, M., & Rasztoivits, E. (2009). Juvenile growth response of European beech (*Fagus sylvatica* L.) to sudden change of climatic environment in SE European trials. *iForest - Biogeosciences and Forestry*, *2*(6), 213-220. doi:10.3832/ifor0519-002
- Monserud, R. A. (2003). Evaluating forest models in a sustainable forest management context. *Forest Biometry, Modelling and Information Sciences*, *1*(1), 35-47.
- Pearse, G., Moltchanova, E., & Bloomberg, M. (2015). Assessment of the accuracy of profile available water and potential rooting depth estimates held within New Zealand's fundamental soil layers geo-database. *Soil Research*, *53*(7), 737-744. doi:https://doi.org/10.1071/SR14012

- Peng, C., Liu, J., Dang, Q., Apps, M. J., & Jiang, H. (2002). TRIPLEX: a generic hybrid model for predicting forest growth and carbon and nitrogen dynamics. *Ecological Modelling*, 153(1–2), 109-130. doi:[http://dx.doi.org/10.1016/S0304-3800\(01\)00505-1](http://dx.doi.org/10.1016/S0304-3800(01)00505-1)
- Pinjuv, G., Mason, E. G., & Watt, M. (2006). Quantitative validation and comparison of a range of forest growth model types. *Forest Ecology and Management*, 236(1), 37-46. doi:<http://dx.doi.org/10.1016/j.foreco.2006.06.025>
- Pinjuv, G. L. (2006). *Hybrid forest modelling of Pinus Radiata D. Don in Canterbury, New Zealand*. (PhD), University of Canterbury, New Zealand.
- Rauscher, H., Isebrands, J., Host, G., Dickson, R., Dickmann, D., Crow, T., & Michael, D. (1990). ECOPHYS: an ecophysiological growth process model for juvenile poplar. *Tree Physiology*, 7(1-2-3-4), 255-281.
- Snowdon, P., Jovanovic, T., & Booth, T. H. (1999). Incorporation of indices of annual climatic variation into growth models for *Pinus radiata*. *Forest Ecology and Management*, 117(1), 187-197.
- Weiskittel, A. R., Hann, D. W., Kershaw, J. A., & Vanclay, J. K. (2011). *Forest Growth and Yield Modeling*: Wiley.
- Woollons, R. C., Snowdon, P., & Mitchell, N. D. (1997). Augmenting empirical stand projection equations with edaphic and climatic variables. *Forest Ecology and Management*, 98(3), 267-275. doi:[http://dx.doi.org/10.1016/S0378-1127\(97\)00090-X](http://dx.doi.org/10.1016/S0378-1127(97)00090-X)

7

A preliminary growth and yield model for *Eucalyptus globoidea* plantations in New Zealand

7. A preliminary growth and yield model for mature *Eucalyptus globoidea* plantations in New Zealand

7.1 Introduction

The New Zealand forestry industry is almost entirely (90%) based on *Pinus radiata* plantations (NZFOA, 2017). However, there are opportunities to introduce new species and overcome the limitations of *Pinus radiata* (Millen et al., 2018). *Eucalyptus* species are considered to be an alternative, including dryland *Eucalyptus*, which can survive in dry conditions as well as produce high-quality timber (Menzies, 1995). However, despite strong advocacy for alternative species, including *Eucalyptus*, the area being planted remains small ($\geq 1\%$) (Maclaren, 2005; NZFOA, 2017). This is because growing *Eucalyptus* in New Zealand has, over the years, been challenging (Berrill & Hay, 2005; Berrill & Hay, 2006) as they have site-specific requirements (Bell & Williams, 1997; Williams & Woinarski, 1997), pests and diseases that affect their health and productivity (Lin, 2017), and the market for *Eucalyptus* wood products was unrecognised (Apiolaza et al., 2011). Recently the situation has started to change as a result of the New Zealand Dryland Forest Initiative (NZDFI), which introduced several ground-durable dryland *Eucalyptus* species as alternatives for ex-pasture lands (NZDFI, 2013). *Eucalyptus globoidea* was one of the top-ranked *Eucalyptus* species in the NZDFI programme for its desirable properties (Nicholas & Millen, 2012b), for example, highly durable heartwood.

A managed forest is a dynamic biological system that continuously changes as a response to natural variations as well as to silvicultural practices. Therefore, it is essential to explore current and future forest dynamics through growth and yield models in order to make effective decisions (Blake et al., 1990; Blanco et al., 2005; Castedo-Dorado. et al., 2007; Clutter et al., 1983). The first generation of models, namely mensurational-statistical models, give little information about the mechanisms of forest dynamics, but provide robust growth predictions (Korzukhin et al., 1996). Moreover, forest growth models are often based on large datasets,

compiling long-term field measurements (Castedo-Dorado et al., 2007; Pienaar & Rheney, 1995) or sophisticated databases, for example, information obtained from remote sensing data (Battaglia et al., 2004; Landsberg et al., 2003).

However, in scenarios where comprehensive data is not available, it may still be desirable to forecast forest growth (Vanclay, 2010). Generally, in data-poor situations, preliminary models can still be developed for new species (Berrill et al., 2007; Kitikidou et al., 2016; Palahí & Grau, 2003). Vanclay (2010) proposed a single parameter robust method for this type of situation. Such models are often inaccurate but may be useful (Box, 1976) to obtain an initial forecast.

Eucalyptus species were planted all over New Zealand in a scattered way, sometimes to satisfy research needs or to pursue the personal interests of farmers. Preliminary and indicative models are available for *Eucalyptus fastigata*, *E. nitens*, and overall stringy-bark groups in New Zealand (Berrill & Hay, 2005; Berrill & Hay, 2006). So, to have a preliminary stand-level model to describe all stand attributes for *E. globoides* is a complementary advancement.

This chapter outlines the development of a stand-level *E. globoides* growth and yield model that describes several important attributes. In particular, mean top height (MTH), basal area (G), maximum diameter at breast height (D_{max}), standard deviation of diameter (SD_D), stand volume (V), self-thinning and height-diameter relationship (H-D). They were developed with available data using a traditional mensurational modelling approach.

7.2 Materials and methods

7.2.1 Data preparation and description

Stand-level *E. globoides* plantation data were available from SCION's (the former New Zealand Forest Research Institute) permanent sample plot system (Pilaar & Dunlop, 1990).

Data from 29 permanent sample plots (PSPs) in ten different localities were available (Table 7.1 and Figure 7.1).

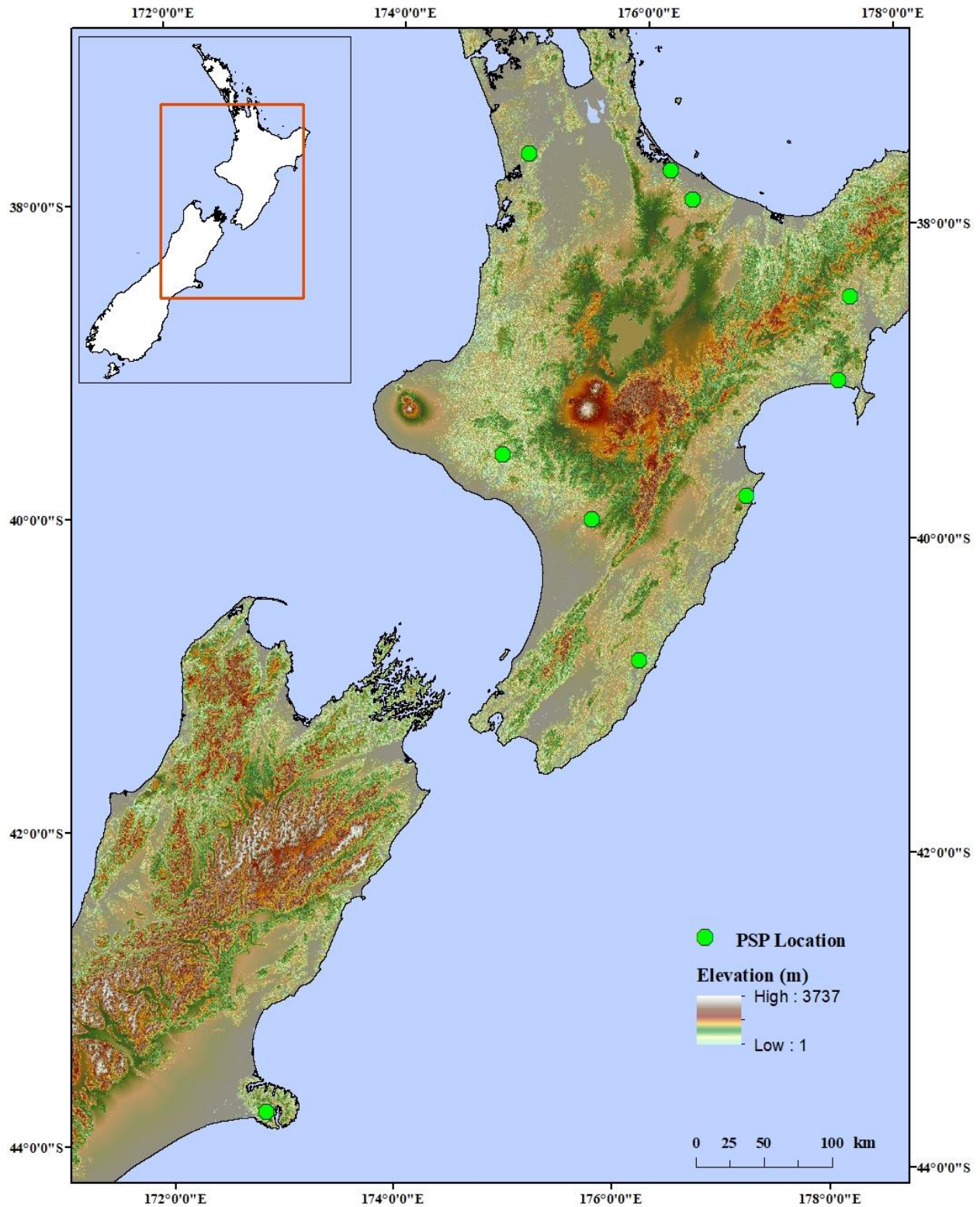


Figure 7.1 Permanent sample plot (PSP) locations and topography.

Table 7. 1 Summary of the variables used for modelling.

Variable	Unit	Statistical summary of variable			
		Mean	Min.	Max.	SD
Plot size	ha	0.06	0.04	0.10	0.02
Age (t)	Years	13.84	3.15	24.85	5.90
Individual tree height (h)	m	12.90	0.10	39.80	9.05
Mean top height (MTH)	m	18.98	3.50	28.80	7.05
Diameter at breast height at 1.4m (DBH)	cm	22.90	0.10	62.30	14.49
Max DBH (D_{max})	cm	39.79	5.40	62.30	13.66
Basal area (G)	m^2ha^{-1}	30.59	0.54	77.88	18.84
Volume (V)	$m^3 ha^{-1}$	161.34	0.40	538.60	130.09
Standard deviation of diameter (SD_D)	cm	5.34	1.35	11.86	2.20
Stocking (N)	stems ha^{-1}	496.99	141.09	1375	317.33
Altitude (Alt)	m	211.70	80	300	100.41
Slope	(°)	23.27	8	42	13.06

Trees were measured from the PSPs at 1 to 10-year intervals with an irregular frequency. Mean top height (MTH) and maximum diameter (D_{max}) of the trees were calculated from the individual tree measurements by following the procedure proposed by Goulding (2005). The standard deviation of DBH (SD_D) was calculated for each PSP. Basal area (G) was calculated as the sum of cross-sectional area at breast height (1.4m), and then this was divided by plot size to provide a per hectare estimate. Stand volume (V) was calculated for each measurement within each sample plot.

The original data were organised to fit both yield and difference equations. The stand level summary data was organised by representing all possible measurement time interval. This equal interval data was used to fit the differential equations. The stand level summary data organised in simple time increment was used to fit stand volume equations. The individual tree measurement data from all stand used to develop a height-diameter relationship.

7.2.2 Modelling and evaluation

The algebraic difference approach (ADA) (Bailey & Clutter, 1974) was applied for modelling mean top height (MTH), basal area (G), maximum diameter (D_{\max}) and standard deviation of diameter (SD_D). Well known and frequently-used polymorphic and anamorphic forms of difference equations (Bailey & Clutter, 1974; Belli & Ek, 1988; Ek, 1974; Vanclay, 1994; Zeide, 1993) (

Table 7.2) were tested by fitting non-linear least-squares (Clutter, 1963), to find the best fitted model based on their residuals distribution and fitting statistics (e.g. RMSE, SE).

Table 7.2 Different forms of difference equations.

	Generic name	Expression	No.
Polymorphic form	Schumacher 1	$Y_2 = e^{\ln(Y_1)(\frac{t_1}{t_2}) + \alpha(1 - \frac{t_1}{t_2})}$	53
	Schumacher 2	$Y_2 = e^{\ln(Y_1)(\frac{t_1}{t_2})^\gamma + \alpha[1 - (\frac{t_1}{t_2})^\gamma]}$	54
	Gompertz 1	$Y_2 = e^{\ln(Y_1)e^{-\beta(t_2-t_1)} + \alpha[1 - e^{-\beta(t_2-t_1)}]}$	55
	Gompertz 2	$Y_2 = e^{\ln(Y_1)e^{-\beta(t_2-t_1) + \gamma(t_2^2 - t_1^2)} + \alpha[1 - e^{-\beta(t_2-t_1) + \gamma(t_2^2 - t_1^2)}]}$	56
	Weibull 1	$Y_2 = Y_1 e^{-\beta(t_2^\gamma - t_1^\gamma)} + \alpha[1 - \beta(t_2^\gamma - t_1^\gamma)]$	57
	Weibull 2	$Y_2 = \alpha - \beta(\frac{\alpha - Y_1}{\beta}) (\frac{t_2}{t_1})^\gamma$	58
	Hossfeld	$Y_2 = \frac{1}{\frac{1}{Y_1} (\frac{t_2}{t_1})^\beta + \alpha[1 - (\frac{t_2}{t_1})^\beta]}$	59
	Von Bertalanffy-Richards 1	$Y_2 = \alpha (\frac{Y_1}{\alpha})^{\frac{\ln[1 - e^{-(\beta t_2)}]}{\ln[1 - e^{-(\beta t_1)}]}}$	60
	Von Bertalanffy-Richards 2	$Y_2 = \alpha \{1 - [1 - (\frac{Y_1}{\alpha})^{1-\vartheta}] (\frac{t_2}{t_1})^{\frac{1}{1-\vartheta}}\}$	61
	Von Bertalanffy-Richards 3	$Y_2 = \alpha \{1 + [(\frac{\alpha}{Y_1})^\vartheta - 1] e^{-\beta(t_2 - t_1)}\}^{\frac{1}{\vartheta}}$	62
Anamorphic form	Schumacher A1	$Y_2 = Y_1 e^{-\beta(\frac{1}{t_2} - \frac{1}{t_1})}$	63
	Schumacher A2	$Y_2 = Y_1 e^{-\beta[(\frac{1}{t_2})^\gamma - (\frac{1}{t_1})^\gamma]}$	64
	Gompertz	$Y_2 = Y_1 \frac{e^{-\beta e^{-\gamma t_2}}}{e^{-\beta e^{-\gamma t_1}}}$	65
	Von Bertalanffy-Richards	$Y_2 = Y_1 \left[\frac{1 - e^{-\beta t_2}}{1 - e^{-\beta t_1}} \right]^\gamma$	66
	Weibull	$Y_2 = Y_1 \frac{1 - e^{-\beta t_2}^\gamma}{1 - e^{-\beta t_1}^\gamma}$	67
	Hossfeld	$Y_2 = \frac{1}{\frac{1}{Y_1} + \beta(\frac{1}{t_2})^\gamma - (\frac{1}{t_1})^\gamma}$	68

Stand volume yields (V) were modelled by testing various simple, established and commonly used functions (Table 7.3), and height yield (H-D) models were created by fitting the Näslund (1936) equation with an exponent, -2, represented as:

$$H = 1.4 + \left(\alpha + \frac{\beta}{D}\right)^{-2} \quad (69)$$

where H is tree height (m), D is diameter (cm) at breast height (1.4m), and α and β are regressions coefficients. The exponent term here is changeable. This function is widely used and can be conveniently expressed in a linear form:

$$\frac{D}{(H-1.4)^{0.4}} = \alpha \times D + \beta \quad (70)$$

A height-diameter relationship can be local at a plot level (Curtis, 1967; Garcia, 1974) or stand level (Zhao, 1999) when few plots are sampled. Therefore, a better height-diameter relationship can be obtained by identifying and incorporating relevant factors accounting for differences among the stands in the sites (Zhao, 1999). This was achieved by separating and linearly expanding the regression coefficients with the relevant factors described previously in Chapters 3 and 4.

Table 7.3 Volume equations.

Expression	Reference	No.
$V = \alpha \times G \times MTH$	(Soalleiro, 1995)	71
$V = G \times MTH^{(\alpha+\beta t)}e^{(\gamma+\delta t)}$	(Jansen et al., 1996)	72
$V = G \times \left(\alpha + \frac{\beta}{MTH}\right)$	(Burkhart, 1977)	73
$V = e^{(\alpha+\beta \log MTH)+\gamma \log G}$	(Candy, 1989)	74

Due to the small number of plots, a conceptual self-thinning/mortality model was established by applying Reineke's stand density index (SDI) approach (Reineke, 1933). This was done by estimating quadratic mean diameter at breast height (DBH) and basal area (G).

All the models except self-thinning were evaluated through the validation procedure described in Chapter 4, which included a full set of visual analyses of residuals, model projection plot as well as RMSE, SE, MAE, BIAS, MAPRESS, MPRESS and adjusted R^2 . Adjusted R^2 were not considered for assessing difference equations.

7.3 Results

7.3.1 Mean top height (MTH) model

The first Von-Bertalanffy Richards polymorphic model (Equation 60) exhibited the most precise fitting statistics. It had minimum bias and the lowest standard error of prediction compared to the other models tested. However, the RMSE and MAE were higher in model fitting statistics, which reduced during validation to 3.852 and 2.512 respectively (Table 7.4). The model residuals were well distributed with minor heteroscedasticity at the beginning of the modelling period. The model was fitted over the measured data by covering all the MTH ranges, although there were a couple of measurements that stood out from the fitting line (Figure 7.2).

Table 7.4 Mean top height (MTH) model fitting and validation statistics.

<i>Action</i>	<i>RMSE</i>	<i>MAE</i>	<i>BIAS</i>	<i>SE</i>	<i>AICc</i>	<i>MPRESS</i>	<i>MAPRESS</i>
Fitting	7.185	5.467	-1.777	1.116	701.226	-	-
Validation	3.852	2.512	0.066	1.112	645.430	0.009	0.946

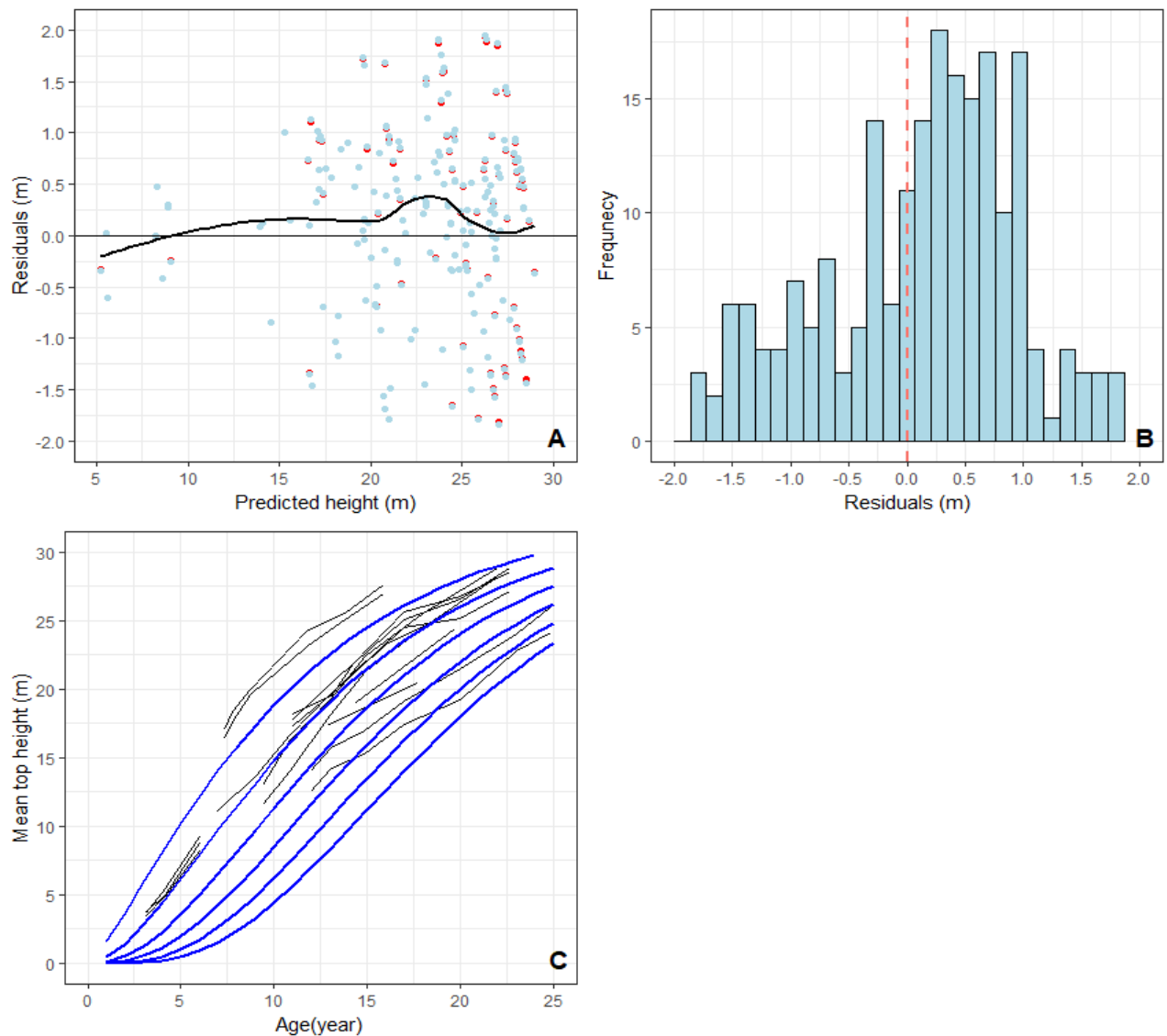


Figure 7.2 Mean top height (MTH) model results: A) Residuals against prediction plot of first Von Bertalanffy-Richards polymorphic equation, light blue points represent model fitting, red points indicate validation residuals, and model fit is shown by the black line; B) Residuals frequency distribution, red dashed line shows the mean; and C) Model fit (blue lines) over measured MTH (thin black lines).

7.3.2 Basal area (G) model

Among tested models, the anamorphic Schumacher model (Equation 63) was found to be the best fitted for basal area prediction. This model had the lowest error and greatest precision. Precision increased during validation with much less error (Table 7.5). The residual plot exhibited minor heteroscedasticity. The residuals distribution was positively biased, which

indicated a slight overprediction. Moreover, the model predicted basal area covering the measured range, except for two stands (Figure 7.3).

Table 7.5 Basal area (G) model fit and validation statistics.

<i>Action</i>	<i>RMSE</i>	<i>MAE</i>	<i>BIAS</i>	<i>SE</i>	<i>AIC_c</i>	<i>MPRESS</i>	<i>MAPRESS</i>
Fitting	25.303	21.250	2.893	6.893	746.594	-	-
Validation	13.431	9.988	0.653	6.800	704.571	1.054	0.841

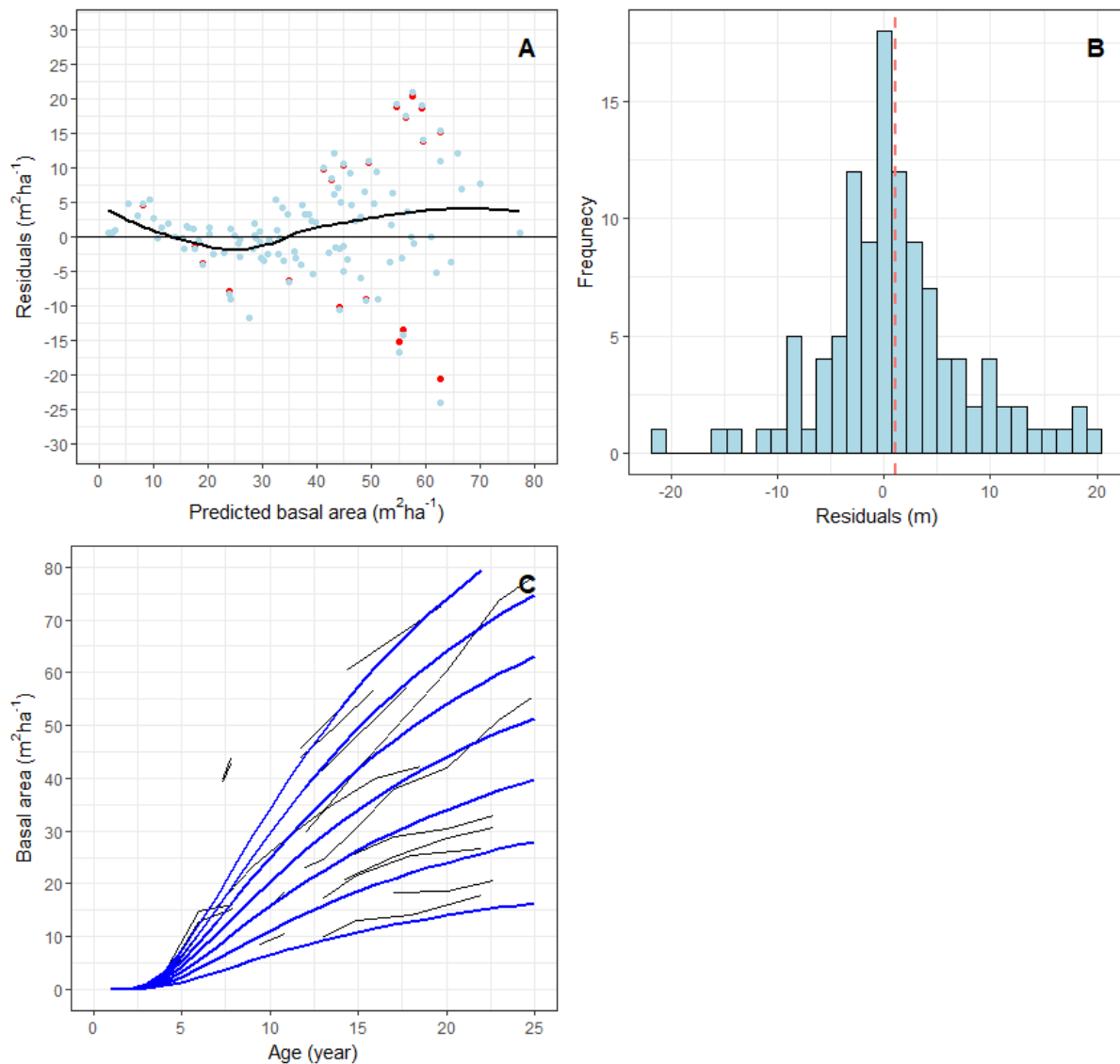


Figure 7.3 Basal area (G) model results: A) Residuals against prediction plot of first Schumacher anamorphic equation, light blue points represent model fitting, the red points indicate validation residuals, and model fit is shown by the black line; B) Residuals frequency distribution, red dashed line shows the mean; and C) Model fit (blue lines) over measured G (thin black lines).

7.3.3 Maximum diameter (D_{\max}) model

The Hossfeld polymorphic model (Equation 59) predicted the maximum diameter (D_{\max}) with most overall precision and least bias in comparison with other models. In this case, RMSE and MAE increased from fitting to validation statistic, and bias went from positive to negative. However, the standard error (SE) reduced slightly for validation compared with fit statistics. The low MPRESS and MAPRESS values also presented model goodness-of-fit (Table 7.6). The residuals plot showed high bias at the beginning and end of the modelling period, though the residuals frequency distribution was normal. The predicted D_{\max} plot covered all the measurements reasonably well (Figure 7.4).

Table 7.6 Maximum diameter (D_{\max}) model fitting and validation statistics.

<i>Action</i>	<i>RMSE</i>	<i>MAE</i>	<i>BIAS</i>	<i>SE</i>	<i>AICc</i>	<i>MPRESS</i>	<i>MAPRESS</i>
Fitting	2.400	1.759	0.054	2.411	1052.299	-	-
Validation	6.699	4.681	-0.061	2.388	973.322	0.059	0.932

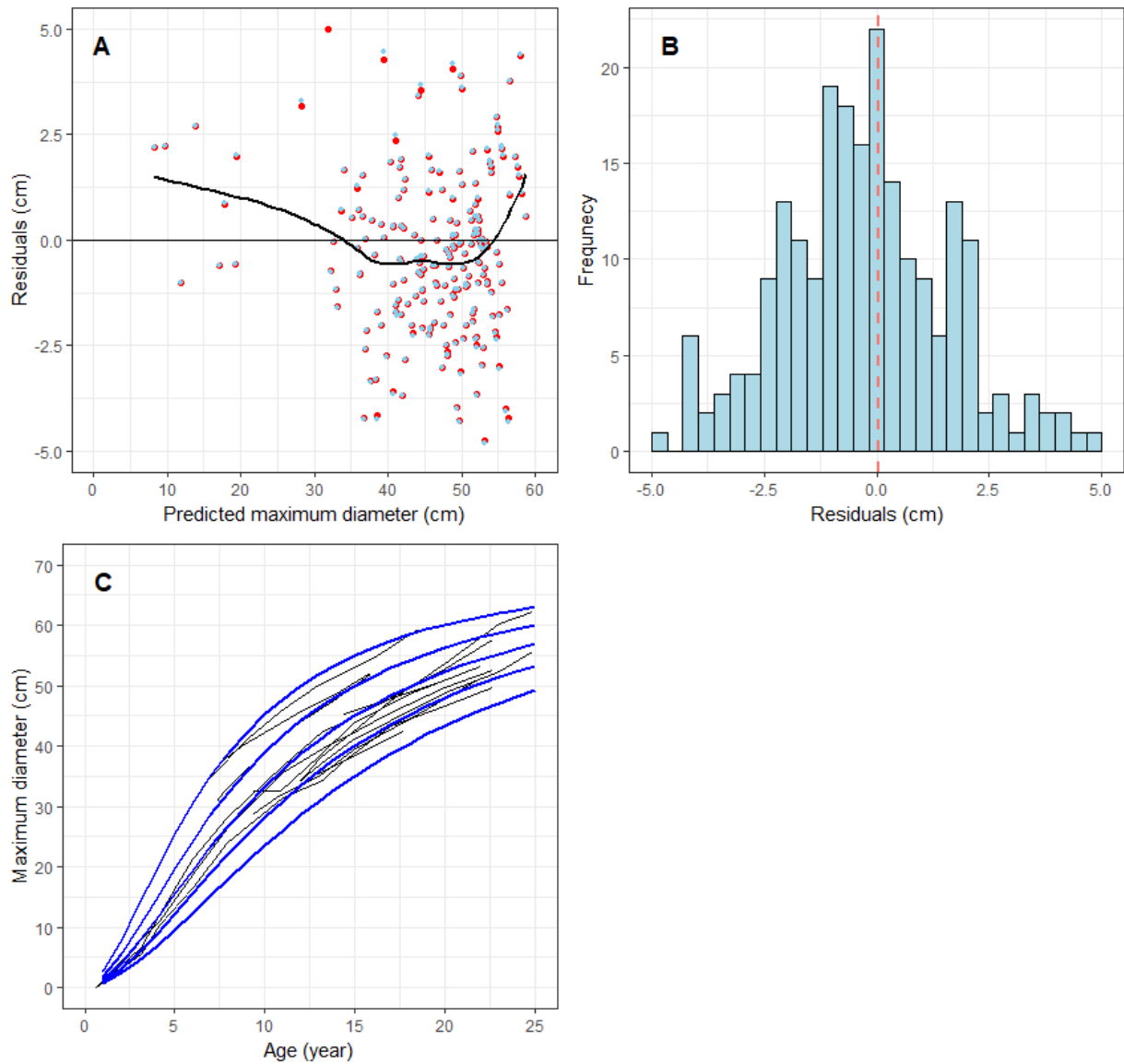


Figure 7.4 Maximum diameter (D_{max}) model results: A) Residuals against prediction plot of Hossfeld polymorphic equation, light blue points represent model fitting, the red points indicate validation residuals, and the model fit is shown by the black line; B) Residuals frequency distribution, red dashed line shows the mean; and C) Model fit (blue lines) over measured D_{max} (thin black lines).

7.3.4 Standard deviation of diameter (SD_D) model

Among all the models, the standard deviation of diameter (SD_D) was best predicted by the second Schumacher polymorphic model (Equation 54). The model showed minimum fitting statistics with the least prediction errors. The statistics increased slightly from fitting to validation. Besides, the model goodness-of-fit confirmed by MPRESS and MAPRESS (Table 7.7).

Table 7.7 Standard deviation of DBH (SD_D) model fitting and validation statistics.

<i>Action</i>	<i>RMSE</i>	<i>MAE</i>	<i>BIAS</i>	<i>SE</i>	<i>AICc</i>	<i>MPRESS</i>	<i>MAPRESS</i>
Fitting	1.571	1.224	0.412	1.577	915.086		-
Validation	1.959	1.513	0.337	1.569	843.225	0.407	0.596

Graphically, the model was well predicted, and residuals showed normal tendencies. The residuals plot shows overprediction and positive bias of the model with few outliers in the frequency distribution plot. The prediction plot shows that the model included the full range of measured SD_D (Figure 7.5).

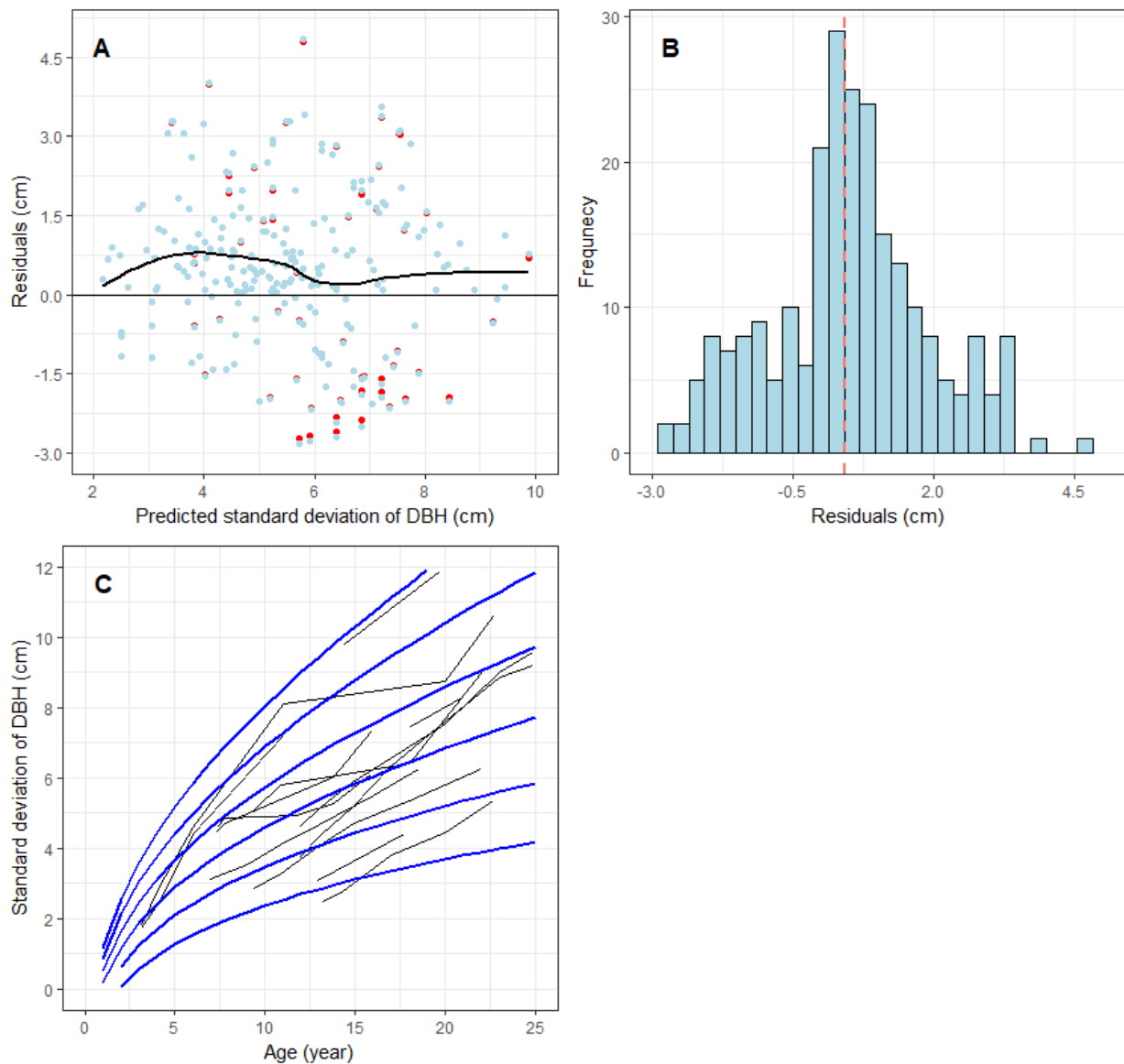


Figure 7.5 Maximum diameter (D_{max}) model results: A) Residuals against prediction plot of Hossfeld polymorphic equation, light blue points represent model fitting, the red points indicate validation residuals, and the model fit is shown by the black line; B) Residuals frequency distribution, red dashed line shows the mean; and C) Model fit (blue lines) over measured SD_D (thin black lines).

7.3.5 Stand volume (V) model

The most satisfactory volume yield model was a four parameter one (Equation 72) by Jansen et al. (1996). The fitting statistics represented minimal prediction error and precision, though validation statistics were greater in both cases. The small MPRESS and MAPRESS confirmed the precision of the model (Table 7.8). These results are also confirmed by the

graphical presentation. Although, residuals against predicted plot displayed minor heteroscedastic tendency (Figure 7.6).

Table 7.8 Stand volume(V) model fitting and validation statistics.

Action	RMSE	MAE	BIAS	SE	AICc	MPRESS	MAPRESS
Fitting	39.122	27.983	-1.102	40.5	621.002	-	-
Validation	140.959	89.827	-0.582	39.413	569.752	-0.845	0.868

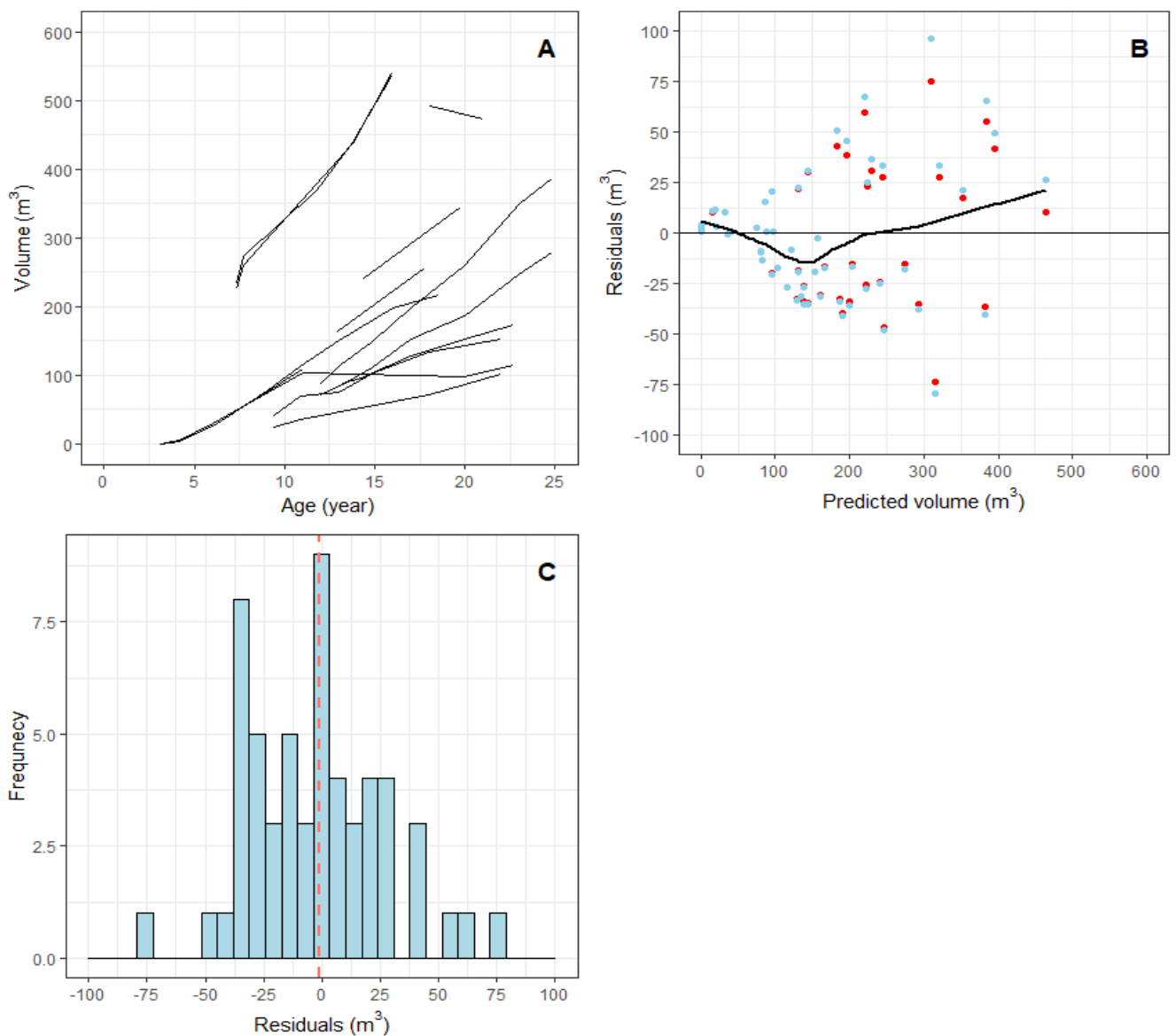


Figure 7.6 Stand volume (V) model results: A) Estimated stand volume from measured data; B) Residuals against prediction plot, light blue points represent model fitting, red points indicate validation residuals, and model fit is shown by the black line; and C) Residuals frequency distribution, red dashed line is shown the mean.

7.3.6 Height diameter (H-D) model

The stand-specific individual height-diameter (H-D) model showed precise prediction (Equation 75). Stand-specific altitude (Altitude), and basal area (G) were found to influence the H-D relationship significantly ($P < 0.05$) and adding them into the final model improved the prediction accuracy of the model. The goodness-of-fit values increased slightly from fitting to validation statistics (Table 7.9). The residuals plot showed a normal distribution, and the model fitted well. The frequency of residuals distribution also showed similar normal attributes (Figure 7.7).

$$H = 1.4 + ((\alpha_0 + \alpha_1 \times \text{Altitude}) + \frac{(\beta_0 + \beta_1 \times G)}{D})^{-2} \quad (75)$$

Table 7.9 Height-diameter relationship (H-D) model fitting and validation statistics.

<i>Action</i>	<i>RMSE</i>	<i>MAE</i>	<i>BIAS</i>	<i>SE</i>	<i>AICc</i>	<i>MPRESS</i>	<i>MAPRESS</i>
Fitting	3.080	2.418	-0.001	3.101	1567.12	-	-
Validation	4.374	3.375	-0.020	3.222	1350.955	-0.001	0.530

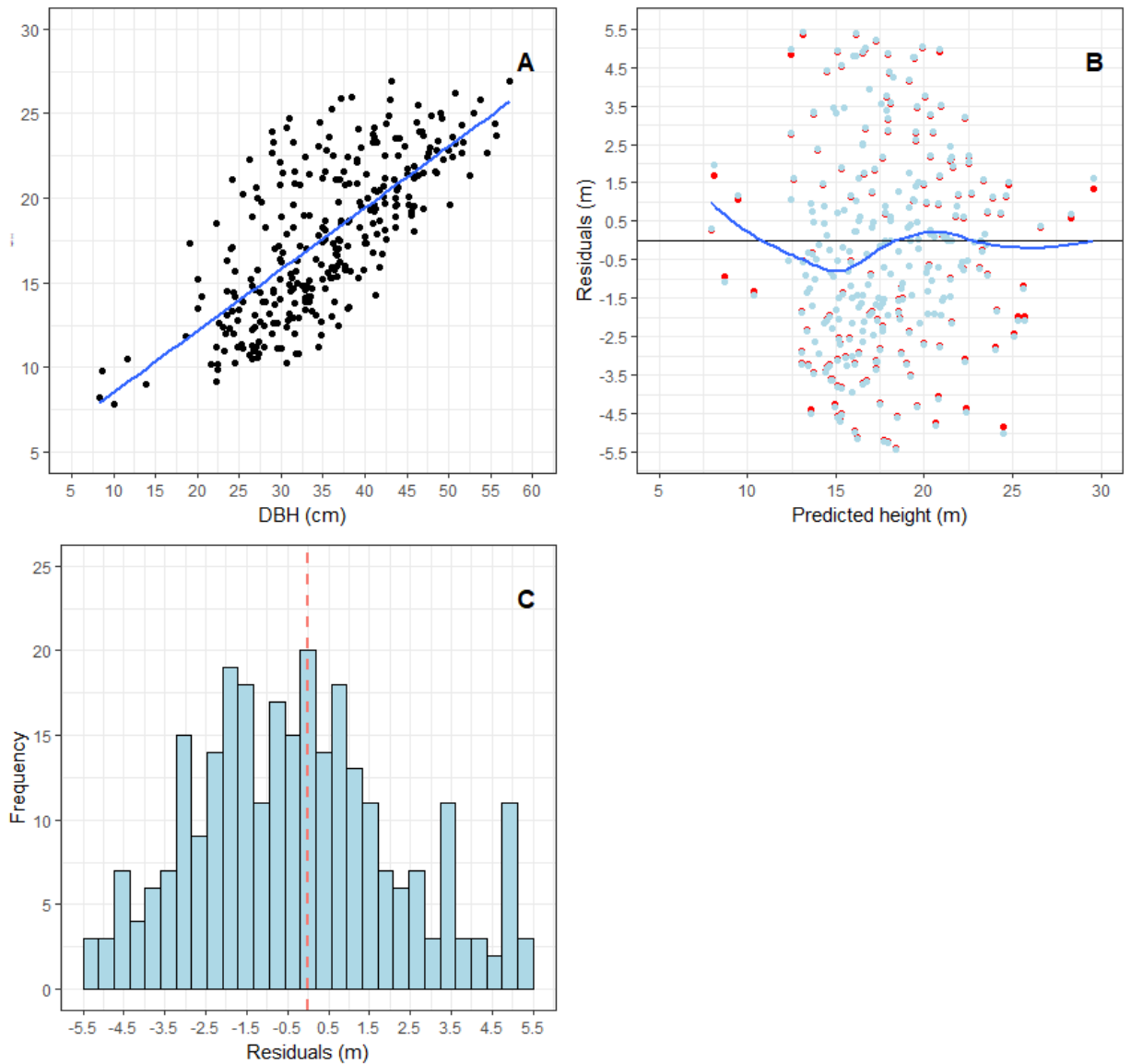


Figure 7.7 A) Measured height-diameter (H-D), blue line shows the linear trend; B) Residuals against prediction plot, light blue points represent model fitting, red points indicate validation residuals, model fit is shown by the blue line; and C) Residuals frequency distribution, red dashed line is shown the mean.

7.3.7 Self-thinning model

The self-thinning model was developed using Reineke's SDI method, and the result showed a precise fit for the data. Stocking ranged from 150-1350 stems ha^{-1} . The trees started to die when they approached 100% of the maximum stocking. Highest stocking frequency showed at 400-650 stems ha^{-1} (Figure 7.8).

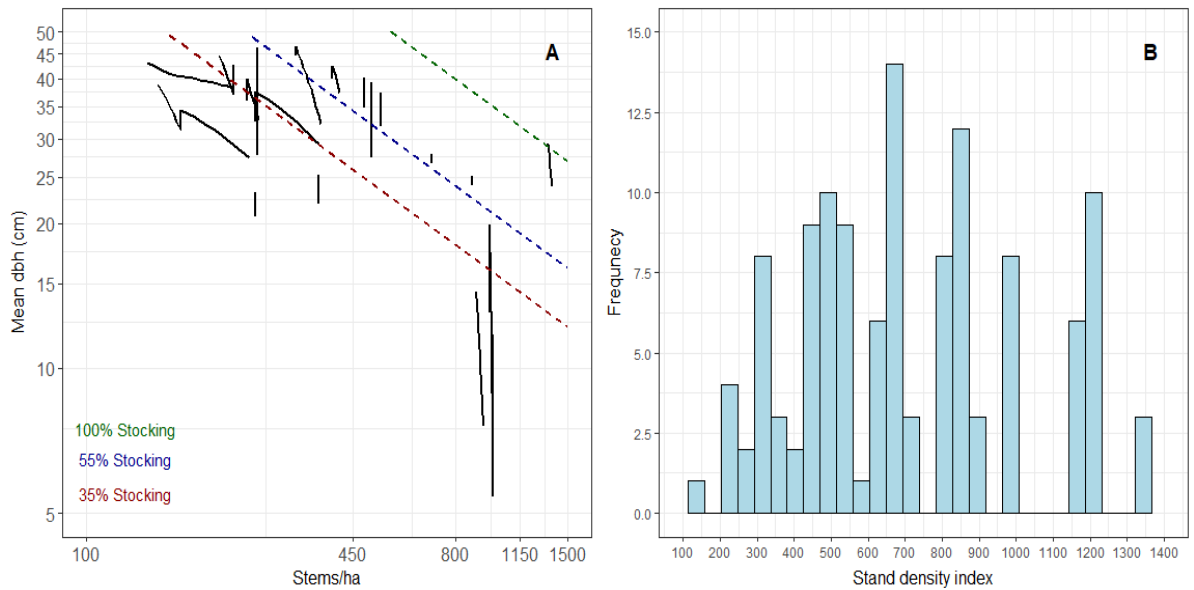


Figure 7.8 A) Reineke's SDI curve represented with self-thinning lines and A) SDI distribution plot.

7.4 Discussion

This study developed and demonstrated a preliminary set of mature stand growth and yield models for *E. globoidea* in New Zealand using sparsely available data. The state of a stand was adequately described by the following state variables: mean top height, basal area, volume yield, stocking, maximum diameter, standard deviation of DBH and the height-diameter relationship. The nature of the scheme is described by the rate of change of these variables over time by their corresponding transition function. All the transitional functions used have a theoretical basis. These models presented in this study fulfil the basic modelling assumptions, being path invariant and having no logical circular issues in prediction.

The final models were the best-fitted models, which generally had the highest accuracy among the tested set of equations from several differential forms. There were some errors in model prediction, which may be due to the irregular measurement intervals for the stands included in the study. Lee (1998) reported that long measurement intervals can produce larger errors than short measurement intervals. Therefore, a regular short interval dataset would likely have given more precision in prediction. Also, the measurement periods were not well

distributed, which may have caused bias and heteroscedasticity through the modelling period (Lee, 1998). Furthermore, model precision could likely have been improved by reinforcing it with more biological, or silvicultural information, for example, thinning information or any natural disturbance events (Park & Wilson, 2007). In this study, such information was not available.

The best MTH, D_{\max} and SD_D models took polymorphic forms, similar to earlier preliminary modelling studies. For example, even-aged *Cupressus lusitanica* and *C. macrocarpa* plantations (Berrill, 2004), *Acacia melanoxylon* (Berrill et al., 2007), *Eucalyptus fastigata* (Berrill & Hay, 2005) in New Zealand and *Pinus nigra* in Catalonia, Spain (Palahí & Grau, 2003). However, the basal area (G) was best fitted with an anamorphic form, which is unusual but can be found in similar types of data-limited situations. For example, Vanclay (2010) suggested one-parameter anamorphic forms to deal with a similar small dataset.

Borders et al. (1988) reported autocorrelation in data while using equal interval datasets, especially in a data-limited situation. This autocorrelation may have influenced the final results of this study. However, it can be overcome by collecting and adding more data to the final modelling dataset. This data should cover all age classes as well as sites (Borders, 1989). Also, all these models are based on mensurational equations and deserve further reinforcement from a biological perspective, by adding physiology into the modelling procedure. Finally, the self-thinning model was based on the SDI concept of Reineke (1933), which requires further testing and elaboration with more data. Pretzsch and Biber (2005) found that the SDI function's power (Reineke, 1933) changed with species and site, in this study the default value (1.605) was used. Specifically, the self-thinning model needs to fit with a differential form by considering different stocking and sites.

Although, these preliminary models offered a first stage indication and reasonably accurate prediction of mature *E. globoidea* in New Zealand, the set of models presented here

did not cover all the age classes so that some extrapolation may occur during projection. Silvicultural and natural disturbances were not accounted for in the models. Therefore the model's performance could be altered. The model set was site specific for mature stands, hence need to be calibrated with new site data.

7.5 Conclusion

This study developed a set of preliminary growth and yield models for *E. globoidea* which satisfy basic mensurational assumptions. Mean top height, maximum diameter, and standard deviation of DBH were represented respectively by first Von-Bertalanffy Richards, Hossfeld, and second Schumacher polymorphic difference equations. They yielded the prediction with the greatest accuracy, whereas, basal area was predicted by Schumacher anamorphic difference equation with higher precision. The SDI approach also fitted well to predict self-thinning and give information about stocking. The performance of stand volume yield and height-diameter relationship models were precise with site-specific factors. These models will provide a first-stage indication of, and understanding about, the growth pattern of *E. globoidea*. The results will vary among the sites because of different site conditions, therefore caution must be exercised. However, more tree measurement data including site characteristics and silvicultural regimes may increase the precision of these models and reduce bias.

7.6 References

- Apiolaza, L., McConnochie, R., & Millen, P. (2011). *Introducing durable species to New Zealand drylands: genetics of early adaptation of Eucalyptus bosistoana*. Paper presented at the developing a Eucalypt resource: learning from Australia and elsewhere, Wood Technology Research Centre.
- Bailey, R. L., & Clutter, J. L. (1974). Base-age invariant polymorphic site curves. *Forest Science*, 20(2), 155-159. doi:10.1093/forestscience/20.2.155
- Battaglia, M., Sands, P., White, D., & Mummery, D. (2004). CABALA: a linked carbon, water and nitrogen model of forest growth for silvicultural decision support. *Forest Ecology and Management*, 193(1), 251-282. doi:https://doi.org/10.1016/j.foreco.2004.01.033
- Bell, D. T., & Williams, J. E. (1997). Eucalypt ecophysiology. *Eucalypt ecology: individuals to ecosystems*. Cambridge University Press, Cambridge, 168-196.
- Belli, K. L., & Ek, A. R. (1988). Growth and survival modeling for planted conifers in the great Lakes Region. *Forest Science*, 34(2), 458-473.
- Berrill, J. (2004). Preliminary growth and yield models for even-aged *Cupressus lusitanica* and *C. macrocarpa* plantations in New Zealand. *New Zealand Journal of Forestry Science*, 34(3), 272.
- Berrill, J., Nicholas, I., & Gifford, H. (2007). Preliminary growth and yield models for even-aged *Acacia melanoxylon* plantations in New Zealand. *New Zealand Journal of Forestry Science*, 37(1), 37.
- Berrill, J. P., & Hay, A. E. (2005). Indicative growth and yield models for even-aged *Eucalyptus fastigata* plantations in New Zealand. *New Zealand Journal of Forestry Science*, 35(2/3), 121-138.
- Berrill, J. P., & Hay, A. E. (2006). Indicative growth and yield models for stringybark eucalypt plantations in northern New Zealand. *New Zealand Journal of Forestry*, 51(1), 19.
- Blake, J., Somers, G., & Ruark, G. (1990). Perspectives on process modeling of forest growth responses to environmental stress. In R. Dixon, R. Meldahl, G. Ruark, & W. Warren (Eds.), *Process modeling of forest growth responses to environmental stress*. (pp. 9-17). Timber Press, Portland, Oregon.
- Blanco, J. A., Zavala, M. A., Imbert, J. B., & Castillo, F. J. (2005). Sustainability of forest management practices: Evaluation through a simulation model of nutrient cycling. *Forest Ecology and Management*, 213(1), 209-228.
- Borders, B. E. (1989). Systems of equations in forest stand modeling. *Forest Science*, 35(2), 548-556.

- Borders, B. E., Bailey, R. L., & Clutter, M. L. (1988). Forest growth models: parameter estimation using real growth series. *USDA Forest Service General Technical Report North Central Forest Experiment Station*.
- Box, G. E. (1976). Science and statistics. *Journal of the American Statistical Association*, 71(356), 791-799.
- Burkhart, H. E. (1977). Cubic-foot volume of loblolly pine to any merchantable top limit. *Southern Journal of Applied Forestry*, 1(2), 7-9.
- Candy, S. (1989). Growth and yield models for *Pinus radiata* in Tasmania. *New Zealand Journal of Forestry Science*, 19(1), 112-133.
- Castedo-Dorado, F., Diéguez-Aranda, U., Barrio-Anta, M., & Álvarez-González, J. G. (2007). Modelling stand basal area growth for radiata pine plantations in north-western Spain using the GADA. *Annals of Forest Science*, 64(6), 609-619. doi:10.1051/forest:2007039
- Castedo-Dorado, F., Diéguez-Aranda, U., & Álvarez-González, J. G. (2007). A growth model for *Pinus radiata* D. Don stands in north-western Spain. *Annals of Forest Science*, 64(4), 453-465. doi:10.1051/forest:2007023
- Clutter, J. L. (1963). Compatible growth and yield models for Loblolly Pine. *Forest Science*, 9(3), 354-371.
- Clutter, J. L., Fortson, J. C., Pienaar, L. V., Brister, G. H., & Bailey, R. L. (1983). *Timber management: a quantitative approach*: John Wiley & Sons, Inc.
- Curtis, R. O. (1967). Height-diameter and height-diameter-age equations for second growth Douglas-fir. *Forest Science*, 13, 365-375.
- Ek, A. R. (1974). Nonlinear models for stand table projection in northern hardwood stands. *Canadian Journal of Forest Research*, 4(1), 23-27.
- Garcia, O. (1974). Height-diameter equations for *Pinus radiata*. *Nota Tecnica*, 19.
- Goulding, C. J. (2005). Measurement of trees. In M. Colley (Ed.), *Forestry handbook* (4th ed., pp. 316). New Zealand: The New Zealand Institute of Forestry (Inc.).
- Jansen, J. J., Sevenster, J., & Faber, J. (1996). *Opbrengsttabellen voor belangrijke boomsoorten in Nederland*. The Netherlands: IBN-DLO
- Kitikidou, K., Papageorgiou, A., Milios, E., & Stampoulidis, A. (2016). Preliminary individual tree growth model, site index model" mortality" model for Aleppo pine (*Pinus halepensis* mill.) in Chalkidiki (Northern Greece). *Journal Ciência Florestal*, 26(4), 1247-1257.

- Korzukhin, M. D., Ter-Mikaelian, M. T., & Wagner, R. G. (1996). Process versus empirical models: which approach for forest ecosystem management? *Canadian Journal of Forest Research*, 26(5), 879-887. doi:10.1139/x26-096
- Landsberg, J. J., Waring, R. H., & Coops, N. C. (2003). Performance of the forest productivity model 3-PG applied to a wide range of forest types. *Forest Ecology and Management*, 172(2), 199-214. doi:https://doi.org/10.1016/S0378-1127(01)00804-0
- Lee, S. H. (1998). *Modelling growth and yield of Douglas-fir using different interval lengths in the South Island of New Zealand*. (PhD), University of Canterbury, New Zealand.
- Lin, H. (2017). *Risk and impact of insect herbivores on the development of dryland Eucalyptus forestry in New Zealand*. (PhD), University of Canterbury, New Zealand.
- Maclaren, P. (2005). Realistic alternatives to radiata pine in New Zealand - a critical review. *New Zealand Journal of Forestry*, 50(1), 3-10.
- Menzies, H. (1995). Eucalypts show potential. *Farm Forestry Review*, 33-34.
- Millen, P., van Ballekom, S., Altaner, C., Apiolaza, L., Mason, E., McConnochie, R., . . . Murray, T. (2018). Durable eucalypt forests—a multi-regional opportunity for investment in New Zealand drylands. *New Zealand Journal of Forestry*, 63(1), 11-23.
- Näslund, M. (1936). Skogsförsöksanstaltens gallringsförsök i tallskog. *Meddelanden från statens skogsförsöksanstalt*, 29(1).
- Nicholas, I., & Millen, P. (2012). Durable Eucalypt leaflet series: *Eucalyptus globoidea* In New Zealand Dryland Forest Initiative (Ed.).
- NZDFI. (2013). New Zealand Dryland Forest Initiative introductory brochure. In M. R. Centre (Ed.). Blenheim, New Zealand.
- NZFOA. (2017). New Zealand plantation forest industry: facts and figures 2016/17. Wellington, New Zealand: Ministry for Primary Industries.
- Palahí, M., & Grau, J. (2003). Preliminary site index model and individual-tree growth and mortality models for black pine (*Pinus nigra* Arn.) in Catalonia (Spain). *Journal of Forest Systems*, 12(1), 137-148.
- Park, A., & Wilson, E. R. (2007). Beautiful plantations: can intensive silviculture help Canada to fulfil ecological and timber production objectives? *The Forestry Chronicle*, 83(6), 825-839. doi:10.5558/tfc83825-6
- Pienaar, L. V., & Rheney, J. W. (1995). Modeling stand-level growth and yield response to silvicultural treatments. *Forest Science*, 41(3), 629-638.

- Pilaar, C. H., & Dunlop, J. D. (1990). The permanent sample plot system of the New Zealand Ministry of Forestry. *Bulletin des Recherches Agronomiques de Gembloux*, 25(1), 5-17.
- Pretzsch, H., & Biber, P. (2005). A re-evaluation of Reineke's rule and stand density index. *Forest Science*, 51(4), 304-320. doi:10.1093/forestscience/51.4.304
- Reineke, L. H. (1933). Perfecting a stand-density index for even-aged forest. *Journal of Agricultural Research*, 4, 627-638.
- Soalleiro, R. R. (1995). *Crecimiento y produccion de masas forestales de pinus pinaster ait. En galicia. Alternativas selvícolas posibles*. Universidad Politécnica de Madrid.
- Vanclay, J. K. (1994). Modeling forest growth and yield. *Applications to Mixed Tropical Forests*. CAB International, Wallingford.
- Vanclay, J. K. (2010). Robust relationships for simple plantation growth models based on sparse data. *Forest Ecology and Management*, 259(5), 1050-1054. doi:10.1016/j.foreco.2009.12.026
- Williams, J., & Woinarski, J. (1997). *Eucalypt ecology: individuals to ecosystems*: Cambridge University Press.
- Zeide, B. (1993). Analysis of growth equations. *Forest Science*, 39(3), 594-616.
- Zhao, W. (1999). *Growth and yield of Pinus radiata in Canterbury, New Zealand*. (PhD), University of Canterbury, New Zealand.

8

Conclusions

8. A general discussion

The findings of this doctoral thesis contribute to advancement in the understanding of growth dynamics of two dryland *Eucalyptus* species (*E. bosistoana* and *E. globoidea*) planted in New Zealand. In addition, this study presents improved modelling approaches for these species. These include both juvenile and mature plantation stands at different modelling resolutions. In particular, this thesis highlights the following models: (i) a purpose-specific non-geostatistical digital elevation model (DEM) interpolation method; (ii) within-site and between sites variables which influence the height growth and survival of juvenile *E. bosistoana* and *E. globoidea*, (iii) different modelling resolutions to accommodate between-site variables for *E. bosistoana* and *E. globoidea*, and (iv) a preliminary mensurational growth and yield model for mature *E. globoidea*.

8.1 Within-site and between-sites growth and survival factors

Within-site topographic attributes were extracted from the DEM, which was developed by the simple process described in Chapter 2. Topographic attributes significantly affected the height growth and survival of juvenile *Eucalyptus* plantations (Chapter 3). Topographic attributes related to surface shape (e.g. curvature) and position (e.g. morphometric protection index, and distance from the top ridge) were most important. These attributes indirectly characterise and represent the soil and climatic variables (Beven & Kirkby, 1979; Böhner & Antonić, 2009; Coops et al., 2000; Zevenbergen & Thorne, 1987). The within-site temperature was independently modelled but was not statistically significant, and therefore was not included in the final model. This may be due to the lack of position-specific climatic data for each plot. Soil information was not tested for similar reasons.

The site-specific models showed consistent results (Chapter 3), where *Eucalyptus* species were influenced by topography. The site-specific models developed here are temperature sensitive. These findings are in line with other studies for *Eucalyptus* (Oparah,

2012; Prior & Bowman, 2014). However, the soil information did not significantly influence the height growth and survival of *Eucalyptus*. The available soil information is very coarse and has been shown to be inaccurate in a previous study (Pearse et al., 2015), which may be the reason for its non-significance.

The final models were statistically sound. The precision and bias of the final models could be improved by including more initial site-specific data, for example, initial height measurements and site characteristics. Furthermore, better soil and climatic information have the potential to provide a better understanding of the ecophysiological process.

8.2 Flexible modelling approach

Different modelling approaches (Chapters 4 and 5) were applied and assessed based on the precision and bias of validation results (Chapter 6). The augmented PULSE modelling approach was the best, offering a robust understanding of the ecophysiological process without violating the basic mensurational assumptions. The model can also be built with minimal available information, though more specific information unequivocally increases the model precision and reduce bias. Casnati (2016) reported similar results for mature stands of *Eucalyptus grandis* and *Pinus taeda* in Uruguay.

8.3 Preliminary growth and yield model for *E. globoides*

Juvenile models provide better understandings of the plantation establishment and site preparation, but mature stand models give better projections of future productivity. Several management decisions can be made from these projections, for example, planning silvicultural regimes. Mason et al. (1997) reported limitations on building growth and yield models by linking juvenile and mature stand data. Therefore, a full set of preliminary growth and yield models was developed for mature stands of *E. globoides* from the available mature stand data only. The final models developed here are comparable to the indicative model of Berrill and Hay (2006) for the stringy-bark *Eucalyptus* group in New Zealand. The models are statistically

sound with satisfactory precision and minimal bias. However, there are some heterogeneous tendencies of the models' residuals, which may be improved by reinforcing the models with more data.

8.4 Management implications

Chapter 2 results show that high-resolution (0.5m × 0.5m) DEMs can be developed from low-cost GNSS (RTK-GPS), especially, where no DEM and LiDAR data exist. This approach could be effectively applied for developing DEMs for small geographic areas, like plots, but the labour involved likely precludes its use for the larger geographic areas, like stands or whole forests.

Chapter 3 reports on a set of models for height growth and survival of two dryland *Eucalyptus* species on a smaller spatial scale than conventional practice. Similar to Chapter 3, Chapters 4 and 5 reported on the site-specific models. These findings can be used to predict and understand the eco-physiology of dryland *Eucalyptus*. The information produced by the models could be used at the time of plantation establishment to aid the process of site-species matching and site preparation.

Among the several dryland *Eucalyptus* species studied, mature stand *E. globoides* inventory data was available from a few PSP plots around New Zealand (Pilaar & Dunlop, 1990). Therefore, the preliminary mature stand growth and yield models were built to represent the growth dynamics of this species over time in Chapter 7. This model will allow projection of future growth and yield for *E. globoides*.

8.5 Research needs and research questions

The interpolation of DEM from GNSS (RTK-GPS) data in this study was tested in particular site-specific conditions, which may need further adjustment by considering different surfaces as well as the environmental situation. The interpolation method could be tested with

different spatial arrangement of the data points collected in order to reduce the effects of any spatial-autocorrelation.

The models developed and the results produced in this study provide a better understanding of the juvenile and mature growth dynamics for the dryland *Eucalyptus* on different spatial scales. However, further research is needed to fully understand the growth process and the behaviour of these species. The models could be tested in different climatic scenarios: they could be altered to include better soil information, particularly drought severity and frequency, and the interaction of the trees with light and other competing vegetation (e.g. weeds). Furthermore, the results presented here were considered without any silvicultural or site preparation data, which should be included in future studies. Finally, all the results are site-specific, the models presented in this study need to be tested and calibrated with many different sites to make the models more orthogonal and increase their applicability.

8.6 Conclusion

This study explored different aspects to understand juvenile and mature dryland *E. bosistoana* and *E. globoidea* growth dynamics in New Zealand. Different modelling techniques were applied and developed for predicting and understanding the *Eucalyptus* species. The ecophysiological models presented in this study showed great potential, and they have important uses compared to other time-based approaches. However further research, including proper soil data, is needed. Finally, a set of mensurational models were built for *E. globoidea* mature stands, which could be able to generate initial mature stand growth dynamics information and identify areas for future research.

8.7 References

- Berrill, J. P., & Hay, A. E. (2006). Indicative growth and yield models for stringybark eucalypt plantations in northern New Zealand. *New Zealand Journal of Forestry*, 51(1), 19.
- Beven, K. J., & Kirkby, M. J. (1979). A physically based, variable contributing area model of basin hydrology. *Hydrological Sciences Bulletin*, 24(1), 43-69. doi:10.1080/02626667909491834
- Böhner, J., & Antonić, O. (2009). Land-surface parameters specific to topo-climatology. *Developments in Soil Science*, 33, 195-226.
- Casnati, A. C. R. (2016). *Hybrid mensurational-physiological models for Pinus taeda and Eucalyptus grandis in Uruguay*. (PhD), University of Canterbury, New Zealand.
- Coops, N. C., Waring, R. H., & Moncrieff, J. B. (2000). Estimating mean monthly incident solar radiation on horizontal and inclined slopes from mean monthly temperatures extremes. *International Journal of Biometeorology*, 44(4), 204-211. doi:10.1007/s004840000073
- Mason, E. G., Whyte, A. G. D., Woollons, R. C., & Richardson, B. (1997). A model of the growth of juvenile radiata pine in the Central North Island of New Zealand: links with older models and rotation-length analyses of the effects of site preparation. *Forest Ecology and Management*, 97(2), 187-195. doi:[http://dx.doi.org/10.1016/S0378-1127\(97\)00099-6](http://dx.doi.org/10.1016/S0378-1127(97)00099-6)
- Oparah, I. A. (2012). *Photosynthetic acclimation to temperature of four Eucalyptus species and Sequoia sempervirens*. (MSc), University of Canterbury, New Zealand.
- Pearse, G., Moltchanova, E., & Bloomberg, M. (2015). Assessment of the accuracy of profile available water and potential rooting depth estimates held within New Zealand's fundamental soil layers geo-database. *Soil Research*, 53(7), 737-744. doi:<https://doi.org/10.1071/SR14012>
- Pilaar, C. H., & Dunlop, J. D. (1990). The permanent sample plot system of the New Zealand Ministry of Forestry. *Bulletin des Recherches Agronomiques de Gembloux*, 25(1), 5-17.
- Prior, L. D., & Bowman, D. M. J. S. (2014). Big eucalypts grow more slowly in a warm climate: evidence of an interaction between tree size and temperature. *Global Change Biology*, 20(9), 2793-2799. doi:doi:10.1111/gcb.12540
- Zevenbergen, L. W., & Thorne, C. R. (1987). Quantitative analysis of land surface topography. *Earth Surface Processes and Landforms*, 12(1), 47-56. doi:doi:10.1002/esp.3290120107

Appendices

Appendix I

Additionally, the top 10 cm of soil was sampled at each pit location for soil chemical analysis. Chemical analyses included quantifying a range of micro- and macro-nutrient concentrations; and additionally, cation exchange capacity (CEC), pH, total base saturation (TBS), volumetric weight (VW), and organic matter (OM) content (Table I). The chemical analyses were undertaken by an analytical testing company (Hill Laboratories, Christchurch, New Zealand) following their standard procedures.

Table I. Summary statistics of the soil chemical analysis data.

Variables	Unit	A				B				C			
		<i>Min</i>	<i>Max</i>	<i>Mean</i>	<i>Sd</i>	<i>Min</i>	<i>Max</i>	<i>Mean</i>	<i>Sd</i>	<i>Min</i>	<i>Max</i>	<i>Mean</i>	<i>Sd</i>
<i>OM</i>	%	0.70	5.60	2.99	1.1	1.0	4.6	2.72	1.05	3	9.1	5.67	1.51
<i>tC</i>	%	0.40	3.20	1.73	0.7	0.6	2.7	1.57	0.61	2	5.3	3.29	0.89
<i>tN</i>	%	0.10	0.30	0.20	0.1	0.1	0.4	0.18	0.05	0.13	0.5	0.26	0.1
<i>TBS</i>	%	62.00	94.0	77.4	7.1	48	80.	65.6	7.45	34	81	49.5	12.9
<i>C/N</i>		3.60	13.1	8.83	2.3	4.7	12	8.50	2.02	11	14	12.6	0.98
<i>AMN/TN</i>		1.00	4.90	2.62	1.1	1.3	6.7	2.20	1.02	1.50	3	2.37	0.45
<i>VW</i>	g/mL	0.91	1.10	0.99	0.1	0.9	1.2	1.06	0.08	0.74	0.98	0.86	0.06
<i>pH</i>	pH unit	5.80	7.10	6.26	0.3	5.5	6.0	5.76	0.15	5.40	6.40	5.69	0.27
<i>OP</i>	mg/L	3.00	16.0	6.45	3.3	3.0	14	5.36	2.25	2	12	6.08	3.19
<i>K</i>	me/100g	0.63	1.38	0.95	0.2	0.4	1.3	0.89	0.25	0.16	0.6	0.36	0.12
<i>Ca</i>	me/100g	5.10	12.8	8.60	2	3.6	9.7	6.80	1.47	2.10	12.4	5.25	2.9
<i>Mg</i>	me/100g	2.95	6.75	4.50	1.1	1.6	6.1	3.23	1.11	0.74	5.87	2.02	1.5
<i>Na</i>	me/100g	9.00	40.0	23.9	9.7	9.0	34	17.9	5.92	1	33	10.54	10.82
<i>CEC</i>	me/100g	13.0	24.0	18.6	2.9	12	22	16.8	2.43	9	24	14.96	3.84
<i>B</i>	mg/kg	0.50	1.20	0.79	0.2	0.4	0.8	0.62	0.11	0.20	1.5	0.48	0.33
<i>tP</i>	mg/kg	282	549	409	64	374	566	484	46.7	165	526	359.62	103.2
<i>AMN</i>	µg/g	14	112	50.6	25	20	182	40.9	28.9	20	111	62.83	22.49

*OM = Organic matter, tC = Total carbon, tN = Total nitrogen, TBS = Total base saturation, C/N = Carbon nitrogen ratio, AMN/TN = Anaerobically mineralisable N/total N, VW = Volume weight, OP = Olsen phosphorus, K = Potassium, Ca = Calcium, Mg = magnesium, Na = Sodium, CEC = Cation exchange capacity, B = Boron, tP = Total phosphorus, AMN = Anaerobically mineralisable N.

Table II. Final juvenile height model summary with parameters

Species	Site	Sat	α_0	α_1	α_2	α_3	α_4	α_5	β_0	β_1	β_2	β_3	β_4	β_5	β_6
<i>E. globoidea</i>	A	Est	-2.051	2.010	0.0043	-	-	-	1.871e+016	-1.398e-02	-1.584e+01	-2.829e+0	-	-	-
		SE	0.525	0.517	0.0005	-	-	-	1.656	9.245e-04	1.652e+00	8.838e-01	-	-	-
		<i>p</i>	0.001	0.0001	2.59e-1	-	-	-	< 0.000002	< 2e-16	< 2e-16	0.001607	-	-	-
<i>E. bosistoana</i>	B	Est	0.53609	-0.0977	0.01260	1.25919	-8.445493	-	1.478807	0.042378	-1.04705	-0.01461	-0.01276	6.573568	0.015729
		SE	0.16774	0.00936	0.00216	0.19244	0.430181	-	0.141687	0.008319	0.154006	0.001257	0.002026	0.337177	0.001469
		<i>p</i>	0.00144	< 2e-16	6.84e-1	9.58e-11	< 2e-16	-	< 2e-16	4.18e-07	1.81e-11	< 2e-16	4.39e-10	< 2e-16	< 2e-16
	C	Est	3.34557	-2.447348	0.00245	-0.0086	-0.016512	-1.36	0.537881	0.0199025	0.0447812	-	-	-	-
		SE	0.73907	0.627552	0.00095	0.00152	0.004243	0.268	0.1293038	0.0015926	0.0046178	-	-	-	-
		<i>p</i>	8.43e-06	0.000117	0.01022	3.83e-08	0.00012	6.62e-07	4.09e-05	< 2e-16	< 2e-16	-	-	-	-

Table III. Final juvenile survival model summary with parameters.

Species	Site	Stat.	α_0	α_1	α_2	β_0	β_1	β_2	β_3
<i>E. globoidea</i>	Avery	Est	0.292	0.0465	-0.04293	-3.2431	3.1882	0.00359	-0.10117
		SE	0.015	0.0187	0.0121	1.1201	1.0708	0.00057	0.04987
		<i>p</i>	< 2e-16	0.0130	0.00043	0.0038	0.0029	5.48e-10	0.04286
<i>E. bosistoana</i>	Dillon	Est	0.01036	-	-	0.51373	0.1154	-	-
		SE	0.0120	-	-	0.8424	0.0519	-	-
		<i>p</i>	0.3907	-	-	0.542	0.0272	-	-

Appendix II

Table IV. Soil description of all the study sites.

Series	Dom. Soil Type	Soil Class	Class Name	Comments
Mairaki	Silt loam	PXM	Mottled fragic pallic	Fragic pallic soils are predominantly silty and severely restrict root movement.
Phoebe	Silt loam	PXM	Mottled fragic pallic	
Jordan	Silt loam and shallow silt loam	PXJ	Argillic fragic pallic	
Wither	Hills soils	PXJN	Argillic-sodic fragic pallic	Argillic pallic soils have a clay accumulation in the sub-soils
Glenmark	Silt loam	PJC	Calcareous argillic pallic	
Flaxbourne	Hill soils	PJT	Typic argillic pallic	
Bideford	Loam	PJM	Mottled argillic pallic	Immature pallic soils are insufficiently developed and brittle
Grower	Hill soils	PIM	Mottled immature pallic	
Kidnappers	Silt loam	PIT	Typic immature pallic	
Halcombe	Silt loam	PPJ	Argillic perch-gley pallic	Perch-gley pallic soils occur on sites which are periodically saturated.
Matapiro	Sandy loam	PPU	Duric perch-gley pallic	
Matapiro	Light sandy loam	PPU	Duric perch-gley pallic	
Pokororo	Steepland soils	BOA	Acidic orthic brown	Orthic brown soils have weak soil strength. Most commonly occur in hilly or steep slopes.
Marokopa	Clay loam	BOA	Acidic orthic brown	
Tuhitarata	Silt loam	BOP	Pallic orthic brown	
Atua	-	BOP	Pallic orthic brown	
Wainui	Heavy silt loam	BOP	Pallic orthic brown	
Ngaumu	Fine sandy loam	BOM	Mottled orthic brown	Orthic pumice soils are well to imperfectly drained but do not severely restrict water movement
Waimarama	Sandy loam	BOC	Calcareous orthic brown	
Tauhara	Steepland soils	MOI	Immature orthic pumice	
Kaharoa	Sand	MOZ	Podzolic orthic pumice	Fluvial recent soils deposited by flowing water.
Awatere	Gravelly sand	RFT	Typic fluvial recent	
Mahoenui	Sandy loam	ROT	Typic orthic recent	Orthic recent soils occur on eroded land.
Opouri	Steepland	UYT	Typic yellow ultic	Yellow ultic soils are clayey and imperfectly drained.

Table V. Height growth model parameter estimates.

Species	Stat.	α_0	α_1	β_0	β_1	β_2
<i>E. globoidea</i>	Estimate	-1.08776	0.09069	-1.35861	0.17674	-
	SE	0.42408	0.02577	0.69570	0.04622	-
	<i>P</i>	0.011690	0.000634	0.053422	0.000220	-
	<i>Sig.</i>	*	***	.	***	-
<i>E. bosistoana</i>	Estimate	2.120282	-1.724324	-0.999457	0.019529	2.189817
	SE	0.412280	0.34617	0.499306	0.019529	2.189817
	<i>P</i>	1.15e-06	2.29e-06	0.04771	0.00228	5.10e-05
	<i>Sig.</i>	***	***	*	**	***

Table VI. Survival model parameter estimates.

Species	Stat.	α_0	α_1	α_2	β_0
<i>E. globoidea</i>	Estimate	-1.36783	0.14865	0.07710	0.74156
	SE	0.24489	0.02742	0.02102	0.14259
	<i>p</i>	1.11e-07	2.40e-07	0.000342	6.59e-07
	<i>Sig.</i>	***	***	***	***
<i>E. bosistoana</i>	Estimate	-0.591724	0.026553	0.022564	0.827190
	SE	0.143901	0.007501	0.008251	0.160142
	<i>p</i>	6.33e-05	0.000527	0.006965	7.23e-07
	<i>Sig.</i>	***	***	**	***

Appendix III

Table VII. PULSE model (R_{TVPD}) parameters estimates.

Species	Stat.	α	β
<i>E. bosistoana</i>	Estimate	8.246e-05	1.077e+00
	SE	8.361e-05	1.039e-01
	<i>P</i>	0.32	<2e-16
	<i>Sig. Codes</i>	-	***
<i>E. globoidea</i>	Estimate	8.246e-05	1.077e+00
	SE	8.361e-05	1.039e-01
	<i>P</i>	0.326	<2e-16
	<i>Sig. Codes</i>	-	***

Sig. Codes: 0 '***'; 0.001 '**'; 0.01 '*'; 0.05 '.'; 0.1 '-'

Table VIII. Parameter estimates for augmented PULSE height yield model (R_{TVPD}).

Species	Stat.	α	β_0	β_1	β_2
<i>E. bosistoana</i>	Estimate	8.959e-05	1.193e+00	1.775e-01	-1.388e-01
	SE	8.019e-05	9.072e-02	8.233e-02	3.709e-02
	<i>P</i>	0.266	<2e-16	0.033	0.0002
	<i>Sig. Codes</i>	-	***	*	***
<i>E. globoidea</i>	Estimate	8.156e-05	1.065e+00	2.589e-01	-
	SE	7.564e-05	9.476e-02	8.432e-02	-
	<i>P</i>	0.283	<2e-16	0.002	-
	<i>Sig. Codes</i>	-	***	**	-

Sig. Codes: 0 '***'; 0.001 '**'; 0.01 '*'; 0.05 '.'; 0.1 '-'

Table IX. Parameter estimates for the survival proportion PULSE model (R_{TVPD}).

Species	Stat.	α	β
<i>E. bosistoana</i>	Estimate	-0.0004242	0.614
	SE	0.0006846	0.168
	<i>P</i>	0.536	0.0003
	<i>Sig. Codes</i>	-	***
<i>E. globoidea</i>	Estimate	-0.003079	0.502222
	SE	0.003545	0.121711
	<i>P</i>	0.386	6.13e-05
	<i>Sig. Codes</i>	-	****

Sig. Codes: 0 '***'; 0.001 '**'; 0.01 '*'; 0.05 '.'; 0.1 '-'

Table X. Parameter estimates for augmented survival proportion PULSE model (R_{TVPD}).

Species	Stat.	α	β_0	β_1
<i>E. bosistoana</i>	Estimate	-0.0001061	0.6839106	0.0096863
	SE	0.0001789	0.172794	0.0024732
	<i>P</i>	0.5541	0.000114	0.000134
	<i>Sig. Codes</i>	-	***	***
<i>E. globoidea</i>	Estimate	-0.003200	0.333132	0.082404
	SE	0.003622	0.150016	0.082404
	<i>P</i>	0.3784	0.027	0.0463
	<i>Sig. Codes</i>	-	*	*

Sig. Codes: 0 '***'; 0.001 '**'; 0.01 '*'; 0.05 '.'; 0.1 '-'

Appendix IV

Table XI. Preliminary models parameter estimates.

Model	Stat.	α	β	γ	δ
<i>MTH</i>	Estimate	33.27801	0.10493	-	-
	SE	0.59493	0.00488	-	-
	<i>p</i>	<2e-16	<2e-16	-	-
	<i>Sig.</i>	***	***	-	-
<i>G</i>	Estimate		15.4329	-	-
	SE		0.4876	-	-
	<i>p</i>		<2e-16	-	-
	<i>Sig.</i>		***	-	-
<i>Dmax</i>	Estimate	1.34350	2.18374	-	-
	SE	0.09103	0.05533	-	-
	<i>p</i>	<2e-16	<2e-16	-	-
	<i>Sig.</i>	***	***	-	-
<i>SD_D</i>	Estimate	-5.88374	-0.22515	-	-
	SE	1.04224	0.02529	-	-
	<i>p</i>	4.62e-08	< 2e-16	-	-
	<i>Sig.</i>	***	***	-	-
<i>V</i>	Estimate	2.91550	-0.11914	-6.58049	0.32620
	SE	0.45295	0.02559	1.37885	0.07908
	<i>p</i>	2.94e-08	2.02e-05	1.35e-05	0.000124
	<i>Sig.</i>	***	***	***	***

Table XII. Height-diameter relationship model

Model	Stat.	α_0	α_1	β_0	β_1
<i>H-D</i>	Estimate	2.814e-01	3.295e-05	9.863e-01	-2.424e+01
	SE	2.751e-02	1.250e-05	4.977e-01	4.841e+00
	<i>p</i>	< 2e-16	0.00884	0.04843	9.38e-07
	<i>Sig.</i>	***	**	*	***

